

PREDICTING PAVEMENT PERFORMANCE
USING TIME-DEPENDENT TRANSFER
FUNCTIONS

SEPTEMBER 1972 - NUMBER 32



BY

R. E. BOYER

JHRP

JOINT HIGHWAY RESEARCH PROJECT
PURDUE UNIVERSITY AND
INDIANA STATE HIGHWAY COMMISSION

Informational Report

PREDICTING PAVEMENT PERFORMANCE USING TIME-DEPENDENT TRANSFER FUNCTIONS

TO: J. F. McLaughlin, Director
Joint Highway Research Project

September 7, 1972

FROM: H. L. Michael, Associate Director
Joint Highway Research Project

File: 2-1

The attached Report is presented to the Board for Information inasmuch as it is concerned with the development of a technique to predict the performance of flexible pavement systems subjected to dynamic load inputs. The Report is titled "Predicting Pavement Performance Using Time-Dependent Transfer Functions". It has been authored by Mr. Robert E. Boyer, Graduate Instructor in Research in the Soil Mechanics area of Civil Engineering. Professor M. E. Harr served as director of the study.

The research was financed by the Civil Engineering Research Division, Air Force Weapons Laboratory and the field tests were made at Kirtland Air Force Base, New Mexico. The Report is presented to the Board for information in accordance with JHRP policy of reporting pertinent research conducted in the School of Civil Engineering to the Board.

Respectfully submitted,



Harold L. Michael
Associate Director

HLM:ms

cc: W. L. Dolch	M. L. Hayes	C. F. Scholer
R. L. Eskew	C. W. Lovell	M. B. Scott
W. H. Goetz	G. W. Marks	J. A. Spooner
M. J. Gutzwiller	R. D. Miles	N. W. Steinkamp
G. K. Hallock	J. W. Miller	H. R. J. Walsh
R. H. Harrell	G. T. Satterly	E. J. Yoder

Informational Report
PREDICTING PAVEMENT PERFORMANCE USING TIME-DEPENDENT
TRANSFER FUNCTIONS

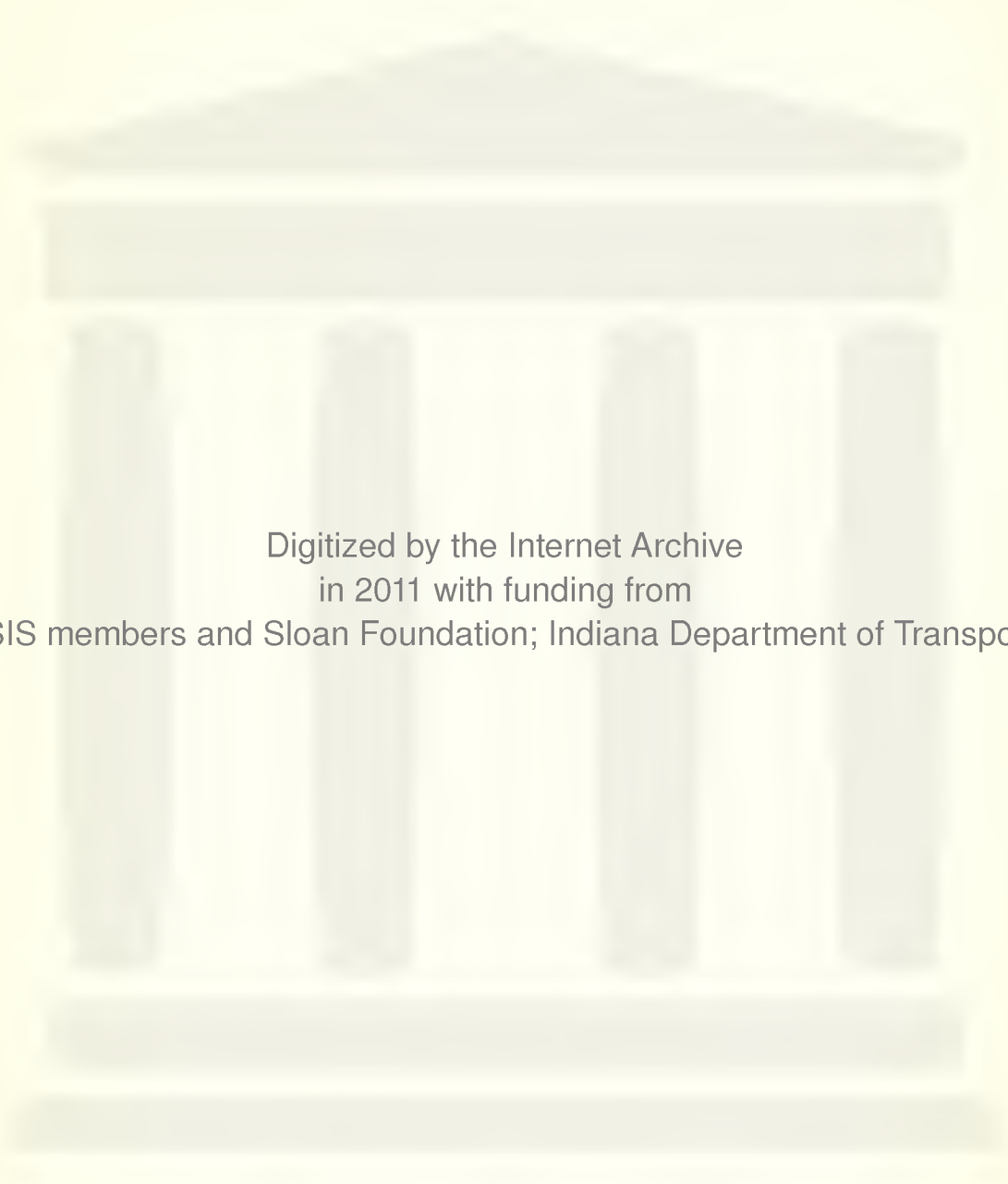
by

Robert E. Boyer
Graduate Instructor in Research
School of Civil Engineering

Joint Highway Research Project

File: 2-1

Purdue University
West Lafayette, Indiana
September 7, 1972



Digitized by the Internet Archive
in 2011 with funding from
LYRASIS members and Sloan Foundation; Indiana Department of Transportation

ACKNOWLEDGMENTS

The author wishes to extend sincere thanks to his advisor, Dr. M. E. Harr, for his helpful suggestions during the long discussions leading to the formulation of this research topic and for his continued guidance throughout the course of this investigation.

The interest and comments of the other members of the research committee, Dr. G. A. Leonards, Professor E. J. Yoder, and Professor E. O. Stitz are greatly appreciated.

Sincere thanks are extended to the Civil Engineering Research Division, Air Force Weapons Laboratory, for financial assistance needed to conduct the research and for making available facilities at Kirtland Air Force Base, New Mexico, to conduct field tests in conjunction with this research effort.

The author also takes this opportunity to thank Mr. L. M. Womack and Mr. H. R. Marien, who were the Air Force project engineers, for their cooperation and assistance during the entire investigation; and to Mr. W. H. Hightner and W. L. DeGroff for their assistance and useful discussions.

To his wife, Sue, the author expresses deep gratitude for her help in successfully completing this work - her consistent patience and understanding.

TABLE OF CONTENTS

	Page
LIST OF TABLES	vi
LIST OF FIGURES	vii
LIST OF SYMBOLS	xii
ABSTRACT	xiv
INTRODUCTION	1
REVIEW OF LITERATURE	4
Elastic Solutions	4
Static Loading	5
Dynamic Loading	6
Elastic-Viscoelastic Solutions	6
Static Loading	7
Dynamic Loading	8
Viscoelastic Solutions	9
Static Loading	10
Dynamic Loading	10
Mechanistic Solutions	11
Transfer Function Concept	12
"A Priori" Modeling	13
"A Posteriori" Modeling	13
Determining Transfer Functions	16
FORMULATION OF A TESTING PROGRAM	18
Formulation of Pavement Transfer Functions	18
An "A Priori" Model Technique	22

TABLE OF CONTENTS (cont'd)

	Page
"A Posteriori" Modeling Techniques	23
Signature and TDT Functions	28
Predicting Performance	32
FIELD INVESTIGATION	35
Exploratory Tests	35
Field Tests	36
Instrumentation	38
Scope of Field Tests	40
RESULTS OF FIELD TESTS	51
Peak Dynamic Deflection Basin	51
Deflection Response Functions	51
TDT Functions	61
DISCUSSION OF RESULTS	82
Peak Dynamic Deflection Basin	83
Form of the Deflection Response Functions	84
Form of the TDT Functions	86
Prediction of Deflection Response Functions	88
CONCLUSIONS	97
SUGGESTIONS FOR FURTHER RESEARCH	99
BIBLIOGRAPHY	101
APPENDICES	
Appendix A: Methods for Determining Transfer Functions	106
Appendix B: Regression Analysis-Normal Distribution Model, Computer Program	112

TABLE OF CONTENTS (cont'd)

	Page
Appendix C: Signature and Time-Dependent Transfer Functions, Computer Program	117
Appendix D: Predicting Pavement Performance, Computer Code CONVLE	124
Appendix E: Exploratory Tests	129
Appendix F: Deflection Gages - Description, Installation, and Calibration	139
Appendix G: Listing of Data, Deflection Response and TDT Functions	159
Appendix H: Listing of Data, Predicted Deflection Response Functions	178
VITA	205

LIST OF TABLES

Table	Page
1. Comparison of Peak Prime Mover Deflections for Each Sensing Device Used in Exploratory Tests	37
2. Prime Mover Characteristics	49
3. Peak Dynamic Deflections--C135 Aircraft	52
4. Peak Dynamic Deflections--C131 Aircraft	53
5. Peak Dynamic Deflections--C130 Aircraft	54
6. Peak Dynamic Deflections--Load Cart	55
7. Model Results of Peak Deflections	56
8. Characteristics of TDT Functions	86

LIST OF FIGURES

Figure	Page
1. "A Priori" Modeling	14
2. "A Posteriori" Modeling	15
3. Physical Situation	19
4. Transfer Function Concept	20
5. Time-Dependent Transfer Function for "A Priori" Model	24
6. Frequency Spectrum Plot for Vibrator Data	25
7. Frequency Spectrum Plot for Simple Model	25
8. Adjustment for Response Functions	30
9. Nondestructive Evaluation Method	33
10. Sensing Device Schematic	39
11. Type I Installations-Distant	41
12. Type I Installations-Close Up	41
13. Type II Installations-Distant	42
14. Type II Installations-Close Up	42
15. Instrumentation Setup	43
16. Recording Equipment Components	43
17. Test Site Locations	44
18. Pavement Cross-Sections	45
19. Prime Mover-C135 Aircraft	47
20. Prime Mover-C131 Aircraft	47
21. Prime Mover-C130 Aircraft	48
22. Prime Mover-Load Cart	48
23. Prime Mover Main Gear Characteristics	50

LIST OF FIGURES (cont'd)

Figure	Page
24. Relationships of A-Factors at Each Test Site	57
25. Range of B-Factors at Each Test Site	58
26. Deflection Response Functions (Data for C135 Site 1) . .	62
27. Deflection Response Functions (Data for C131 Site 1) . .	63
28. Deflection Response Functions (Data for C130 Site 1) . .	64
29. Deflection Response Functions (Data for C135 Site 2) . .	65
30. Deflection Response Functions (Data for C131 Site 2) . .	66
31. Deflection Response Functions (Data for C130 Site 2) . .	67
32. Deflection Response Functions (Data for C135 Site 3) . .	68
33. Deflection Response Functions (Data for C131 Site 3) . .	69
34. Deflection Response Functions (Data for C130 Site 3) . .	70
35. TDT Functions (Data for C135 Site 1)	72
36. TDT Functions (Data for C131 Site 1)	73
37. TDT Functions (Data for C130 Site 1)	74
38. TDT Functions (Data for C135 Site 2)	75
39. TDT Functions (Data for C131 Site 2)	76
40. TDT Functions (Data for C130 Site 2)	77
41. TDT Functions (Data for C135 Site 3)	78
42. TDT Functions (Data for C131 Site 3)	79
43. TDT Functions (Data for C130 Site 3)	80
44. Prediction of Deflection Response Functions	88
45. Typical Calculated and Measured Deflection Response Functions for C135, Using TDT Functions from C131 . . .	90

LIST OF FIGURES (cont'd)

Figure		Page
46.	Typical Calculated and Measured Deflection Response Functions for C130, Using TDT Functions from C131 . . .	91
47.	Typical Calculated and Measured Deflection Response Functions for C135 Using Predicted TDT Functions, With C131 as Standard Prime Mover	92
48.	Typical Calculated and Measured Deflection Response Functions for C130 Using Predicted TDT Functions, With C131 as Standard Prime Mover	93
49.	Revised Performance Evaluation Method	95
50.	Simple Second Order Model	107
51.	Asymptotic Approximation of a System's Frequency Spectrum	107
52.	Layout of Sensing Devices	130
53.	Instrumentation Setup	130
54.	Load Cart	131
55.	Boeing 727 Aircraft	131
56.	LVDT Installation Detail	133
57.	Aluminum Sleeve (with cap) Installed	133
58.	Holder Assembly Components	134
59.	Holder Assembly-Partially Assembled	134
60.	Typical Data, Boeing 727-25 MPH	136
61.	Typical Data, Load Cart-8 MPH	137
62.	Typical Data, Load Cart-12 MPH	138
63.	Components of Deflection Gage Type I	141
64.	Components of Deflection Gage Type II	141
65.	Partially Assembled Deflection Gage Type I	143
66.	Partially Assembled Deflection Gage Type II	143

LIST OF FIGURES (cont'd)

Figure	Page
67. Gage Installation-Type I	144
68. Gage Installation-Type II	145
69. Reference Beam Support	146
70. Schematic Representation of the Transient Deflection Measuring System	147
71. Drilling Reference Rod Holes	148
72. Holes Ready for Reference Rods	148
73. Bushing for Lateral Alignment	150
74. Styrofoam Sleeve In-Place	150
75. Paper Filler	152
76. Plate for Vertical Alignment	152
77. Unassembled Alignment Components	153
78. Assembled Alignment Components	153
79. Mount Installation, Close-up	154
80. Mount Installation, Distant	154
81. Epoxy Curing, Close-up	155
82. Epoxy Curing, Distant	155
83. Calibration Devices	157
84. Method of Calibration	157
85. Typical Calculated and Measured Deflection Response Functions for C131 Using Predicted TDT Functions, With C135 as Standard Prime Mover	185
86. Typical Calculated and Measured Deflection Response Functions for C130 Using Predicted TDT Functions, With C135 as Standard Prime Mover	186

Part of the ...

Date	Description	Amount
1891
1892
1893
1894

1895
1896
1897
1898
1899
1900

LIST OF FIGURES (cont'd)

Figure		Page
87.	Typical Calculated and Measured Deflection Response Functions for C135 Using Predicted TDT Functions, With C130 as Standard Prime Mover	192
88.	Typical Calculated and Measured Deflection Response Functions for C131 Using Predicted TDT Functions With C130 as Standard Prime Mover	193
89.	Typical Calculated and Measured Deflection Response Functions for C135 Using Predicted TDT Functions, With C131 as Standard Prime Mover	199
90.	Typical Calculated and Measured Deflection Response Functions for C130 Using Predicted TDT Functions, With C131 as Standard Prime Mover	200

LIST OF SYMBOLS

A	- Normal distribution model parameter, peak dynamic deflection of a signature input
a	- Damping factor
B	- Normal distribution model parameter, a measure of the rate at which a pavement system is capable of dissipating energy.
c	- Damping coefficient
C_{x_i}	- Scaling factor used to adjust deflection response functions spatially
d	- Gage spacing
e	- Base of natural logarithms
$G(t)$	- Time-dependent transfer function
$\bar{G}(s)$	- Transfer function
$I(t)$	- Signature input function
$\bar{I}(s)$	- Laplace transform of $I(t)$
i	- Spatial sequence counter ($i = 0$ represents signature; $i = 1, 2, \dots$ represents output functions)
j	- $\sqrt{-1}$
k	- Elastic spring constant
l	- Dummy variable
m	- Lumped mass of a system
n	- Dummy variable
$O(t)$	- Deflection response output function
$\bar{O}(s)$	- Laplace transform of $O(t)$
s	- A complex variable ($=j\omega$)
t	- Time
x_i	- Distance transverse from point of a signature application

LIST OF SYMBOLS (cont'd)

y	- Velocity
y	- Acceleration
α	- Frequency
λ	- Offset distance of signature input
ϕ	Phase angle
τ	- Dummy time variable
ω	- Frequency

ABSTRACT

Boyer, Robert Elston, Ph.D., Purdue University, August 1972.
Predicting Pavement Performance Using Time-Dependent Transfer Functions.
Major Professor: Dr. Milton E. Harr.

An approach using a real world modeling technique was developed to predict the performance of flexible pavement systems subjected to dynamic load inputs. "A posteriori" modeling was presented in contrast to the normally accepted "a priori" modeling technique. With this approach, the initial hypothesis was:

"that time-dependent functions could be calculated from a pavement's dynamic input and output deflection responses; that these functions could be obtained, in a mathematical sense, without the need to simulate respective material performance to determine values for preselected descriptors; and that these time-dependent functions could be employed to predict deflection output responses when the pavement was subjected to any imposed load".

The investigation was carried out by extending transfer function theory in connection with a discretized convolution procedure to define the pavement's time-dependent transfer functions. The time-dependent transfer functions were calculated from data measured during full scale tests in a service environment (three pavement cross-sections and three aircraft of different weights and gear configurations were used). Subsequently, a method to predict deflection output responses was developed for use in conjunction with the calculated time-dependent transfer functions.

It was concluded that the characteristics of a flexible pavement could be represented by a series of time-dependent transfer functions obtained from a series of dynamic tests using a common prime mover. It was also concluded that the time-dependent transfer



functions contained certain isolated descriptors which were related to the aircraft gear configurations, and other descriptors which were only indicative of the pavement's behavior. In addition, agreement was achieved between the calculated and measured time-dependent deflection functions resultant from employing the procedures in the proposed performance evaluation method.



Pavement evaluation techniques commonly employed in practice follow two approaches. The more common method (empirical approach) is to base the evaluation on noted changes of certain material descriptors of the pavement system; e.g., changes in strength as measured by CBR tests. An evaluation is then made by correlating the measured descriptor or descriptors with similar data obtained from previous experience on a similar structure in a similar geographic locale. These procedures consider only a few material descriptors, and offer great difficulty in extrapolating to greater magnitudes, or different types of loadings in new environments.

Another approach used to evaluate pavement system requires the theoretical postulation of an analytical model, or combinations of models, followed by field and/or laboratory tests to determine the system parameters. This approach does provide a mechanism for extrapolating to greater magnitudes of loadings, and, in general, is capable of incorporating a greater number of material descriptors; however, the degree of complexity associated with a theoretical approach is proportional to the number of material descriptors contained in the selected model. A shortcoming of this technique is measured by the degree to which the preselected model actually represents the real system.

A new approach to the pavement evaluation problem is advanced by this investigation. The objective of this approach is to overcome some of the shortcomings of the two discussed above. In this method it is hypothesized that time-dependent functions can be calculated from a pavement's input and output deflection responses; that these

functions (transfer functions) can be obtained, in a mathematical sense, without the need to simulate respective material performance to determine values for preselected descriptors; and that these time-dependent functions can be employed to predict deflection output responses when the pavement is subjected to most imposed loads.

REVIEW OF LITERATURE

The more common empirical method of design and/or evaluation of a pavement system emerged nearly a century ago in the form of rule-of-thumb procedures. Around the turn of the century prototype test roads were used to determine the pavement needs to accomodate given traffic; then, between World Wars I and II highway engineers introduced the classification of soils to correlate performance with subgrade types. During World War II, however, a new problem surfaced. Engineers were faced with the need to predict the performance of pavement systems for greater wheel loads and frequencies than they had ever before experienced (references 2 and 3). The urgency for better design techniques led to consideration of available theoretical developments; thus, a rational design procedure was introduced (reference 4). Since that time many investigators have attempted to model various pavement components and systems in their search to be better able to design and/or to evaluate a pavement.

The discussion of literature which follows places primary emphasis on solutions derived from the classical theories of elasticity and viscoelasticity. The nature of applied loads (i.e., static and dynamic) is treated separately. Lastly, some developed uses of the so-called mechanistic models are explored.

Elastic Solutions

The application of analytical models to pavement systems has evolved over the years principally through the use of the theory of

elasticity. Common to the approaches to stress analysis problems using the theory of elasticity are the assumptions that the medium is homogeneous and isotropic, and that its material properties can be defined by linear elastic relationships.

Static Loading

In the latter part of the 19th century, J. Boussinesq developed the stresses and deflections within a semi-infinite mass under a concentrated vertical force by applying the theory of elasticity. Beginning in 1926, Westergaard (references 5, 6, 7, and 8) modeled a pavement as a flexible, elastic beam supported by a subgrade consisting of isolated elastic springs (Winkler foundation). A later refinement was introduced by Hogg (reference 9) who used a flexible, elastic plate on a semi-infinite foundation to model a pavement system. Harr and Leonards (reference 10) first employed the model of a partially supported slab. Their analysis included provisions for predicting stresses and deflections produced by moisture and temperature gradients within concrete slabs in addition to the stresses and deflections induced by some superimposed vehicular loadings. Numerous investigators (references 11, 12, 13, 14, and 15) have presented variations to refine Westergaard's model.

In 1943, Burmister (reference 16) extended the Boussinesq solution to layered systems. His models (reference 17) proved to predict deflections better than the earlier Boussinesq model. Subsequently, the theory of elasticity has been invoked to provide a multitude of models which consider additional layers and variable thicknesses with

consequent multiplication of more material parameters (references 18, 19, 20, 21, and 22).

Dynamic Loading

Elastic solutions for steady-state dynamic loadings have received considerable attention during the past twenty years. In 1951, Van der Poel (reference 23) measured velocities of elastic waves on the surface of soils and roads. Later, in 1954, Pickett (reference 24) provided a theoretical explanation for the propagation of waves on the surface of a concrete slab. Only in the past decade, however, has emphasis been placed on the so-called surface wave technique. The procedure involves measuring the wavelength and velocity of waves at the surface of the pavement under test. The more recent theoretical developments, advanced by Jones (reference 25) and Jones and Thrower (reference 26), explain the propagation of waves in a multilayered pavement structure in terms of the elastic properties and thicknesses of the composite layers. In 1967, practical applications of the surface wave method were provided by Jones, Thrower, and Gatfield (reference 27). Good correlation between estimates of thickness and strength of in-situ pavement sections were obtained using this method. Current attention is being focused toward refinement of this technique (reference 27).

Elastic-Viscoelastic Solutions

Recent studies (references 28, 29, 30, 31, 32, 34, 35, 36, and 37) have incorporated time-dependent attributes to a portion of a pavement system by using either a viscoelastic model to represent a pavement

layer over a Winkler foundation, or an elastic* pavement layer over a viscoelastic foundation. These investigations (for both static and dynamic loadings), like those using purely elastic methods, assume component materials to be homogeneous and isotropic.

Static Loading

Freudenthal and Lorsch (reference 28) analyzed an infinite, elastic beam on three different types of linear viscoelastic foundations under various loadings. Reissner (reference 29) provided the solution for a model consisting of a plate resting on a viscoelastic foundation and incorporated shear interactions between the plate and foundation interface. Hoskin and Lee (reference 30) showed that for some special but important cases the time-dependent problem could be reduced to an elastic model with the same geometry as the parent problem ("correspondence principle", after Lee (reference 31)). Pister and Williams (reference 32) modified Reissner's (reference 29) concept to obtain the continuity of horizontal displacements at the interface between an elastic plate and a viscoelastic foundation; i.e., in addition to permitting horizontal shearing stresses at the plate/foundation interface, the horizontal displacements were also preserved (not taken equal to zero). Here, also the elastic plate equation was coupled with the viscoelastic modeling of the foundation through the use of the correspondence principle. A Voigt (spring and dashpot in parallel) model was employed to represent the foundation behavior.

*Here and in subsequent uses the term "elastic" is understood to plead as assuming the assumptions of the classical "theory of elasticity".

Pister and Monismith (reference 33) used a 3-element viscoelastic model to represent an asphalt concrete beam supported on a Winkler foundation. The viscoelastic solution was obtained from the classical solution of an elastic beam on a Winkler foundation through the use of the correspondence principle. Monismith and Secor (reference 34) later employed a 4-element viscoelastic model to represent an asphalt concrete layer supported on a Winkler foundation. In contrast to the earlier work of Pister and Monismith (reference 34), an additional free-dashpot was added to the model to account for irrecoverable viscous flow. The correspondence principle was again invoked to solve the problem, and laboratory tests were conducted which demonstrated that the model could provide a reasonable approximation of the properties of the asphaltic concrete material.

Barksdale and Leonards (reference 35) investigated long term effects due to repeated loads by applying the correspondence principle to the solution of a multilayer elastic model. A series of Kelvin (spring and dashpot in parallel) elements with both short term and long term creep compliance characteristics were used to obtain an operational modulus for the elastic equations. Predictions of immediate deflection and rutting of asphalt pavements at the AASHO Road Test compared favorably with the measured data.

Dynamic Loading

In 1962, Pister and Westman (reference 36) introduced a quasi-static approximation of a moving load for the static load, elastic-viscoelastic model presented earlier by Pister and Monismith (reference

33). Many aspects of their results were found to be in good qualitative agreement with field pavement performance; e.g., maximum deflections varied with the velocity of load, viscoelastic profiles were not symmetrical as in the elastic case, and deflections preceding the load were found to be less than those that followed.

Harr and Lewis (reference 37) developed a theory whereby stresses and deflections could be calculated for a series of rectangular slabs lying on a viscoelastic foundation and subjected to a moving load. Inertia forces and partial support consequent to linear temperature variations within the slab were also taken into account. This investigation revealed that, contrary to prevailing beliefs, an increase in velocity of load could produce an increase in deflection and stress.

Viscoelastic Solutions

A number of investigators have modeled pavement systems as being entirely viscoelastic. These approaches normally consider inertia forces in contrast to the aforementioned elastic and elastic-viscoelastic solutions (with the exception of Harr and Lewis (reference 37)). The foundation for these studies was provided by Biot (reference 38) in 1955 when he introduced new principles for the formulation of dynamic problems in viscoelasticity for the most general case of anisotropy. Biot's approaches were based on a variational principle derived from irreversible thermodynamics and the correspondence principle.

Static Loading

Pister (reference 39) presented the solution of a viscoelastic plate on a viscoelastic foundation, wherein the effect of transverse shear deformations were accounted for within the plate. Viscoelastic material properties were included in both the plate and the foundation; however, inertia forces were neglected.

Dynamic Loading

Harr (reference 40) used a simple Voigt element to show the influence of vehicle speed on pavement deflection. The analytical results compared favorably with AASHO Road Test data secured at Ottawa, Illinois (reference 41). Perloff and Moavenzadeh (reference 42) presented an analysis for the deflection due to a point load moving across the surface of a semi-infinite, homogeneous, linear viscoelastic medium. A Kelvin model was used to characterize the material; inertia forces were neglected. Recently, Szendrie and Freeme (reference 43), in conjunction with vibration tests, modeled a pavement system using seven system parameters derived from a series of springs, dashpots, and layered mass representations.

Viscoelastic models have been employed recently in conjunction with the load-deflection stiffness method (references 44, 45, 46, and 47). In this method the dynamic input is in the form of a steady-state vibratory load, and the ratio of the applied load magnitude to the measured deflection is termed the dynamic stiffness of a pavement structure.

Mechanistic Solutions

Each successive investigation appears to add insight into the action of pavement systems; however, none of the models thus far presented are able to represent field situations with sufficient predicative capability to satisfy either existing or contemplated needs. For example, in the classical theory of elasticity, the requirements of equilibrium and the definitions of strain (and the compatibility relations), even at a point, provide less equations than the unknowns contained within them. Hence, additional assumptions are required to provide a tractable system. Additional independent relations are generally introduced at a point by inferring certain mechanistic properties to the materials -- commonly referred to as "constitutive relations". In elastic theory the "constitutive relations" are assumed to relate stresses and strains in a linear, homogeneous manner; i.e., by generalizing Hooke's law. The action of real materials under field conditions indicate that the true relationship between stresses and strains are neither linear nor homogeneous and depend greatly on time, temperature, and previous history.

The present investigation offers an alternate approach, which is based on the observed input and output responses of real materials under actual field conditions. This method incorporates a far greater degree of versatility to the description of component materials, while at the same time, it introduces a global concept to the response of these materials to loading (in lieu of the point concept and subsequent assumption of homogeneity and isotropy required in the case of the

classical theories).

The approach has its basis in three earlier investigations: Busching, Goetz, and Harr (reference 48), concerning the mechanistic description of a deformable, transversely anisotropic bituminous mixture; Lal, Goetz, and Harr (reference 49), obtaining properties of sheet-asphalt mixtures under conditions of plain strain; and Swami, Goetz, and Harr (reference 50), predicting behavior of bituminous mix under a variety of conditions including temperature differentials. As a result of the latter study, it was concluded that the viscoelastic, or time-dependent, characteristics of an asphalt concrete could be represented by a time dependent expression called a "transfer function"; that the transfer function was unique for the sample of the material at a given temperature; and that the parameters inherent in the transfer function were better indicators of the material characteristics than previously employed models (such as, Young's Modulus, Poisson's ratio, etc.).

Transfer Function Concept

By definition, a transfer function is the ratio of an operational output (expressed as the Laplace transform of the output) to an operational input (Laplace transform of the input) of a time-dependent system (references 51, 52, and 53). If a system is subjected to a dynamic input, $I(t)$, and evidences a resulting output, $O(t)$, then mathematically, the transfer function is depicted as

$$\bar{G}(s) = \frac{\bar{O}(s)}{\bar{I}(s)} \quad (1)$$

where,

$\bar{G}(s)$ = transfer function,

$\bar{I}(s)$ = Laplace transform of input function, $I(t)$, and

$\bar{O}(s)$ = Laplace transform of output function, $O(t)$.

Note that the transfer function is the ratio of two Laplace transforms, and hence is a function of the complex variable, "s" (references 54 and 55).

"A Priori" Modeling

Use of the classical (elasticity and viscoelasticity) theories normally use "a priori" modeling; i.e. a model is employed to simulate the response of the system to loading, as depicted in Figure 1. Inputs of interest are induced in the model after material and system parameters are identified and predictions are made of the behavior of the system. Since the model is chosen "a priori", the number of system parameters are predetermined. Inherent in this approach is the existence of specifically designed laboratory and/or field tests to evaluate the necessary parameters. Comparisons with "real world" behavior indicates the degree to which success is achieved.

"A Posteriori" Modeling

When "a posteriori" modeling inputs are set forth, consequent outputs are measured and the two are related in a purely mathematical way (transfer functions) without regard to simulating anticipated effects. Hence, there is neither the preselection of system parameters nor a modeling in the "simulation world" (see Figure 2). In contrast



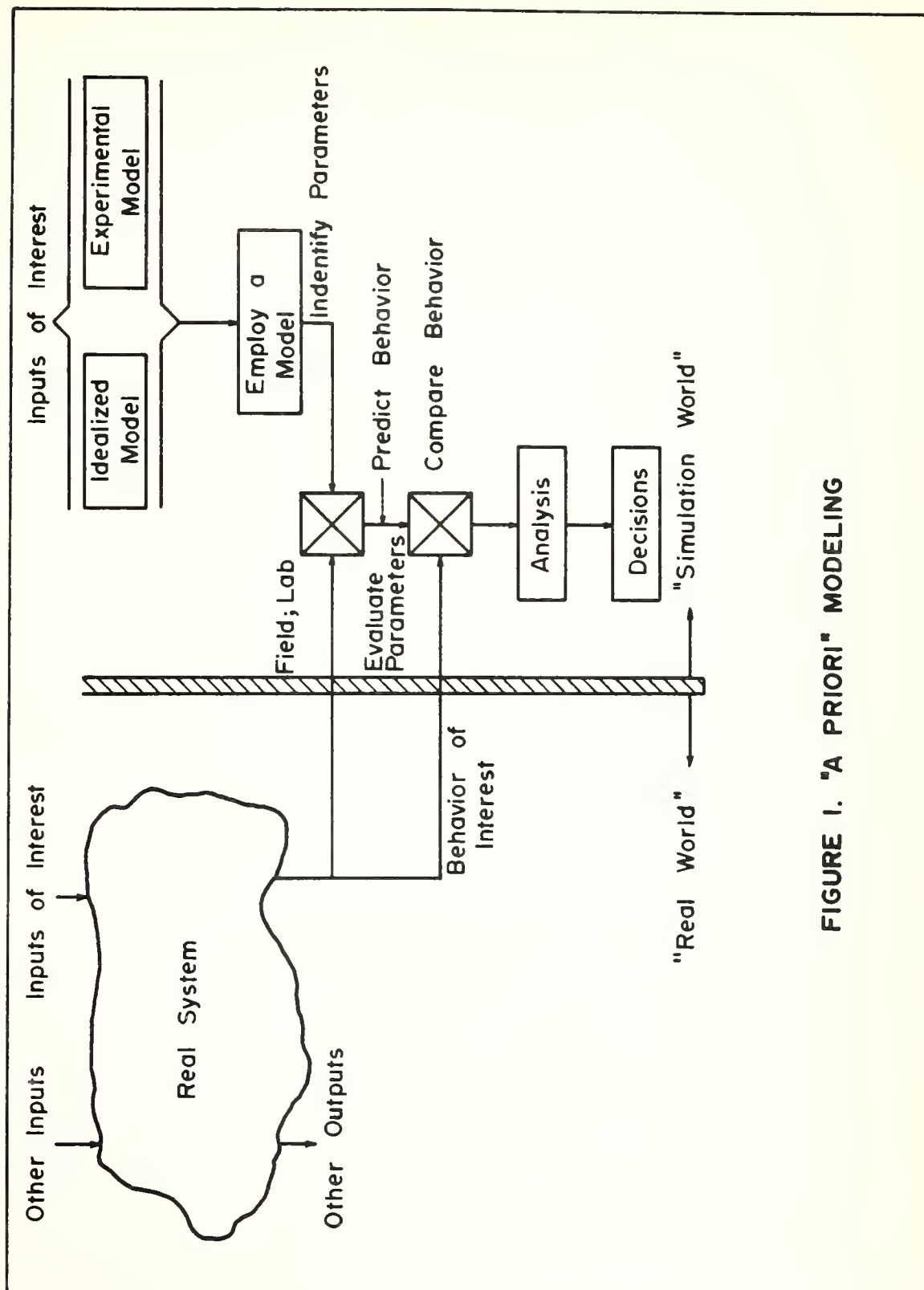


FIGURE 1. "A PRIORI" MODELING

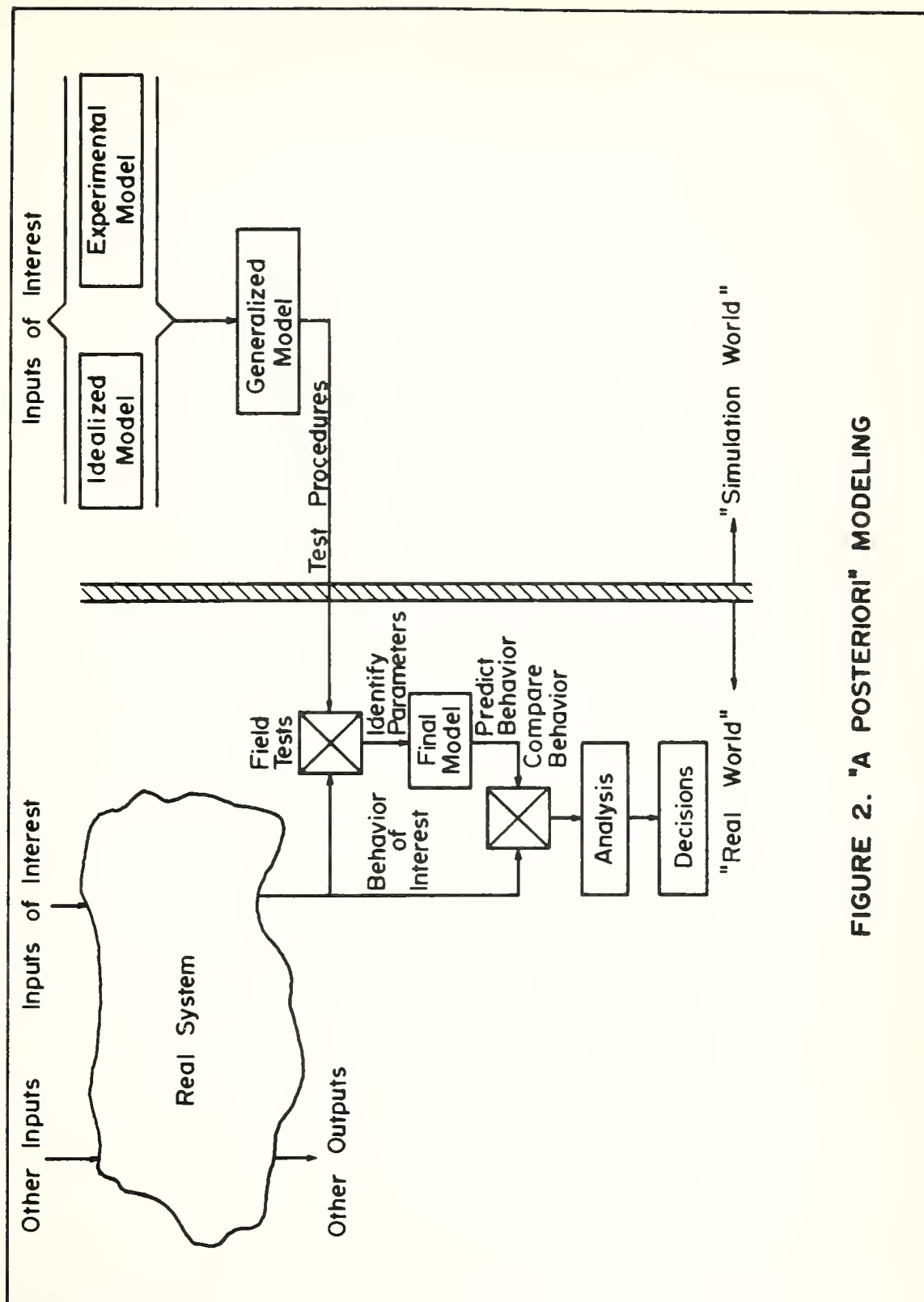


FIGURE 2. "A POSTERIORI" MODELING

to "a priori" modeling, the technique involves the desired use of the real world system itself.

Determining Transfer Functions

Transfer functions for predicting system behavior can be obtained by either "a priori" or "a posteriori" modeling techniques. In the case of "a priori" modeling, generally, a mechanical system is hypothesized and a mathematical expression is obtained relating the transfer of input to output. An example of how the transfer function is obtained using "a priori" modeling is given in Appendix A (reference 56).

In "a posteriori" modeling, several methods can be used to determine a transfer function. One method is to approximate the transfer function from input and output data obtained from field tests (viz., by analyzing the frequency spectrum of the measured inputs and outputs) as proposed by Tsein (reference 53) and Crafton (reference 51) for certain types of input and output data from laboratory tests. Swami (reference 57) obtained the transfer function of asphaltic concrete specimens in the absence of any prior knowledge of their dynamic properties by using input and output data in the manner indicated above. The transfer functions, thus obtained, define an "a posteriori" type experimental model. A second way to determine the transfer function for a system is to find the output of the system due to an unit impulse, or Dirac Delta function input. In this case the measured output provides directly the transfer function. A third method for finding a system's transfer function is to implicitly invoke

the process of real convolution (to input and output data) in the time domain, and subsequently, if desired, to invert the function to a complex domain. Appendix A presents some details of each of the above methods for finding a system's transfer function.



FORMULATION OF A TESTING PROGRAM

Figure 3 represents an aircraft moving on a pavement system. Figure 4a depicts a detail of this figure which provides a series of three dimensional plots of time-dependent deflection responses (along a line normal to the direction of aircraft movement). A time-dependent deflection response function represents the vertical movement at a point on the surface of pavement system as a "prime mover" passes in the vicinity of the point. The deflection response may be a measure of the surface movement in terms of an acceleration, a velocity, or a displacement. In the present work only displacement responses shall be considered in further developments.

Formulation of Pavement Transfer Functions

The "signature" of a prime mover is the vertical response at some convenient point on a pavement's surface (defined at $x = x_0 = 0$) corresponding to the input of a prime mover's tires. In this regard the prime mover can be thought of as providing a "quasi input force" equivalent to the lumped prime mover input (e.g., truck duals, aircraft gear, single tire, etc.). In subsequent developments, the signature is taken to be the time-dependent input function to the pavement system.

The time-dependent deflection response at $x = x_1$ represents a time-dependent output function at that point corresponding to the signature input function at $x = x_0$. Similarly the response at $x = x_2$ represents the time-dependent output function at the point $x = x_2$ due

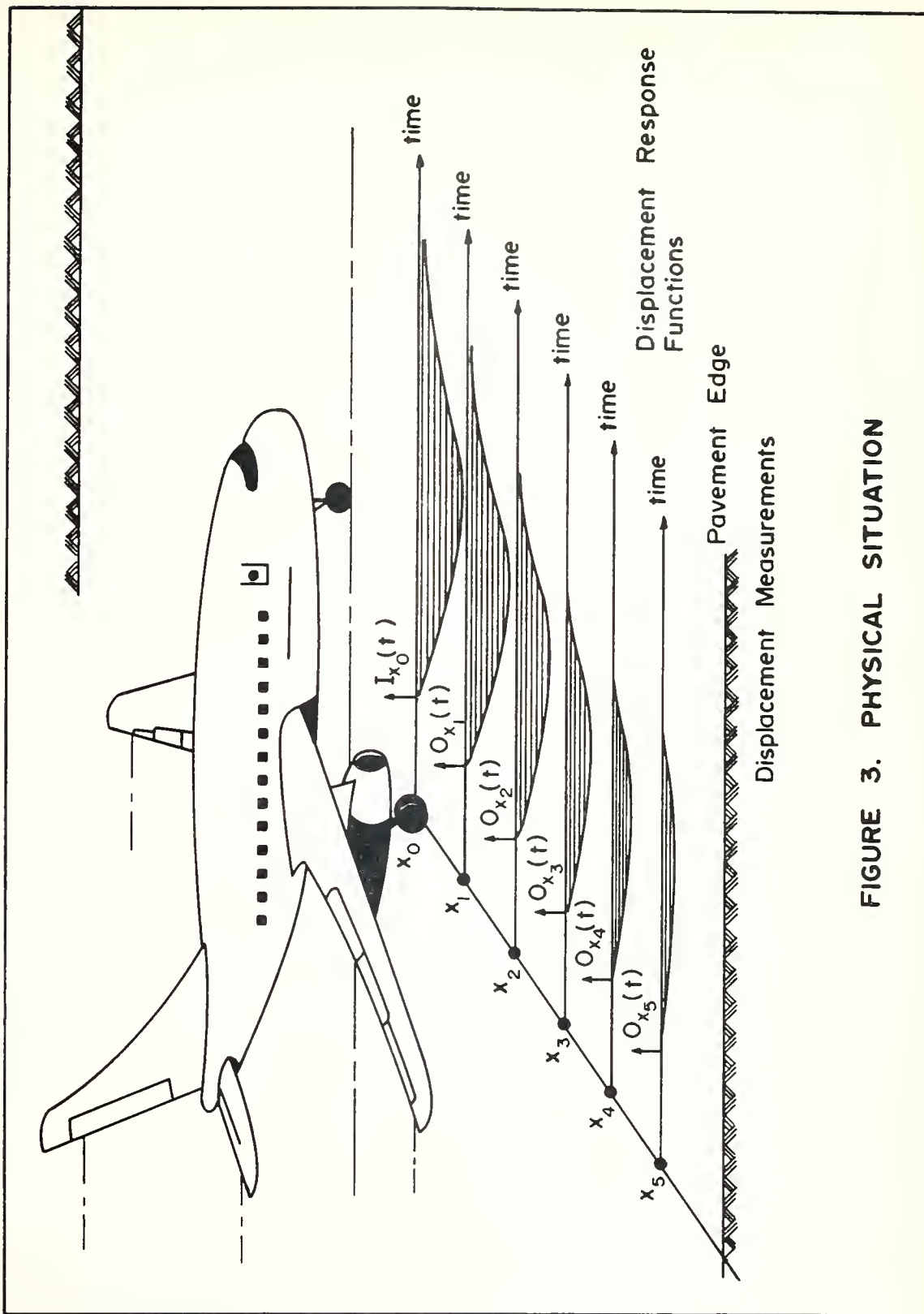


FIGURE 3. PHYSICAL SITUATION



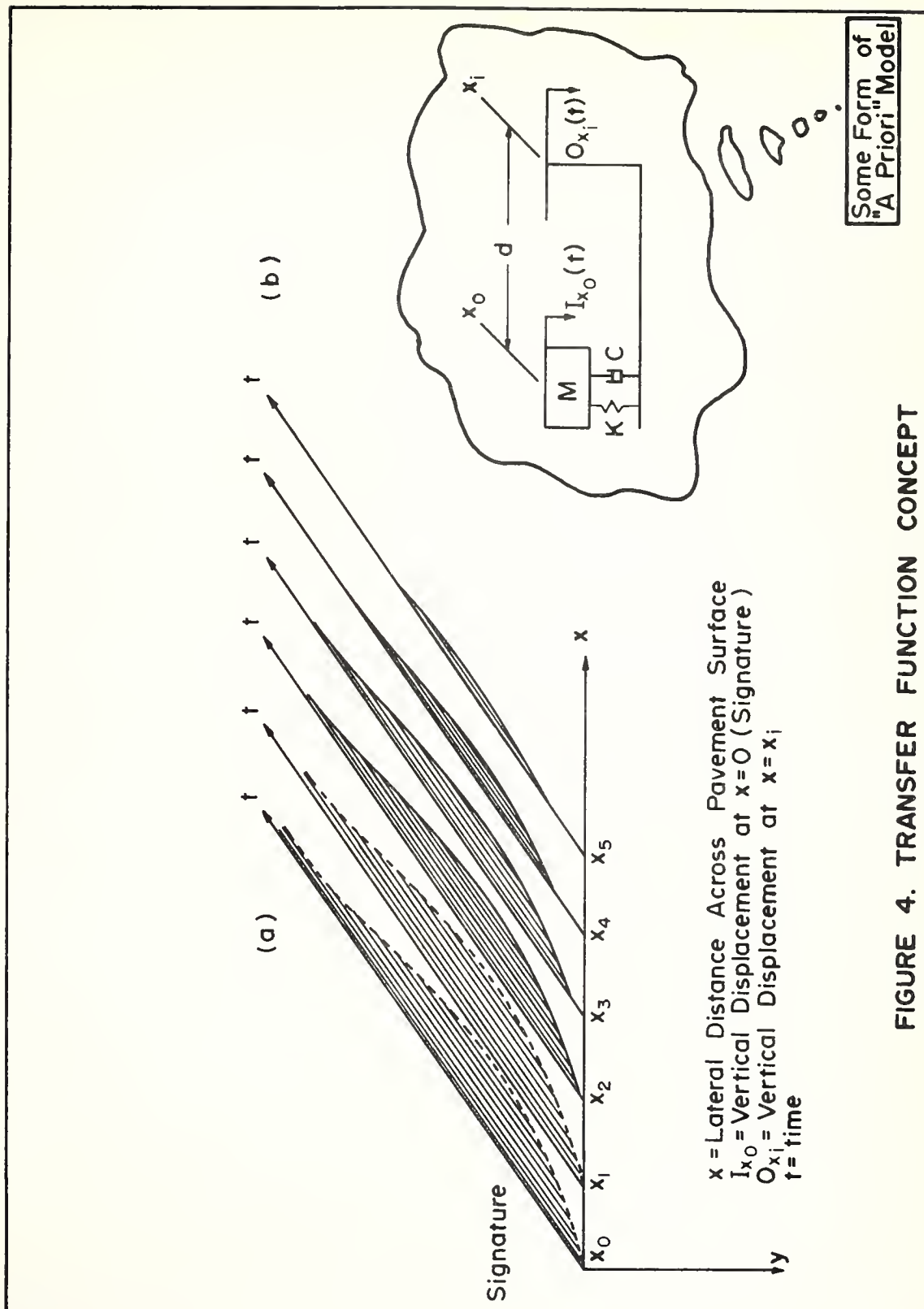


FIGURE 4. TRANSFER FUNCTION CONCEPT



to the signature at $x = x_0$, etc. In essence, each successive time-dependent deflection function is defined to be a time-dependent output function of the signature at the corresponding points, $x = x_1$, $x = x_2, \dots, x = x_i$, respectively.

In general, following equation (1), the transfer function at a point on the pavement at $x = x_i$ due to the signature at $x = x_0$ can be written as

$$\bar{G}_{x_i}(s) = \frac{\bar{O}_{x_i}(s)}{\bar{I}_{x_0}(s)} \quad (2)$$

where,

$\bar{I}_{x_0}(s)$ = Laplace transform of the signature at $x = x_0$ (an input response),

$\bar{O}_{x_i}(s)$ = Laplace transform of an output response function at $x = x_i$, and

$\bar{G}_{x_i}(s)$ = the transfer function between the operational signature at $x = x_0$ and an operational output response function at $x = x_i$.

The transfer function is seen here to be expressed as deflection response functions at two different points due to a quasi input force at $x = x_0$. An examination of equation (2) also shows that to be meaningful the transfer function must reflect pertinent material parameters which characterize the pavement system between points $x = x_0$ and $x = x_i$. Hence, in philosophy, the transfer function provides a "body concept" to the pavement in contrast to the "point concept" inherent in "a priori" modeling by classical (elasticity and viscoelasticity) theories.



In summary, the signature reflects both the input of the prime mover and the consequent feedback of the pavement system. The time-dependent transfer functions are seen to act as filters which attenuate the available energy of the signature. As such, they must contain component parameters of the pavement which, in turn, indicate the performance of the system.

An "A Priori" Model Technique

The simple theoretical spring-dashpot model depicted in Figure 4b will be used to further illustrate the concept of a transfer function for an "a priori" system. The differential equation of motion for this particular model may be written as (references 53 and 57).

$$\ddot{O}_{x_i}(t) + \frac{c}{m} \dot{O}_{x_i}(t) + \frac{k}{m} O_{x_i}(t) = \frac{c}{m} \dot{I}_{x_o}(t) + \frac{k}{m} I_{x_o}(t) \quad (3)$$

Taking the Laplace transform of both sides of equation (3) and rearranging,

$$\bar{G}_{x_i}(s) = \frac{\bar{O}_{x_i}(s)}{\bar{I}_{x_o}(s)} = \frac{\frac{c}{m}s + \frac{k}{m}}{s^2 + \frac{c}{m}s + \frac{k}{m}} \quad (4)$$

or,

$$\bar{G}_{x_i}(s) = \frac{2\omega a s + \omega^2}{s^2 + 2\omega a s + \omega^2} \quad (5)$$

where,

$$\omega = \sqrt{\frac{k}{m}}$$

and

$$a = \frac{c}{2m\omega}$$

The inverse Laplace transform produces the time-dependent transfer function for the theoretical, "a priori" model as

$$G_{x_i}(t) = \frac{\omega}{\sqrt{1-a^2}} \cdot e^{-a\omega t} [2a \sin(\omega\sqrt{1-a^2}t + \phi) + \sin(\omega\sqrt{1-a^2}t)] \quad (6)$$

and

$$\tan \phi = \frac{\sqrt{1-a^2}}{a} \quad (7)$$

A characteristic plot of $G_{x_i}(t)$ versus t (for $a < 1$) is shown in Figure 5.

"A Posteriori" Modeling Techniques

In the early stages of this research, it was thought that a low frequency vibrator could excite a pavement system sufficiently to provide the transfer function from a frequency spectrum analysis. To investigate this possibility, a testing program was undertaken at the Civil Engineering Research Facility, Kirtland Air Force Base, New Mexico, using a low frequency vibrator. The vibrator was capable of inducing a constant force between 50 and 1500 pounds over a frequency range of approximately 15 to 50 cycles per second. The output responses were measured with Columbia Model 1107-4 accelerometers. A typical set of data with amplitude of surface motion plotted versus frequency of input force is depicted in Figure 6. Figure 7 represents calculated responses for a theoretical second order viscoelastic model. A comparison of the two plots led to the conclusion that the vibrator used in the tests at Kirtland Air Force Base contained frequencies less than that of the natural frequency of

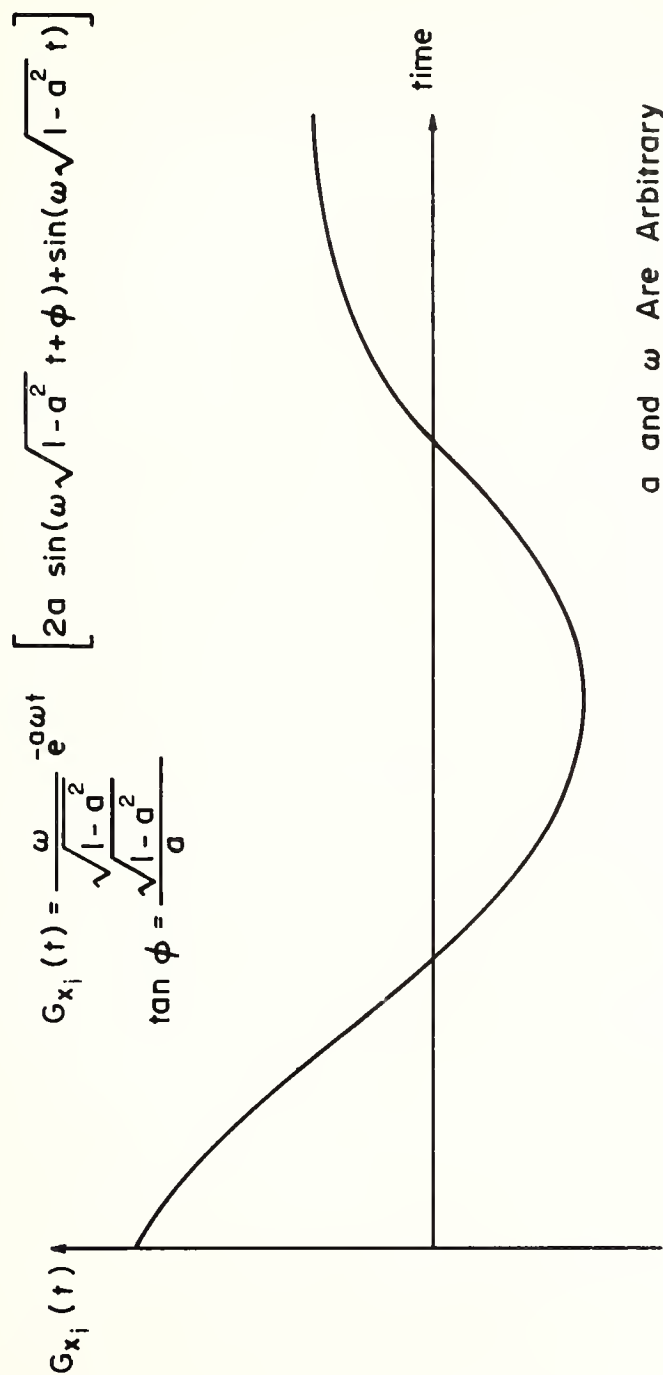


FIGURE 5. TIME-DEPENDENT TRANSFER FUNCTION FOR "A PRIORI" MODEL.

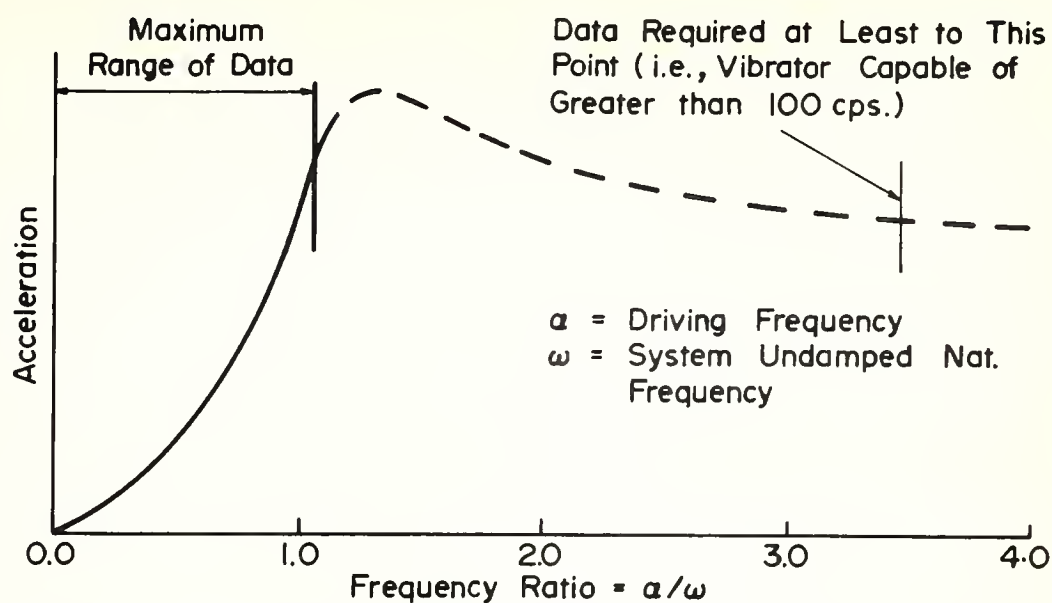


FIGURE 6. FREQUENCY SPECTRUM PLOT FOR VIBRATOR DATA

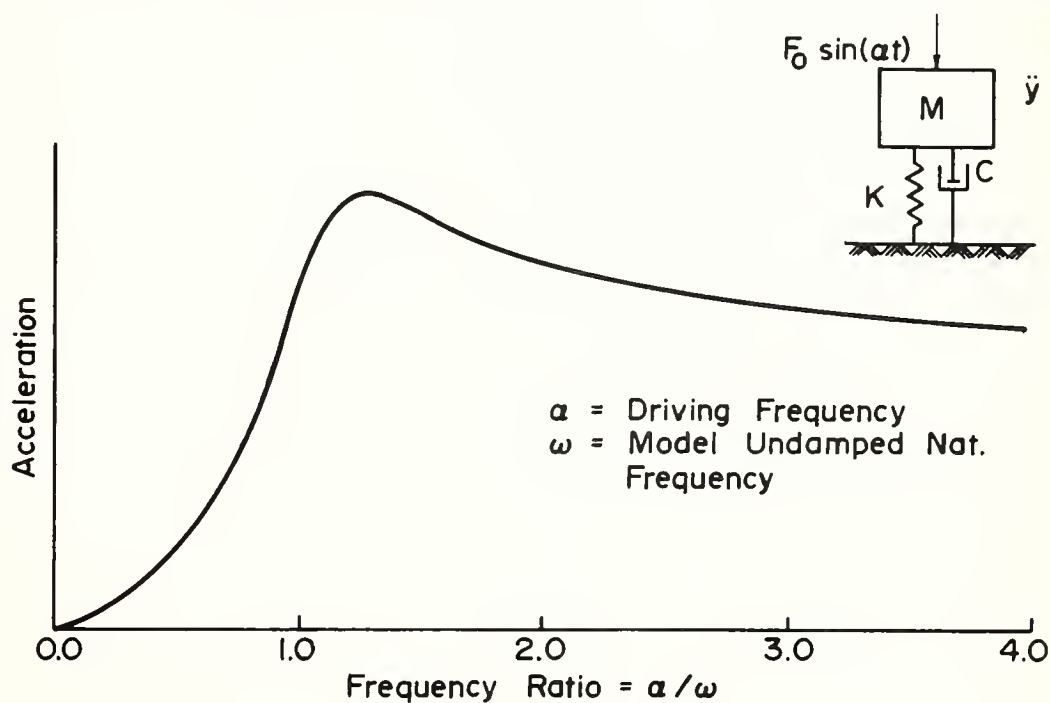


FIGURE 7. FREQUENCY SPECTRUM PLOT FOR SIMPLE MODEL

the pavement system tested. To determine the transfer functions for a system from its frequency spectrum, it is necessary to excite the system to frequencies three to four times that of its natural frequency; that is, it is necessary to reach magnitudes of frequency which display a constant slope at the upper bound of the frequency spectrum curve for the system. This observation coupled with the lead time and cost required to design and fabricate an adequate vibrator negated the frequency spectrum technique.

Attention was then directed to the "a posteriori" impulse input method (see Appendix A). Unfortunately, this method also necessitated new and expensive equipment; hence, it was also deemed unfeasible.

Finally, the "a posteriori" real convolution technique (see Appendix A) was explored. This technique provides a time domain solution which permits the deflection responses to be used directly in calculating a time domain transfer function. The method also eliminates the need to obtain Laplace transforms and inverse transforms.

Beginning with the definition of a transfer function for the physical situation as given in equation (2), it follows that

$$\bar{O}_{x_i}(s) = \bar{G}_{x_i}(s) \cdot \bar{I}_{x_o}(s) \quad (8)$$

As equation (8) is seen to represent the product of two Laplace transforms, $O_{x_i}(t)$ is said to be the "real convolution of $G_{x_i}(t)$ and $I_{x_o}(t)$ ". Invoking the real convolution theorem (references 54, 58, and 59) equation (8) can be expressed as

$$O_{x_i}(t) = \int_0^t G_{x_i}(\tau) \cdot I_{x_o}(t-\tau) d\tau \quad (9)$$

An implicit solution of equation (9) was devised to yield $G_{x_i}(t)$, termed the inverse transform of the transfer function, or the time domain transfer (TDT) function, hereinafter referred to as a TDT function. Equation (9) was discretized to facilitate numerical solutions by a computer. The integral was solved implicitly for $G_{x_i}(t)$, provided $O_{x_i}(t)$ and $I_{x_o}(t)$ were available, say, as arrays of numerical values. Conversely, an explicit solution was obtained for $O_{x_i}(t)$, when $G_{x_i}(t)$ and $I_{x_o}(t)$ were known. Recursion formulas used to develop computer subroutines for the implicit and explicit solutions of the real convolution integral are provided as equations (10) and (11).

Implicit convolution--

$$G_{x_i}(k) = \frac{O_{x_i}(k) - \sum_{j=1}^{k-1} G_{x_i}(j) \cdot I_{x_o}(k-j+1) \cdot \Delta t_{x_i}}{I_{x_o}(1) \cdot \Delta t_{x_i}} \quad (10)$$

Explicit convolution--

$$O_{x_i}(k) = \sum_{j=1}^k G_{x_i}(j) \cdot I_{x_o}(k-j+1) \cdot \Delta t_{x_i} \quad (11)$$

Accelerations and/or velocities could be used to determine the TDT functions, although displacements have been indicated here. For example, if the output responses are given as the accelerations of a pavement systems surface,

$$\bar{G}_{x_i}(s) = \frac{s^2 \bar{O}_{x_i}(s)}{s^2 \bar{I}_{x_o}(s)} = \frac{\bar{O}_{x_i}(s)}{\bar{I}_{x_o}(s)} \quad (12)$$

Signature and TDT Functions

Equation (10) establishes the TDT function once a pavement's response functions are known at two points. To obtain the requisite response functions, the time history of the vertical motion of a pavement's surface is required at specific locations adjacent to the vehicle's path. The actual location of a prime mover's signature is arbitrary; however, once selected, its position must be fixed relative to the gages used to measure the deflection responses. This is necessary because a TDT function serves as a filtering mechanism to transform a signature at one point into a deflection response at an adjacent point; therefore, the distance over which a TDT function is calculated must remain constant.

It was not considered feasible to confine the path of a prime mover to a precise location relative to the installed gages; so, a method was developed to accomodate the shifting of the response function measurements. The technique employed to accomplish the minor spatial adjustments for the deflection response functions is predicated on the assumption that the peak dynamic deflection basin attenuates according to a normal distribution curve. The spatial adjustments were considered to be small compared to the extent of the dynamic deflection basin, so that any error in the modeling process would thereby be minimized. This was later found to be the case. The correction necessary to shift

a response function must, in essence, scale the response function spatially; yet, it must also retain its shape. This was accomplished by forming a scaling factor defined as

$$c_{x_i+\lambda, x_i} = O_{x_i+\lambda}(\text{peak}) / O_{x_i}(\text{peak}) \quad (13)$$

where,

λ = Offset distance of input (i.e., distance between the actual point where a prime mover's signature is applied and a defined signature input point on the pavement relative to the gages),

$O_{x_i+\lambda}(\text{peak})$ = The peak value of the deflection response function at a point located at $x = x_i + \lambda$ from the defined signature input point,

$i = 0, 1, 2, \dots, i$ ($i = 0$ represents the signature),

and,

$$O_{x_i}(\text{peak}) = A \cdot e^{-B(.0417 x_i)^2} \quad (14)$$

or,

$$O_{x_i+\lambda}(\text{peak}) = A \cdot e^{-B(.0417(x_i+\lambda))^2} \quad (15)$$

The A and B parameters associated with the normal distribution model are obtained by a regression analysis on peak deflection values. Figure 8 shows a 2-dimensional representation of how the method is employed. For example, consider that a prime mover passes the gages at a distance $x = \lambda$ to the left of the first gage. The peak dynamic deflections are fitted to a normal distribution model; the factors,

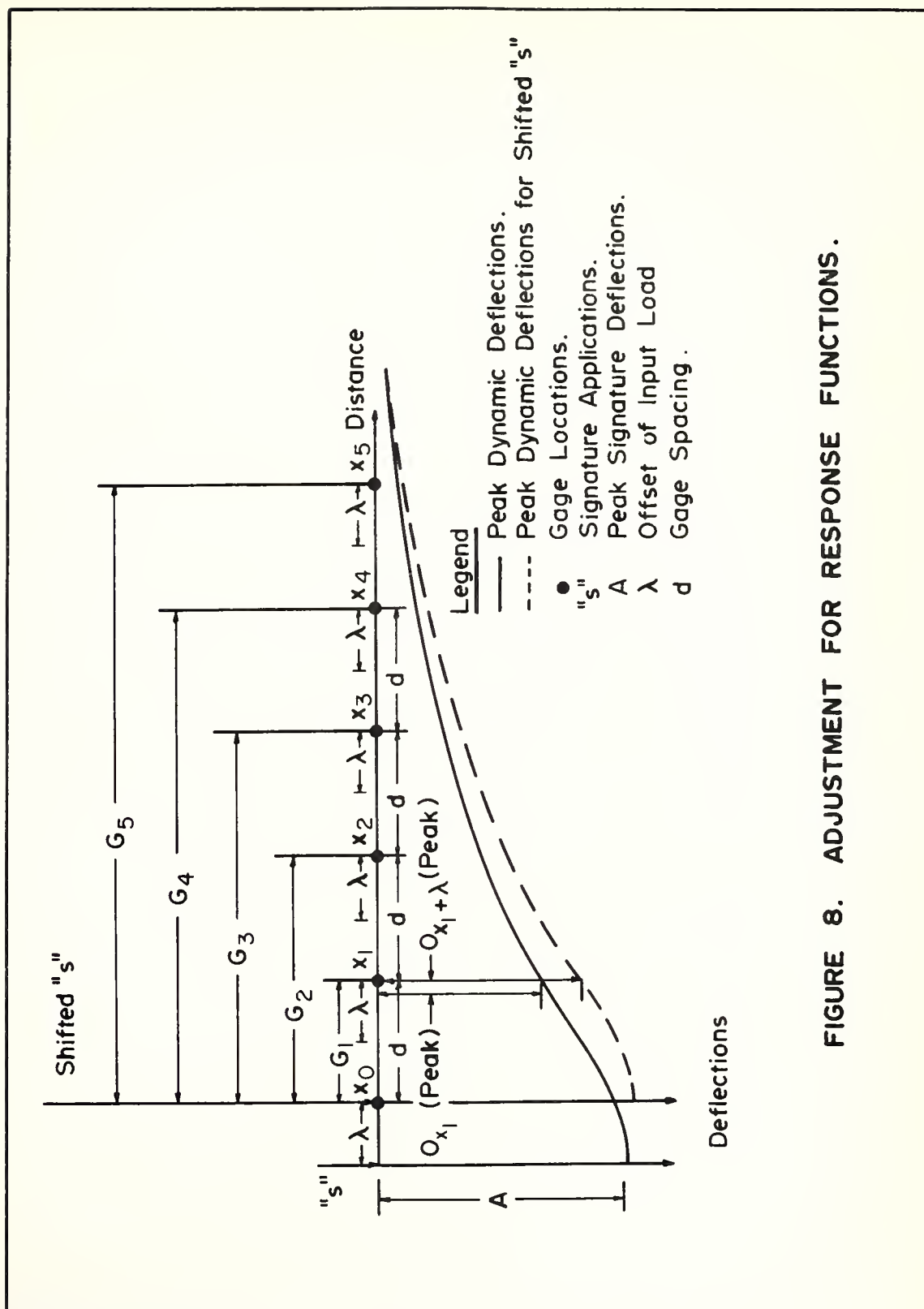


FIGURE 8. ADJUSTMENT FOR RESPONSE FUNCTIONS.

${}^c x_0 + \lambda, x_0, \dots, {}^c x_i + \lambda, x_i$, are computed; and the correction process is employed.

The testing program had as an objective the identification of the individual tests necessary to validate the hypothesis for this investigation. The hypothesis, as initially set forth, stated that TDT functions could be calculated from a pavement's input and output deflection responses; and that these TDT functions could be obtained, in a mathematical sense, without the need to simulate respective material performance to determine values for preselected descriptors.

In summary, the deflection response functions at $x = x_i$ ($i = 0, 1, 2, \dots, i$) relative to a signature applied at $x = x_0$, as transferred from $x = x_0 + \lambda$, are given when the measured deflection responses are multiplied by the factors defined from equation (13). Then, equation (10) is invoked to determine the pavement's TDT functions. Once deflection response functions are measured, the pavement's respective prime mover's signature and TDT functions may be determined as follows:

- (1) Fit peak dynamic deflections to a normal distribution model - least squares fit of equation (14).
- (2) Determine signature and deflection responses with respect to a common origin - apply correction factor defined by equation (13).
- (3) Calculate TDT functions - apply technique defined by equation (10).

A listing of computer code NMLFIT for accomplishing item (1) is provided in Appendix B. Appendix C provides a listing of computer

code CONVLI which contains maneuvers for items (2) and (3).

Predicting Performance

As a secondary feature, and dependent on being able to calculate a pavement's TDT functions, it was further hypothesized that these functions could be employed to predict output deflection response functions when the pavement was subject to any imposed load. In the previous section, the procedures for ascertaining a prime mover's signature and a pavement's TDT functions were outlined. Once sufficient catalogues of the signatures and TDT functions of different prime movers and pavement systems are obtained, estimates can be had of combinations of vehicles and pavements for which tests were not conducted. For example, with a cataloged signature and, say, TDT functions obtained from a particular vehicle, a third computer code CONVLE (see Appendix D for a listing) may be invoked to calculate deflection response functions at the x_i points. Figure 9 summarizes a complete procedure for predicting a pavement's performance when subjected to a particular prime mover. The procedure outlines the combinations of catalogued signatures and TDT functions necessary to perform these predictions.

Referring to Figure 9, two arbitrary pavements are shown: pavement A on the left is the pavement for which signatures of both prime movers #1 and #2 have been previously cataloged (the pavement's TDT functions are also known); and pavement B on the right is the pavement whose deflection response functions for prime mover #2 are desired. Since the deflection response functions are desired for

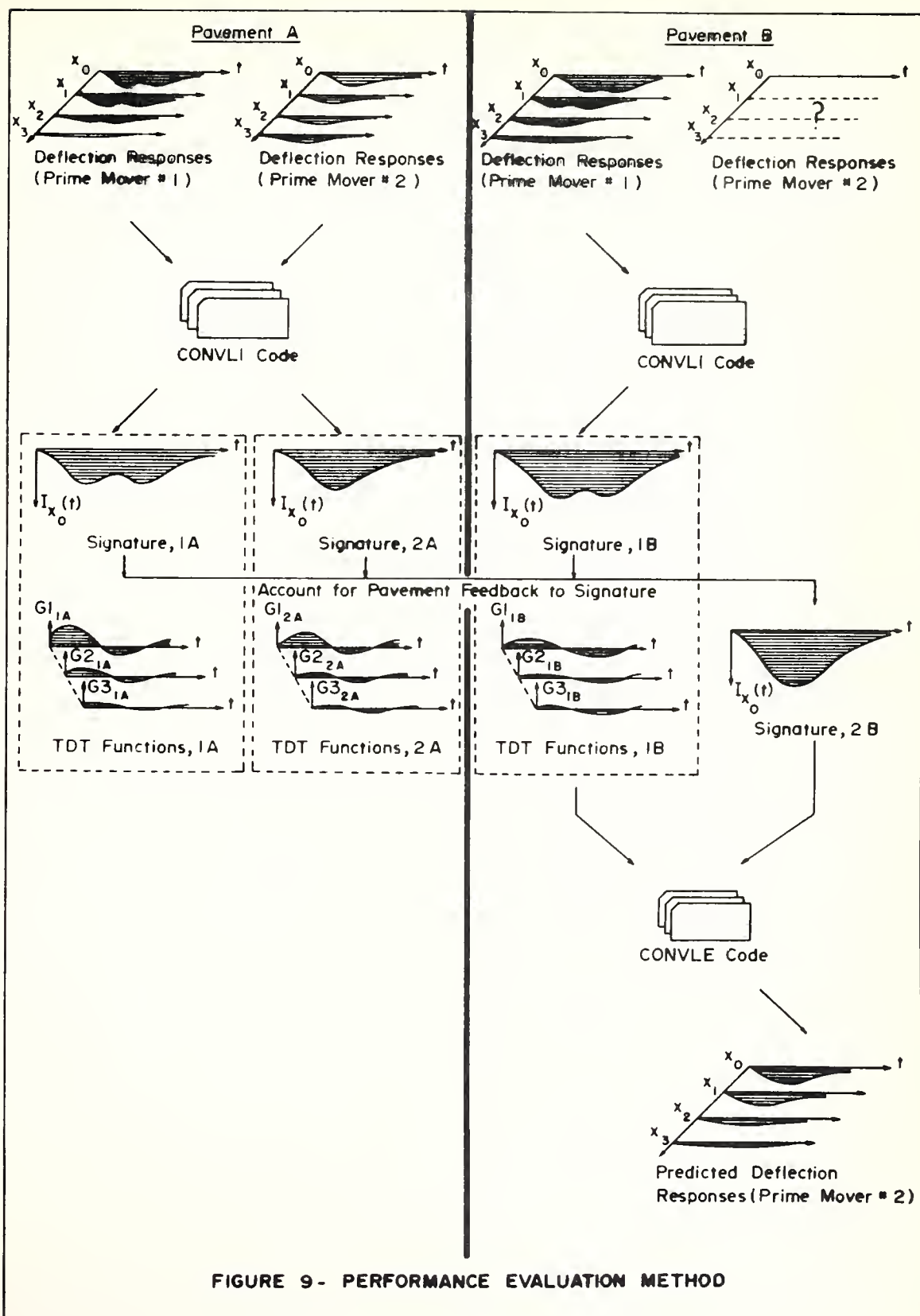


FIGURE 9 - PERFORMANCE EVALUATION METHOD

prime mover #2, prime mover #1 shall be termed a "standard" vehicle to illustrate the prediction method. As a first step, consider the standard vehicle (prime mover #1) on pavement B. Deflection response functions are measured, and the vehicle's signature and the pavements TDT functions are calculated using computer code CONVLI. The next step accounts for the pavement's feedback to the signature. In the early part of this investigation, it was assumed that the deflection magnitudes of a particular prime mover's signatures on different pavements could be treated linearly. This was later found to be the case. Therefore, by using the three known signatures, it follows that the fourth signature for prime mover #2 on pavement B may be expressed as

$$I_{x_{o2B}}(t) = \frac{I_{x_{o1B}}(\text{peak})}{I_{x_{o1A}}(\text{peak})} \cdot I_{x_{o2A}}(t) \quad (16)$$

Lastly, the fourth signature, equation (16), and the pavement B TDT functions, from the first step, are used in computer code CONVLE to calculate the corresponding deflection response functions for prime mover #2 on pavement B. Thus, the desired performance predictions are achieved.

The deflection response functions provide the true deflection basin for any instant of time desired. In addition, the deflection basin is not predicated on use of predetermined parameters as is done in the "a priori" modeling approaches. Inherent in the TDT functions are the numerous pavement "properties"; yet, none have to be evaluated directly in order to assess the pavement's performance.

FIELD INVESTIGATION

The field investigation phase of this study had as its objective the development and use of techniques for obtaining all the data required to determine a pavement's TDT functions by the convolution method. The main feature of the technique was to devise a system which could accurately measure the time-dependent deflection response functions of a pavement when subjected to a prime mover's dynamic load input.

Exploratory field tests were conducted to ascertain the criteria needed to design the measuring system. These tests were necessary as the deflection response functions were transient in nature, rather than steady state, and neither the magnitude of deflections nor their time durations were known. Once the information from these tests had been analysed, it was possible to design an adequate measuring system. After fabrication and installation of the measuring components, a full scale field test program was carried out to obtain the data required to validate the performance evaluation method summarized by Figure 9.

Exploratory Tests

Field exploratory tests were conducted on an operational taxiway at Kirtland AFB, New Mexico (Albuquerque International Airport). They had as their primary objective acquisition of data necessary to select a suitable energy sensing device, and to determine locations on the pavement adjacent to a prime mover's path which could adequately define the dynamic deflection basin. Both vertical deflections and

accelerations of the pavement's surface were considered, and a series of tests were conducted using a specially built load cart and a Boeing 727 aircraft (see Appendix E). Appendix E also provides details concerning installation and calibration of the sensing devices employed as well as typical plots of deflection response functions obtained. Table 1 gives a comparison of the test results for each prime mover with respect to the particular sensing device used. Conclusions from the data acquired in these tests indicated that a deflection gage employing a linear variable differential transformer (LVDT) was the device best suited for measuring the time-dependent functions.

The peak magnitudes of the deflection response functions and their relative attenuation with distance from the prime mover's path guided the design of the deflection gages; e.g., they established the required LVDT sensitivity and the gage spacing, respectively.

Field Tests

The prototype field tests were also conducted at Kirtland, AFB, N.M. (Albuquerque International Airport). In contrast to the exploratory tests, however, this testing program was designed to control certain variables which were thought to influence a pavement's TDT functions; e.g., data was only secured when pavement temperatures were between 55°F and 65°F, and the prime mover speeds were controlled to approximately five miles per hour for each data run.

TABLE 1.

COMPARISON OF PEAK PRIME MOVER DEFLECTIONS FOR
EACH SENSING DEVICE USED IN EXPLORATORY TESTS

SENSING DEVICE	TYPE AND MODEL	METHOD OF INSTALLATION @	CHARACTER OF RESPONSE*					REMARKS
			1 Ft	6 Ft	1 Ft	6 Ft	727	
Linear Variable Differential Transformer	Schaevitz Type 500S1	Reference @ 18' depth	None	None	None	None	None	Insensitive
Linear Variable Differential Transformer	Hewlett-Packard Model 24DCDT-100	Reference @ 18' depth	.022"	.004"	.070"	.010"	.010"	Good performance
Linear Variable Differential Transformer	C & E Electronics Model 15-020-DG	Reference @ 18' depth	-	.004"	-	.010"	.020"	range
Accelerometer	Columbia Model 1107-4	Surface mounted	None	None	.35-1.4g	None	None	Accelerations attenuate rapidly
Accelerometer	Columbia Model 306-4	Surface mounted	None	None	None	None	None	Insensitive

*Response refers to peak deflection at noted distance from point of dynamic load input.

Instrumentation

Time-dependent deflection response functions were measured with specially designed deflection gages using LVDT displacement transducers. The overall system was designed to monitor a pavement's vertical movement at six different locations simultaneously; six locations on a line normal to a prime mover's path. Also, since it was necessary to direct the prime movers close to some of the sensing devices, special consideration had to be given to protect these gages from a prime mover's tire; these special gages were placed within the pavement's wearing course, and were labelled type I installations. When provisions were not required to protect the gages, a beam was used to serve as the LVDT mounts. The regular deflection gages were labelled type II installations.

Following from the combination of theory and experience associated with the exploratory tests, deflection gage locations relative to the path of a prime mover were selected as shown in Figure 10 (both type I and type II installations are depicted). Appendix F describes each type gage, installation details, and the method used to calibrate the deflection gages.

The following provisions were incorporated into the overall data acquisition technique:

- (1) The gage outputs were recorded on magnetic tape with an Ampex FR 1300 tape recorder and, in order to ascertain the validity of the data, selected gages were monitored on an oscilloscope at the time of a test run.

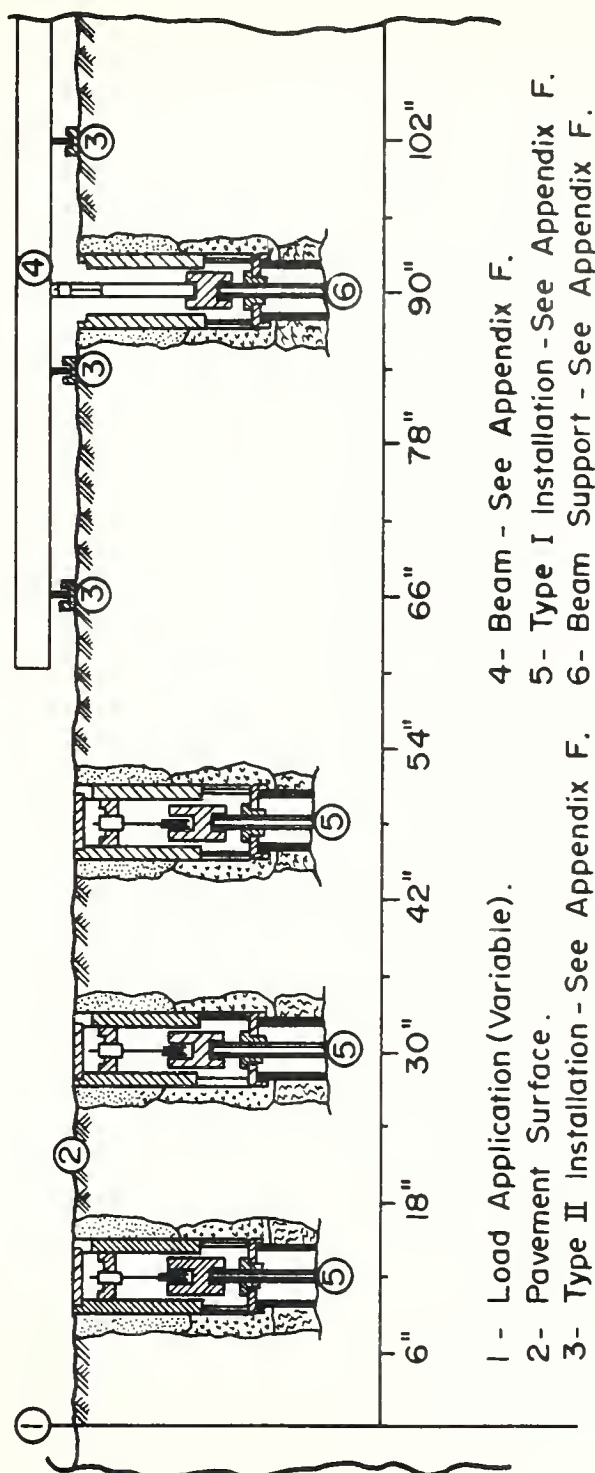


FIGURE 10. SENSING DEVICE SCHEMATIC.

(2) An IRIG time generator (Culton Industries) was used to record a time scale on the magnetic tape. This record was later used to select time intervals for digitizing and analyzing the data.

(3) The temperature of the asphaltic concrete wearing course was monitored with a thermometer embedded approximately one inch into the pavement's surface.

(4) A DC triggering circuit, actuated by pressure switches located 24 feet on each side of the deflection gages, was installed for checking the velocity of the prime mover for each test run. The DC voltage was also recorded on the magnetic tape.

(5) Adhesive tape was applied to the pavement's surface parallel to the line of deflection gages to facilitate a physical measurement of the prime mover tire relative to the first deflection gage. The distance between the location of the first deflection gage and the centroid of the prime mover tire's imprint on the tape provided the offset distance.

Figures 11 through 14 represent the type I and type II installations, respectively. Figure 15 shows the overall instrumentation setup, and Figure 16 is a view of the recording equipment components.

Scope of the Field Tests

The prototype investigations were conducted at three sites (see Figure 17) with pavement cross-sections as shown in Figure 18. Four different prime movers were used at each test site; C135, C131 and C130

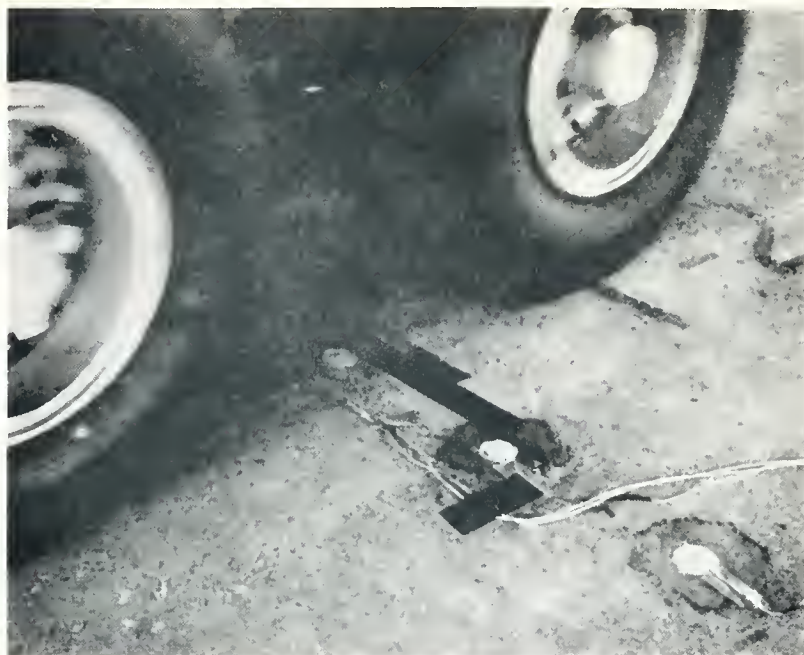


FIGURE 11. TYPE I INSTALLATIONS, DISTANT



FIGURE 12. TYPE I INSTALLATIONS, CLOSE-UP

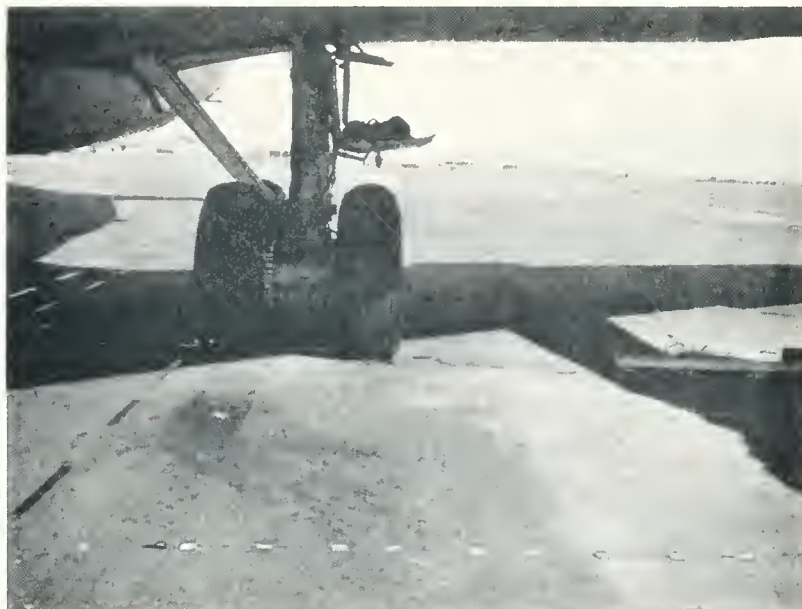


FIGURE 13. TYPE II INSTALLATIONS, DISTANT

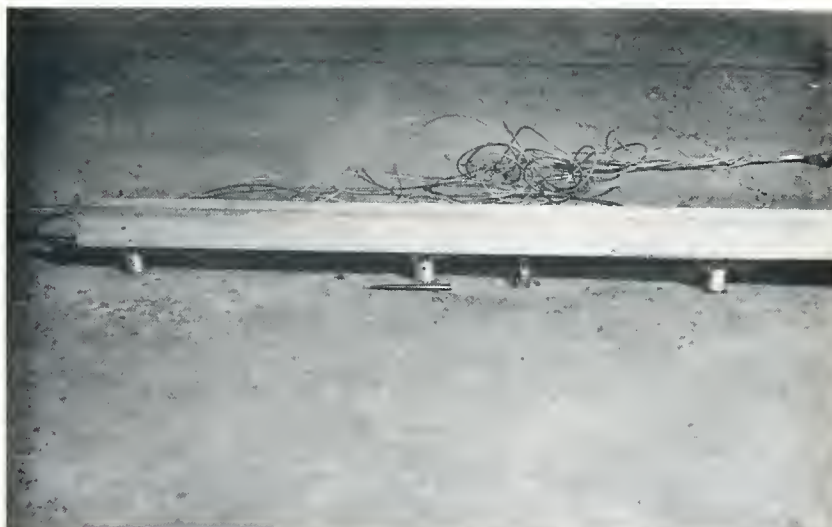


FIGURE 14. TYPE II INSTALLATIONS, CLOSE - UP



FIGURE 15. INSTRUMENTATION SETUP



FIGURE 16. RECORDING EQUIPMENT COMPONENTS

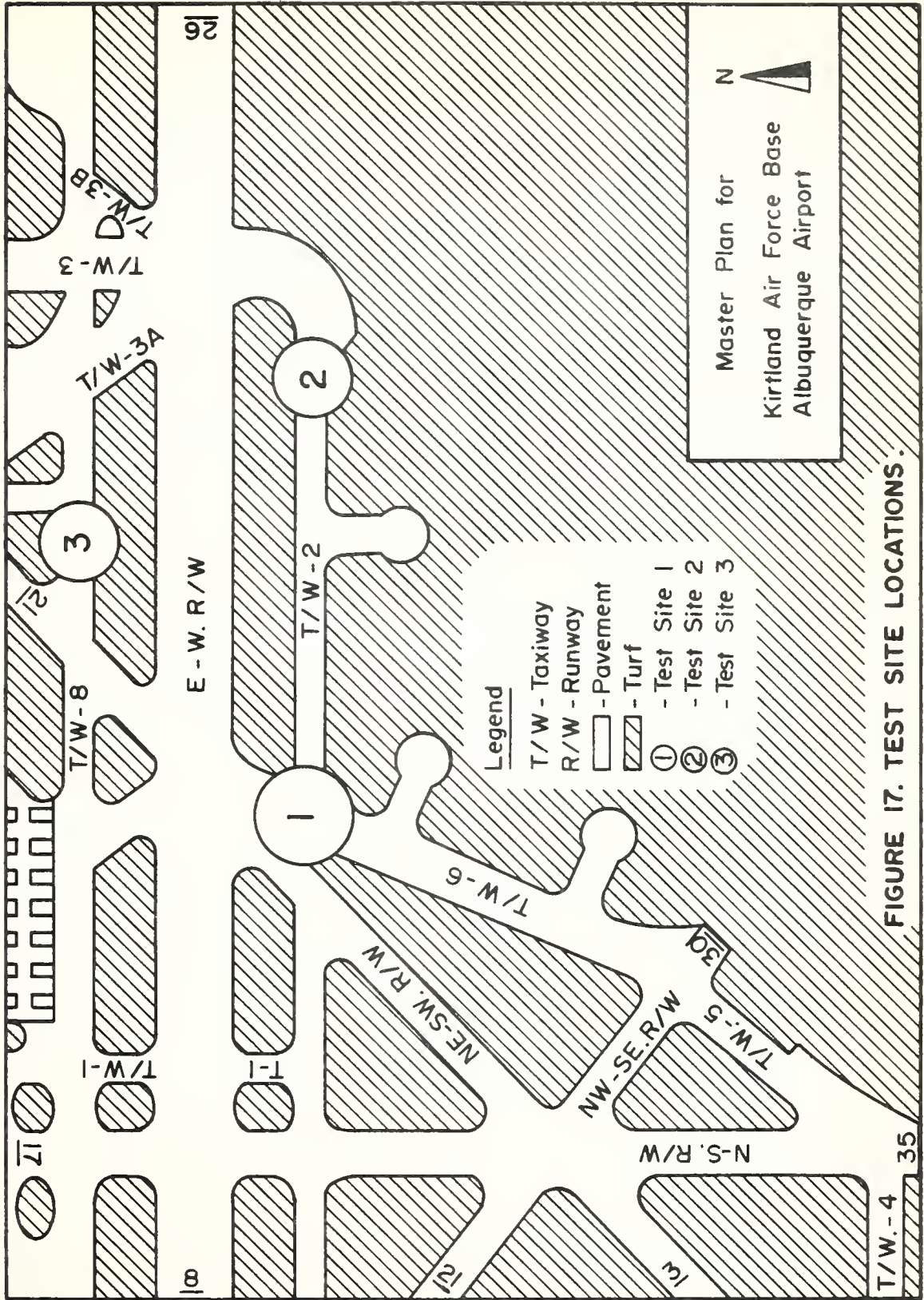
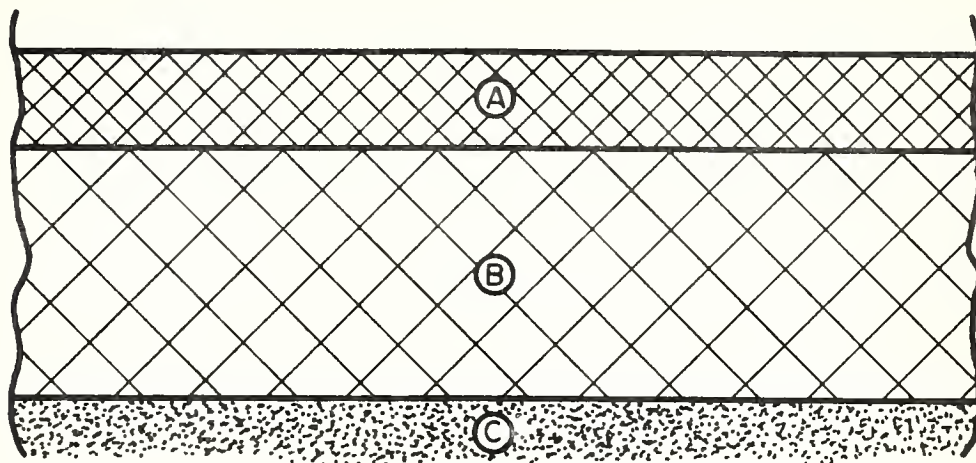


FIGURE 17. TEST SITE LOCATIONS.



Test Site No.	Taxiway No.	(A) Asphalt Concrete	(B) Base Course	(C) Subgrade
1	6	3"	9"	Silt / Sand
2	2	6.5"	8"	Silt / Sand
3	8	10"	6"	Highly Compacted Silt / Sand

FIGURE 18. PAVEMENT CROSS-SECTIONS.

type aircraft, and a load cart. Figures 19 through 22 depict each prime mover, respectively. A minimum of four forward passes of each prime mover was made at each site; the number of passes of the prime movers was limited by two factors -- cost and availability of the prime movers, and the number of passes considered necessary to provide a good definition of the dynamic deflection basin. Table 2 summarizes the physical characteristics of each prime mover. The main wheel and/or gear configurations are illustrated in Figure 23.





FIGURE 19. PRIME MOVER - C 135 AIRCRAFT



FIGURE 20. PRIME MOVER - C 131 AIRCRAFT



FIGURE 21. PRIME MOVER - C 130 AIRCRAFT

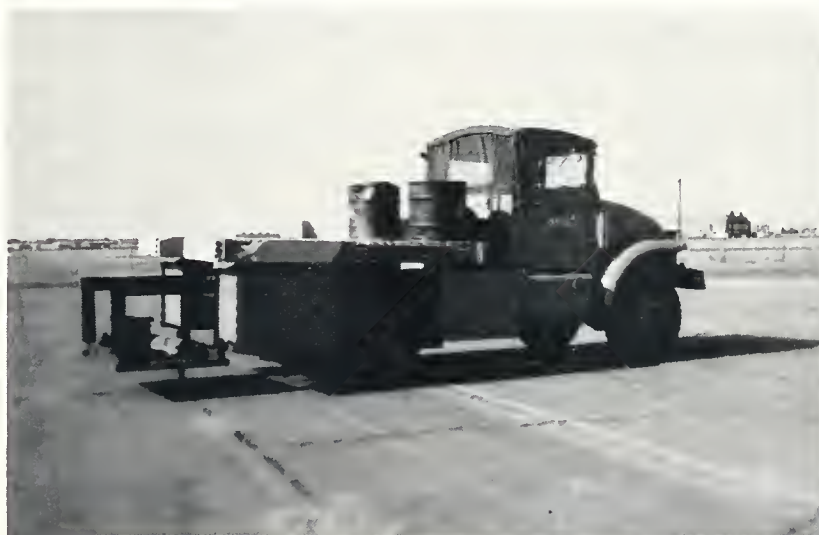


FIGURE 22. PRIME MOVER - LOAD CART

TABLE 2.
PRIME MOVER CHARACTERISTICS^(a)

Prime Mover	Standard Test ^(b) Weight	Tread ^(c)	Wheelbase ^(d)	Wheel Configuration
CL35	210,000 Lbs	265 in.	548 in.	twin-tandem
CL31	40,000 Lbs	300 in.	314 in.	twin
CL30	90,000 Lbs	131 in.	388 in.	single-twin
Load cart	23,000 Lbs	* ^(e)	* ^(e)	single wheel ^(f)

Notes:

- (a) See reference (56) for detailed aircraft characteristics.
- (b) Aircraft weights were variable depending on amount of fuel on-board; standard test weights were selected so that linear adjustments could be applied to deflections for comparison purposes.
- (c) Tread. The center-to-center distance between the main gear tires for single-wheel configurations or between the centroids of the main gear tires for multiple-wheel configurations.
- (d) Wheelbase. The center-to-center distance between the centroid of the main gear and the nose gear.
- (e) Not applicable for load cart.
- (f) Single wheel configuration is indicative for this prime mover because of the way loading is applied.

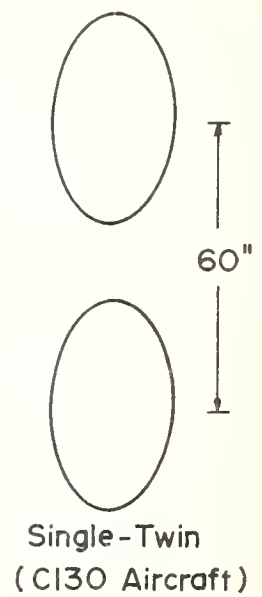
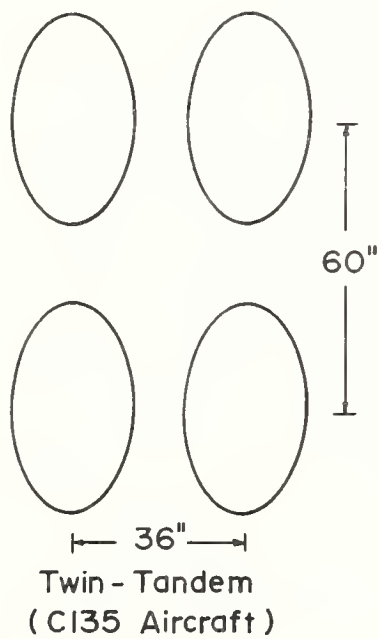
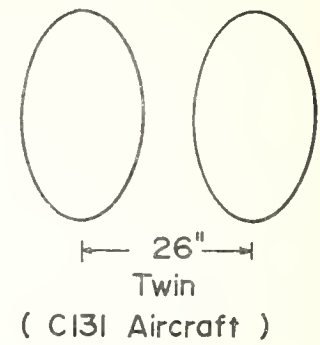
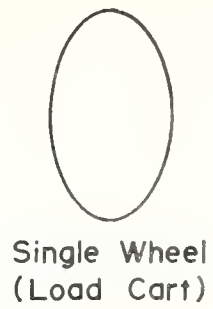


FIGURE 23. PRIME MOVER MAIN GEAR CHARACTERISTICS.

RESULTS OF THE FIELD TESTS

Peak Dynamic Deflection Basin

Peak deflection response values of the dynamic tests for all the prime movers at the three test sites are summarized in Tables 3 through 6. These values were then fitted to a normal distribution model of the form $O_{x_i}(\text{peak}) = A \cdot e^{-B(.0417X_i)^2}$ by conducting a least squares regression analysis. The resulting parameter values and correlation coefficients are provided in Table 7. The A factors were adjusted linearly to an arbitrary standard prime mover weight because the weights of the aircraft varied from site to site depending on the quantity of fuel on-board at the time the tests were conducted. Finally, a ratio factor defined as the ratio of the A factor divided by the largest A factor at each test site was calculated for each prime mover, respectively. The adjusted A factors and the ratio factors as defined above are also provided in Table 7.

The relationship between A factors and the ratio factors are shown in Figure 24; and the range of the B parameters are provided in Figure 25.

Deflection Response Functions

In each of the dynamic tests, deflections were recorded over a one to two minute period starting from the time a prime mover began to accelerate until it had passed beyond the vicinity of the deflection gages. Oscillographs of the recorded data reflected measurable deflections over only an approximate two second period, or whenever

TABLE 3.
PEAK DYNAMIC DEFLECTIONS - C135 AIRCRAFT

RUN	SITE NO. 1			SITE NO. 2			SITE NO. 3		
	Gage	X(IN.)	Y(IN.)	Gage	X(IN.)	Y(IN.)	Gage	X(IN.)	Y(IN.)
1	2L	21.5	.0250	2L	7.0	.0680	3L	17.0	.0240
	3L	39.5	.0020	3L	25.0	.0200	4L	35.0	.0100
	4L	57.5	.0020	4L	43.0	.0080	5H	53.0	.0030
				5H	61.0	.0030			
2	2L	7.5	.0830	2L	10.0	.0500	2L	26.0	.0130
	3L	25.5	.0060	3L	28.0	.0160	3L	44.0	.0040
	4L	43.5	.0040	4L	46.0	.0070	4L	62.0	.0020
	5H	61.5	.0010	5H	64.0	.0030			
3	2L	12.0	.0600	1L	3.5	.0680	2L	4.0	.0400
	3L	30.0	.0040	2L	15.5	.0370	3L	22.0	.0160
	4L	48.0	.0030	3L	33.5	.0100	4L	40.0	.0080
				4L	51.5	.0040	5H	58.0	.0020
4	2L	5.0	.0900	2L	10.0	.0530	2L	10.0	.0350
	3L	23.0	.0090	3L	28.0	.0160	3L	28.0	.0170
	4L	41.0	.0050	4L	46.0	.0070	4L	46.0	.0050
	5H	59.0	.0000	5H	64.0	.0030	5H	64.0	.0010
5	2L	16.5	.0320	2L	1.5	.0800	3L	10.0	.0390
	3L	34.5	.0040	3L	19.5	.0280	4L	28.0	.0190
	4L	52.5	.0020	4L	37.5	.0100	5H	46.0	.0060
				5H	55.5	.0040	6H	64.0	.0020

Notes: (1) Centroid of outside wheel of main gear truck taken as point for signature applications.

(2) Deflections measured at negative x points were not used.

(3) X represents distance from point where signature was applied to a respective gage location; Y is the peak vertical deflection of the pavement's surface at a respective gage location.

TABLE 4.

PEAK DYNAMIC DEFLECTIONS - C131 AIRCRAFT

RUN	SITE NO. 1			SITE NO. 2			SITE NO. 3		
	Gage	X(IN.)	Y(IN.)	Gage	X(IN.)	Y(IN.)	Gage	X(IN.)	Y(IN.)
1	2L	1.5	.0456	2L	9.0	.0176	2L	7.0	.0287
	3L	19.5	.0099	3L	21.0	.0122	3L	25.0	.0103
	4L	37.5	.0016	4L	39.0	.0010	4H	43.0	.0034
	5H	55.5	.0000	5H	57.0	.0008	5H	55.0	.0004
2	3L	14.0	.0231	2L	5.0	.0232	3L	16.0	.0162
	4L	32.0	.0024	3L	23.0	.0078	4H	34.0	.0066
	5H	50.0	.0000	4L	41.0	.0020	5H	70.0	.0010
	2L	0.0	.0470	2L	12.5	.0247	2L	6.5	.0276
3	3L	18.0	.0128	3L	24.5	.0119	3L	23.5	.0114
	4L	36.0	.0016	4L	42.5	.0025	4H	41.5	.0039
	5H	54.0	.0000	5H	60.5	.0013	5H	59.5	.0005
	2L	0.0	.0484	2L	6.0	.0204	2L	14.5	.0194
4	3L	18.0	.0127	3L	24.0	.0050	3L	32.5	.0063
	4L	36.0	.0016	4L	42.0	.0019	4H	50.5	.0021
	5H	54.0	.0000						
	2L	10.0	.0236				3L	20.0	.0125
5	3L	28.0	.0012	3L	6.5	.0212	4H	38.0	.0050
	4L	46.0	.0006	4L	24.5	.0065	5H	56.0	.0007
	5H	64.0	.0000	5H	42.5	.0013			

Notes: (1) Centroid of outside wheel of main gear truck taken as point for signature application.

(2) Deflections measured at negative x points were not used.

TABLE 5.
PEAK DYNAMIC DEFLECTIONS - C130 AIRCRAFT

RUN	SITE NO. 1		SITE NO. 2		SITE NO. 3	
	Gage	X(IN.)	Y(IN.)	Gage	X(IN.)	Y(IN.)
1	2L	13.0	.0560	1L	1.0	.0487
	3L	31.0	.0028	2L	13.0	.0315
	4L	49.0	.0022	3L	31.0	.0061
	5H	67.0	.0005	4L	49.0	.0024
2	2L	13.0	.0525	1L	1.5	.0402
	3L	31.0	.0027	2L	10.5	.0395
	4L	49.0	.0022	3L	28.5	.0093
	5H	67.0	.0005	4L	46.5	.0032
3	3L	18.7	.0174	1L	4.0	.0584
	4L	36.7	.0059	2L	14.0	.0322
	5H	54.7	.0005	3L	16.0	.0139
				4L	32.0	.0104
4	2L	8.0	.0781	2L	7.5	.0449
	3L	26.0	.0057	3L	10.5	.0386
	4L	44.0	.0034	4L	25.5	.0162
	5H	62.0	.0006	5H	43.5	.0035
5	2L	6.5	.0727	2L	8.5	.0483
	3L	24.5	.0039	3L	9.5	.0404
	4L	42.5	.0030	4L	26.5	.0142
	5H	60.5	.0004	5H	27.5	.0109

Notes: (1) Centroid of main gear truck taken as point for signature application.

(2) Gages 2L and 3L became inoperative at Site No. 3 after first run.

TABLE 6.
PEAK DYNAMIC DEFLECTIONS - LOAD CART

RUN	SITE NO. 1		SITE NO. 2		SITE NO. 3	
	Gage	X(IN.)	Y(IN.)	Gage	X(IN.)	Y(IN.)
1	2L	1.0	.0667	2L	3.5	.0413
	3L	19.0	.0336	3L	21.5	.0215
	4H	37.0	.0211	4H	39.5	.0102
	5H	55.0	.0022	5H	57.5	.0048
2	2L	3.5	.0604	2L	1.0	.0418
	3L	21.5	.0300	3L	19.0	.0204
	4H	39.5	.0161	4H	37.0	.0111
	5H	57.5	.0010	5H	59.0	.0043
3	2L	3.5	.0608	2L	5.0	.0404
	3L	21.5	.0304	3L	23.0	.0198
	4H	39.5	.0160	4H	41.0	.0100
	5H	57.5	.0010	5H	59.0	.0043
4	2L	2.5	.0608	2L	0.0	.0408
	3L	20.5	.0309	3L	18.0	.0222
	4H	38.5	.0167	4H	36.0	.0133
	5H	56.5	.0015	5H	54.0	.0055
5	2L	3.5	.0649	2L	6.0	.0368
	3L	21.5	.0295	3L	24.0	.0191
	4H	39.5	.0158	4H	42.0	.0090
	5H	57.5	.0015	5H	60.0	.0039
6	2L	0.5	.0651	2L	2.5	.0418
	3L	18.5	.0342	3L	20.5	.0209
	4H	36.5	.0206	4H	38.5	.0116
	5H	54.5	.0016	5H	56.5	.0047

Notes: (1) Centroid of single load wheel taken as point for signature application.

TABLE 7.

MODEL RESULTS OF PEAK DEFLECTIONS

Prime Mover	Site	Input* Load(Kips)	Peaks Fitted	Weight Factor	A Factor	Adjusted A Factor	Ratio Factor	B Factor	Correlation Coefficient
CL35 ACFT	1	95	17	1.00	0.1010	0.1010	1.00	2.1763	0.9874
CL35 ACFT	2	95	20	1.00	0.0706	0.0706	1.00	1.2006	0.9616
CL35 ACFT	3	72	18	1.32	0.0392	0.0517	1.00	0.6818	0.9538
CL31 ACFT	1	24	19	0.75	0.0463	0.0345	0.34	2.4138	0.9868
CL31 ACFT	2	18	17	1.00	0.0231	0.0231	0.33	1.2292	0.9698
CL31 ACFT	3	28	17	0.64	0.0278	0.0178	0.34	0.8704	0.9683
CL30 ACFT	1	52	19	0.77	0.0950	0.0731	0.73	2.2597	0.9783
CL30 ACFT	2	39	20	1.03	0.0493	0.0508	0.72	1.2097	0.9174
CL30 ACFT	3	40	9	1.00	0.0394	0.0394	0.76	0.4062	0.9806
Load Cart	1	23	24	1.00	0.0607	0.0607	0.60	0.6458	0.9537
Load Cart	2	23	24	1.00	0.0387	0.0387	0.55	0.5731	0.9422
Load Cart	3	23	24	1.00	0.0278	0.0278	0.54	0.3797	0.9097

*Aircraft input loads were variable due to amount of fuel on-board.

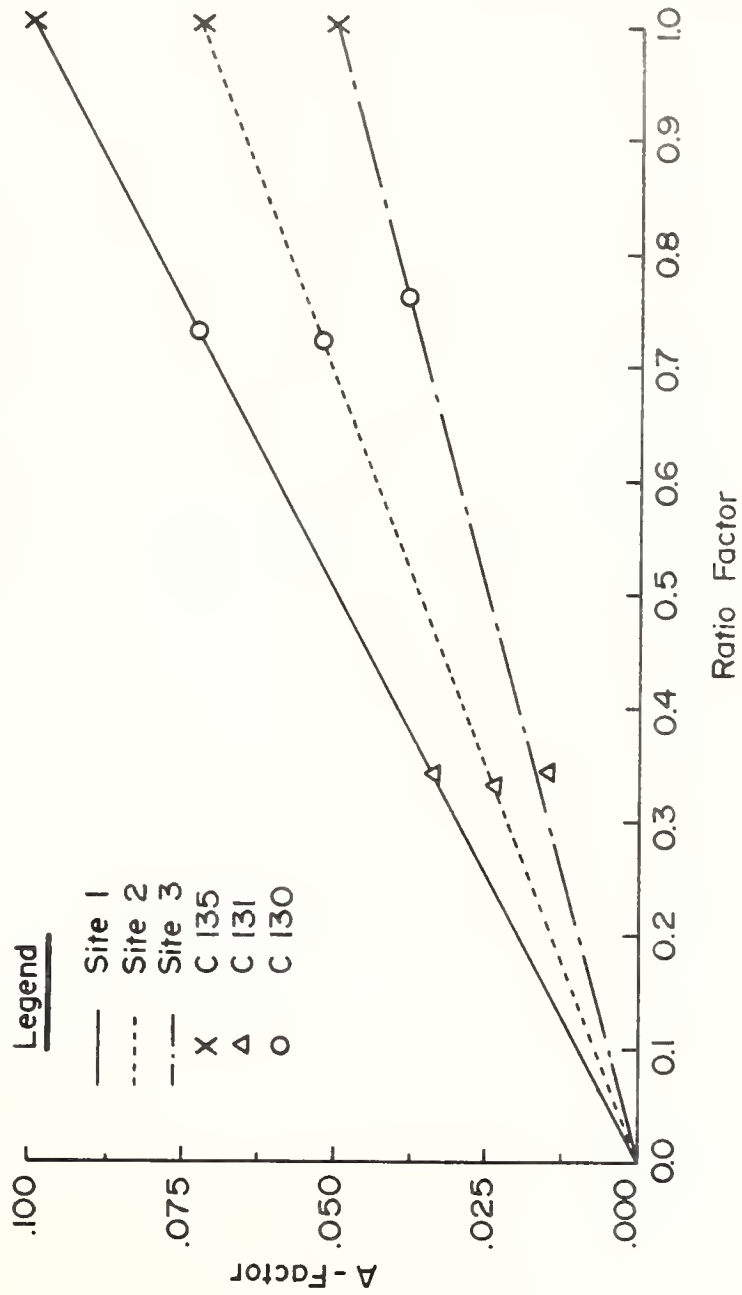


FIGURE 24. RELATIONSHIPS OF A-FACTORS AT EACH TEST SITE

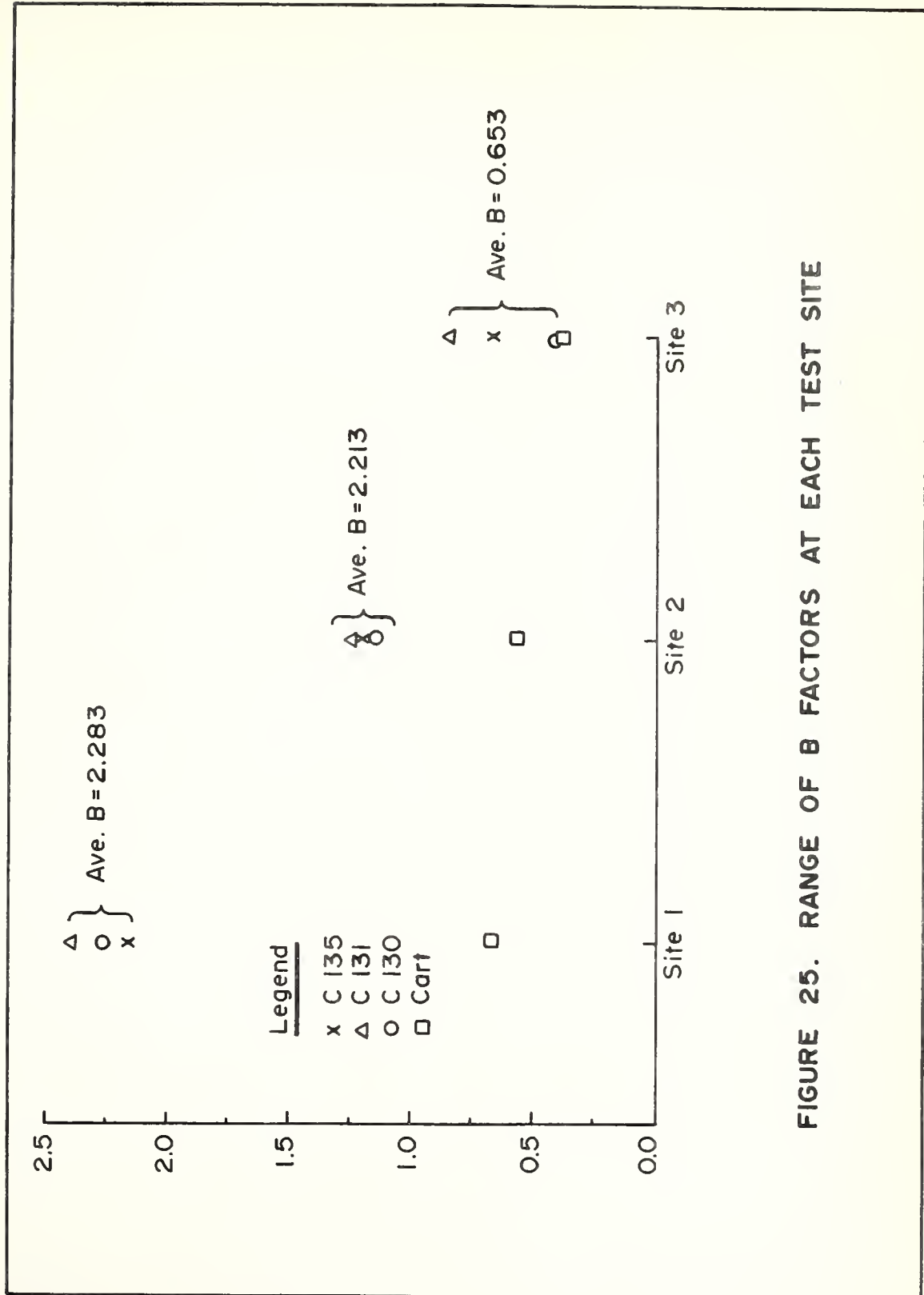


FIGURE 25. RANGE OF B FACTORS AT EACH TEST SITE

the prime mover passed within 14 to 18 feet of the gage locations. The IRIG time signal was used to select a 9.5 second interval over which to convert the gage output voltages to digital units. Prior to ditigitizing, however, the data were filtered electronically to remove any interference having frequencies greater than 100 Hz. A sampling rate of 40 units/second was used in the ditigitizing process, thus, providing 380 discrete values for each deflection response function.

To achieve a common null point for all the data, the first ten discrete values of each deflection response function was averaged and, in turn, this average value was subtracted from each discrete value in the array. This procedure was necessary since it was observed that the null for the respective gages were different. Some of the null values also changed after each test run because of the pavement's viscoelastic behavior. The null for the gages close to the point of signature application changed most, whereas, it changed very little for gages at adjacent locations. In the extreme case, it was noted that the null could change by as much as ten percent of the peak dynamic deflection for a gage located at a point where the signature was applied.

The data contained in the deflection response function arrays were truncated to reduce the computer time required to calculate TDT functions and to predict the desired deflection functions. This procedure follows from using the 9.5 second interval over which to ditigitize the recorded data. An approximate two second interval would have been large enough had sufficient experience been obtained

with the digitizing process. Therefore, it was decided to truncate the deflection response function arrays containing 380 discrete values to retain only the significant data. The truncation was accomplished by deleting all initial values in a signature array which were smaller than .002 inch. Subsequently, the number of discrete values between the first array value that was retained and the peak array value was counted. The length of the array was then established as three times this counted number. After the length of the array was established in this manner, the latter array values (which were of no particular significance) were deleted. The interval of the signature array containing only the significant values was taken as the common interval over which to retain the discrete values for successive deflection response functions that were adjacent to the point where the signature was defined.

Linear interpolation between successive discrete values of the response functions was then employed so that a common time base of 1.84 seconds containing 47 discrete values could be achieved. The reason for providing a common time base was twofold: (1) to standardize the number of discrete values for the calculated TDT functions; and (2) to account for fluctuations in prime mover velocities.

Lastly, the deflection response function arrays were shifted with respect to their respective offset distance as defined in Figure 8. The scaling factors given by equation (13) were multiplied by the deflection array values for each set of test data. This shift would not have been necessary had the deflection functions been

measured relative to the prime mover instead of at fixed locations on the pavement.

Computer code CONVLI (Appendix C) has been provided with all the instructions required to accomplish the procedures outlined above. Figures 26 through 34 show plots of the deflection response functions after these procedures were applied. It is to be noted that the ordinate scales are variable in these plots, and because a number of data runs were available for each prime mover at each test site, the plots represent an average of the measured data. Appendix G contains computer sheets listing the discretized data, printed out to six decimal places.

TDT Functions

The denominator in equation (10) is always equal to the product of the first discrete signature array value times the discretized time interval; i.e., $I_{x_0}(1) \cdot \Delta t$. It was found necessary to substitute a value larger in magnitude for $I_{x_0}(1)$ in order to obtain convergence for the implicit convolution process. This substitution was accomplished with the understanding that a reciprocal value would have to be used to obtain the suitable inverse when using the explicit convolution technique defined by equation (11). A value of ten times the peak signature deflection was chosen to replace the initial signature array value. In essence, this substitution provided a value for $I_{x_0}(1)$ which was near unity, or practically 500 times its true value.

The procedure outlined above was initiated because in the early stages of this analysis, the discretized TDT functional values were

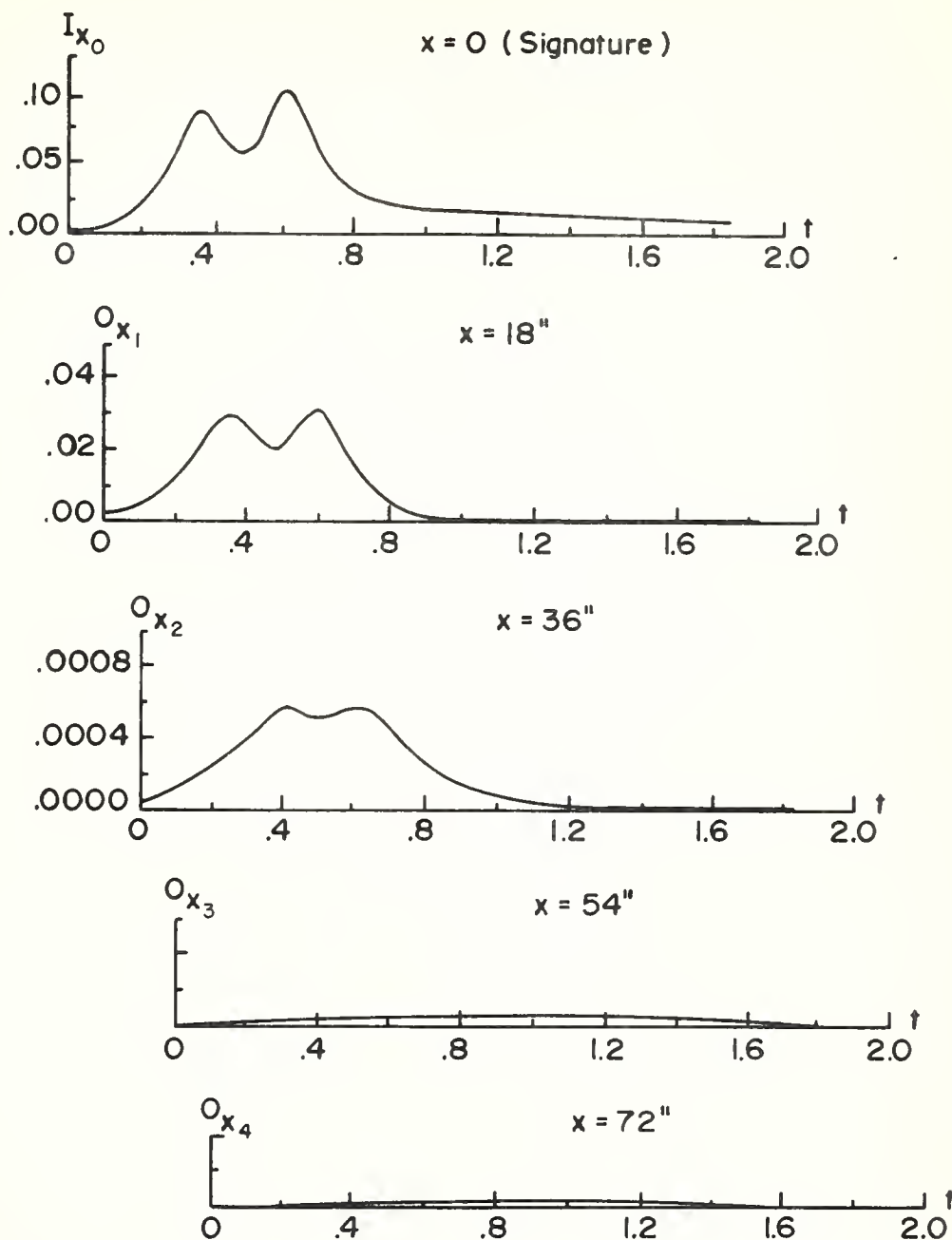
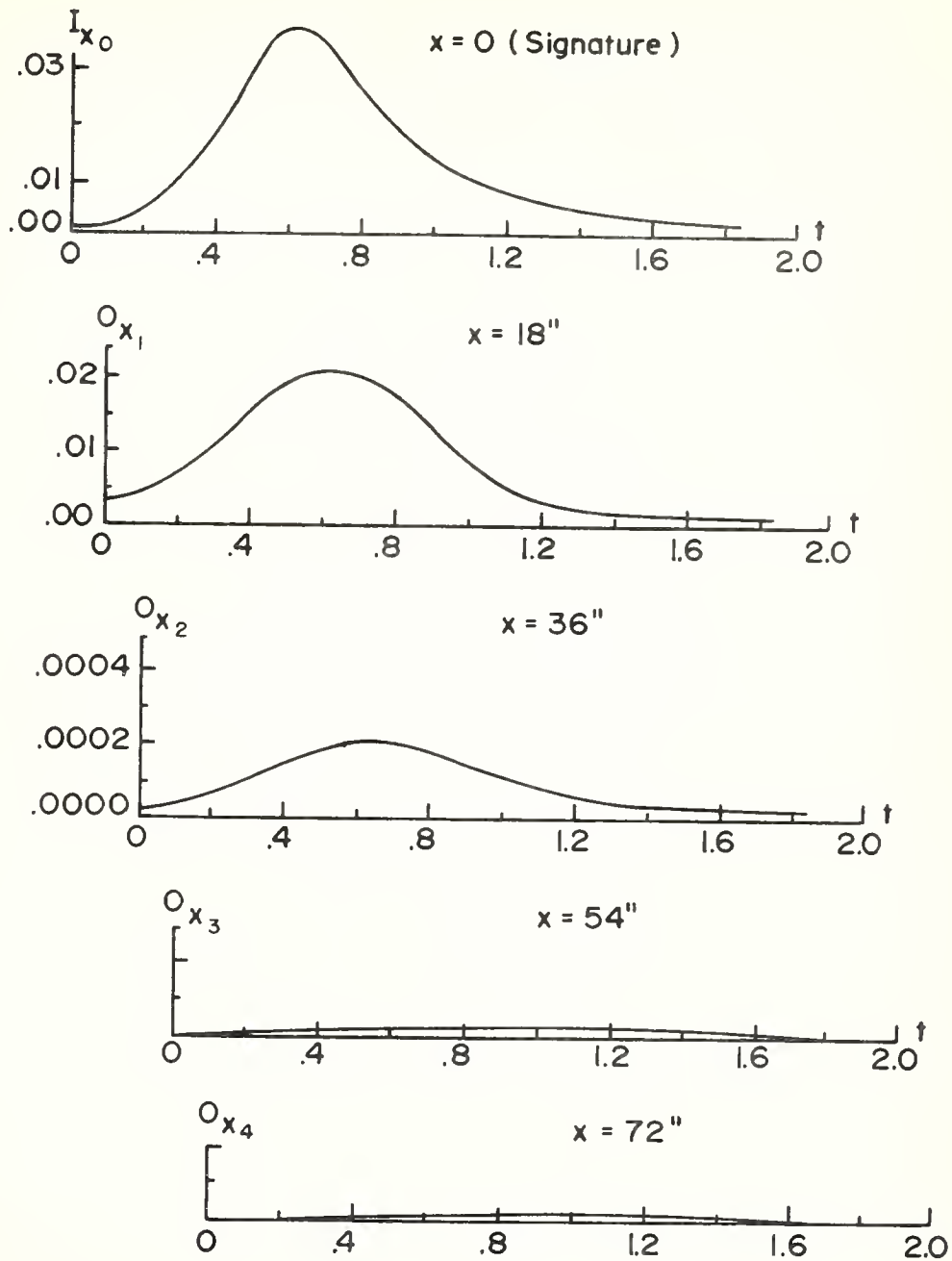


FIGURE 26. DEFLECTION RESPONSE FUNCTIONS
(DATA FOR C 135 SITE 1)



**FIGURE 27. DEFLECTION RESPONSE FUNCTIONS
(DATA FOR C 131 SITE 1)**

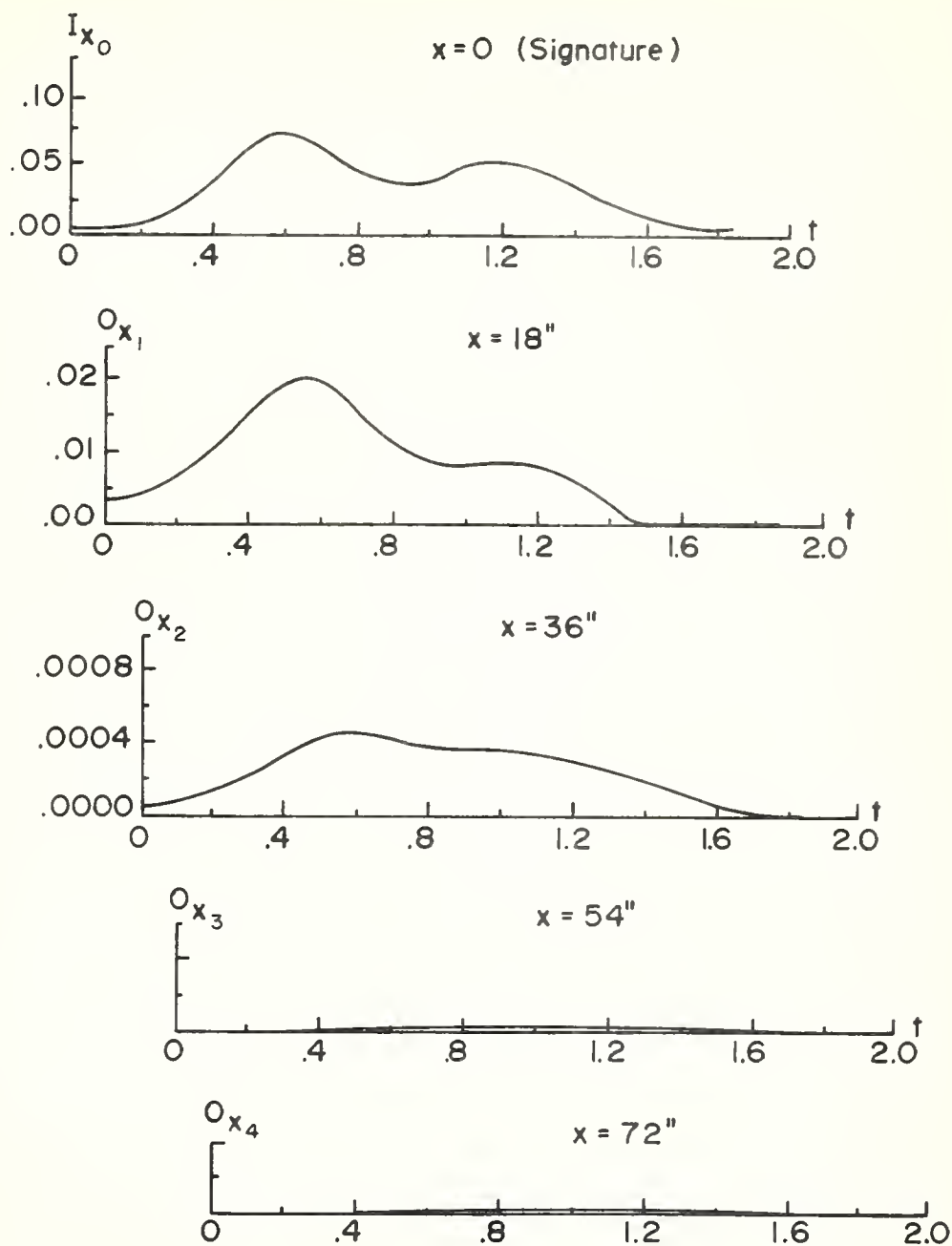


FIGURE 28. DEFLECTION RESPONSE FUNCTIONS
(DATA FOR C 130-SITE 1)

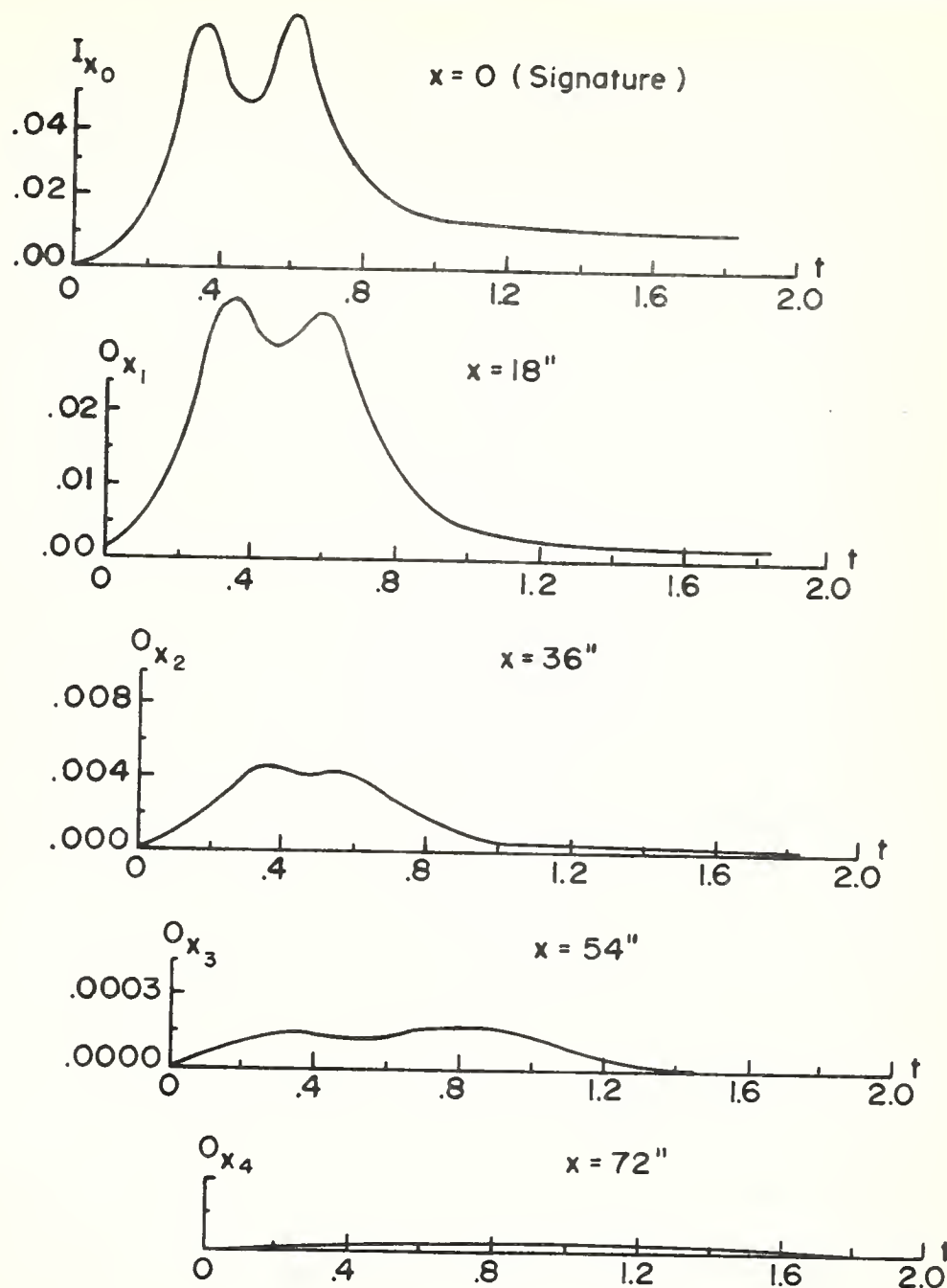
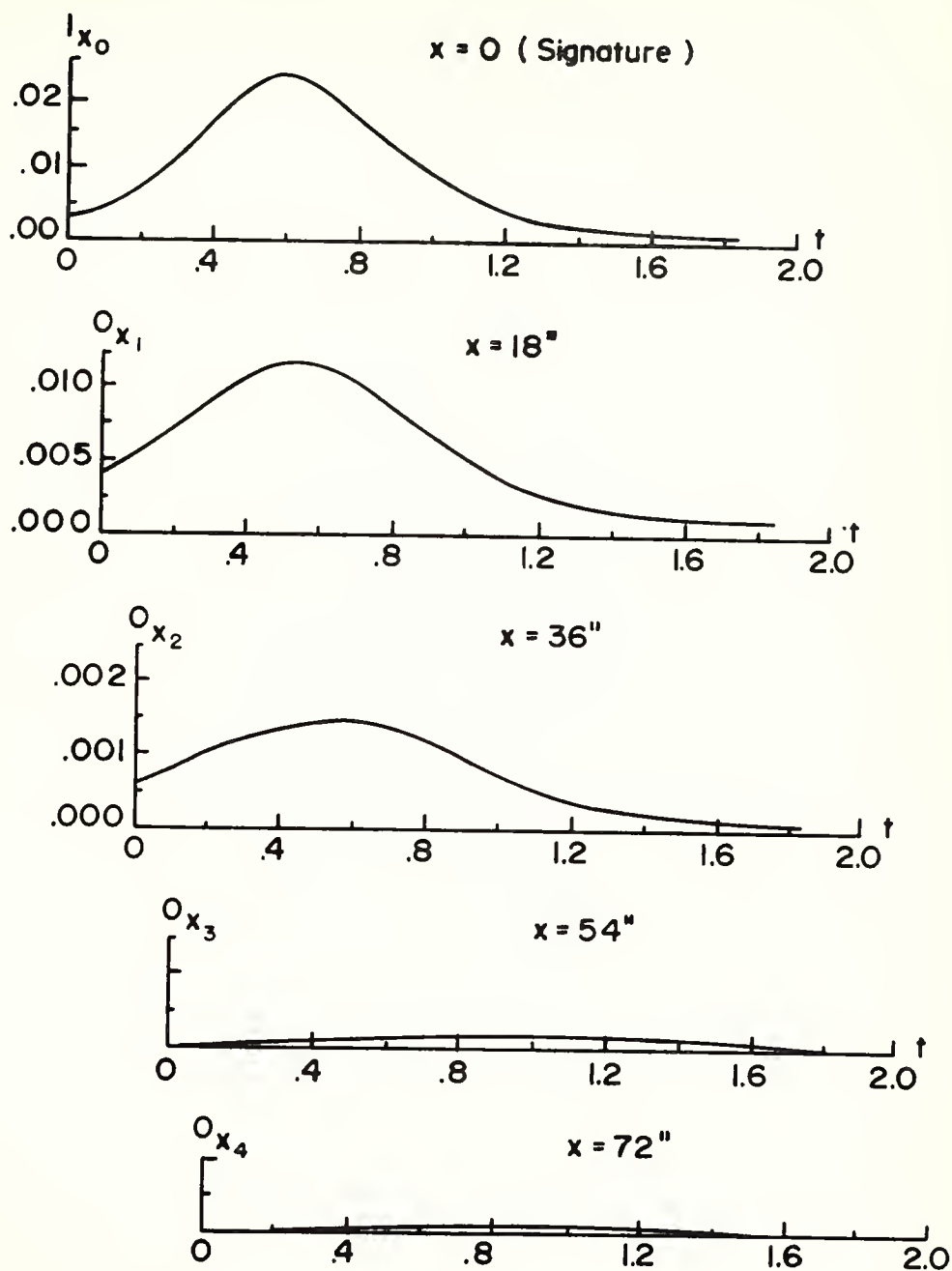
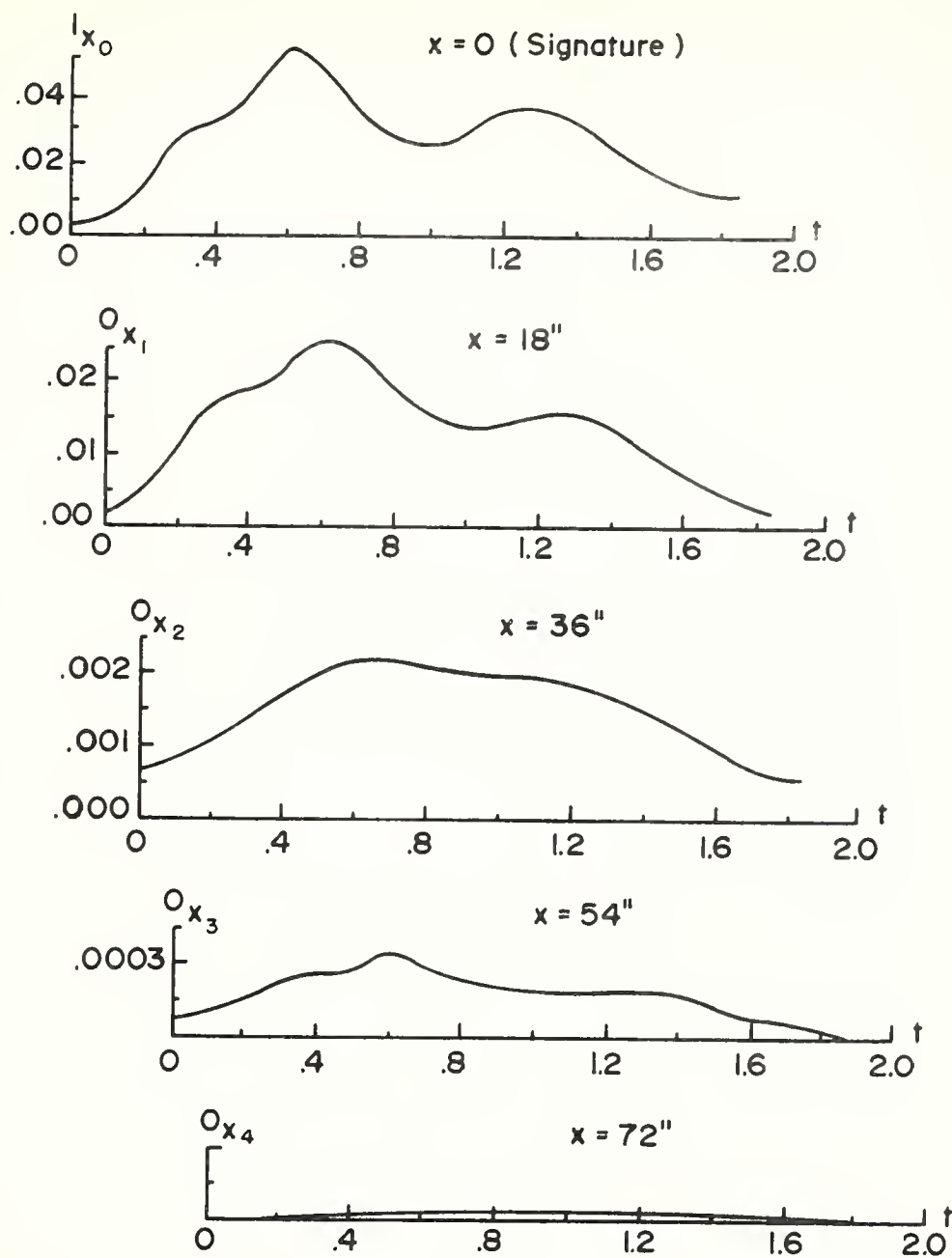


FIGURE 29. DEFLECTION RESPONSE FUNCTIONS
(DATA FOR C 135 SITE 2)



**FIGURE 30. DEFLECTION RESPONSE FUNCTIONS
(DATA FOR C 131 SITE 2)**



**FIGURE 31. DEFLECTION RESPONSE FUNCTIONS
(DATA FOR C 130 SITE 2)**

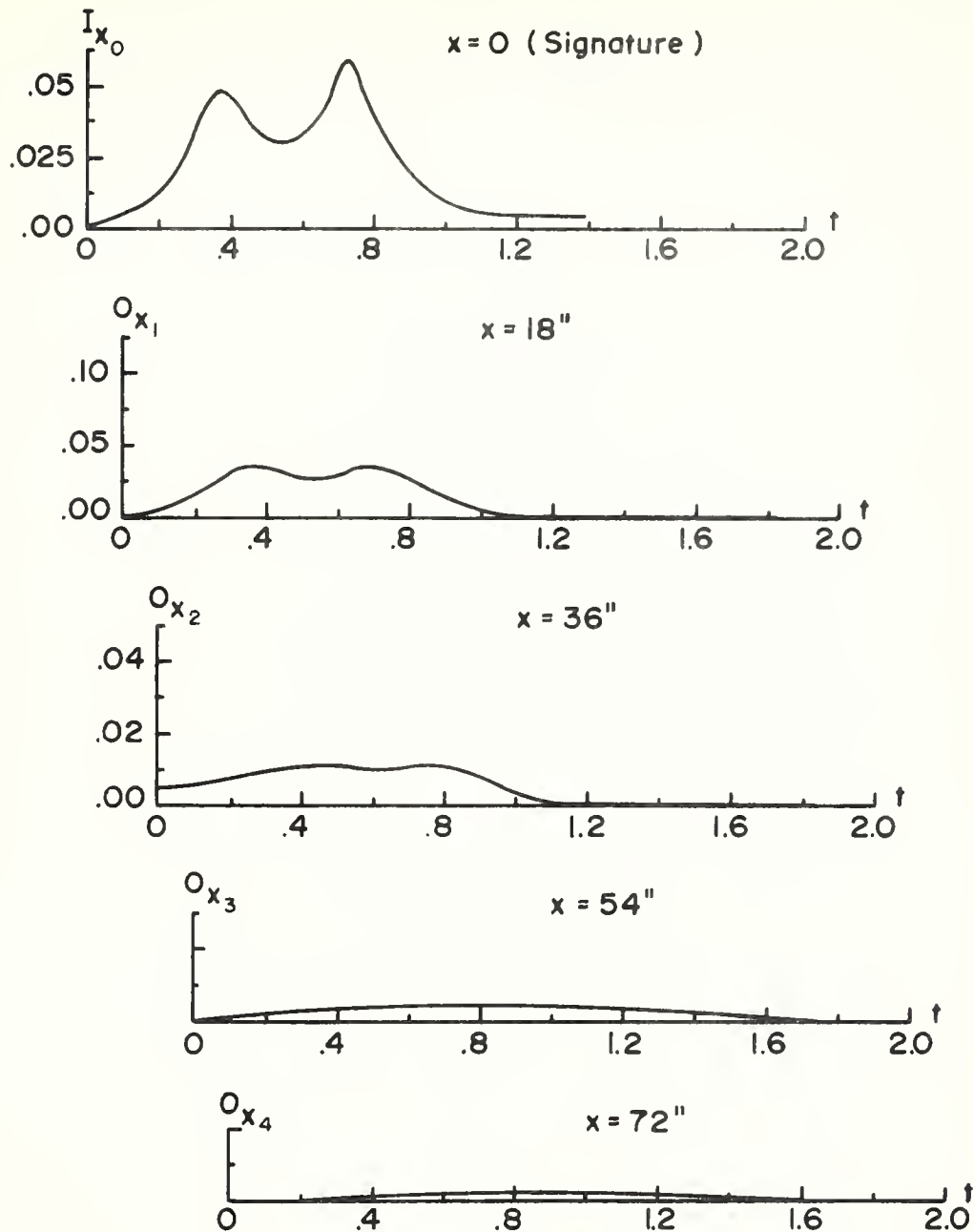


FIGURE 32. DEFLECTION RESPONSE FUNCTIONS
(DATA FOR C 135 SITE 3)

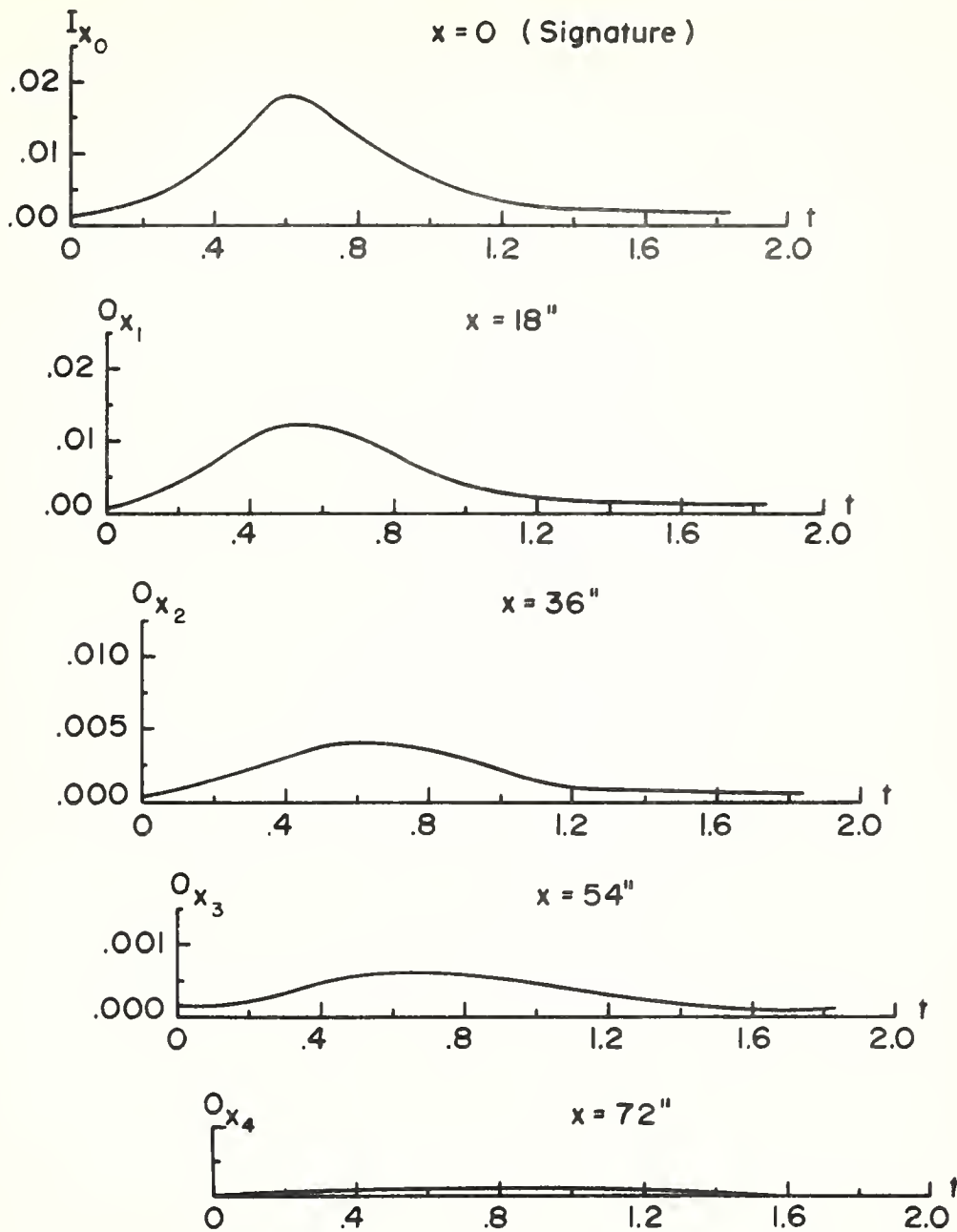


FIGURE 33. DEFLECTION RESPONSE FUNCTIONS
(DATA FOR C 131 SITE 3)

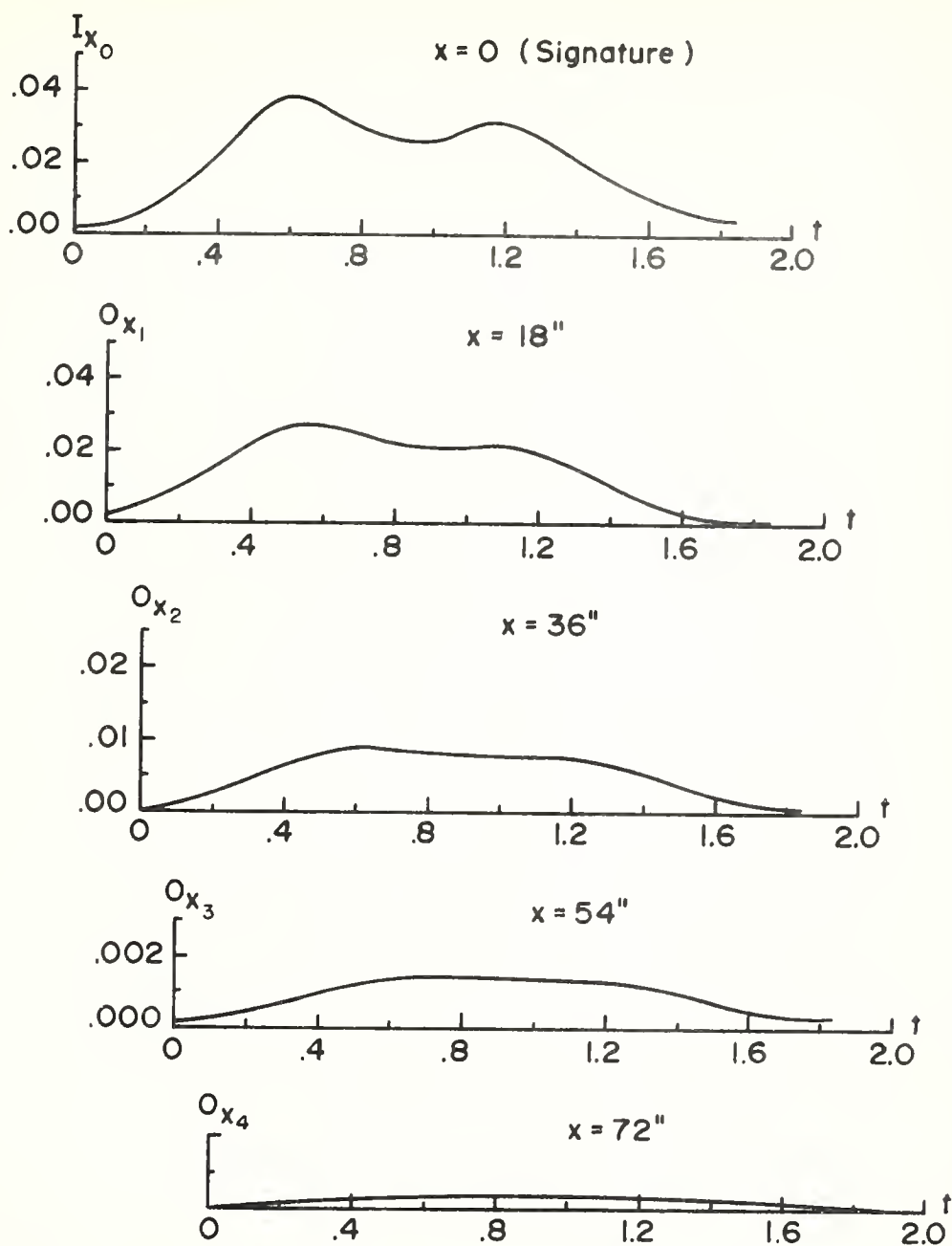


FIGURE 34. DEFLECTION RESPONSE FUNCTIONS
(DATA FOR C 130 SITE 3)

found to increase in magnitude, almost without bound, as time increased (or as consecutive array values were computed). Close examination of the implicit convolution technique revealed that the constant denominator in equation (10) was of the order of magnitude of 10^{-5} ; and since the summation process was repeated 46 times, there was reason to believe that repeated division by such a small number could cause this difficulty. It was also noted that each consecutive step carried over inflation of its result to the next step in the summation process. To examine the effect of this division in the procedure, discretized analytical input and output functions were used to simulate deflection response functions. The implicit convolution procedure was used to calculate a discretized TDT function. Then, explicit convolution between this calculated TDT function and the original analytical input function was used in an effort to reproduce the original analytical output function. Good agreement was achieved when 16 digits beyond the decimal point were retained, but when only six digits beyond the decimal point were retained, considerable error was observed in attempting to reproduce the discretized analytical output function. The conclusion from this exercise was that an apparent rounding error in the consecutive computer operations, due to the small magnitude of the divisor in equation (10), led to increasingly large magnitudes for the discretized TDT array values (i.e., as the summation procedure was carried out).

Once the deflection response functions had been obtained as shown in Figures 26 through 34, the TDT functions were calculated by implicit convolution (equation (10)) of the signatures with their

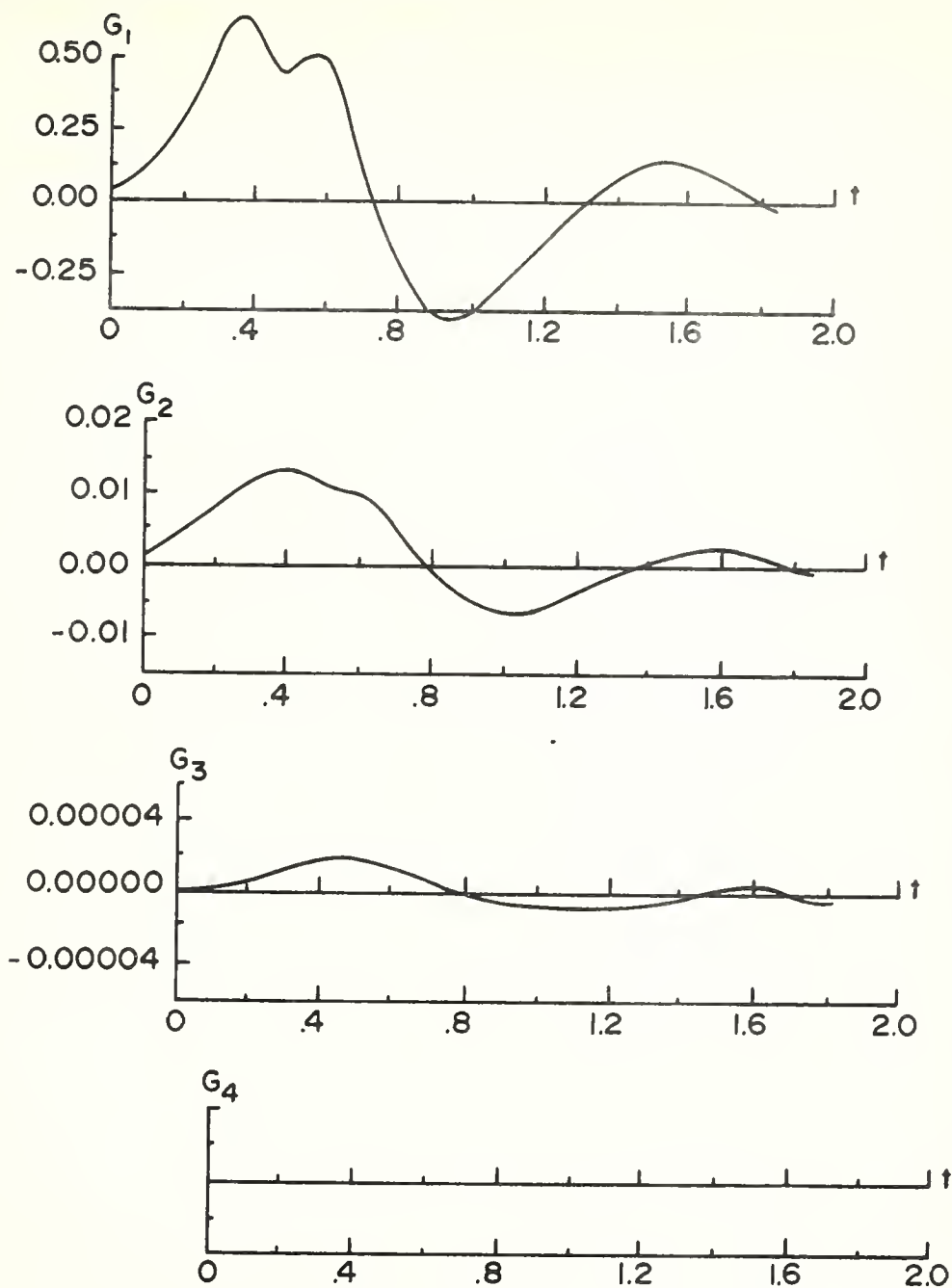
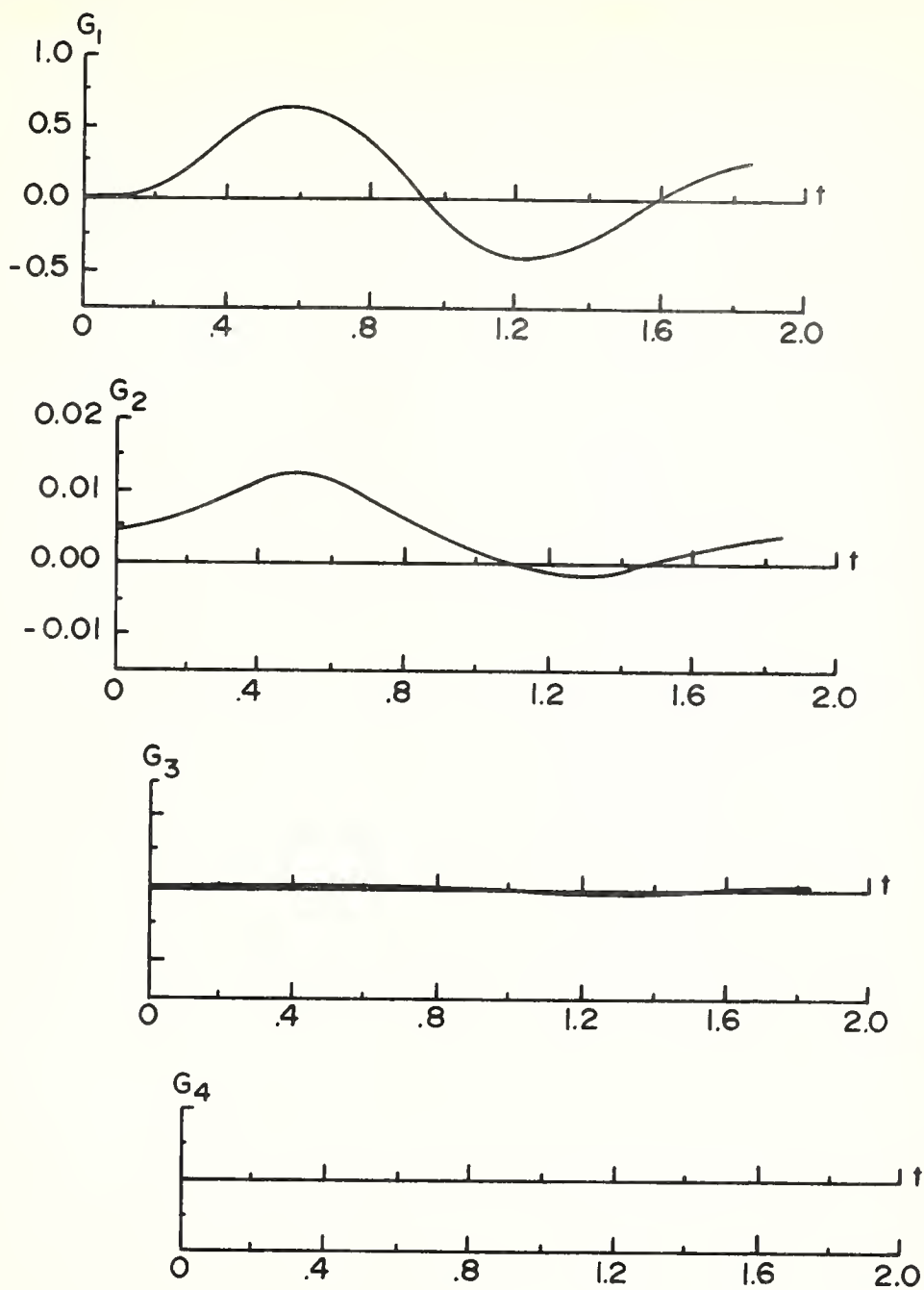


FIGURE 35. TDT FUNCTIONS
(DATA FOR C135 SITE 1)



**FIGURE 36. TDT FUNCTIONS
(DATA FOR C131 SITE 1)**

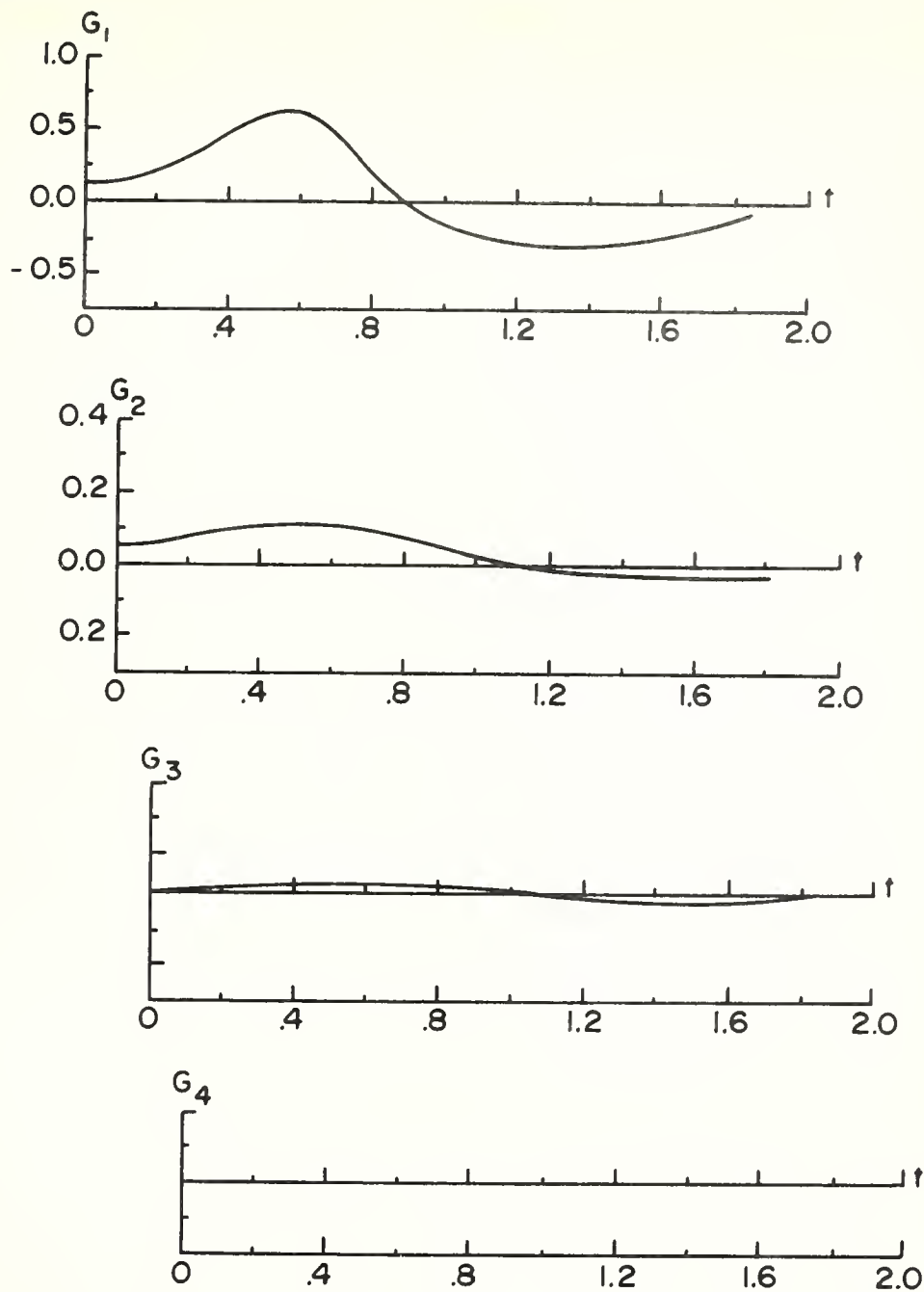
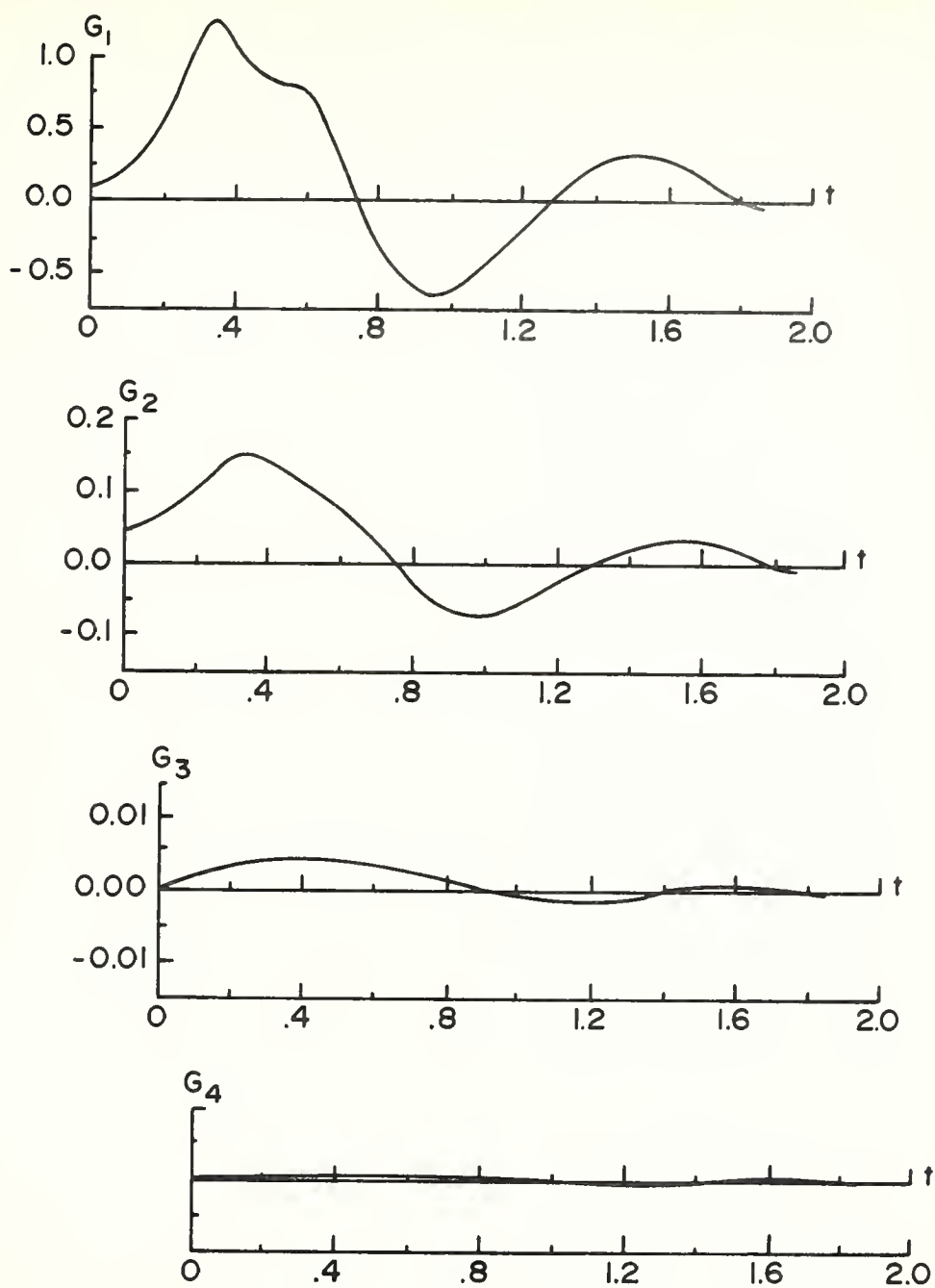
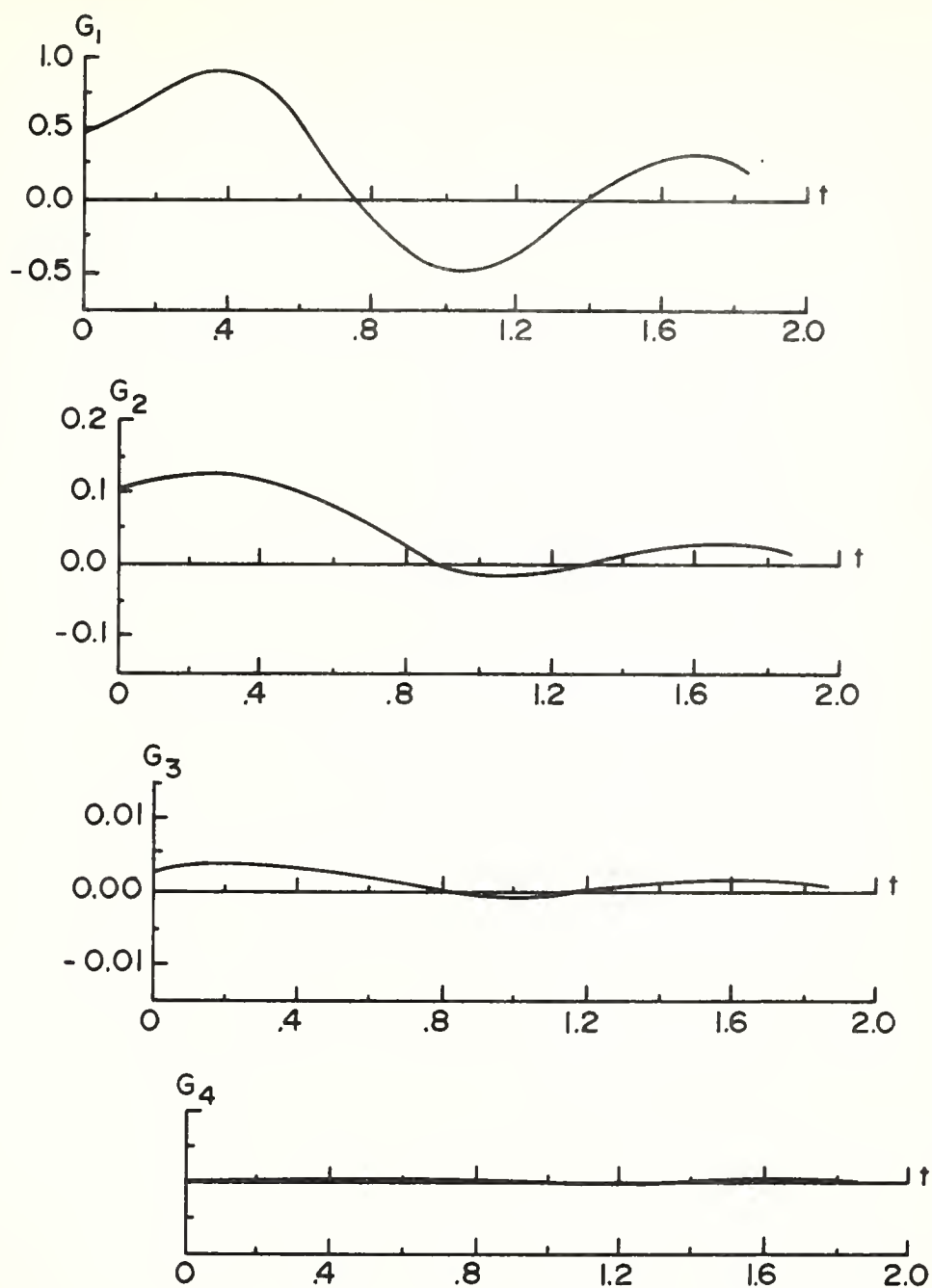


FIGURE 37. TDT FUNCTIONS
(DATA FOR C130 SITE 1)



**FIGURE 38. TDT FUNCTIONS
(DATA FOR C135 SITE 2)**



**FIGURE 39. TDT FUNCTIONS
(DATA FOR C13I SITE 2)**

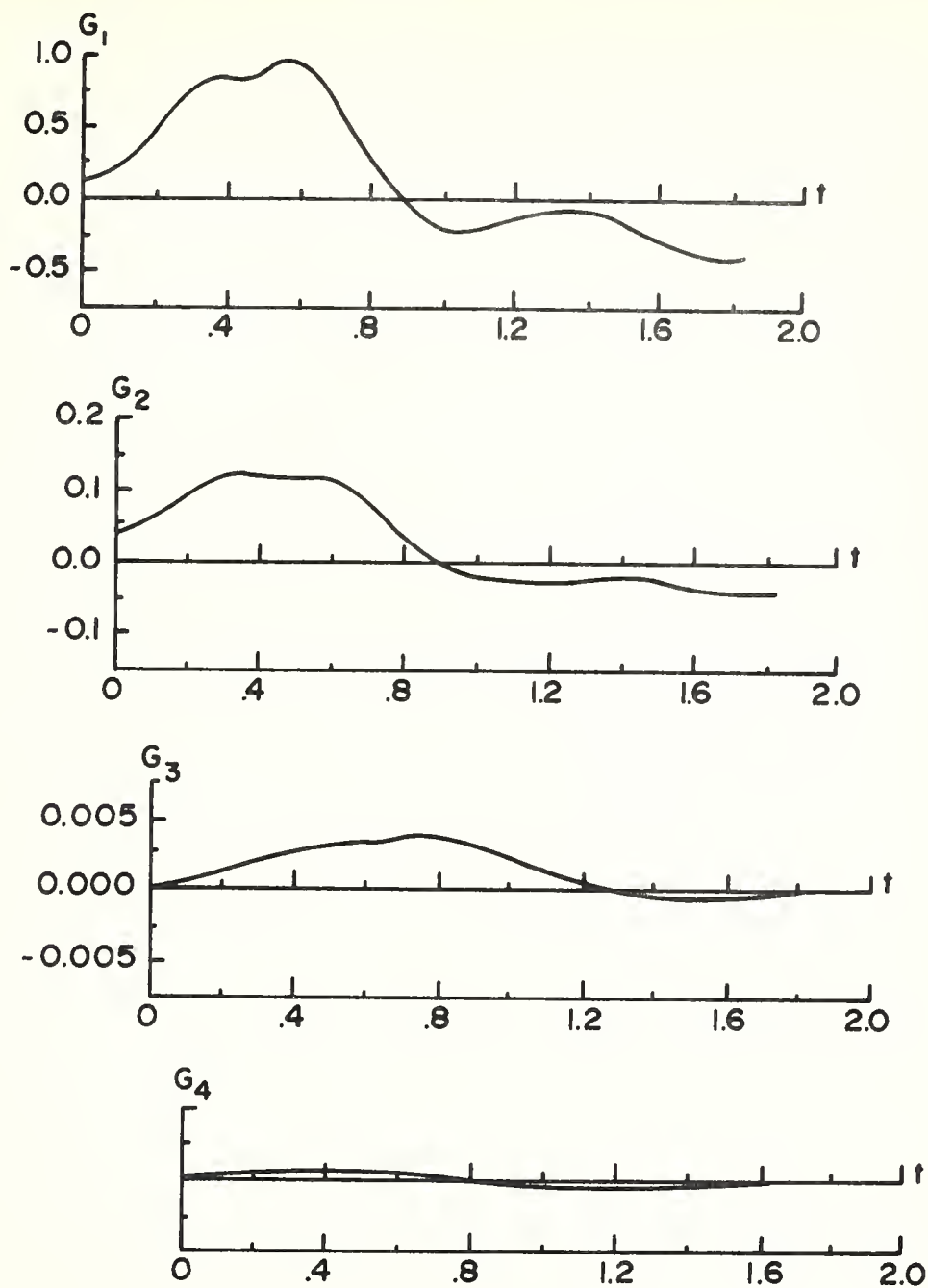


FIGURE 40. TDT FUNCTIONS
(DATA FOR C130 SITE 2)

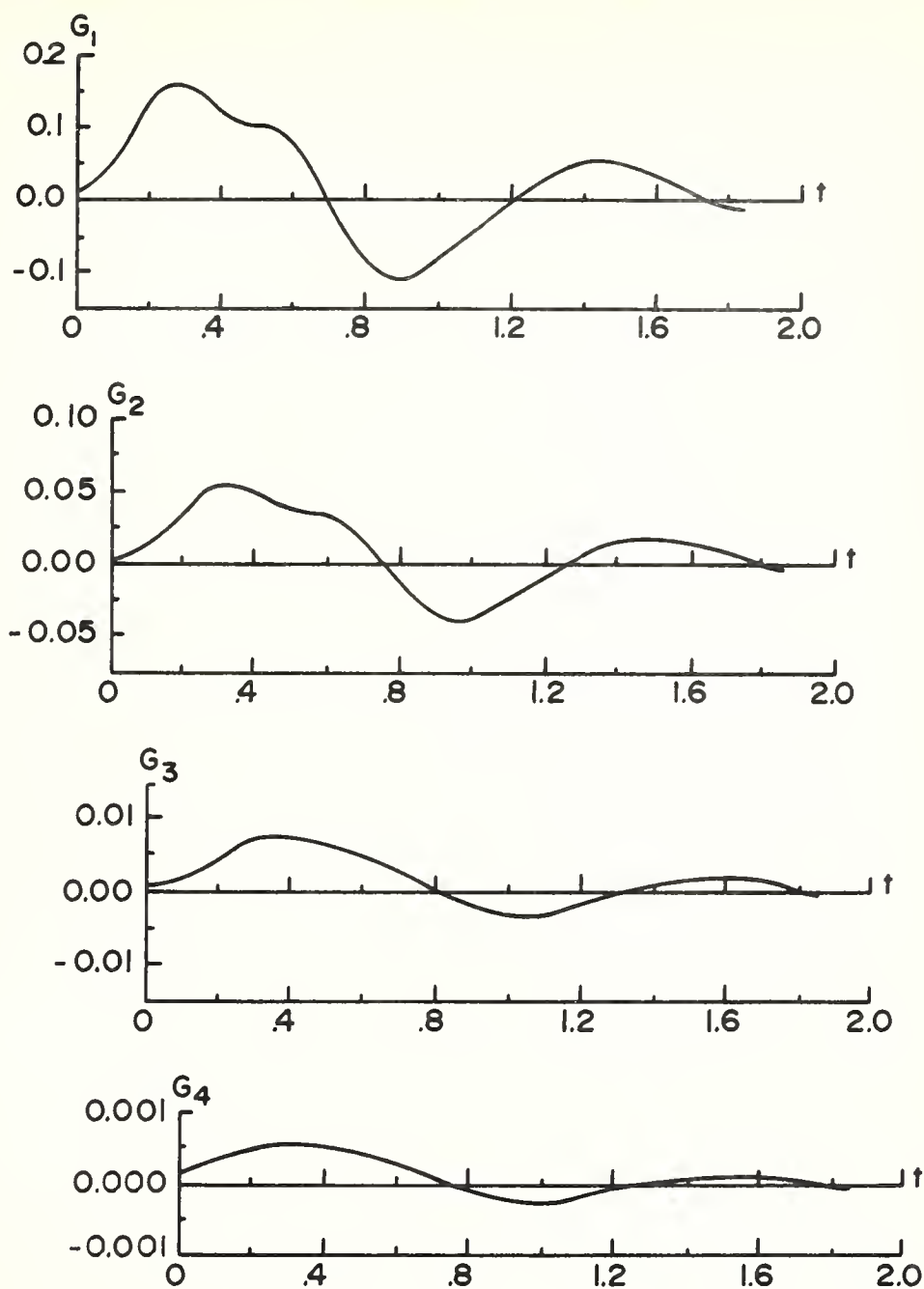


FIGURE 41. TDT FUNCTIONS
(DATA FOR C135 SITE 3)

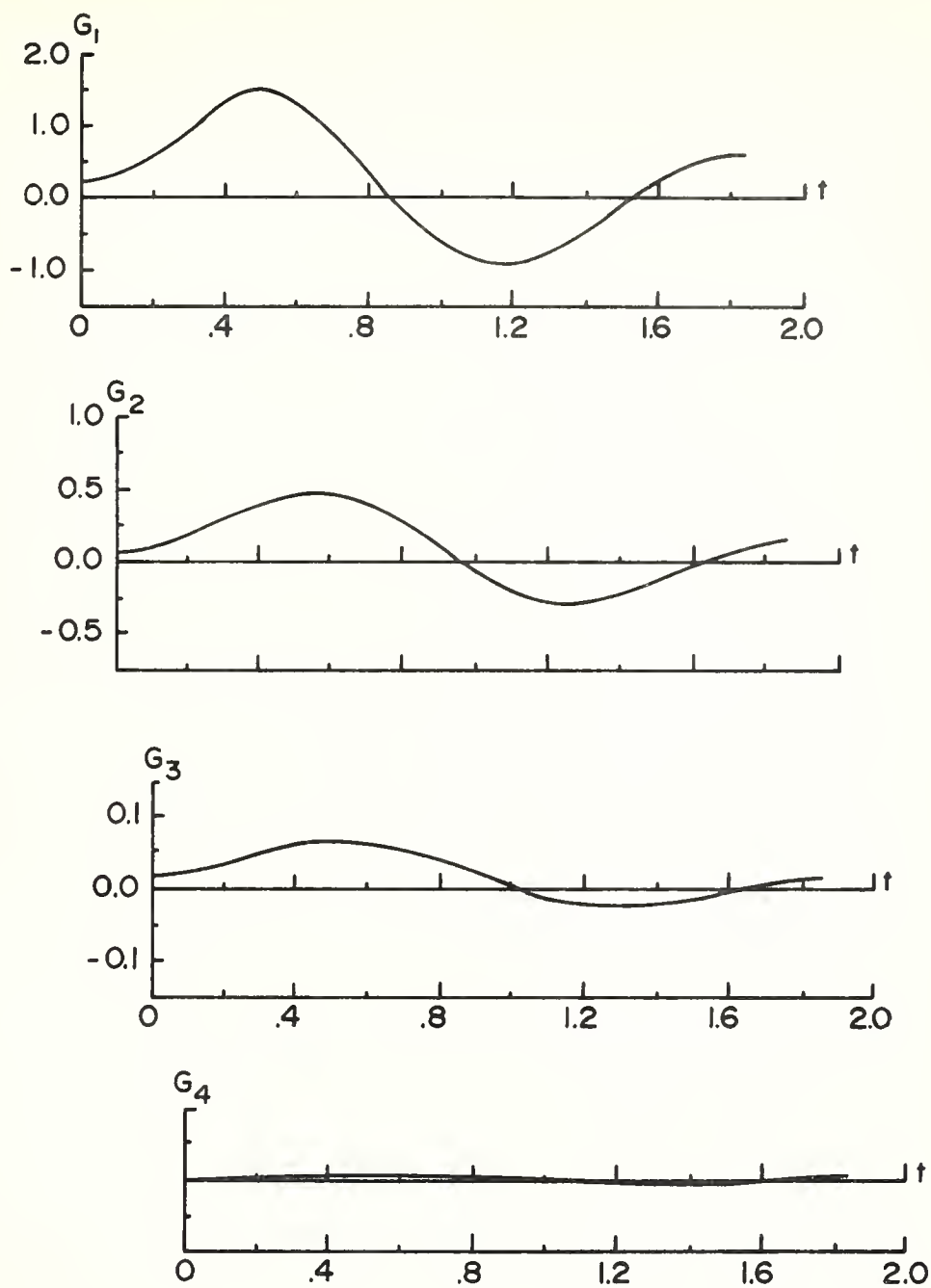


FIGURE 42. TDT FUNCTIONS
(DATA FOR C131 SITE 3)

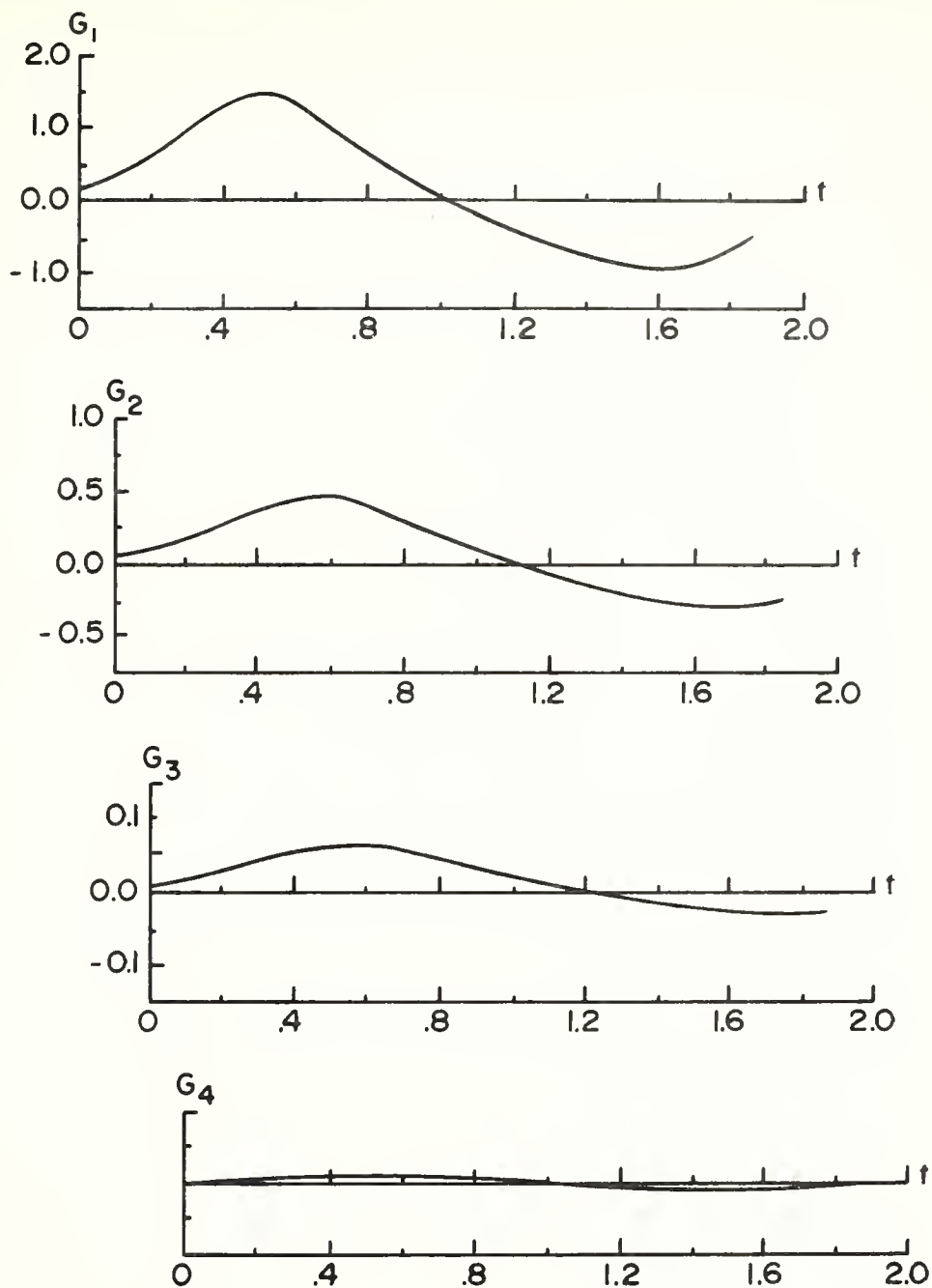


FIGURE 43. TDT FUNCTIONS
(DATA FOR C130 SITE 3)

respective output response functions. Figures 35 through 43 contain plots of the TDT functions calculated for each aircraft at each test site. Computer sheets containing the discretized functions, printed out to six decimal places, are provided in Appendix G.

DISCUSSION OF RESULTS

It was initially hypothesized that a pavement's TDT functions could be calculated from a prime mover's time-dependent deflection input and its respective time-dependent deflection outputs at adjacent locations on the pavement surface; that these functions could be obtained in a mathematical sense, without the need to simulate material performance to determine values for preselected descriptors; and secondarily, that these TDT functions could be employed to predict deflection outputs when the pavement was subjected to an arbitrarily imposed loading.

The secondary hypothesis also formed the basis for the non-destructive performance evaluation method presented in Figure 9. The procedures for obtaining TDT functions and those set forth in the performance evaluation method were employed in conjunction with the dynamic deflection data from the field tests. Analysis of the data included:

- (1) modeling the peak dynamic deflection basin;
- (2) presenting the measured deflection response functions;
- (3) calculating the TDT functions; and
- (4) predicting deflection response functions for arbitrarily chosen prime movers and test sites in accordance with the procedures of the developed performance evaluation method.

Items (1) and (2) had to be accomplished before the primary hypothesis could be employed. Item (3) (implicit convolution) provided the

mechanism to investigate the validity of the primary hypothesis. Item (4) (explicit convolution) permitted the secondary hypothesis, concerning predicting a pavement's performance, to be explored.

The discussion of these results are contained in this section.

Peak Dynamic Deflection Basin

The peak dynamic deflections were found to form a normal distribution about the point where a signature was applied. The validity of this model was established by the correlation coefficients calculated as part of the regression analysis (See Table 7). The parameters in the model, $O_{x_i}(\text{peak}) = A \cdot e^{-B(.0417X_i)^2}$, relate significant information about the shape of the deflection basin adjacent to the signature point, or spatial origin. The A factor is merely the peak dynamic deflection of a signature input, whereas, the B factor is a measure of the rate at which the pavement system is capable of dissipating an energy input, or a measure of the rate at which the system deflections attenuate spatially.

From Figure 24, it is noted that the relationships between the A-factors and ratio factors were found to be linear for a particular test site. A slight deviation was observed with respect to aircraft between sites, apparently due to difference in prime mover weights. In general, however, the ratio factors for each aircraft could be taken to be constant. The ratio factors used for the C135, C131, and C130 aircraft were 1.00, 0.34, and 0.74, respectively. Once these factors were known, equation (16) was employed to calculate the required signature array (see Figure 9). This technique provided

for the influence of a pavement's feedback to an input signature.

The range of B factors for a prime mover at a particular test site was observed to be small and was taken to be constant, with exception of the load cart. For the load cart, it was determined that a significant amount of the single wheel load was carried by stabilizing wheels located approximately 30" adjacent and to each side of the load wheel. This was ascertained by the correspondingly small B factors -- which indicated that the deflections decreased with lateral distance at a lesser rate than for the other prime movers. In view of this, it was decided that the load cart data should be deleted from further consideration. Figure 25 shows, that for the aircraft prime movers, a single B factor could be used at each test site.

Form of the Deflection Response Functions

The general characteristics of the deflection response functions for a particular aircraft were found to be similar at each test site. Some observations from these results are:

- (1) The C135 aircraft (twin-tandem gear) had its peak deflection resultant from the second set of tires in the gear truck. This reflected the pavement's viscoelastic behavior.
- (2) The C131 aircraft displayed only one peak deflection. This was consistent with its twin gear truck. Some viscoelastic action of the pavement was also evident.
- (3) The C130 aircraft (single-twin gear) had two peak deflections like that of the C135, but the largest peak resulted from the first wheel in the gear in contrast to the second wheel for the C135. This

appears to be due to the load distribution on the gear. Again, viscoelastic behavior of the pavement was observed.

Form of the TDT Functions

Figures 35 through 43 represent the TDT functions that were calculated by computer code CONVLI without the need to simulate material performance or to determine values for preselected descriptors. Various characteristics of these functions are summarized in Table 8; viz. the maxima, minima, and zero values which may be thought of as the more basic descriptors in the functions. The magnitudes of the maxima and minima values are seen to be independent of the aircraft. For example, these values can be taken to be constant for all the aircraft at a particular site. In view of this independence, the values can be thought of as representing parameters which indicate the performance of the pavement system itself. It is also of interest that, in comparison with the pavement cross-sections (see Figure 18), the absolute maxima and minima values increase with increasing thickness of pavement. The time required to reach sequential zeroes of the TDT functions appears to be independent of site; e.g. the time for each zero can be taken to be constant for all the sites for a particular aircraft. The zero time values seem to represent parameters which indicate how each of the prime movers influence the performance of the pavement system. In considering the prime mover main gear characteristics (see Figure 23), it is reasonable to believe that these sequential zero time values represent indicators of the influence of the different aircraft gear configurations. This finding

was not anticipated in the earlier stages of this investigation. It is, however, considered to be very significant.

The significant features of the TDT functions are seen to be (1) that indicators can be isolated which are independent of the prime mover (indicators which reflect the way a pavement system attenuates the energy imparted by a prime mover's signature); and (2) that indicators can be identified which represent a pavement's response to the configuration of a prime mover's input.

Prediction of Deflection Response Functions

The discussion so far has indicated the general validity of the concepts associated with the dynamic deflection basin; time-dependent deflection response functions (including signatures); and, time-dependent transfer functions. It was indicated previously ("Formulation of Testing Program" in the section on "Predicting Performance") that once catalogues of the signatures and TDT functions of different prime movers and pavement systems were obtained, estimates would be had for combinations of prime movers and pavements for which tests were not conducted. In keeping with the performance evaluation method as initially advanced by Figure 9, it was seen that one aircraft and one test site could be chosen arbitrarily as standards. Subsequently, predictions of the deflection response functions for the other two aircraft at the other two sites could be predicted from results of only the standard vehicle at those locations (using computer code CONVLE). Figure 44 represents a sample scheme where the C131 aircraft and site 2 are taken as the standards.

<u>Aircraft</u>	<u>Site 1</u>	<u>Site 2</u>	<u>Site 3</u>
C135	Prediction	Standard	Prediction
C131	Standard	Standard	Standard
C130	Prediction	Standard	Prediction

FIGURE 44. PREDICTION OF DEFLECTION RESPONSE FUNCTIONS.

A typical set of calculated and measured deflection response functions for the C135 and C130 aircraft, consistent with the scheme in Figure 44, are shown in Figures 45 and 46. In all cases the predicted peak deflection values are seen to be in close agreement with the measured peak deflection values; however, the time history of the predicted deflection response functions are slightly out of phase with the measured ones. This small difference was thought to be due to not taking into account the difference in the sequential zero time values for the various gear configurations. Therefore, in an effort to improve upon the predictions of the deflection response functions, computer code CONVLE was further refined so as to reduce even these small differences. This was done by using linear interpolation to predict a fourth set of TDT functions from the three known sets as had been done previously for the signatures (equation 16). Hence, it was found that the times to the sequential zero values of the TDT functions for the respective aircraft would be in better correspondence. From this, it follows that the fourth set of TDT functions for, say, prime mover 2 on pavement B may be expressed as

$$G_{x_{12B}}(t) = \frac{G_{x_{11B}}(\text{first peak})}{G_{x_{11A}}(\text{first peak})} \cdot G_{x_{12A}}(t) \quad (17)$$

A typical set of calculated and measured deflection response functions for the C135 and C130 aircraft, consistent with the scheme in Figure 44, are shown in Figures 47 and 48, respectively. In all cases the calculated deflection response functions correspond well in time to the measured functions, and in all cases the calculated peak deflections

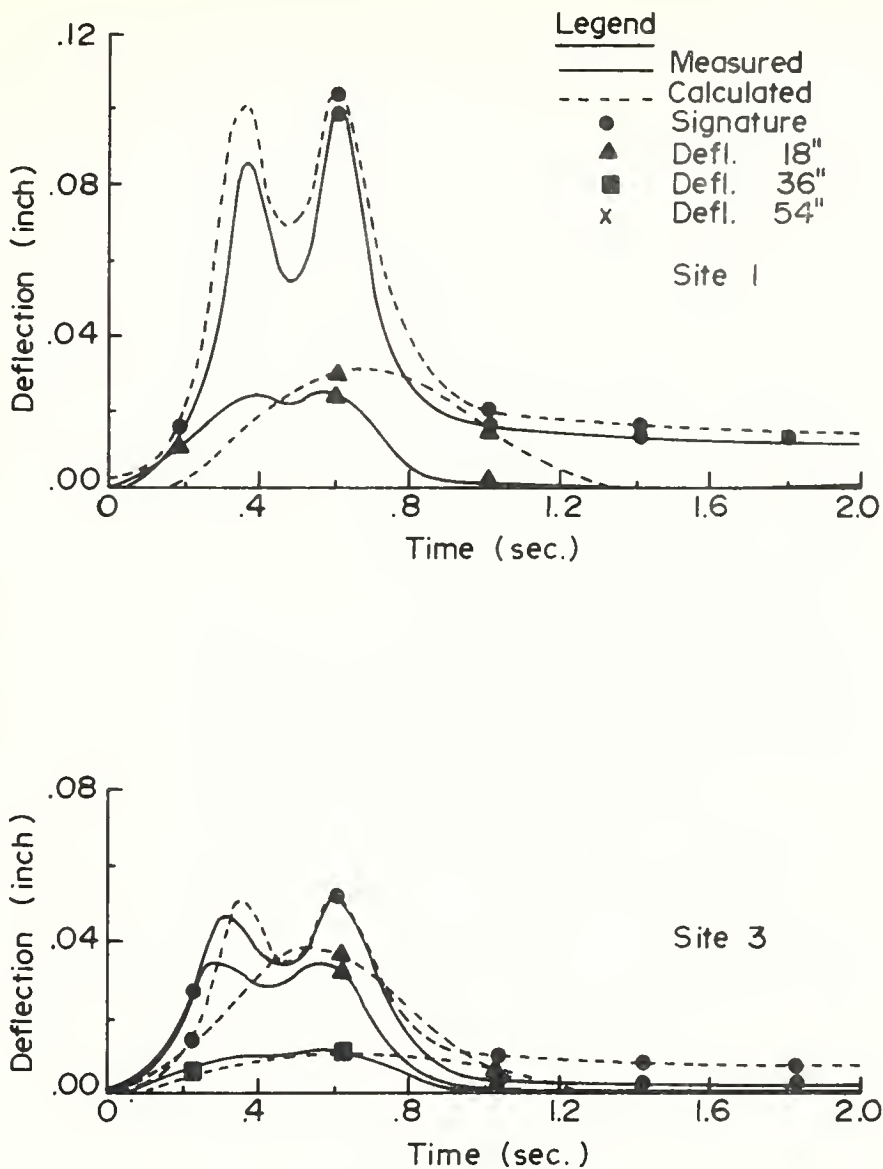


FIGURE 45. TYPICAL CALCULATED AND MEASURED DEFLECTION RESPONSE FUNCTIONS FOR C135 USING PREDICTED TDT FUNCTIONS WITH C131 AS STANDARD PRIME MOVER .

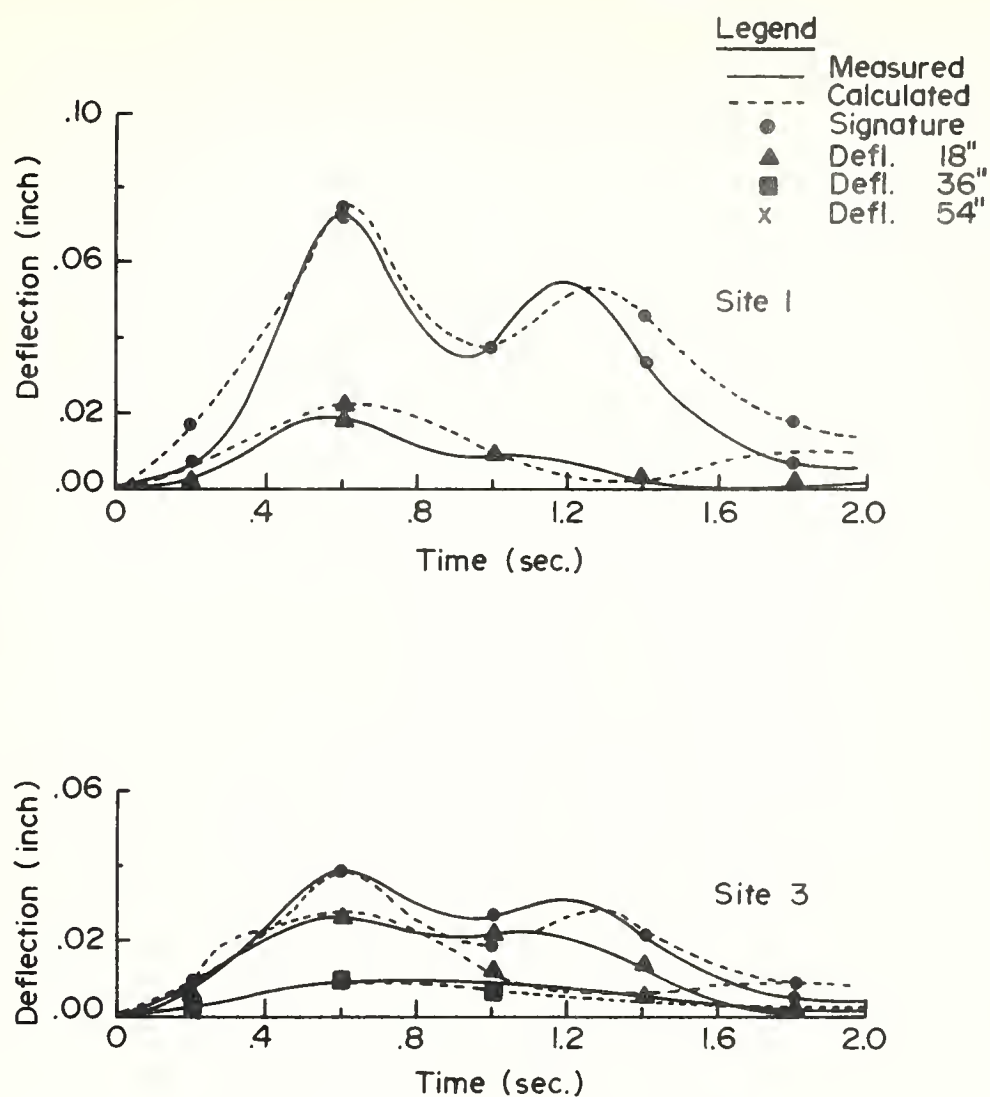


FIGURE 46. TYPICAL CALCULATED AND MEASURED DEFLECTION RESPONSE FUNCTIONS FOR C135, USING TDT FUNCTIONS FROM C131 WITH C131 AS STANDARD PRIME MOVER.

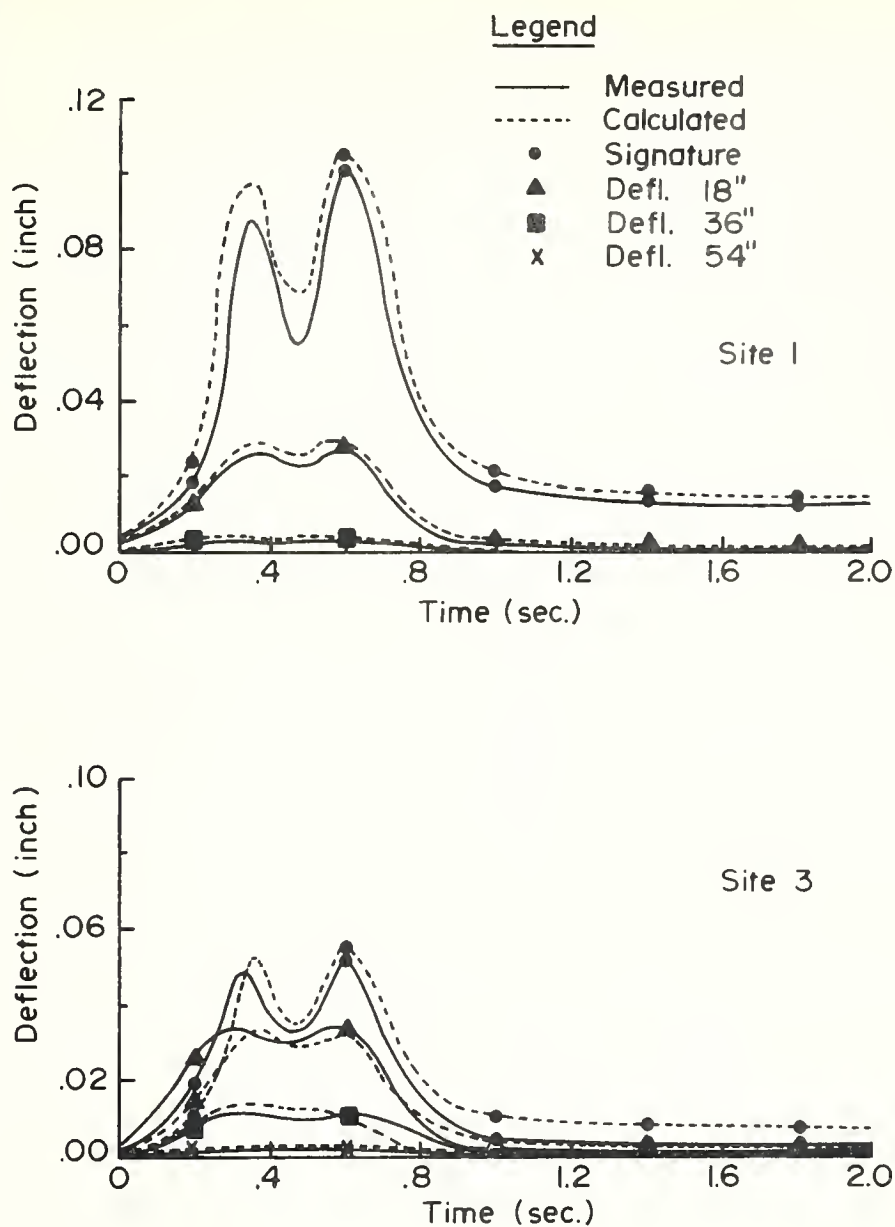


FIGURE 47. TYPICAL CALCULATED AND MEASURED RESPONSE FUNCTIONS FOR C135 USING PREDICTED TDT FUNCTIONS WITH C131 AS STANDARD PRIME MOVER.

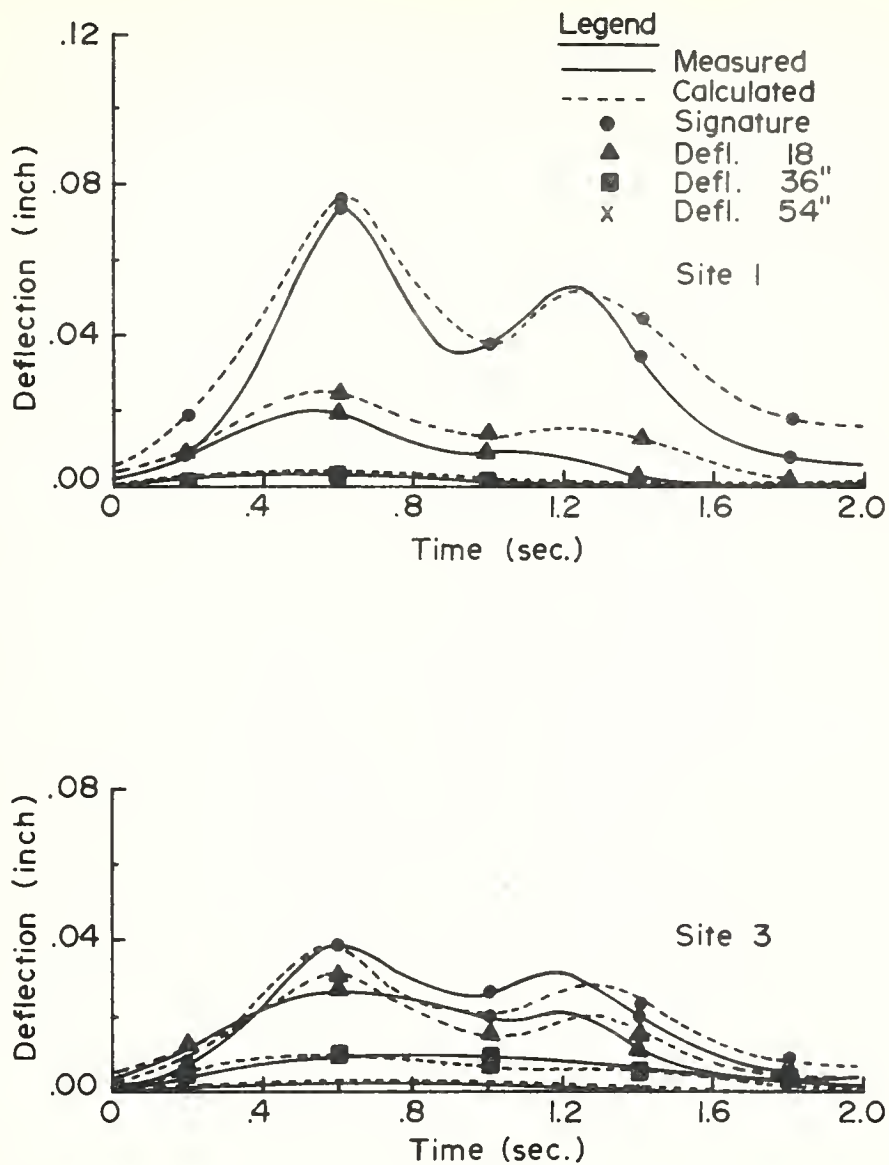
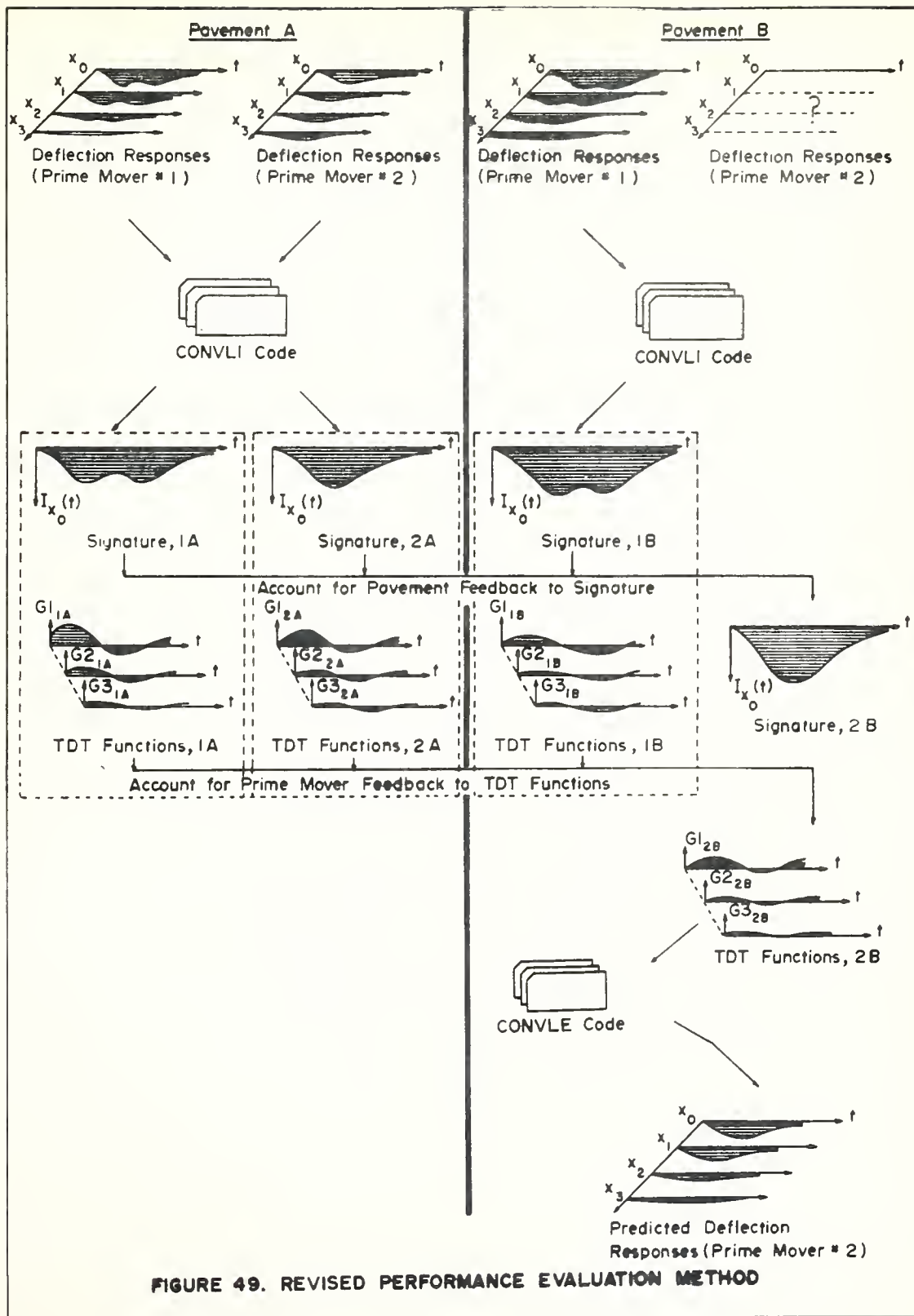


FIGURE 48. TYPICAL CALCULATED AND MEASURED RESPONSE FUNCTIONS FOR C130 USING PREDICTED TDT FUNCTIONS WITH C131 AS STANDARD PRIME MOVER.

were within 10% of the measured ones. A schematic of the revised performance evaluation method is provided as Figure 49.

Just as various forms of the constitutive relations may change outputs for a given input, it could be expected that the TDT functions could also reflect these characteristics. Radical differences between a standard vehicle and a prime mover in question could lead to large discrepancies between predicted and observed deflections. The two phenomena responsible for this are the relative contact area of the load inputs and the comparative stress levels of the vehicles; these should be matched to some degree to insure good predictions. It is not believed, however, that these limitations are restrictive in the world of real aircraft and real pavements.

Some additional plots of measured and calculated deflection response functions for other combinations of the scheme depicted in Figure 44 are given in Appendix H. Case 1 in Appendix H represents the scheme shown in Figures 44 through 48. Cases 2 and 3 use site 2 as standard with C135 and C130, respectively, as standard prime movers. Case 4 uses the C130 and site 1 as standards.



SUMMARY AND CONCLUSIONS

Transfer function theory in connection with discretized real convolution can be extended to define a pavement's time-dependent transfer functions. The time-dependent transfer functions can be calculated from an implicit solution of the convolution integral using data measured in a field environment. Dynamic deflection response functions can be calculated to predict pavement performance by employing the convolution procedure in an explicit manner.

A procedure ~~was~~ advanced to predict a pavement's performance for a particular load or situation which had not been previously experienced. As an example, two sites (labeled site 1 and site 2) and two prime movers (A and B) are involved. One site and one prime mover are considered to be standard, say site 1 and prime mover A. It is desired to predict the pavement's performance at site 2 incident to prime mover B. Signatures and time-dependent transfer functions are catalogued for both prime movers at the standard site. The standard prime mover is then run at site 2 so that its signature and time-dependent transfer functions may be calculated. The relationships between signatures and time-dependent transfer functions at the standard site and the signature and time-dependent transfer functions from the standard prime mover at site 2 (site under question) permit prediction of the deflection response functions for prime mover B at site 2 to be carried out.

To validate the transfer function approach and the prediction

method, full scale field tests were conducted. The time-dependent transfer functions were calculated for three different pavement cross-sections using the data collected for three operational military aircraft.

The results of these tests indicate the following conclusions:

(1) There is a unique set of time-dependent transfer functions at a particular site for a particular prime mover. These functions do appear to provide the basis for a proposed performance evaluation method.

(2) The peak deflections form a normal distribution about the point where a signature is applied. Excellent correlation between the measured data and the normal distribution model
$$O_{x_i}(\text{peak}) = A e^{-B(.0417X_i)^2}$$
 was achieved. The A parameters were found to be dependent on the pavement and prime mover; whereas, the B parameters were taken to be constant for a given pavement, independent of prime mover.

(3) The time-dependent transfer functions are independent of magnitude of load input but reflect to a minor extent some characteristics of the prime mover gear configurations.

(4) In philosophy, the transfer function provides a measure

of "global properties" of a pavement in contrast to the "point-wise aspects" inherent in classical (elasticity and viscoelasticity) theories.

(5) The time-dependent characteristics of a flexible pavement can be represented by a series of time-dependent transfer dynamic tests using a common prime mover.

SUGGESTIONS FOR FUTURE RESEARCH

This investigation has been a first step in formulating and testing the concept of using transfer function theory to evaluate a pavement system. Conclusions from the full scale field tests, although limited in scope, clearly establish the validity of the hypotheses as initially conceived. In view of the favorable results and the experience gained by conducting this investigation, the following recommendations for further research are provided:

1. The transfer function approach advances a global concept wherein the TDT functions are sensitive to the distance over which the input and output functions are measured. A more reliable deflection measuring system should be developed to measure the time-dependent input and output functions relative to the prime mover instead of at fixed locations on the pavement surface. Such a system would eliminate the need to shift the deflection response functions, and thereby reduce any errors associated with the modeling used in the shifting procedure.
2. Develop a vibration testing device capable of determining a pavements transfer functions by the frequency spectrum technique. The device must be capable of delivering a constant input force between 5 and 150 Hz. Successful employment of this technique would negate use of a standard vehicle.
3. Perform a study to isolate and identify system parameter contained in the TDT functions. These

parameters could then be correlated with current theoretical models and existing evaluation and design methods.

4. Conduct a parameter study to incorporate a greater number of variables, including temperature, speed, environmental, and geographic conditions, etc.
Application and correlation of the concept to layered systems and different materials, such as soil and concrete, should be considered.
5. Initiate a program to monitor TDT functions over a long-time period to permit correlation of parameters with pavement deterioration. Emphasis could be placed on establishing a distress criteria and standards for maintenance and repair of pavements.

BIBLIOGRAPHY

BIBLIOGRAPHY

1. "Deteriorating Airport Pavements Spur Efforts to Head off Crisis", Engineering News Record, page 11, November 4, 1971.
2. Horonjeff, B., Planning and Design of Airports, McGraw-Hill Book Company, Inc., New York, 1962.
3. Yoder, E. J., Principles of Pavement Design, John Wiley and Sons, Inc., New York, 1959.
4. "Development of CBR Flexible Pavement Design Methods for Airfields", Symposium, Transactions, American Society of Civil Engineers, Vol. 115, 1950.
5. Westergaard, H. M., "Stresses in Concrete Pavements Computed by Theoretical Analysis", Public Roads, Vol. 7, 1926.
6. Westergaard, H. M., "Theory of Concrete Pavement Design," Proceedings, Highway Research Board, 1927.
7. Westergaard, H. M., "Stresses in Concrete Runways of Airports," Proceedings, Highway Research Board, 1939.
8. Westergaard, H. M., "New Formulas for Stresses in Concrete Pavements of Airfields," Transactions, ASCE, 1948.
9. Hogg, A. H. A., "Equilibrium of a Thin Plate, Symmetrically Loaded, Resting on an Elastic Foundation of Infinite Depth," Philosophical Magazine, Vol. 25, 1928.
10. Harr, M. E., and Leonards, G. A., "Analysis of Concrete Slabs on Ground", Journal of the Soil Mechanics and Foundations Division, Proceedings of the ASCE, Vol. 85, No. SM3, June, 1959.
11. Gazi, D. C., "Analysis of Finite Beams on Elastic Foundations," Journal of the Structural Division, Proceedings of the ASCE, Vol. 84, No. ST4, July, 1958.
12. Hetenyi, M., Beams on Elastic Foundations, The University of Michigan Press, Ann Arbor, 1946.
13. Klepikov, S. N., "Calculation of Beams on an Elastic Foundation with a Variable Modulus of Subgrade Reaction", Soil Mechanics and Foundation Engineering, No. 5, September-October, 1965, Consultants Bureau, New York.
14. Ray, K. C., "Influence Lines for Pressure Distribution under a Finite Beam on Elastic Foundations", Journal of American Concrete Institute, Vol. 30, No. 6, December, 1958.

15. Terzaghi, K., "Evaluation of Coefficients of Subgrade Reaction", Geotechnique, Vol. 5, No. 4, December, 1955.
16. Burmister, D. M., "The Theory of Stresses and Displacements in Layered Systems and Application to the Design of Airport Runways", Proceedings, Highway Research Board, 1943.
17. Burmister, D. M., "The General Theory of Stresses and Displacements in Layered Soil Systems," Journal of Applied Physics, Vol. 16, 1945.
18. Acum, W. E. A., and Fox, L., "Computation of Load Stresses in a Three-Layer Elastic System", Geotechnique, Vol. II, 1951.
19. Burmister, D. M., "Evaluation of Pavement Systems of the WASHO Road Test by Layered Systems Methods", Highway Research Board Bulletin 177, 1958.
20. Fox, L., "Computation of Traffic Stresses in a Single Road Structure", Proceedings, Second International Conference on Soil Mechanics, Vol. 2, Rotterdam, 1948.
21. Malter, H., "Numerical Solutions for Beams on Elastic Foundations", Transactions of the ASCE, Vol. 125, 1960.
22. Schiffman, R. L., "The Numerical Solution for Stresses and Displacements in a Three-Layer Soil System", Proceedings, Fourth International Conference on Soil Mechanics and Foundation, Vol. 2, 1957.
23. Van der Poel, C. "Dynamic Testing of Road Constructions", Journal of Applied Chemistry, Vol. 1, 1951.
24. Pickett, G., "Dynamic Testing of Pavements", Journal of American Concrete Institute, Vol. 16, 1945.
25. Jones, R., "Surface Wave Technique for Measuring Elastic Properties and Thickness of Roads; Theoretical Development", British Journal of Applied Physics, Vol. 13, 1962.
26. Jones, R. and Thrower, E. N., "An Analysis of Waves in a Two-Layer Composite Plate and Its Application to Surface Wave Propagation on Roads," Journal of Sound Vibrations, Vol. 2, 1965.
27. Jones R., Thrower, E. N., and Gatfield, E. N., "Surface Wave Method", Proceedings, International Conference on the Structural Design of Asphalt Pavements, University of Michigan, 1967.
28. Freudenthal, A. M., and Lorsch, H. G., "The Infinite Elastic Beam on a Linear Viscoelastic Foundation", Journal of the Engineering Mechanics Division, Proceedings of the ASCE, Vol. 83, No. EM1, January, 1957.

29. Reissner, E., "A Note on Deflections of Plates on a Viscoelastic Foundation", Transactions of the ASME, Vol. 25, No. 1, March, 1958.
30. Hoskin, B. C., and Lee, E. H., "Flexible Surfaces on Viscoelastic Subgrades," Journal of the Engineering Mechanics Division, Proceedings of the ASCE, Vol. 85, No. EM4, October, 1959.
31. Lee, E. H., "Viscoelastic Stress Analysis", Structural Mechanics, Proceedings, First Symposium on Naval Structural Mechanics, Pergamon Press, New York, 1960.
32. Pister, K. S., and Williams, M. L., "Bending of Plates on a Viscoelastic Foundation", Journal of the Engineering Mechanics Division, Proceedings of the ASCE, Vol. 86, No. EM5, October, 1960.
33. Pister, K. S., and Monismith, C. L., "Analysis of Viscoelastic Flexible Pavements," Flexible Pavement Design Studies 1960, Highway Research Bulletin 269, 1960.
34. Monismith, C. L., and Secor, K. E., "Viscoelastic Behavior of Asphalt Concrete Pavements", Proceedings, International Conference on the Structural Design of Asphalt Pavements, University of Michigan, 1962.
35. Barksdale, R. D., and Leonards, G. A., "Predicting Performance of Bituminous Surfaced Pavements", Proceedings, International Conference on the Structural Design of Asphalt Pavements, University of Michigan, 1967.
36. Pister, K. S., and Westmann, R. A., "Analysis of Viscoelastic Pavements Subjected to Moving Loads," Proceedings, International Conference of the Structural Design of Asphalt Pavements, University of Michigan, 1963.
37. Harr, M. E., and Lewis, K. H., "Analysis of Concrete Slabs Subjected to Warping and Moving Loads", Highway Research Board Record No. 291, 1969.
38. Biot, M. A., "Dynamics of Viscoelastic Anisotropic Media", Proceedings, Fourth Midwestern Conference on Soil Mechanics, September, 1955.
39. Pister, K. S., "Viscoelastic Plate on a Viscoelastic Foundation", Journal of the Engineering Mechanics Division, Proceedings of the ASCE, Vol. 87, No. EM1, February 1961.
40. Harr, M. E., "Influence of Vehicle Speed on Pavement Deflection", Proceedings, Highway Research Board, Vol. 44, 1962.

41. AASHO Road Test Data, "Final Report on Road Test One-MD", Highway Research Board Special Report 4, 1952.
42. Perloff, W. H., and Moavenzadeh, F., "Deflection of Viscoelastic Medium due to a Moving Load", Proceedings, International Conference on the Structural Design of Asphalt Pavements, University of Michigan, 1967.
43. Szendrei, M. E., and Freeme, C. R., "Road Responses to Vibration Tests", Journal of the Soil Mechanics and Foundations Division, Proceedings of the ASCE, Vol. 96, No. SM6, November, 1970.
44. Hall, J. W., "Nondestructive Testing of Flexible Pavements, "A Literature Review", Technical Report No. AFWL-TR-68-147, Air Force Weapons Laboratory, Kirtland Air Force Base, New Mexico, May 1970.
45. Nijboer, I. L. W., "Investigation into the Dynamic Properties of Road Constructions", Science and Industry, Reprint, Vol. 2, 1955.
46. Maxwell, A. A., "Nondestructive Testing of Pavements", Highway Research Board Bulletin 277, 1960.
47. Heukelom, W., "Analysis of Dynamic Deflections of Soils and Pavements", Geotechnique, Vol. 11, No. 3, 1961.
48. Busching, H. W., Goetz, W. H., and Harr, M. E., "Stress-Deformation Behavior of Anisotropic Bituminous Mixtures," Proceedings, Assn. Asphalt Paving Technology, Vol. 36, 1967.
49. Goetz, W. H., Harr, M. E., and Lal, H. B., "Invariant Properties of a Sheet-Asphalt Mixture", Highway Research Record No. 158, 1967.
50. Swami, S. A., Goetz, W. H., and Harr, M. E., "Time and Load Independent Properties of Bituminous Mixtures", Highway Research Record No. 313, 1970.
51. Crafton, P. A., Shock and Vibration in Linear Systems, Harper and Brothers, Inc., N. Y., 1961.
52. Harrison, H. L., and Bollinger, J. G., Introduction to Automatic Controls, International Textbook Company, Inc., Scranton, 1963.
53. Tsien, H. S., Engineering Cybernetics, McGraw-Hill Book Company, Inc., New York, 1954.
54. Harr, M. E., Application of Mathematics for Engineers and Scientists, Unpublished Notes, Purdue University, 1969.

55. Wylie, C. R., Jr., Advanced Engineering Mathematics, McGraw-Hill Book Company, Inc., New York, 1960.
56. Lago, G., and Benningfield, L. M., Control System Theory, The Ronald Press Company, New York, 1962.
57. Swami, S. A., "The Response of Bituminous Mixtures to Dynamic and Static Loads Using Transfer Functions", Ph.D. Thesis Submitted to Purdue University, 1969.
58. Senaut, C. J., Jr., Fundamentals of the Laplace Transform, McGraw-Hill Book Company, Inc., New York, 1962.
59. Senaut, C. J., Jr., Control System Design, McGraw-Hill Book Company, Inc., New York, 1968.
60. Hay, D. R., "Aircraft Characteristics for Airfield Pavement Design and Evaluation", Technical Report No. AFWL-TR-69-54, Air Force Weapons Laboratory, Kirtland Air Force Base, New Mexico, October 1969.
61. Brown, R. G., and Nilsson, J. W., Introduction to Linear Systems Analysis, John Wiley and Sons, Inc., 1966.
62. Raven, F. H., Automatic Control Engineering, McGraw Hill Book Company, New York, 1968.

APPENDICES

APPENDIX A

METHODS FOR DETERMINING TRANSFER FUNCTIONS

"A Priori" Modeling

When "a priori" modeling is employed, a transfer function is normally obtained through a three-stage process. First, a free-body diagram is constructed to model the real system; secondly, an appropriate law, or principle, is invoked (e.g., Newton's Second Law of Motion, Conservation of Energy, etc.) to obtain the governing (differential) equations; and lastly, the (differential) equations are solved so that the ratio of input to output can be formed. As an example of the process, consider the schematic representation of a simple model of a pavement system as shown in Figure 50. Assuming motion to be in the vertical direction only, applying Newton's Second Law of Motion, the governing differential equation of motion becomes

$$m\ddot{x}(t) + c\dot{x}(t) + kx(t) = f(t) \quad (18)$$

Solving equation (18) by Laplace transform method (with initial conditions equal zero) results in (reference 55)

$$\bar{x}(s) = \frac{1}{ms^2 + cs + k} \cdot \bar{f}(s) \quad (19)$$

or,

$$\frac{\bar{x}(s)}{\bar{f}(s)} = \bar{G}(s) = \frac{1}{ms^2 + cs + k} \quad (20)$$

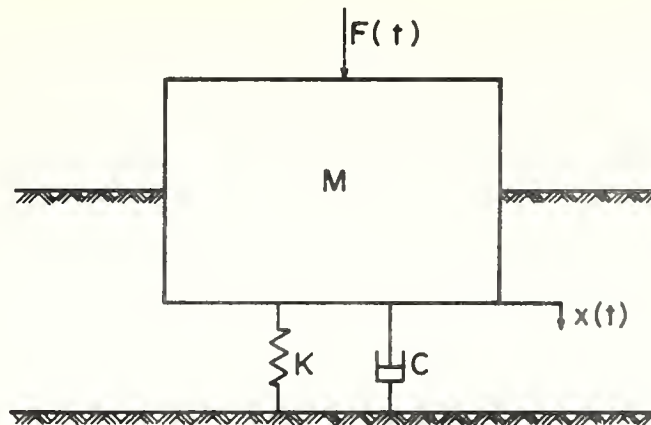


FIGURE 50. SIMPLE SECOND ORDER MODEL

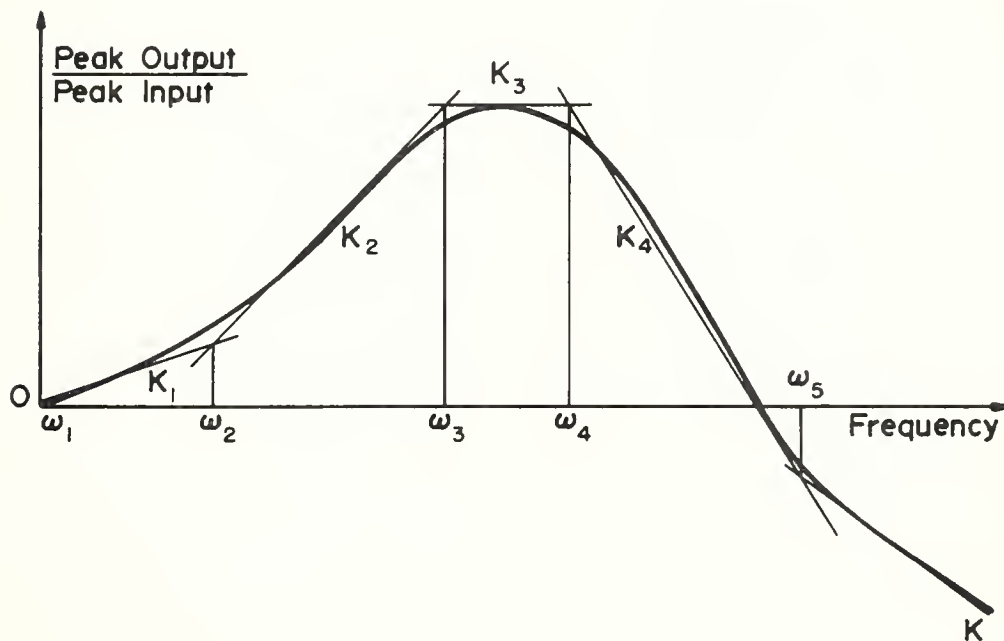


FIGURE 51. ASYMPTOTIC APPROXIMATION OF A SYSTEM'S FREQUENCY SPECTRUM

where,

$\bar{G}(s)$ = transfer function, with displacement of the mass as the operational output and the forcing function as the operational input.

"A Posteriori" Modeling

In "a posteriori" modeling, methods for determining a transfer function are basically experimental. Three commonly used methods are presented below:

Frequency Spectrum

Suppose a sinusoidal input of known magnitude and frequency is applied to a system whose transfer function is sought. The magnitude of the steady-state peak input and the steady-state peak output (and generally the phase angle between the two) are measured. The ratio of the magnitude of the peak output to that of the peak input is plotted for a range of frequencies. The resulting plot is called the "frequency spectrum" for the system. The frequency range need cover only those frequencies wherein the slope of the frequency spectrum curve possesses a changing slope. The curve is then approximated by a series of straight lines as shown in Figure 51. The straight lines are selected so as to provide asymptotes to the curve. The closer the approximation to the actual frequency spectrum curve, the better will be the approximation of the transfer function (reference 51). The intersections of the selected approximating asymptotes determine the "break" frequencies, or "corner" frequencies. In Figure

51, for example, there are five; shown as $\omega_1 = 0$, ω_2 , ω_3 , ω_4 and ω_5 . The slopes of the asymptotes are given as K_1 , K_2 , K_3 , K_4 and K_5 , respectively. Once the break frequencies and the slopes of the approximating asymptotes are ascertained, the modified transfer function which describes the frequency spectrum can be expressed (reference 51) as

$$G(j\omega) = A(j\omega + \omega_1)^{K_1} \cdot (j\omega + \omega_2)^{K_2 - K_1} \dots (j\omega + \omega_n)^{K_n - K_{n-1}} \quad (21)$$

Substituting for the complex variable $s = j\omega$ in equation (21) the experimental transfer function for the system is obtained as

$$G(s) = A(s + \omega_1)^{K_1} \cdot (s + \omega_2)^{K_2 - K_1} \dots (s + \omega_n)^{K_n - K_{n-1}} \quad (22)$$

The constant A can be determined from any one experimental frequency in the frequency spectrum by calculating the absolute value of the transfer function from equation (21) at that frequency and equating it to the corresponding ratio of the magnitude of the peak output to that of the peak input in the frequency spectrum.

Impulse Input

The mathematical nature of an impulse, or Dirac delta function input resolves the transfer function for this system directly as the corresponding output. This input is characterized mathematically as

$$\delta(t) = \lim_{\epsilon \rightarrow 0} F_{\epsilon}(t) = \begin{cases} 1/\epsilon, & 0 \leq t \leq \epsilon \\ 0, & t > \epsilon \end{cases} \quad (23)$$

where,

$\delta(t)$ = impulse, or Dirac delta function

$F_{\epsilon}(t)$ = Heaviside's unit function

It can also be shown (reference 54) that the Laplace transform of the Dirac delta function is unity, or

$$\mathcal{L}[\delta(t)] = 1 \quad (24)$$

Consequently from the definition of a transfer function it is readily seen that for an impulse input

$$\bar{O}(s) = \bar{G}(s) \quad (25)$$

Therefore, theoretically all that need be done to determine a system's transfer function when the system is excited by an impulse input is to measure its output response.

Real Convolution

Both the frequency response and impulse input methods for obtaining a transfer function are frequency, or Laplace, domain approaches: inversion of the solution is required in order to get a time domain solution. Real convolution is essentially a time domain approach. Since it is a time domain response technique, convolution eliminates the transform and inverse transform steps associated with the applications of transfer functions. Basically, the analytical concepts provided by convolution are: (1) proof of multiplicative nature of transfer functions, and (2) duality between multiplication in frequency (or Laplace) domain and convolution in the time domain.

Of equal importance with the concepts identified above, convolution can be used as a numerical and/or graphical tool for computation of responses without resorting to analytical expressions for input.

Convolution introduces the concept of a "system response function".

A system's transfer function is defined as

$$\bar{O}(s) = \bar{G}(s) \cdot \bar{I}(s) \quad (26)$$

where,

$\bar{O}(s)$ = system operational output

$\bar{I}(s)$ = system operational input

$\bar{G}(s)$ = system transfer function

Taking the inverse Laplace transform of equation (25), it follows that

$$\bar{O}(t) = \mathcal{L}^{-1} [\bar{G}(s) \cdot \bar{I}(s)] \quad (27)$$

Equation 27 can then be written in the form (references 54, 58, 61, and 62) of the real convolution integral as

$$O(t) = \int_0^t G(\tau) \cdot I(t-\tau) \cdot d\tau \quad (28)$$

APPENDIX B

REGRESSION ANALYSIS-NORMAL DISTRIBUTION MODEL

COMPUTER PROGRAM

```

PROGRAM NMLFIT(INPUT,OUTPUT,TAPE5=INPUT,TAPE6=OUTPUT)
C.....
C.....PROGRAM NMLFIT
C
C .....
C PURPOSE
C   TO COMPUTE PARAMETER VALUES IN NORMAL
C   DISTRIBUTION MODEL FOR PEAK DYNAMIC DEFLECTION
C   BASIN USING LEAST SQUARES REGRESSION ANALYSIS
C DESCRIPTION OF PARAMETERS
C   X   -VECTOR OF VALUES WHERE DEFLECTIONS WERE MEASURED (INCHES)
C   Y   -VECTOR OF DEFLECTION VALUES TO BE FITTED BY MODEL
C   Z   -VECTOR OF FITTED DEFLECTION VALUES
C   J   -DATA SET NUMBER.
C   K   -NUMBER OF DATA SETS.
C   M   -SETS OF DATUM IN X-Y ARRAYS.
C   XMAX-MAXIMUM VALUE IN X ARRAY.
DIMENSION Y(200), Z(200), W(200)
COMMON/AXIS/X(200)
  9 READ(5,100) J,K,M,XMAX
100 FORMAT(2I1,I2,F10.5)
  DO 8 I=1,M
    8 READ(5,102) Y(I),X(I)
102 FORMAT(32X,2F8.5)
  DO 36 I=1,M
    36 WRITE(6,110) X(I),Y(I)
110 FORMAT(2F10.6)
    F=3.0/XMAX
    DO 30 I=1,M
      30 X(I)=X(I)*F
    CALL NMLFII(Y,Z,M)
    WRITE(6,104)
104 FORMAT(1H1,24X, #X#, 10X, #Z#)
    DO 35 I=1,72
      X(I)=FLOAT(I)
C   PRINT OUT FITTED DATA.
    35 WRITE(6,105) X(I),Z(I)
105 FORMAT(20X,2F10.5)
    IF(J.NE.K) GO TO 9
    STOP
    END

```



```

SUBROUTINE NMLFII(Y,Z,JJJ)
C
C ... SUBROUTINE NMLFII
C
C .....
C PURPOSE
C   LEAST SQUARE METHOD BY USING NEG. EXP. FUNCTION TO FIT VECTOR
C   OF VALUES Y(I) WITH THE HELP OF NEWTON ITERATION METHOD TO
C   SOLVE THE ROOT OF FUNCTION GB.
C DESCRIPTION OF PARAMETERS
C   X -THE AXIS AT WHICH Y(I) IS TABULATED.
C   Y -VECTOR OF VALUES TO BE FITTED BY NEG. EXP. FUNCTIONS.
C   Z -THE CALCULATED VALUES OF NEG. EXP. FUNCTION ON X(I)
C   JJJ-THE DIMENSION OF X,Y,Z.
C SUBROUTINE AND FUNCTION SUBPROGRAM NEEDED.
C   FUNCTION GB AND SUBROUTINE NEWTON.
C METHOD.
C   1. GB IS THE FUNCTION DEDUCED FROM THE LEAST SQUARE METHOD BY
C   USING NEG. EXP. FUNCTIONS. IT ALSO COMPUTES SOME DERIVATIVES
C   VALUES OF GB WITH RESPECT TO EXP(-B).
C   2. CALL SUBROUTINE TO FIND OUT THE ROOT OF GB(EXP(-B)) = 0.
C   3. THEN COMPUTES A AND Z(I).
C
C .....
C
COMMON/AXIS/X(200)
DIMENSION Y(1),Z(1),XGB(200)
J=JJJ
PRINT 5
WRITE(6,212)
212 FORMAT(1H1,1X,*RECORD OF SMOOTH OPERATIONS *//)
DX=.01
XM=1.E-7
XGB(101)=GB(X,Y,XM,J)
XM=1.E-14
XGB(102)=GB(X,Y,XM,J)
XM=1.E-19
XGB(103)=GB(X,Y,XM,J)
DO 40 I=1,100
XM=FLOAT(I)*DX
XGB(I)=GB(X,Y,XM,J)
40 CONTINUE
PRINT 5
PRINT 30,(XGB(K),K=1,103)
CALL NEWTON(X,Y,ROOT,J)
IF(ROOT.EQ.0.) GO TO 150
310 B=-ALOG(ROOT)
VX=0.
VX=VY=0.
DO 20 K=2,J
VX=VX+Y(K)*ROOT**(X(K)*X(K))

```



```

      VY=VY+ROOT**(X(K)*X(K)*2.)
20  CONTINUE
      A=VX/VY
      PRINT 5
      PRINT 100,A,B
100  FORMAT(*0   A=*,F12.6,*   B=*,F12.6)
      GO TO 200
150  PRINT 90
      90  FORMAT(*0   ERROR IN SUBROUTINE ROOTFINDER*)
200  CONTINUE
      PRINT 6
      J=72
      DO 25 I=1,J
      X(I)=FLOAT(I-1)*(3./72.)
      Z(I)=A*(ROOT**(X(I)**2))
25  CONTINUE
      PRINT 30,(Z(I),I=1,J)
      PRINT 6
      5  FORMAT(*+++++*)
      6  FORMAT(*0  =====*)
30  FORMAT(1H0,10F12.6)
      RETURN
      END

```

```

      FUNCTION GB(X,Y,BX,J)

```

```

C
C ... FUNCTION GB
C
C .....
C PURPOSE AND METHOD.
C   GB IS THE FUNCTION DERIVED FROM THE LEAST SQUARE METHOD FOR NEG.
C   EXPONENTIAL FUNCTION  $A \cdot \exp(-B \cdot X \cdot X) = A \cdot (BX^{**}(X \cdot X))$ , WHERE
C    $BX = \exp(-B)$ . DERIVE TWO EQUATIONS FOR TWO UNKNOWNNS A AND
C   BX. ELIMINATE A AND OBTAIN A FUNCTION ONLY DEPENDING
C   ON BX. THIS IS THE GB FUNCTION.
C SUBROUTINE AND FUNCTION SUBPROGRAM DEEDED.
C   NONE.
C DESCRIPTION OF PARAMETERS (SAME AS IN NMLFII J=JJJ)
C   BX - THE INDEPENDENT VARIABLE OF GB. IT RANGES FROM 0. TO 1.
C
C .....
C
C DIMENSION X(1),Y(1)
C XYA=XYB=XYC=XYD=0.
C XYE=XYF=0.
C L=2
C IF(X(1).NE.0.) L=1
C DO 100 I=L,J
C XX=X(I)*X(I)
C IF(XX.EQ.0.) GO TO 200

```



```

      YY=Y(I)*BX**XX
      ZZ=(BX**XX)*(BX**XX)
      GO TO 150
200  YY=Y(I)
      ZZ=1.
150  CONTINUE
      XYA=XYA+YY*XX
      XYB=XYB+XX*ZZ
      XYC=XYC+YY
      XYD=XYD+ZZ
      XYE=XYE+YY*XX*XX
      XYF=XYF+ZZ*XX*XX
100  CONTINUE
      GB=XYA/XYB-XYC/XYD
      X(195)=XYA
      X(196)=XYB
      X(197)=XYC
      X(198)=XYD
      X(199)=XYE
      X(200)=XYF
      RETURN
      END

```

SUBROUTINE NEWTON(X,Y,ROOT,J)

```

C
C ... SUBROUTINE NEWTON
C
C .....
C PURPOSE AND METHOD
C   USE NEWTON RALPSON METHOD TO SOLVE FOR THE ROOT OF GB FUNCTION
C   WITH THE INITIAL VALUE IN UU.
C   WITH THE INITIAL VALUE IN UU, DERIVATIVE OF GB IS CALCULATED IN
C   GB FUNCTION ROUTINE. THE NO. OF ITERATIONS (ICOUNT) CANNOT
C   EXCEED OVER 150 TIMES. THE ROOT WILL BE RETURNED IN ROOT.
C SUBROUTINE AND FUNCTION SUBPROGRAM DEEDED.
C   GB FUNCTION ROUTINE.
C
C .....
C
C DIMENSION X(1),Y(1)
C UU=.99999999
C UU=.6
C TEST=1.E-7
C ICOUNT=0
10 GUU=GB(X,Y,UU,J)
   DUU=X(199)/X(196)-2.*X(200)*X(195)/(X(196)*X(196))-X(195)/X(198)
   1-2.*X(196)*X(197)/(X(198)*X(198))
   IF(DUU.EQ.0.) GO TO 150
   IF(ABS(GUU).LT.TEST) GO TO 100
   U=UU*(1.-GUU/DUU)

```



```
IF(U.LT.0.) U=UU/2.
IF(ABS(U-UU).LT.TEST) GO TO 100
IF(ICOUNT.GE.150) GO TO 160
ICOUNT=ICOUNT+1
UU=U
PRINT 20,ICOUNT,GUU,U
GO TO 10
100 ROOT=U
RETURN
150 PRINT 5
5 FORMAT(=0 *** ZERO DERIVATIVE OF GB,EXITS ≠)
STOP
160 PRINT 6
6 FORMAT(=0 *** ITERATIONS OVER 150 TIMES,EXITS ≠)
20 FORMAT(* +++,I4,* +++,2F12.6)
GO TO 100
END
```


APPENDIX C

SIGNATURE AND TIME-DEPENDENT TRANSFER FUNCTIONS

COMPUTER PROGRAM

```

PROGRAM CONVLI(INPUT,OUTPUT,TAPE5=INPUT,TAPE6=OUTPUT,PLOT)
DIMENSION XINP(150),XOUT(150),XG(150),W(10)
DIMENSION DEFL(6,500),Z(500),GT(6,500),Y(500),GF(6,500)
COMMON/AXIS/X(500)
DIMENSION RDD(10),RDN(10),RDF(10,150),M(10)
DIMENSION IPS(9),NAME(10),PEAK(12),CONT(10),MONT(10),SPK(10)
DIMENSION V1(200),V2(200),V3(200),V4(200),V5(200),V6(200)
INTEGER CONT,BEGIN,END
REAL MOD,INCR
C      .....READ DATA BEGIN AND END, DATA SET NUMBERS, NUMBER OF SEQUENCE
C      VALUES, DIGITIZED TIME INCREMENT, PLOT COMMAND, NORMAL
C      MODEL PARAMETER VALUES, TIME RANGE, NUMBER OF DESIRED
C      ARRAY VALUES, AND COMMON ORIGIN COMMAND
READ(5,100) BEGIN, END, N, DT, IPLOT, A, B, RANGE, NY, IMOD
N1=N
IF(IPLOT.NE.0) CALL PLOTS
CALL FACTOR(0.6)
INS=2
INL=6
NMY=NY-1
DY=RANGE/FLOAT(NMY)
DO 410 K=1,NY
410 Y(K)=FLOAT(K-1)*DY
C      .....BEGIN LOOP TO CALCULATE SIGNATURE AND TDT FUNCTIONS
DO 1000 J=BEGIN, END
C      .....READ IDENTIFICATION AND DATA
WRITE(6,208) J
READ (8,106) (NAME(I),I=1,9)
WRITE(6,107) (NAME(L),L=1,9)
DO 30 I=1,6
30 READ(8) (DEFL(I,K),K=1,N)
READ (8) ICC
IF(FOF,8) 405,50
405 CONTINUE
C
C      FOR EACH RESPONSE FUNCTION-
C      (1) MODIFY RESPONSE FUNCTIONS TO OBTAIN COMMON ORIGIN(IF NECESSARY)
C      (2) DETERMINE PEAK VALUE OF EACH RESPONSE FUNCTION
C      (3) STORE SEQUENCE NUMBER OF EACH PEAK VALUE
C
DO 396 I=1,6
PEAK(I)=0.
IF(IMOD.EQ.0) GO TO 394

```



```

    AVE=0.
    DO 391 K=1,10
391 AVE=AVE+DEFL(I,K)
    MOD=AVE/10.
393 DO 399 K=1,N
399 DEFL(I,K)=DEFL(I,K)-MOD
394 DO 395 K=1,N
    IF(ABS(PEAK(I)).LT.ABS(DEFL(I,K))) CONT(I)=K
395 IF(ABS(PEAK(I)).LT.ABS(DEFL(I,K))) PEAK(I)=DEFL(I,K)
396 CONTINUE
C
C    FOR PRIMARY RESPONSE FUNCTION (I.E.,DEFL(2,K))-
C    (1)ESTABLISH PERCENT OF PEAK VALUE TO RETAIN SEQUENCE VALUES
C    (2)TEST SEQUENCE VALUES VERSUS PERCENT OF PEAK(RETAIN .GT.)
C    (3)ZERO ALL SEQUENCE VALUES LESS THAN PERCENT OF PEAK VALUE
C    (4)REDEFINE N
C
    GAP=.002
    DO 273 L=1,N
    IF(ABS(DEFL(INS,L)).GT.GAP.AND.L.GT.2) GO TO 290
    LI=L
    DEFL(INS,1)=DEFL(INS,LI)
273 CONTINUE
290 DEFL(INS,2)=DEFL(INS,LI+1)
    LK=CONT(INS)-LI
    N=3*LK+3
    DO 397 K=3,N
    DEFL(INS,K)=DEFL(INS,K+LI-1)
    IF(DEFL(INS,K).LT.0.) DEFL(INS,K)=0.
397 CONTINUE
    INB=INS+1
    DO 299 I=INB,INL
    DO 299 K=1,N
    DEFL(I,K)=DEFL(I,K+LI-1)
    IF(DEFL(I,K).LT.0.)DEFL(I,K)=0.
299 CONTINUE
    NK=N+1
    DO 295 I=INS,INL
    DO 295 K=NK,N1
    DEFL(I,K)=0.
295 CONTINUE
    DO 298 I=1,6
    PEAK(I)=0.
    DO 298 K=1,N
    IF(ABS(PEAK(I)).LT.ABS(DEFL(I,K))) CONT(I)=K
    IF(ABS(PEAK(I)).LT.ABS(DEFL(I,K))) PEAK(I)=DEFL(I,K)
298 CONTINUE
C    .... EXTEND OR COMPRESS DEFL ARRAY TO LENGTH = NY
    DZ=RANGE/FLOAT(N-1)
    IF(N.EQ.NY) GO TO 429
    DO 411 K=1,N

```



```

411 Z(K)=FLOAT(K-1)*DZ
    DO 420 I=2,6
        IPT=1
        GT(I,1)=DEFL(I,1)
        GT(I,NY)=DEFL(I,N)
        DO 421 K=2,NMY
425 IF(Y(K) .LE. Z(IPT+1)) GO TO 424
        IPT=IPT+1
        IF(IPT.GT.N+5) GO TO 50
        GO TO 425
424 OMG=(Y(K)-Z(IPT))/DZ
421 GT(I,K)=OMG*DEFL(I,IPT+1)+(1.-OMG)*DEFL(I,IPT)
420 CONTINUE
    DO 426 I=2,6
        DO 427 K=1,NY
            DEFL(I,K)=GT(I,K)
427 GT(I,K)=0.
        DEFL(I,NY+1)=DEFL(I,NY+2)=DEFL(I,NY+3)=DEFL(I,NY)
426 CONTINUE
        N=NY
429 CONTINUE
431 CONTINUE
C
C     PRINT NEW TIME-DEPENDENT DEFLECTION RESPONSE FUNCTIONS(TRUNCATED)
C
        JL=0
1098 DO 1099 I=INS,INL
        W(I)=FLOAT(I-INS)*.75
        RDD(I)=A*EXP(-B*W(I)**2)
        RDN(I)=RDD(I)/PEAK(I)
        RDF(I,1)=RDN(I)
        DO 1100 K=1,N
1100 DEFL(I,K)=DEFL(I,K)*RDN(1)
        JK=100*J
        DO 800 K=1,N
            800 GT(I,K+JK)=DEFL(I,K)
1099 CONTINUE
        IF(JL.EQ.1) GO TO 802
        IF(J.NE.3) GO TO 1001
        DO 801 I=INS,INL
            DO 801 K=1,N
                DEFL(I,K)=(GT(I,K+100)+GT(I,K+200)+GT(I,K+300))/3.
801 CONTINUE
        JL=1
        DO 805 I=INS,INL
            PEAK(I)=0.
            DO 805 K=1,N
                IF(ABS(PEAK(I)).LT.ABS(DEFL(I,K))) CONT(I)=K
                IF(ABS(PEAK(I)).LT.ABS(DEFL(I,K))) PEAK(I)=DEFL(I,K)
805 CONTINUE
        GO TO 1098

```



```

802 CONTINUE
    WRITE(6,213)
    WRITE(6,214)
    WRITE(6,215)
213 FORMAT(1H1,1X////,12X'                DEFLECTION RESPONSE F
*UNCTIONS')
C      .....INPUT AIRCRAFT AND SITE IDENTIFICATION
214 FORMAT(38X,'C135 AIRCRAFT-SITE 1')
215 FORMAT(1X//,'                TIME                RESPONSE 0  RESPONSE 1  R
*ESPONSE 2  RESPONSE 3  RESPONSE 4')
    DO 1103 K=1,N
    DEFL(1,K)=0.
1103 PRING 201,Y(K),(DEFL(1,K),I=2,6)
    DO 1104 K=1,N
1104 PUNCH 108,(DEFL(I,K),I=2,6)
500 DO 501 I=1,6
    DO 501 K=1,N
501 GF(I,K)=0.0
    DO 404 K=1,N
404 XINP(K)=DEFL(INS,K)
    INB=INS+1
    DO 401 I=INB,INL
    DO 402 K=1,N
402 XOUT(K)=DEFL(I,K)
    CALL CONVL1(XINP,XOUT,XG,DY,N,PEAK(2))
    DO 403 K=1,N
403 GF(I,K)=XG(K)
401 CONTINUE
    WRITE(6,216)
    WRITE(6,217)
    WRITE(6,218)
216 FORMAT(1H1,1X////,'                TDT FUNCTI
*ONS')
C      .....INPUT AIRCRAFT AND SITE IDENTIFICATION
217 FORMAT(32X,'C135 AIRCRAFT-SITE 1')
218 FORMAT(1X//,'                TIME                FUNCTION 1  FUNCTION 2  FU
*UNCTION 3  FUNCTION 4')
    DO 502 K=1,N
502 PRINT 201,Y(K),(GF(I,K),I=3,6)
    DO 503 K=1,N
503 PUNCH 108,(GF(I,K),I=2,6)
    IF(IPLOT.EQ.0) GO TO 1001
C
C      .....PLOT TDT FUNCTIONS AND SIGNATURE
C
    DO 530 K=1,N
    V2(K)=0.0
    V3(K)=0.0
    V4(K)=0.0
    V5(K)=0.0
    V6(K)=0.0

```



```

530 CONTINUE
C
C     .....DETERMINE SCALING PARAMETERS FOR TDT FUNCTIONS
C
    DO 506 K=1,N
    V2(K)=GF(2,K)
    V3(K)=GF(3,K)
    V4(K)=GF(4,K)
    V5(K)=GF(5,K)
    V6(K)=GF(6,K)
506 CONTINUE
    CALL SCALES(10.0,V2,N,1,V3,N,1,V4,N,1,V5,N,1,V6,N,1)
    CALL SCALE(X,10.0,N,1)
C
C     ..... PLOT AXES AND ANNOTATION
C
    CALL AXIS(0.0,0.0,12HTIME,SECONDS,-12,10.0,0.0,X(N+1),X(N+2),0)
    CALL AXIS(0.0,0.0,17HRESPONSE FUNCTION,17,10.0,90.0,V2(N+1),V2(N+2
*) , -1)
    CALL SYMBOL(3.5,10.0,0.2,18HRESPONSE FUNCTIONS,0.0,18)
    CALL SYMBOL(8.0,8.2,0.08,1,0.0,-1)
    CALL SYMBOL(8.1,8.14,0.08,11H-RESPONSE 1,0.0,11)
    CALL SYMBOL(8.0,8.1,0.08,2,0.0,-1)
    CALL SYMBOL(8.1,8.04,0.08,11H-RESPONSE 2,0.0,11)
    CALL SYMBOL(8.0,8.0,0.08,3,0.0,-1)
    CALL SYMBOL(8.1,7.94,0.08,11H-RESPONSE 3,0.0,11)
    CALL SYMBOL(8.0,7.9,0.08,4,0.0,-1)
    CALL SYMBOL(8.1,7.84,0.08,11H-RESPONSE 4,0.0,11)
    CALL SYMBOL(8.0,7.8,0.08,5,0.0,-1)
    CALL SYMBOL(8.1,7.74,0.08,11H-RESPONSE 5,0.0,11)
    CALL SYMBOL(8.0,7.7,0.08,6,0.0,-1)
    CALL SYMBOL(8.1,7.64,0.08,11H-RESPONSE 6,0.0,11)
C
C     .....PLOT TDT FUNCTIONS
C
    DO 517 I=INB,INL
    DO 509 K=1,N
509 Z(K)=GF(I,K)
    Z(N+1)=V2(N+1)
    Z(N+2)=V2(N+2)
    CALL LINE(X,Z,N,1,10,1)
517 CONTINUE
    CALL PLOT(18.0,0.0,-3)
    DO 615 K=1,N
615 XG(K)=DEFL(INS,K)
    CALL SCALE(X,10.0,N,1)
    CALL SCALE(XG,10.0,N,1)
C
C     .....PLOT AXES AND ANNOTATION
    CALL AXIS(0.0,0.0,12HTIME,SECONDS,-12,10.0,0.0,X(N+1),X(N+2),0)
    CALL AXIS(0.0,0.0,17HDEFLECTION,INCHES,17,10.0,90.0,XG(N+1),XG(N+2
*) , -1)

```



```

CALL SYMBOL(3.5,10.0,0.2,14HSIGNATURE PLOT,0.0,14)
CALL SYMBOL(8.0,8.2,0.08,1,0.0,-1)
CALL SYMBOL(8.1,8.14,0.08,11H-RESPONSE 1,0.0,11)
CALL SYMBOL(8.0,8.1,0.08,2,0.0,-1)
CALL SYMBOL(8.1,8.04,0.08,11H-RESPONSE 2,0.0,11)
CALL SYMBOL(8.0,8.0,0.08,3,0.0,-1)
CALL SYMBOL(8.1,7.94,0.08,11H-RESPONSE 3,0.0,11)
CALL SYMBOL(8.0,7.9,0.08,4,0.0,-1)
CALL SYMBOL(8.1,7.84,0.08,11H-RESPONSE 4,0.0,11)
CALL SYMBOL(8.0,7.8,0.08,5,0.0,-1)
CALL SYMBOL(8.1,7.74,0.08,11H-RESPONSE 5,0.0,11)
CALL SYMBOL(8.0,7.7,0.08,6,0.0,-1)
CALL SYMBOL(8.1,7.64,0.08,11H-RESPONSE 6,0.0,11)
C      .....PLOT SIGNATURE.....
      CALL LINE(X,XG,N,1,10,1)
      CALL PLOT(18.0,0.0,-3)
1001 N=N1
1000 CONTINUE
      IF(IPL0T.NE.0) CALL PLOT(0,0,999)
C      =====
C
100 FORMAT(3I3,F10.5,411)
102 FORMAT(8F10.5)
103 FORMAT(12)
104 FORMAT('0==== FOURIER COEFFICIENTS FOR G FUNCTION NO.',I2,/,
*      '      A(I) =',10F11.4)
105 FORMAT('0      B(I) =',10E11.4)
106 FORMAT(9R8)
107 FORMAT(1H0,1X///1X,9R8)
108 FORMAT(5F16.12)
200 FORMAT(1H1,1X,'      RECORD OF RAW DATA      '//1X,'      TIME      RESPON
*SE 1 RESPONSE 2 RESPONSE 3 RESPONSE 4 RESPONSE 5 RESPONSE 6')
201 FORMAT(12X,7F12.6)
208 FORMAT(1H1,1X//////////////////////////1X,'
*      DATA SET NUMBER',2X,I2)
210 FORMAT(21(8E10.3/),7E10.3)
211 FORMAT(1H1,1X,'RECORD OF RESPONSE FUNS '//1X,'      TIME      RESPON
*SE L RESPONSE 2 RESPONSE 3 RESPONSE 4 RESPONSE 5 RESPONSE 6')
250 FORMAT('0      ILLEGAL EOF ENCOUNTERED')
      STOP
50 PRINT 250
      STOP
      END

SUBROUTINE CONVLI
C      PURPOSE
C      TO COMPUTE THE VECTOR OF VALUES OF
      XG FROM CONVOLUTION EQUATION XINP*XG=XOUT.
      FOR GIVEN XINP(I) AND XOUT(I)
C      DISCRIPTION OF PARAMETERS

```



```

C      XINP-INPUT VECTOR OF VALUES
C      XOUT-OUTPUT VECTOR OF VALUES AFTER CONVOLUTION
C      XG-VECTOR OF VALUES OF CONVOLUTION FUNCTION
C      DT-INCREMENT OF THE SUMMATION POINTS
C      N-NUMBER OF SUBINTERVAL PLUS 1.
C      SUBROUTINES AND FUNCTION SUBPROGRAMS NEEDED
C      NONE
C      METHOD
C      1. SET THE VALUE OF 'TEST'. THEN TEST THE VALUES OF XINP(I) TO
C          SEE WHETHER XINP(I) IS GREATER THAN TEST OR NOT
C      2. IF MAGNITUDE OF XINP(K) IS GREATER THAN 'TEST' THEN MAKE UP
C          K MORE VALUES OF XOUT(I) AND K MORE SUMMATION EQUATIONS
C      3. CONSIDER THE SUMMATION EQUATIONS WHICH IS TRANSFERED FROM
C          INTEGRATION EQUATION OF CONVOLUTION.
C      4. BY FORWARD SUBSTITUTION METHOD TO
C          SOLVE FOR XG(I), I=1,...,N.
C      SUBROUTINE CONVLI(XINP,XOUT,XG,DT,N,PEAK)
C
C      .....
C
C      DIMENSION XINP(1),XOUT(1),XG(1)
C      DIMENSION Z(200),Y(200),W(200)
C      A=0.
C      TEST=.000001
C      DO 150 I=1,N
150  XG(I)=0.0
C      DO 151 K=1,N
C      IF(ABS(XINP(K)).LT.TEST) GO TO 151
C      L=K
C      GO TO 152
151  CONTINUE
152  IN=L-1
C      IM=N+L-1
C      DO 153 K=1,IN
153  XOUT(N+K)=XOUT(N)
C      DO 155 I=L,IM
C      II=I-1
C      DO 154 K=L,II
154  A=A+XG(K-L+1)*XINP(I-K+L)
C      XINP(L)=10.*PEAK
C      XG(I-L+1)=(XOUT(I)-A*DT)/(XINP(L)*DT)
155  A=0.0
C      RETURN
C      END

```


APPENDIX D

PREDICTING PAVEMENT PERFORMANCE

COMPUTER PROGRAM

```

PROGRAM CONVLE(INPUT,OUTPUT)
C
C ///////////////////////////////////////////////////
C
C PROGRAM CONVLE
C
C .....
C
C ... PURPOSE
C   READ IN DEFLECTION RESPONSE AND TDT FUNCTIONS TO PREDICT
C   SIGNATURES AND TDT FUNCTIONS. THEN USE THE PREDICTED
C   SIGNATURE AND TDT FUNCTIONS TO REPRODUCE THE DEFLECTION
C   FUNCTIONS( BY CONVLE2)
C ... DESCRIPTIONS OF VARIABLES
C   XINP,XOUT,XG - VARIABLES FOR SUBROUTINE CONVLE2
C   Y - THE COORDINATE ARRAY
C   FUNS - INPUT TDT FUNCTIONS
C         FIRST INDEX IS THE SITE AND AIRCRAFT NUMBER
C         SECOND INDEX IS THE TDT-X FUNCTION
C         THIRD INDEX IS THE ARRAY NUMBER IN THE TDT-X FUNCTION
C   DEFL - INPUT DEFLECTION FUNCTIONS
C         INDICES ARE SAME AS IN FUNS
C   PFUN - PREDICTED TDT FUNCTIONS
C         INDICES ARE SAME AS THE SECOND AND THIRD INDEX OF FUNS
C   PDEFL - PREDICTED DEFLECTION FUNCTIONS
C         INDICES ARE SAME AS IN PFUN
C   PTDT - THE PEAK VALUES FOR EVERY TDT-3 FUNCTIONS
C   FCTOR - MULTIPLICATION FACTORS FOR SIGNATURE PREDICTION
C   NT - TOTAL NO. OF SITES TIMES TOTAL NO. OF AIRCRAFTS
C   N - THE LENGTH OF EACH INPUT DEFL AND TDT FUNCTIONS
C   IST - STANDARD SITE NUMBER
C   IAIR - 1=C135,2=C131,3=C130
C   JA - STANDARD AIRCRAFT ON STANDARD SITE
C   JJ - STANDARD AIRCRAFT ON CURRENT SITE
C   JB - CURRENT AIRCRAFT ON CURRENT SITE
C   JC - CURRENT AIRCRAFT ON STANDARD SITE
C
C ... ROUTINES AND FUNCTIONS NEEDED
C   CONVLE2
C
C ... METHOD
C   1. USE FACTOR MULTIPLICATION FOR PREDICTING SIGNATURE ( BY
C       FCTOR(M,N))

```



```

C      2. USE FACTOR MULTIPLICATION FOR PREDICTING TDT FUNCTIONS
C      OTHER THAN TDT-3 (BY FTR)
C      3. FOR TDT-3 USE SAME METHOD BUT WITH PEAK AJUSTED TO THE
C      CORRESPONDING PEAK OF STANDARD AIRCRAFT ON CURRENT SITE
C      4. MAIN LOOP IS ON SITE 1 AIRCRAFT 123 (EXCEPT IAIR)
C      THEN TO SITE 2,3 (EXCEPT STANDARD SITE) FOR EXAMPLE,
C      IST=2,IAIR=2, THE PREDICTIONS AND REPRODUCTIONS WILL
C      BE ON SITE 1 AIRCRAFT 1,3 AND SITE 3 AIRCRAFT 1,3
C
C      .....
C
C      DIMENSION XINP(70),XOUT(70),XG(70),Y(51),FUNS(9,6,51),PFUN(6,51)
C      DIMENSION DEFL(9,6,51),PDEFL(6,51)
C      DIMENSION IAP(3),PTDT(9)
C      DIMENSION FCTOR(3,3)
C      IAP(1)=4RC135
C      IAP(2)=4RC131
C      IAP(3)=4RC130
C      DO 91 I=1,3
C      DO 91 J=1,3
C 91 FCTOR(I,J)=1.
C      FOLLOWING FOUR CARDS ARE REQUIRED TO INPUT FACTORS FOR
C      CALCULATING FOURTH SIGNATURE
C      FCTOR(1,1)=1.49
C      FCTOR(1,3)=1.49
C      FCTOR(3,1)=0.77
C      FCTOR(3,3)=0.77
C      NT=9
C      N=47
C      DY=.04
C      IST=2
C      IAIR=2
C      INPUT KNOWN DEFLECTION RESPONSE FUNCTIONS TDT FUNCTIONS
C      DO 10 I=1,NT
C      DO 30 K=1,N
C 30 READ 101,(DEFL(I,L,K),L=2,6)
C      DO 35 K=1,N
C 35 READ 101,(FUNS(I,L,K),L=2,6)
C 10 CONTINUE
C      DO 40 I=1,NT
C      PTDT(I)=0.
C      DO 41 K=1,N
C      IF(ABS(PTDT(I)).LT.ABS(FUNS(I,3,K))) PTDT(I)=FUNS(I,3,K)
C 41 CONTINUE
C 40 CONTINUE
C      USE FACTOR MULTIPLICATION TO MODIFY THE PREDICTED TDT FUNCTIONS
C      DO 50 I=1,3
C      JA=(IST-1)*3+IAIR
C      JJ=(I-1)*3+IAIR
C      IF(I.EQ.IST) GO TO 50
C      DO 51 J=1,3

```



```

      JB=(I-1)*3+J
      JC=(IST-1)*3+J
      IF(J.EQ.IAIR) GO TO 51
      DO 81 M=3,6
      AJ=DJ=0.
      DO 80 K=1,N
      IF(ABS(AJ).LT.ABS(FUNS(JA,M,K))) AJ=FUNS(JA,M,K)
      IF(ABS(DJ).LT.ABS(FUNS(JJ,M,K))) DJ=FUNS(JJ,M,K)
80  CONTINUE
      IF(AJ.EQ.0.) AJ=1.E-13
      IF(M.NE.3) GO TO 16
C    FOR TDT-3 OF CURRENT AIRCRAFT ON CURRENT SITE, AJUST THE PEAK
C    VALUE TO BE SAME AS THE CORRESPONDING STANDARD AIRCRAFT
C    ON CURRENT SITE, THEN COPY THE CORRESPONDING TDT-3 FROM THE
C    CURRENT AIRCRAFT ON STANDARD SITE WITH FACTOR MULTIPLICATION
C    TO AJUST THE PEAK VALUE SPECIFIED AS ABOVE.
      AJ=PTDT(JC)
      DJ=PTDT(JJ)
16  FTR=DJ/AJ
      DO 14 K=1,N
14  PFUN(M,K)=FUNS(JC,M,K)*FTR
81  CONTINUE
C .... PREDICT SIGNATURE BY RATIO MULTIPLICATION
      DO 15 K=1,N
      PDEFL(2,K)=DEFL(JC,2,K)*FCTOR(I,J)
15  CONTINUE
      DO 82 MY=1,5
      PRINT 216
      PRINT 217,IAP(J),I
      PRINT 218
      DO 70 LA=1,N
      Y(LA)=FLOAT(LA-1)*DY
70  PRINT 201,Y(LA),(FUNS(JB,KA,LA),KA=2,5)
      PRINT 226
      PRINT 217,IAP(J),I
      PRINT 218
      DO 71 LA=1,N
71  PRINT 201,Y(LA),(PFUN(KA,LA),KA=2,5)
82  CONTINUE
      DO 45 II=3,6
      PEA=0.
      DO 46 K=1,N
      XINP(K)=PDEFL(2,K)
      IF(ABS(PEA).LT.ABS(XINP(K))) PEA=XINP(K)
46  XG(K)=PFUN(II,K)
      MK=0
      M=N
C    REPRODUCTION BY CALLING CONVL2
      CALL CONVL2(XINP,XOUT,XG,DY,M,PEA)
      DO 47 K=1,N
      IF(XOUT(K+MK).LT.0.) XOUT(K+MK)=0.

```



```

47 PDEFL(I,I,K)=XOUT(K+MK)
45 CONTINUE
    DO 83 MY=1,5
      PRINT 213
      PRINT 214,IAP(J),I
      PRINT 215
      DO 76 NB=1,N
67 PRINT 201,Y(NB),(DEFL(JB,KA,NB),KA=2,6)
      PRINT 223
      PRINT 214,IAP(J),I
      PRINT 215
      DO 72 NB=1,N
72 PRINT 201,Y(NB),(PDEFL(KA,NB),KA=2,6)
83 CONTINUE
51 CONTINUE
50 CONTINUE
    STOP
101 FORMAT(5F16.12)
201 FORMAT(13X,F11.2,5F11.6)
213 FORMAT(1H1,////36X,ORIGINAL DEFL. RESPONSE FUNCS)
214 FORMAT(40X,R4, AIRCRAFT SITE-,I1,/)
215 FORMAT(20X,TIME RESP 0 RESP 1 RESP 2 RESP 3
*ESP 4)
216 FORMAT(1H1,////33X,ORIGINAL TDT FUNCTIONS)
217 FORMAT(34X,R4, AIRCRAFT SITE-,I1,/)
218 FORMAT(20X,TIME FUNC 1 FUNC 2 FUNC 3 FUNC 4)
223 FORMAT(1H1,////24X,PREDICTED DEFL. RESPONSE FUNCS (BY RATIO MULTIP
*LOCATION))
226 FORMAT(1H1,////33X,PREDICTED TDT FUNCTIONS)
END

```

```
C      SUBROUTINE CONVL2(XINP,XOUT,XG,DT,N,PEAK)
C
C      //////////////////////////////////////
C      SUBROUTINE CONVL2
C      .....
C      PURPOSE
C          TO COMPUTE THE VECTOR OF VALUES OF XOUT(I) FOR GIVEN
C          VECTORS...XINP(I) AND XG(I) BY USING CONVOLUTION TECHNIQUE.
C          (I.E. CONVOLUTE XINP(I) AND XG(I) BY SUMMATION METHOD)
C      DISCRPTION OF PARAMETERS
C          XINP-INPUT VECTOR OF VALUES
C          XOUT-OUTPUT VECTOR OF VALUES AFTER CONVOLUTION
C          XG-VECTOR OF VALUES OF CONVOLUTION FUNCTION
C          DT-INCREMENT OF THE SUMMATION POINTS
C          N-NUMBER OF SUBINTERVAL PLUS 1.
C
C      SUBROUTINES AND FUNCTION SUBPROGRAMS NEEDED
C          NONE
C      METHOD
```



```

C      TRANSFER THE INTEGRATION FORMULA OF CONVOLUTION INTO
C      FINITE SUMMATION EQUATIONS WITH SUBINTERVALS OF LENGTH DT AND
C      NUMBER N-1. COMPUTE XOUT(I) BY GIVEN VALUES OF XINP
C      AND XG DIRECTLY
C
C      .....
C
      DIMENSION XINP(1),XOUT(1),XG(1)
      XINP(1)=10.*PEAK
      DO 100 I=1,N
      XOUT(I)=0.
      DO 150 J=1,I
      XOUT(I)=XOUT(I)+XG(J)*XINP(I-J+1)*DT
150 CONTINUE
100 CONTINUE
      RETURN
      END

```


APPENDIX E

EXPLORATORY TESTS

A series of exploratory tests were conducted on an operational taxiway at Kirtland AFB, New Mexico (Albuquerque International Airport). The sensing devices used to measure deflection response functions consisted of linear variable differential transformers (LVDT) and accelerometers. The placement of these sensing devices relative to the path of travel of a prime mover are as shown in Figure 52. Figure 53 shows the instrumentation setup and the sensing devices in place prior to a data run with a prime mover; both LVDT and accelerometer devices are depicted.

The prime movers selected for these tests included a load cart with a 25,000 pounds single wheel load and a Boeing 727 aircraft with a 65,000 pounds single main gear load. Figures 54 and 55 show the load cart and aircraft, respectively.

Installation and Calibration

Linear Variable Differential Transformer (LVDT). The differential transformer was installed in a holder which could be removed when not in use. First, a six inch diameter hole was drilled through the pavement system to a depth of approximately 16 feet into the subgrade; a four inch diameter galvanized steel pipe casing was then inserted in the hole; and, subsequently, a 3/8 inch steel reference rod was placed inside the galvanized steel pipe to serve as a reference for the core of the differential transformer (see Figure 56 for a detail

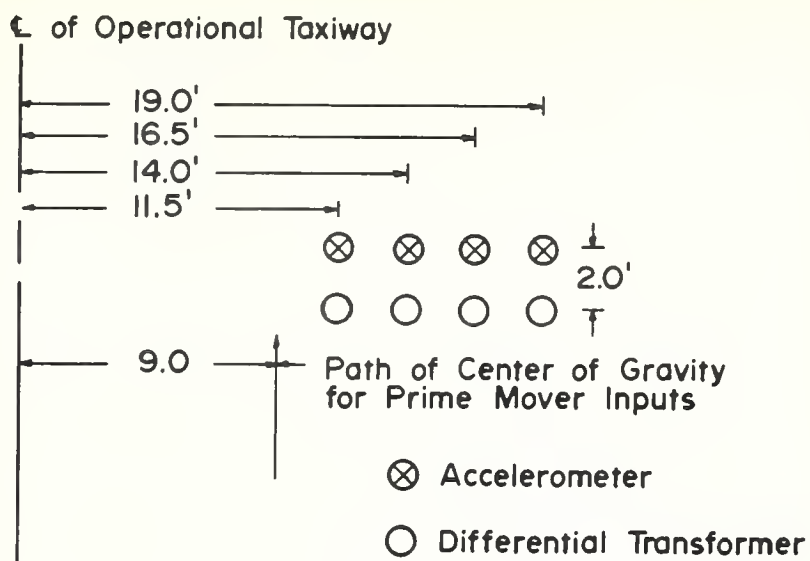


FIGURE 52. LAYOUT OF SENSING DEVICES



FIGURE 53. INSTRUMENTATION SETUP



FIGURE 54. LOAD CART



FIGURE 55. BOEING 727 AIRCRAFT

representation of the assembly). The holder was composed of an interior threaded aluminum sleeve permanently fixed to the pavement wearing course with an epoxy (see Figure 57). The differential transformer coil was held by three set screws in a brass sleeve which mated with the aluminum sleeve fixed to the pavement surface. A cap with an extension rod internally threaded to receive a LVDT core was fitted over the reference rod. The brass sleeve containing the LVDT coil was then placed in position within the aluminum sleeve; wherein, the coil moved with the aluminum sleeve fixed in the pavement wearing course, while the core remained in a fixed position on top of the reference rod. Components of the holder assembly are shown in Figures 58 and 59.

Once the entire assembly was completed, calibrations were achieved by turning the brass sleeve a predetermined number of revolutions from a null position within the fixed aluminum sleeve. One revolution of the brass sleeve provided a displacement of 0.005 inch. After the calibrations were obtained the differential transformer was placed in a null position. Data was placed on magnetic tape using an Ampex FR1300 tape recorder as a prime mover proceeded along the taxiway.

Accelerometer. The accelerometers were installed on a removable pedestal to facilitate removal of the sensing devices when not in use (see Figure 53). The pavement surface was polished slightly with carborundum paper where the accelerometer was to be placed. Subsequently, a quick-drying epoxy was used to fix a small plug to the pavement surface. The plug was internally threaded to accept the external threads on the accelerometer. The accelerometer was precalibrated so

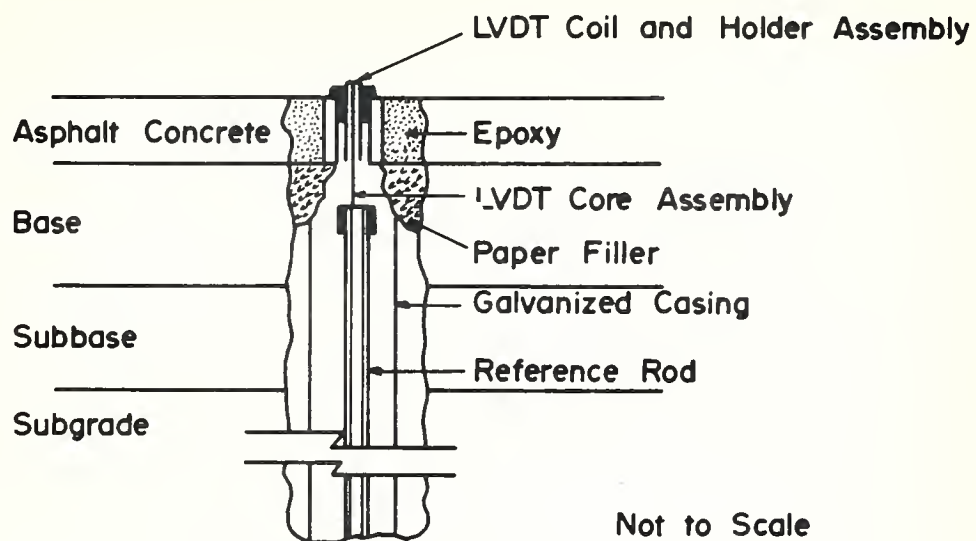


FIGURE 56. LVDT INSTALLATION DETAIL

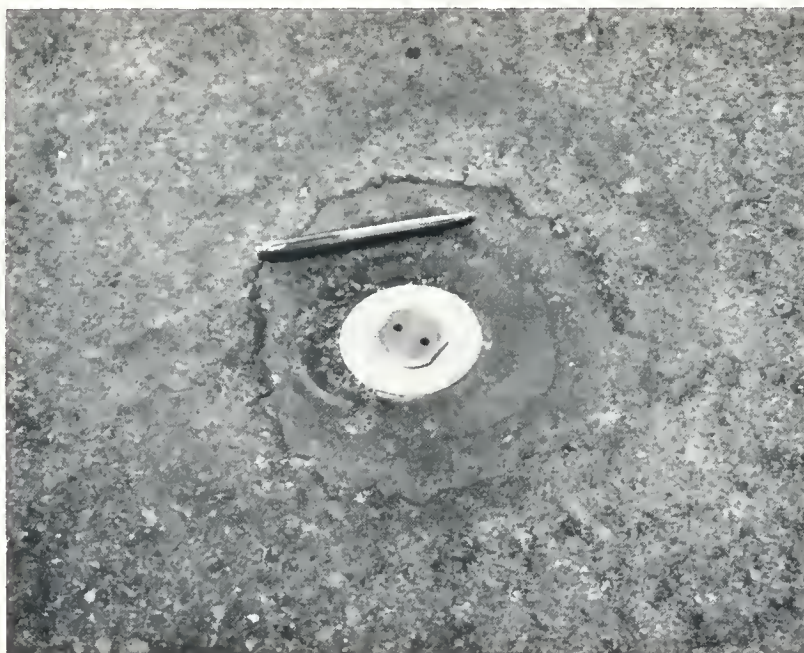


FIGURE 57. ALUMINUM SLEEVE (with cap) INSTALLED

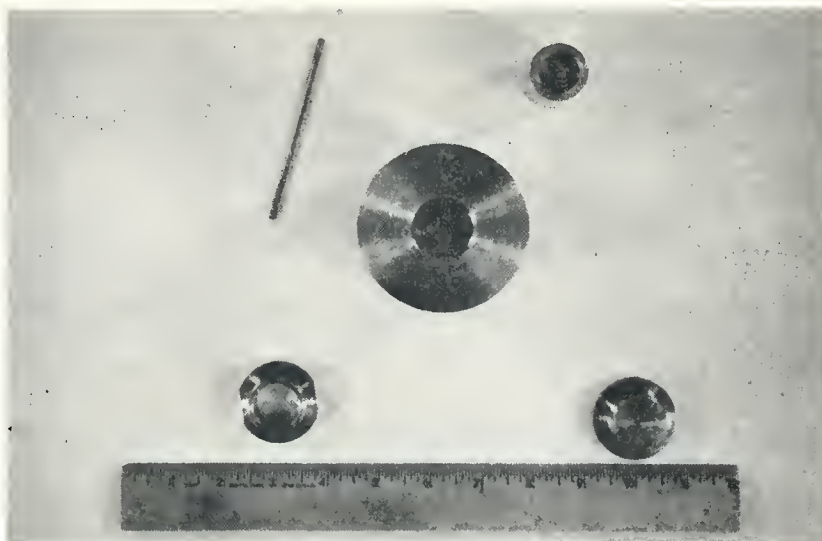


FIGURE 58. HOLDER ASSEMBLY COMPONENTS

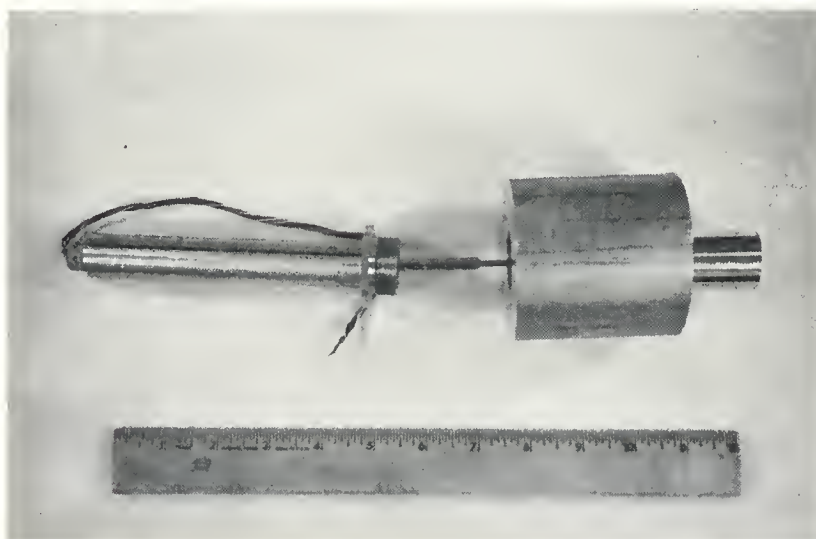


FIGURE 59. HOLDER ASSEMBLY - PARTIALLY ASSEMBLED

that it could be turned into the plug and placed into immediate operation. Data was recorded in the same manner as described above for the LVDT.

Results of Exploratory Tests

A comparison of peak prime mover deflections for each sensing device is summarized in Table 1 of the Field Investigation Section. It was concluded that accelerometers were generally too insensitive to be used at the slower speeds used in the tests. Deflection response functions measured with LVDT sensing devices were good when the sensitivity range of the LVDT was correctly selected.

Figures 60, 61, and 62 depict typical deflection response functions. Attenuation of the peak deflections were used as criteria for selecting a sensitivity range for the sensing devices, and additionally, as the criteria for spacing the deflection gages for the field investigation.

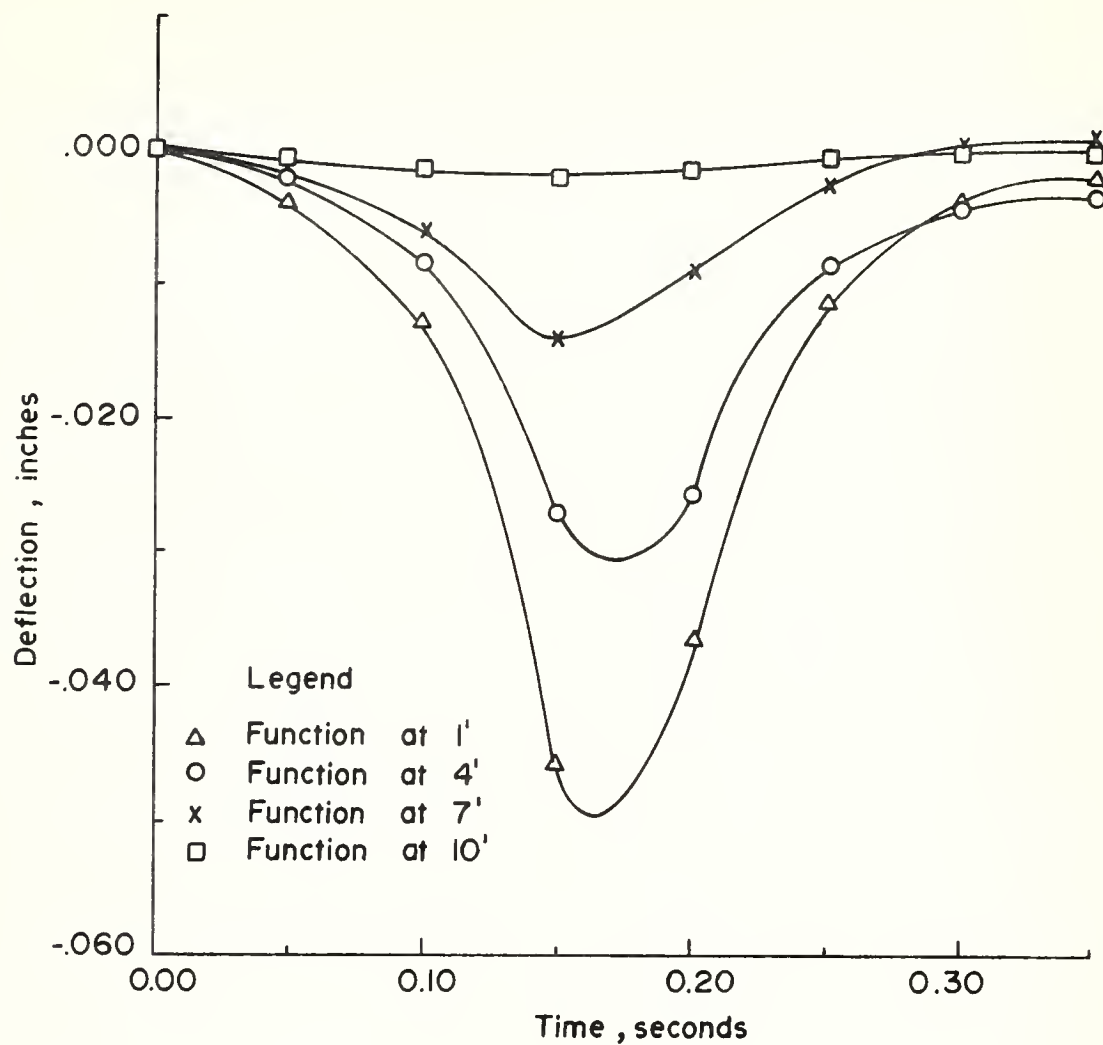


FIGURE 60. TYPICAL DATA SET, BOEING 727 - 25 MPH

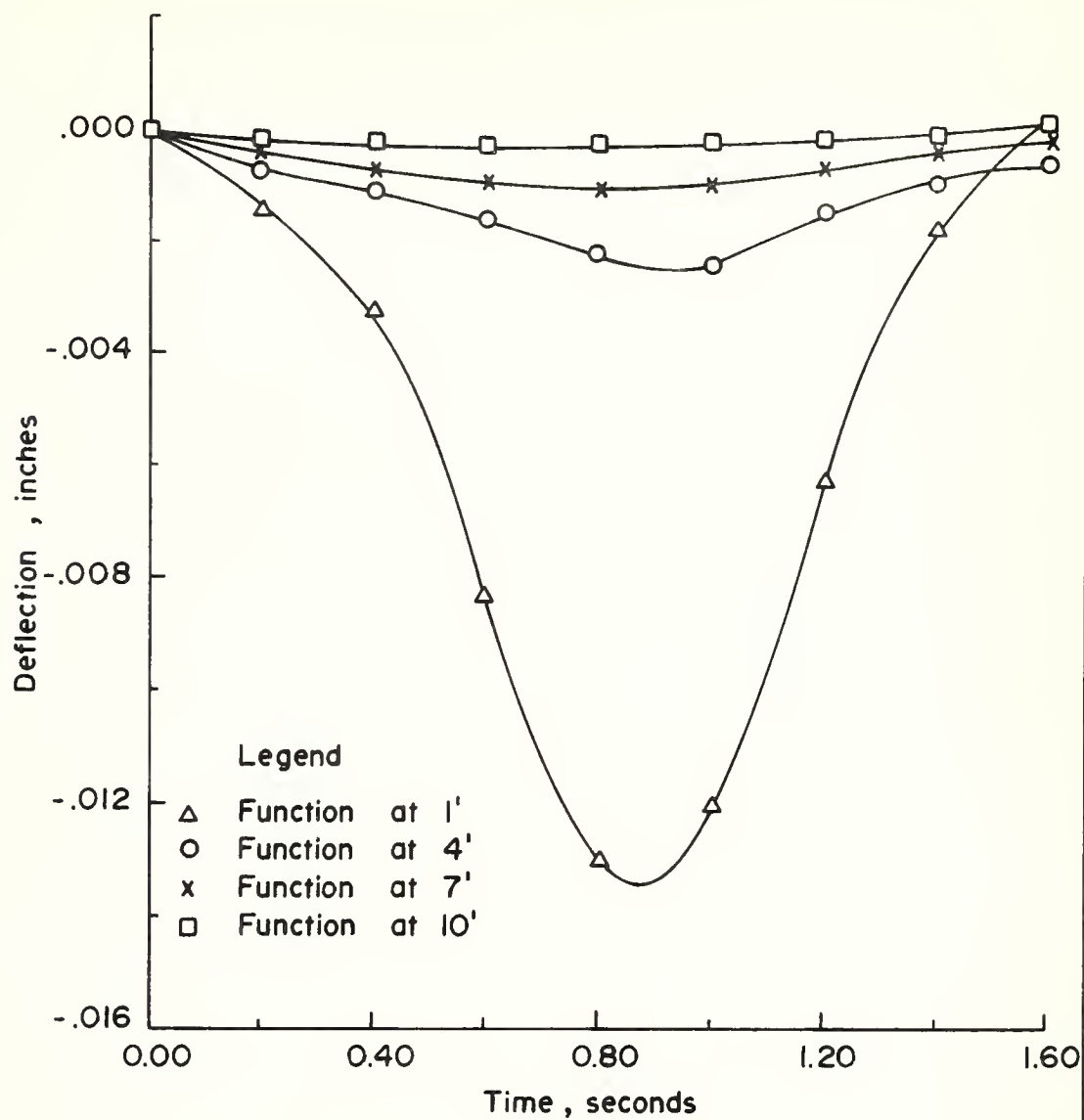
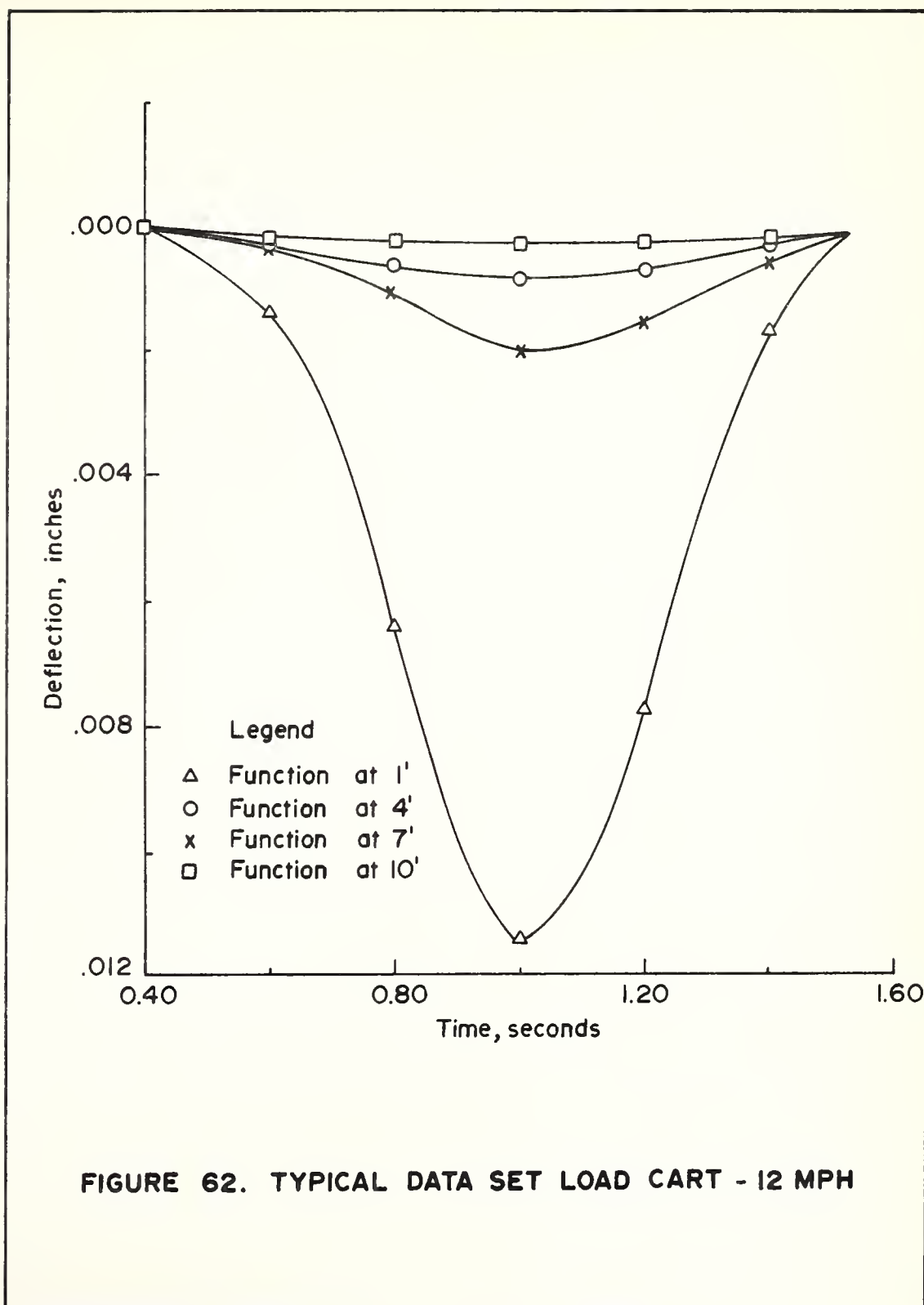


FIGURE 61. TYPICAL DATA SET, LOAD CART - 8 MPH



APPENDIX F

DEFLECTION GAGES - DESCRIPTION, INSTALLATION, AND CALIBRATION

DESCRIPTION

The deflection gages described in this Appendix were specifically designed and fabricated for use in the field investigation associated with this study to predict pavement performance using a transfer function approach. Both type I and II installations employed commercial displacement transducers (Models 24DCDT-250, 24DCDT-100, and 24DCDT-050) manufactured by Hewlett Packard. A DCDT coil assembly consists of a differential transformer coil, a DC-excited solid-state oscillator, a phase-sensitive demodulator, all in one small package 0.75 in. in diameter with variable lengths depending on the particular model. The oscillator converts DC input power to AC, which is used to excite the primary winding. The axial core position determines the amount of voltage induced in the secondary windings. Each of two secondary circuits contains a secondary winding, a full-wave bridge, and an RC filter. These secondary circuits are connected in series opposition so that the resultant output is a DC voltage linearly proportional to the core displacement from the electrical center. The polarity of the voltage is a function of the location of the core with respect to the electrical center, which is located approximately half way along the coil length. Input and output circuits are electrically isolated from each other and the coil assembly case, making them usable directly in floating or ground-return systems. The DC output is sufficient to drive most standard DC indicators, recorders, or control systems. The

design of these transducers eliminates the usual phase-shift correction and harmonic-and-quadrature null problems associated with externally excited AC differential transformers.

The LVDT elements utilized in the instrumentation system had linear ranges of ± 0.250 in., ± 0.100 in., and ± 0.050 in. from the core center for the 24DCDT-250, 24DCDT-100 and 24DCDT-050 models, respectively. Each instrument provided for a total core movement of twice the linear range when the movement in both the positive and negative directions were considered.

For the type I installation, the coil assembly was mounted in a holder which was attached to the top of a reference rod. The core was mated to a vernier holder that was secured to a mount in the asphalt concrete wearing surface. The components of the type I installation are shown in Figure 63. The top row of elements consists of the components which remain stationary as the pavement deflects (viz., from right to left - casing, reference rod, casing cap with teflon bushing, coil holder, and LVDT coil). The bottom row of elements consists of the components that move with the asphalt concrete surface (viz., from right to left - LVDT core, vernier holder, vernier, pavement mount, and the mount cap).

For the type II installation, the coil assembly was mounted in a holder which was attached to the asphalt concrete surface. The core was secured in a beam that was mounted on two reference rods. The components of the type II installation (excluding the beam) are shown in Figure 64. The uppermost and lefthand elements consist of the components which remain stationary as the pavement deflects (viz.,

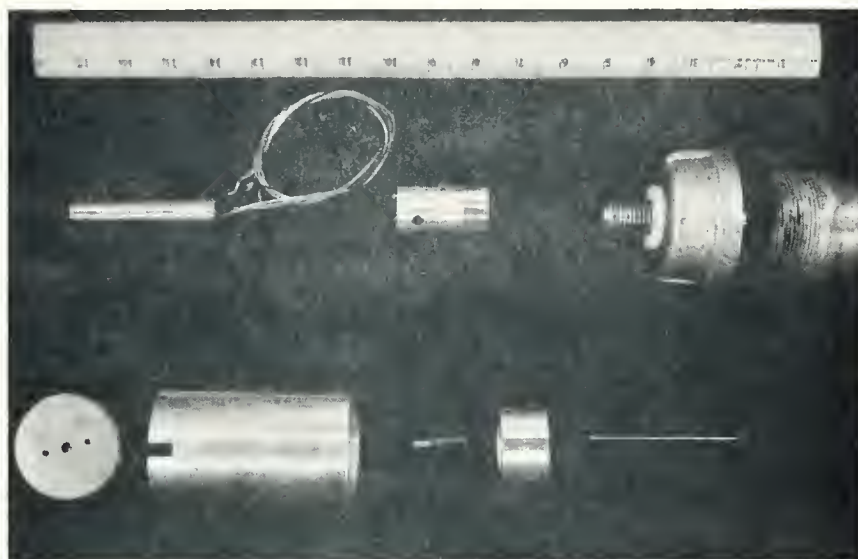


FIGURE 63. COMPONENTS OF DEFLECTION GAGE TYPE I

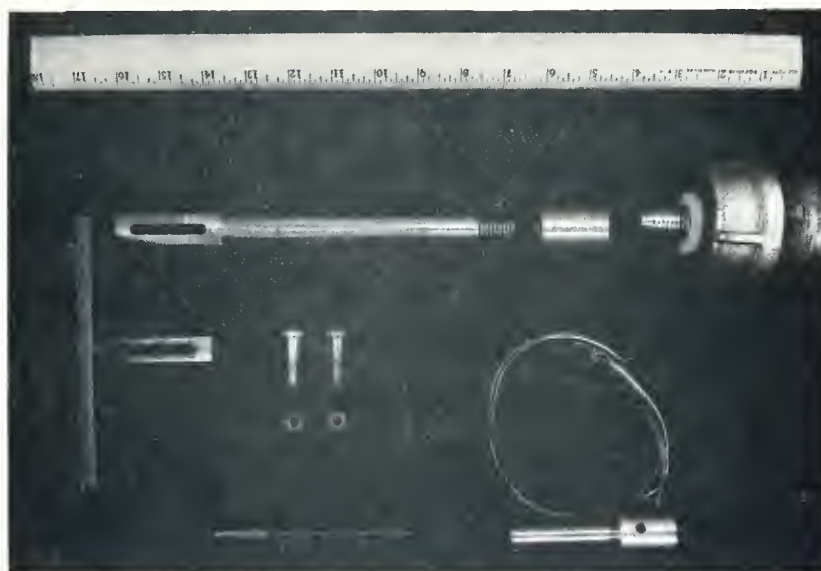


FIGURE 64. COMPONENTS OF DEFLECTION GAGE TYPE II

from right to left and down casing and cap with teflon bushing, reference rod, connector, beam mount extension, beam mount, connector bolts, LVDT core, and the beam vernier). The elements located at the bottom and to the right of the figure (i.e., the LVDT coil holder and LVDT coil) were attached to the asphalt concrete surface.

Figures 65 and 66, respectively, show partially assembled views of both type installations. Figures 67 and 68, respectively, show detailed design views of each type installation. Figure 69 shows a detailed view of the support for the reference beam.

Both Type I and Type II deflection gage installations were employed at each test site. Normally five gages were employed; however, at one site six gages were used so that a direct measurement of prime mover signatures could be monitored. A schematic representation of the transient deflection measuring system is shown in Figure 70. Three regulated power supplies were used to drive the six LVDT's. The time of a specific data run was recorded by use of an IRIG B generator (Culton Industries), and a constant DC voltage trigger provided event marks on the magnetic tape when a prime mover passed locations 24 feet on each side of the deflection gages.

INSTALLATION

The reference rod positions were located on 18 inch centers. Holes six inches in diameter and approximately 18 feet deep were drilled at each reference rod location (see Figures 71 and 72). Reference rods were then cut and placed in each hole. At each location a reference rod was fitted with a driving head and driven to a depth of six to



FIGURE 65. PARTIALLY ASSEMBLED DEFLECTION GAGE TYPE I

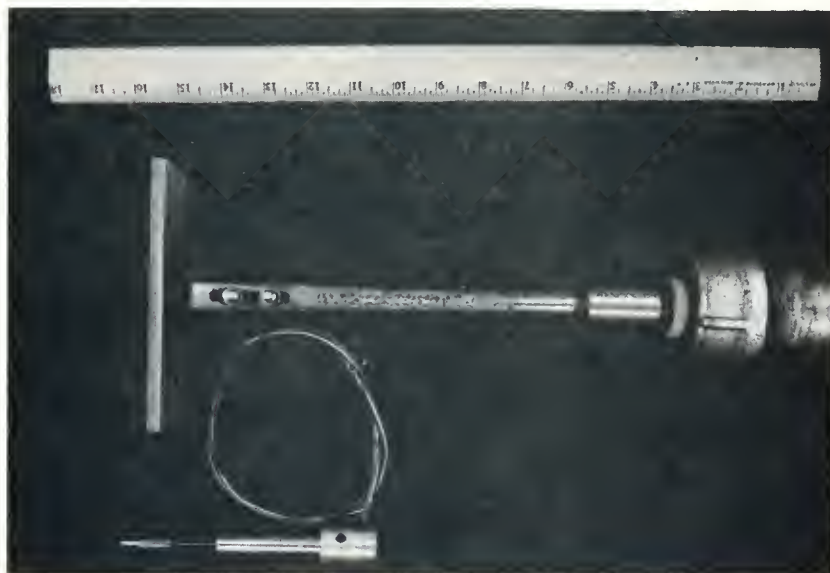


FIGURE 66. PARTIALLY ASSEMBLED DEFLECTION GAGE TYPE II

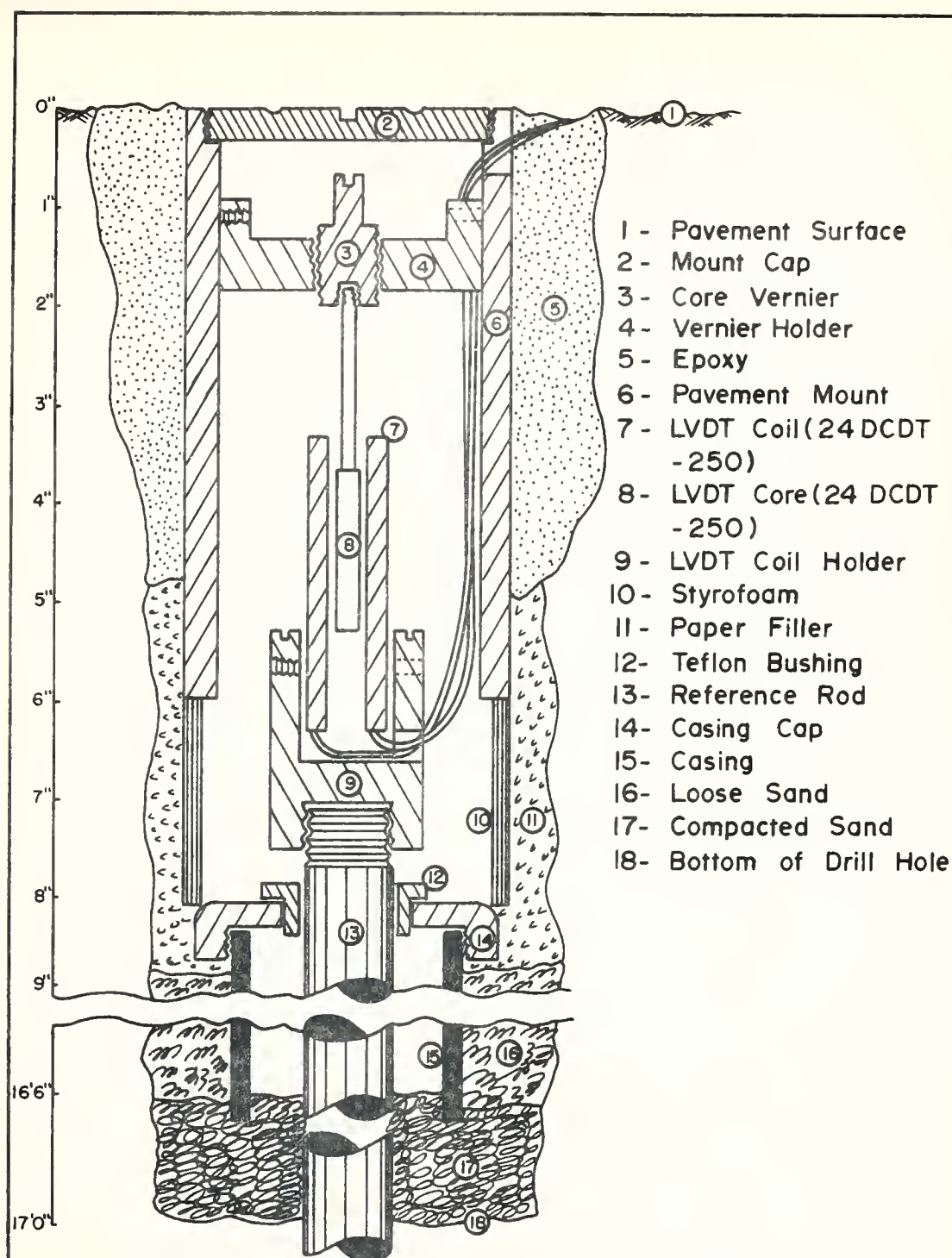


FIGURE 67. GAGE INSTALLATION - TYPE I

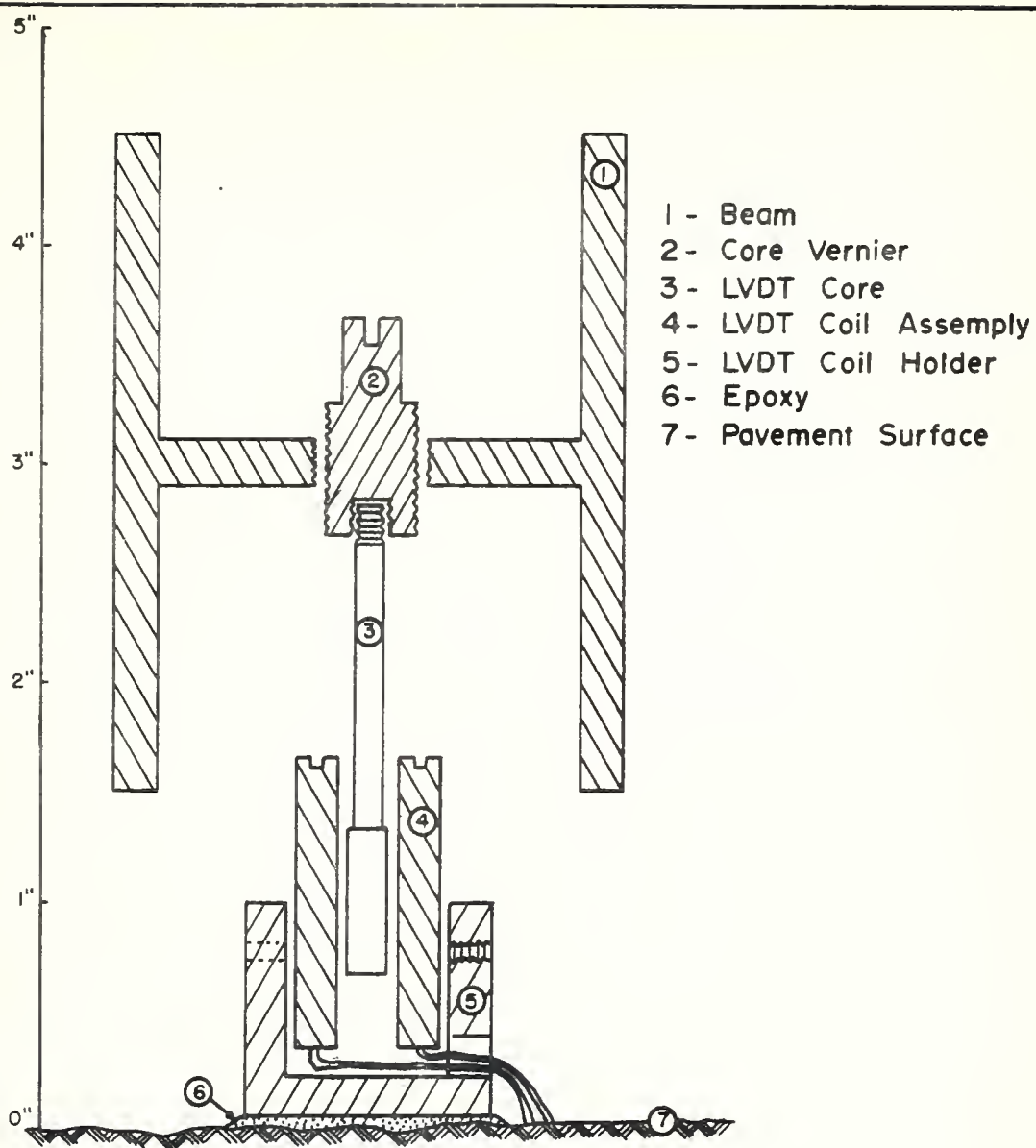
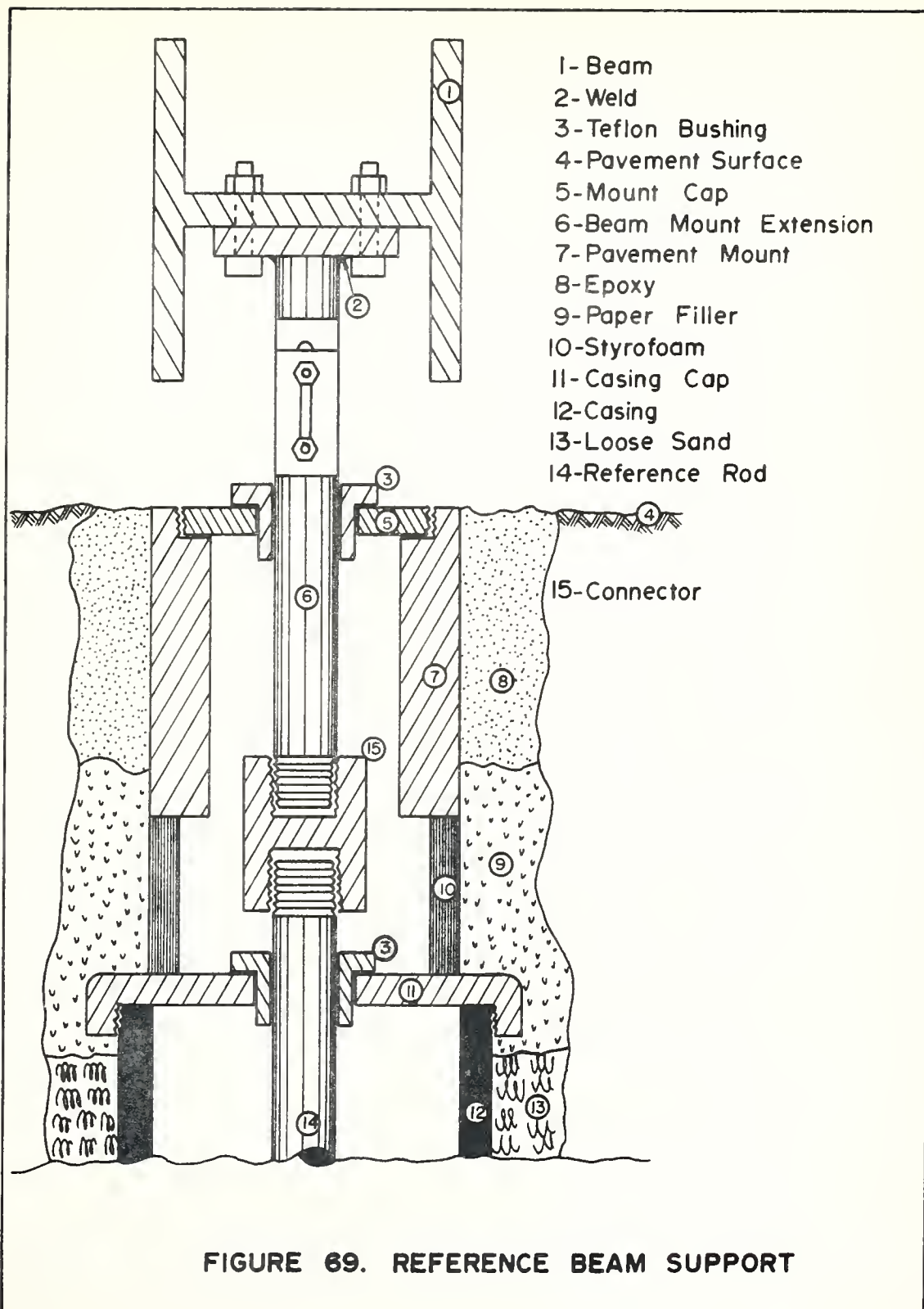


FIGURE 68.GAGE INSTALLATION - TYPE II



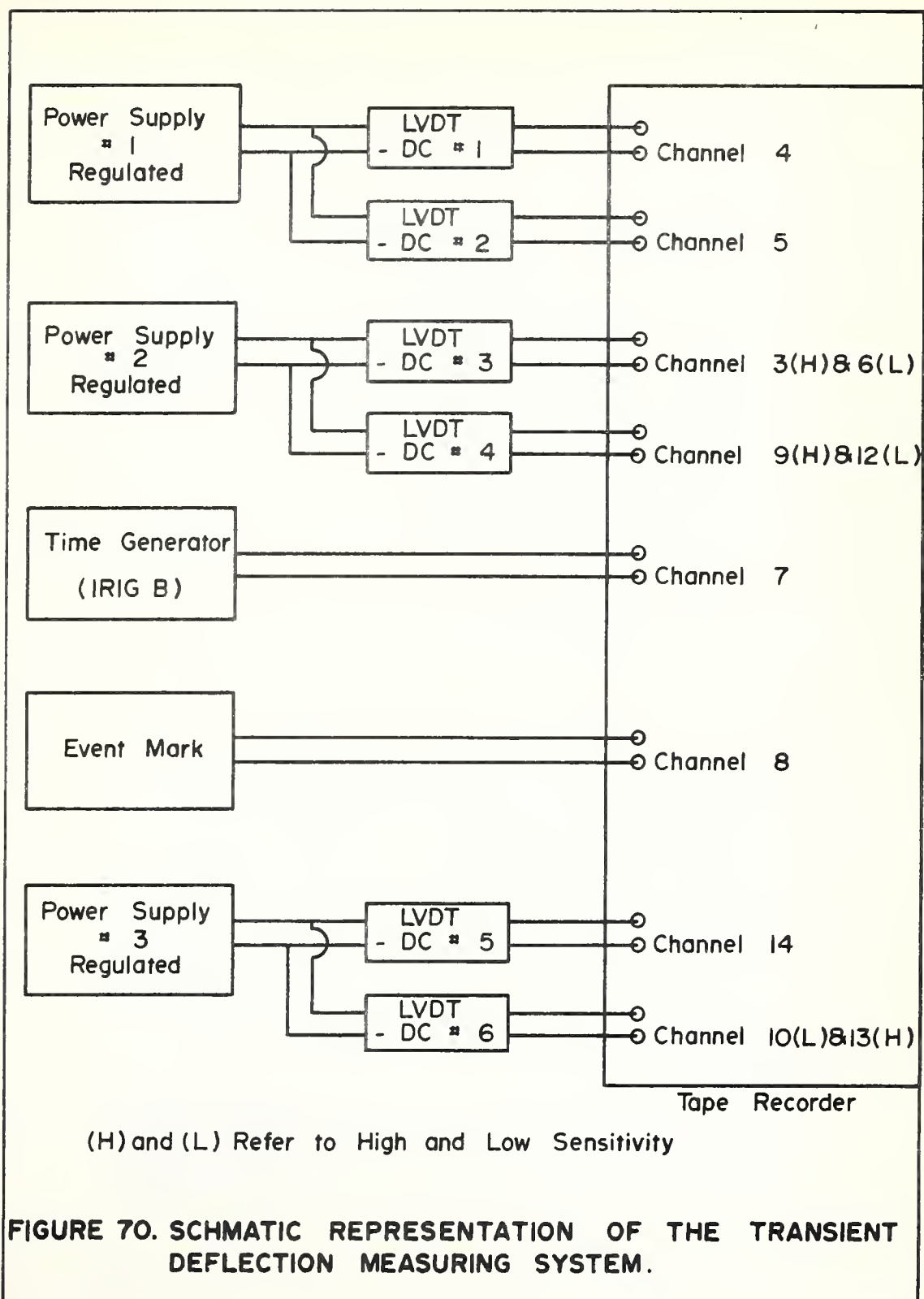




FIGURE 71. DRILLING REFERENCE ROD HOLES

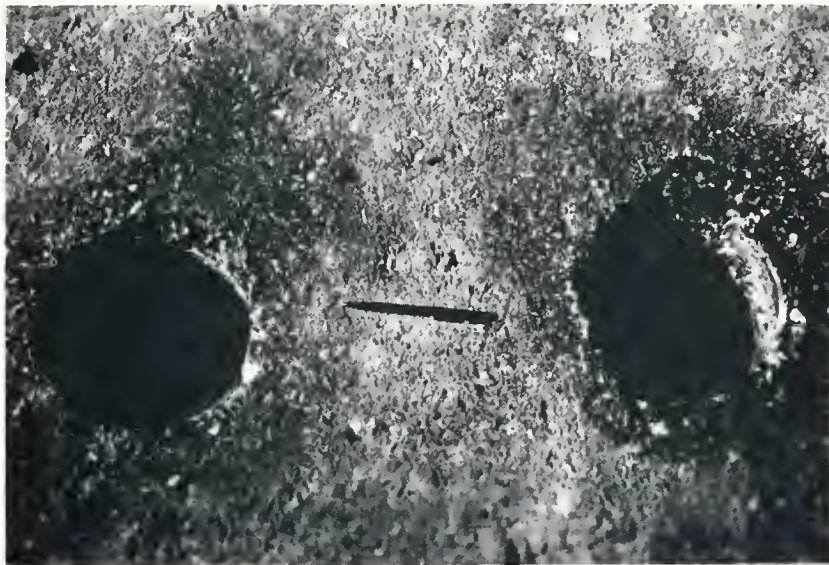


FIGURE 72. HOLES READY FOR REFERENCE RODS

nine inches below the bottom of the drilled hole. The hole was then back filled and tamped with approximately 12 inches of subgrade material. A three inch diameter galvanized pipe casing was cut to appropriate length and placed over and around each reference rod. A casing cap with a teflon bushing was placed over the protruding portion of the reference rod and turned into place on the top of the pipe casing. Each reference rod was fixed at the bottom of the drilled hole by virtue of driving it six to nine inches and then placing approximately 12 inches of tamped backfill. The casing cap fitted with a teflon bushing provided alignment and lateral support for the reference rod near the top of a drilled hole. Subsequently, loose subgrade material was placed in the space between the pipe casing and the wall of each drilled hole to an elevation approximately one inch below the casing cap.

To provide for lateral alignment of the pavement mount with respect to the reference rod, a bushing (Figure 73) was placed over each reference rod, and inserted into the pavement mount. A styrofoam sleeve (Figure 74) was then inserted over and around the bushing between the casing cap and the pavement mount. This sleeve prevented epoxy (when poured to fix pavement mount to wearing surface) from getting near the reference rod and casing cap components. Later, this sleeve served to keep the paper filler from interfering with placement of a LVDT coil, or a reference rod extension. Paper filler was then placed around the pavement mount and styrofoam sleeve to approximately three inches below the pavement surface (Figure 75). This paper filler served as a compressible medium between reference components and



FIGURE 73. BUSHING FOR LATERAL ALIGNMENT

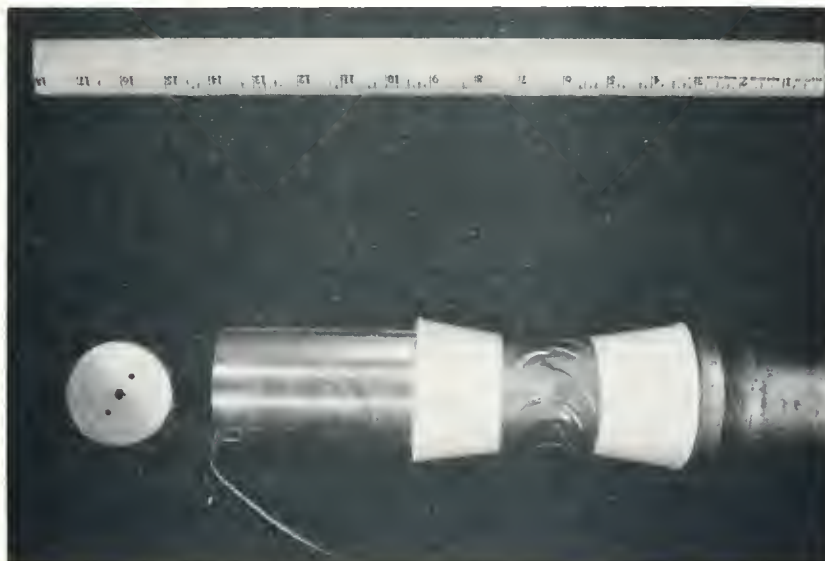


FIGURE 74. STYROFOAM SLEEVE IN - PLACE

movable components of the deflection gages. Vertical alignment between the pavement surface and the pavement mount was achieved by fixing a horizontal steel plate to the mount cap (Figure 76). The plate in-turn rested on the horizontal pavement surface, thereby, providing vertical alignment between the pavement surface and the mount cap. Figures 77 and 78 show the unassembled and assembled components, respectively, and how both lateral and vertical alignment of the pavement mount with respect to the reference rod was achieved. Figures 79 and 80 depict views of the mounts installed subsequent to pouring and curing the epoxy.

An epoxy (Hysol, Resin R8-2038 and Hardener H2-3475) and sand mixture was poured in the volume between the pavement mount paper filler and the inside of the drilled hole. Herman Nelson, Type H-1 400,000 BTU/Hr heaters, were used to cure the epoxy for a period of two hours at a temperature of approximately 140°F. Figures 81 and 82 show the epoxy curing operation.

Type I Installation - The major objective of this type installation was to achieve measurements of the deflection response functions while at the same time protect the sensing device from the tire of a prime mover. After a pavement mount was securely fixed to the pavement's wearing course with the epoxy mixture, a LVDT coil holder and LVDT coil was placed on the top threaded end of a reference rod. Then, a LVDT core, core vernier, and vernier holder assembly was placed inside the pavement mount. This assembly was adjusted to an approximate null position inside the pavement mount and securely fixed in place by tightening the three set screws in the



FIGURE 75. PAPER FILLER

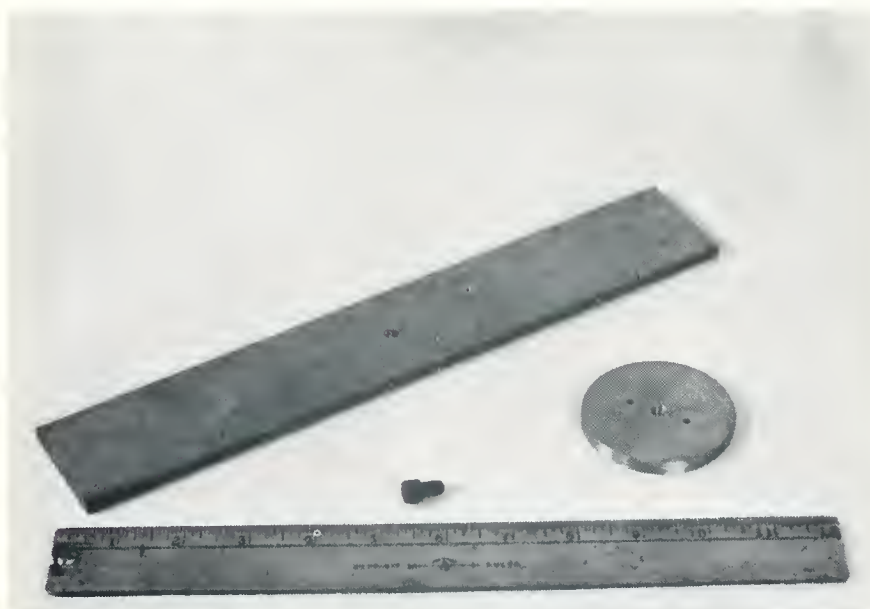


FIGURE 76. PLATE FOR VERTICAL ALIGNMENT

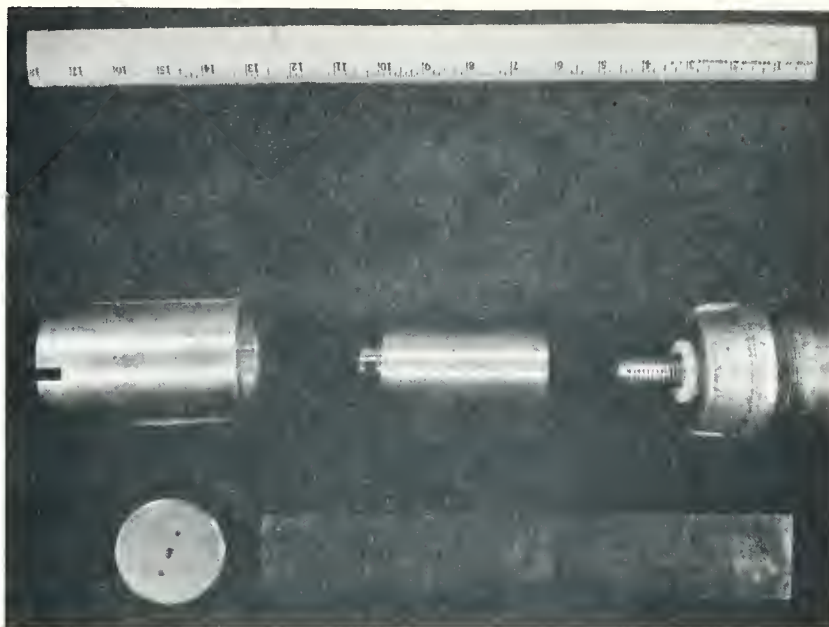


FIGURE 77. UNASSEMBLED ALIGNMENT COMPONENTS



FIGURE 78. ASSEMBLED ALIGNMENT COMPONENTS



FIGURE 79. MOUNT INSTALLATION, CLOSE-UP



FIGURE 80. MOUNT INSTALLATION, DISTANT



FIGURE 81. EPOXY CURING,CLOSE-UP



FIGURE 82 . EPOXY CURING , DISTANT

vernier holder. The deflection gage was then nulled, calibrated, and the mount cap installed.

Type II Installation - The reference beam was first put in place by placing a connector and beam mount extension on top of each of two reference rods. Lateral support for the beam mount extension was provided by a mount cap fitted with a teflon bushing which was placed over the extension rod and secured in the top of the pavement mount. The beam was then secured to the beam mount extensions and adjusted to a predetermined height of approximately three inches above the pavement surface. At each gage position on the beam a LVDT coil and holder assembly was aligned with a LVDT core and vernier in the beam, and the holder glued to the pavement surface with Hysol 608 Epoxy-Patch.

CALIBRATION

Each gage was nulled for zero voltage output prior to calibration. The gages were nulled by turning the core vernier until zero voltage output was achieved. The gage output was monitored by an oscilloscope. Once a null position had been obtained for each gage, the tape recorder was started and a zero reading was taken for each gage. Subsequently, the LVDT core for each deflection gage was displaced a known amount by turning the core vernier a predetermined rotation. With 20 threads per inch on the core vernier, this rotation permitted calculation of the actual displacement of the core. Figure 83 shows the calibration devices used to achieve a desired rotation of the core vernier. Figure 84 represents actual manner in which calibrations were performed. After each core had been displaced, the tape recorder was started and a step

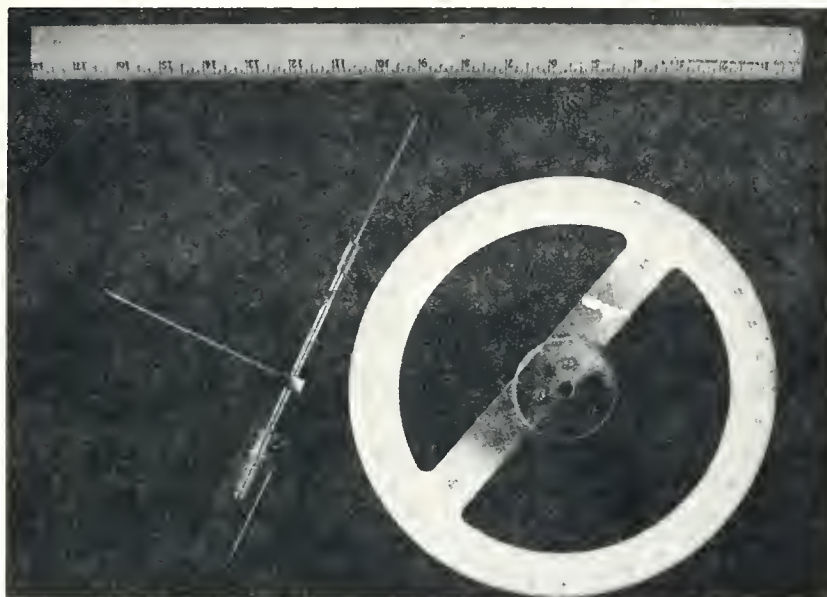


FIGURE 83. CALIBRATION DEVICES



FIGURE 84. METHOD OF CALIBRATION

calibration reading taken for each gage. This calibration procedure was repeated a minimum of two times daily. Occasionally a third calibration step was taken to check linearity of the instruments. All linearity checks proved the gages be within two percent error.

APPENDIX G

DEFLECTION RESPONSE AND TDT FUNCTIONS

Data for the deflection response functions and TDT functions are contained in this Appendix. The deflection response function data are listed first for all the aircraft at each test site. These are followed by the calculated TDT functions. All data was printed out to six decimal places from computer code CONVLI.

DEFLECTION RESPONSE FUNCTIONS
C135 AIRCRAFT-SITE 1

TIME	RESP 0	RESP 1	RESP 2	RESP 3	RESP 4
.00	.002424	.002771	.000094	.000000	.002000
.04	.003222	.004103	.000128	.000000	.000000
.08	.004206	.005104	.000163	.000001	.000000
.12	.006091	.006565	.000199	.000001	.000000
.16	.009971	.009223	.000257	.000001	.000000
.20	.017516	.012592	.000322	.000001	.000000
.24	.030209	.016503	.000382	.000001	.000000
.28	.048391	.020912	.000455	.000001	.000000
.32	.070398	.025591	.000528	.000001	.000000
.36	.086980	.027449	.000577	.000001	.000000
.40	.070956	.025667	.000588	.000001	.000000
.44	.051398	.022773	.000580	.000001	.000000
.48	.033648	.021820	.000574	.000001	.000000
.52	.020119	.023834	.000578	.000001	.000000
.56	.002603	.027508	.000593	.000001	.000000
.60	.001000	.027954	.000594	.000001	.000000
.64	.000016	.023846	.000562	.000001	.000000
.68	.005437	.018214	.000504	.000001	.000000
.72	.047744	.012718	.000431	.000001	.000000
.76	.035545	.008084	.000349	.000001	.000000
.80	.027721	.004759	.000279	.000001	.000000
.84	.023205	.002637	.000230	.000001	.000000
.88	.020337	.001185	.000191	.000000	.000000
.92	.018623	.000813	.000161	.000000	.000000
.96	.017670	.000843	.000143	.000000	.000000
1.00	.016762	.000304	.000121	.000000	.000000
1.04	.016172	.000638	.000104	.000000	.000000
1.08	.015979	.000853	.000096	.000000	.000000
1.12	.015412	.000643	.000080	.000000	.000000
1.16	.014848	.000598	.000063	.000000	.000000
1.20	.014529	.000319	.000056	.000000	.000000
1.24	.014308	.000303	.000050	.000000	.000000
1.28	.013759	.000253	.000033	.000000	.000000
1.32	.013544	.000148	.000028	.000000	.000000
1.36	.013538	.000368	.000031	.000000	.000000
1.40	.013179	.000178	.000020	.000000	.000000
1.44	.013000	.000248	.000016	.000000	.000000
1.48	.013427	.000017	.000013	.000000	.000000
1.52	.012749	0.000000	.000017	.000000	.000000
1.56	.012654	0.000000	.000007	.000000	.000000
1.60	.012869	0.000000	.000025	.000000	.000000
1.64	.012750	.000012	.000013	.000000	.000000
1.68	.012555	0.000000	.000011	.000000	.000000
1.72	.012908	.000263	.000014	.000000	.000000
1.76	.012966	.000438	.000022	.000000	.000000
1.80	.012678	.000288	.000012	.000000	.000000
1.84	.012562	.000482	.000012	.000000	.000000

DEFLECTION RESPONSE FUNCTIONS
CL30 AIRCRAFT-STIFF 1

TIME	RESP 0	RESP 1	RESP 2	RESP 3	RESP 4
0.0	.001532	.000177	.000064	1.000000	.000000
.05	.001850	.000160	.000074	1.000000	.000000
.1	.002295	.000185	.000082	0.999999	.000000
.12	.002440	.000246	.000090	0.999999	.000000
.15	.003572	.000369	.000098	0.999999	.000000
.2	.004526	.000705	.000110	0.999999	.000000
.2	.006159	.001335	.000122	0.999999	.000000
.2	.008134	.002337	.000137	0.999999	.000000
.3	.010793	.003542	.000157	0.999999	.000000
.35	.014224	.005109	.000171	0.999999	.000000
.4	.018650	.006573	.000190	0.999999	.000000
.45	.023779	.007973	.000200	0.999999	.000000
.4	.029216	.009159	.000210	0.999999	.000000
.5	.034888	.010128	.000219	0.999999	.000000
.55	.037248	.010481	.000222	0.999999	.000000
.6	.038900	.010521	.000223	0.999999	.000000
.65	.036394	.010353	.000221	0.999999	.000000
.7	.033126	.010145	.000218	0.999999	.000000
.75	.029211	.009867	.000211	0.999999	.000000
.7	.024871	.009615	.000205	0.999999	.000000
.8	.021263	.008697	.000204	0.999999	.000000
.85	.018245	.007706	.000201	0.999999	.000000
.8	.015694	.006535	.000199	0.999999	.000000
.9	.013542	.005387	.000189	0.999999	.000000
.9	.011626	.004459	.000181	0.999999	.000000
1.0	.009952	.003761	.000172	0.999999	.000000
1.05	.008557	.003196	.000163	0.999999	.000000
1.05	.007459	.002716	.000156	0.999999	.000000
1.15	.006463	.002262	.000146	0.999999	.000000
1.15	.005710	.001887	.000140	0.999999	.000000
1.25	.005089	.001546	.000131	0.999999	.000000
1.25	.004593	.001306	.000124	0.999999	.000000
1.25	.004207	.001117	.000121	0.999999	.000000
1.35	.003853	.000929	.000116	0.999999	.000000
1.35	.003597	.000752	.000102	0.999999	.000000
1.45	.003354	.000622	.000095	0.999999	.000000
1.45	.003193	.000519	.000092	0.999999	.000000
1.4	.003031	.000437	.000090	0.999999	.000000
1.52	.002869	.000383	.000085	0.999999	.000000
1.5	.002785	.000371	.000082	0.999999	.000000
1.65	.002734	.000343	.000078	0.999999	.000000
1.65	.002596	.000332	.000073	0.999999	.000000
1.6	.002580	.000342	.000077	0.999999	.000000
1.72	.002525	.000342	.000074	0.999999	.000000
1.75	.002476	.000321	.000070	0.999999	.000000
1.85	.002402	.000294	.000069	0.999999	.000000
1.85	.002338	.000294	.000061	0.999999	.000000

DEFLECTION RESPONSE FUNCTIONS
CIRCULAR PLATE (STIFF)

TIME	RESP. 0	RESP. 1	RESP. 2	RESP. 3	RESP. 4
1.0	.002182	.003182	.000135	.000000	.000000
.04	.002552	.003355	.000148	.000000	.000000
.08	.003150	.003490	.000150	.000000	.000000
.12	.004117	.004330	.000170	.000000	.000000
.16	.005332	.005270	.000194	.000001	.000000
.20	.007267	.006613	.000217	.000001	.000000
.24	.009964	.008019	.000238	.000001	.000000
.28	.013860	.010245	.000267	.000001	.000000
.32	.019150	.013881	.000299	.000001	.000000
.36	.025785	.018403	.000330	.000001	.000000
.40	.034482	.025180	.000350	.000001	.000000
.44	.044100	.034880	.000380	.000001	.000000
.48	.055452	.048804	.000403	.000001	.000000
.52	.064107	.060018	.000424	.000001	.000000
.56	.070252	.070212	.000427	.000001	.000000
.60	.073600	.078092	.000429	.000001	.000000
.64	.074956	.084837	.000427	.000001	.000000
.68	.075533	.091623	.000428	.000001	.000000
.72	.075874	.098493	.000429	.000001	.000000
.76	.0751297	.092340	.000425	.000001	.000000
.80	.0744412	.0810018	.000410	.000001	.000000
.84	.0739225	.069194	.000412	.000001	.000000
.88	.0735798	.068584	.000407	.000001	.000000
.92	.0734225	.068584	.000405	.000001	.000000
.96	.0734916	.068177	.000400	.000001	.000000
1.00	.0737766	.068176	.000397	.000001	.000000
1.04	.0742412	.068564	.000391	.000001	.000000
1.08	.0747478	.068731	.000390	.000001	.000000
1.12	.0751633	.068705	.000387	.000001	.000000
1.16	.0754690	.068654	.000383	.000001	.000000
1.20	.0756518	.068587	.000377	.000001	.000000
1.24	.0757150	.068412	.000367	.000001	.000000
1.28	.0756174	.068255	.000350	.000001	.000000
1.32	.0754914	.068125	.000342	.000001	.000000
1.36	.0753638	.068014	.000310	.000001	.000000
1.40	.0752260	.067983	.000290	.000001	.000000
1.44	.0750982	.067932	.000272	.000001	.000000
1.48	.0750558	0.000000	.000255	.000001	.000000
1.52	.0751536	0.000000	.000230	.000001	.000000
1.56	.07518247	0.000000	.000217	.000000	.000000
1.60	.07515197	0.000000	.000190	.000000	.000000
1.64	.07512793	0.000000	.000169	.000000	.000000
1.68	.07510981	0.000000	.000150	.000000	.000000
1.72	.07509501	0.000000	.000140	.000000	.000000
1.76	.07508728	0.000000	.000130	.000000	.000000
1.80	.07507777	0.000000	.000118	.000000	.000000
1.84	.07506346	0.000000	.000104	.000000	.000000

DEFLECTION RESPONSE FUNCTIONS
C135 AIRCRAFT-SITE 2

TIME	RESP 0	RESP 1	RESP 2	RESP 3	RESP 4
0.00	.001827	.002958	.001033	.00002P	.000001
.04	.002741	.003751	.001237	.00003R	.000001
.08	.003918	.005124	.001509	.000052	.000001
.12	.005755	.007050	.001819	.000068	.000001
.16	.009091	.010021	.002221	.000086	.000001
.20	.015234	.014676	.002746	.000103	.000001
.24	.026194	.021436	.003327	.000120	.000001
.28	.043947	.029536	.003964	.000136	.000001
.32	.064234	.035201	.004483	.000147	.000001
.36	.068679	.035887	.004634	.000152	.000001
.40	.058346	.033281	.004507	.000152	.000001
.44	.049410	.030571	.004340	.000153	.000001
.48	.045905	.029757	.004243	.000152	.000001
.52	.049776	.031297	.004201	.000153	.000001
.56	.060765	.033967	.004247	.000153	.000001
.60	.071000	.034390	.004186	.000152	.000001
.64	.064987	.031551	.003851	.000152	.000001
.68	.051437	.026052	.003327	.000152	.000001
.72	.039728	.020467	.002807	.000151	.000001
.76	.031230	.015600	.002294	.000150	.000001
.80	.025507	.011923	.001839	.000149	.000001
.84	.021051	.009159	.001439	.000146	.000001
.88	.018082	.007301	.001154	.000139	.000001
.92	.016199	.006085	.000942	.000129	.000001
.96	.014910	.005110	.000770	.000119	.000001
1.00	.014051	.004504	.000636	.000108	.000001
1.04	.013412	.004093	.000519	.000099	.000001
1.08	.012845	.003621	.000415	.000090	.000001
1.12	.012478	.003389	.000322	.000082	.000000
1.16	.012170	.003091	.000255	.000074	.000000
1.20	.011892	.002912	.000186	.000068	.000000
1.24	.011658	.002699	.000136	.000064	.000000
1.28	.011179	.002413	.000088	.000060	.000000
1.32	.011033	.002481	.000053	.000056	.000000
1.36	.010873	.002194	.000015	.000053	.000000
1.40	.010634	.002152	0.000000	.000051	.000000
1.44	.010557	.001963	0.000000	.000049	.000000
1.48	.010522	.002022	0.000000	.000047	.000000
1.52	.010177	.001908	0.000000	.000046	.000000
1.56	.010126	.001838	0.000000	.000045	.000000
1.60	.010123	.001876	0.000000	.000043	.000000
1.64	.009940	.001690	0.000000	.000042	.000000
1.68	.009772	.001730	0.000000	.000041	.000000
1.72	.009785	.001716	0.000000	.000040	.000000
1.76	.009738	.001712	0.000000	.000040	.000000
1.80	.009747	.001648	0.000000	.000039	.000000
1.84	.009540	.001653	0.000000	.000039	.000000

DEFLECTION RESPONSE FUNCTIONS
C131 AIRCRAFT-SITE 2

TIME	RESP 0	RESP 1	RESP 2	RESP 3	RESP 4
0.00	.003280	.004297	.000994	.000030	.000000
.04	.003989	.004784	.001059	.000037	.000000
.08	.004639	.005016	.001067	.000041	.000000
.12	.005497	.005697	.001126	.000041	.000000
.16	.006602	.006461	.001204	.000031	.000000
.20	.007653	.006869	.001204	.000036	.000000
.24	.009083	.007991	.001276	.000030	.000000
.28	.010561	.008448	.001278	.000030	.000000
.32	.012642	.009350	.001354	.000033	.000000
.36	.014642	.010086	.001391	.000030	.000000
.40	.016610	.010419	.001399	.000038	.000000
.44	.018532	.010800	.001418	.000045	.000000
.48	.020513	.011532	.001465	.000039	.000000
.52	.021914	.011607	.001487	.000042	.000000
.56	.022727	.011625	.001475	.000048	.000000
.60	.023000	.011496	.001501	.000036	.000000
.64	.022424	.010850	.001437	.000039	.000000
.68	.021247	.010640	.001407	.000042	.000000
.72	.020207	.009805	.001365	.000041	.000000
.76	.018406	.008780	.001308	.000037	.000000
.80	.016699	.008077	.001306	.000044	.000000
.84	.015102	.007459	.001277	.000040	.000000
.88	.013362	.006542	.001182	.000042	.000000
.92	.011647	.006052	.001115	.000046	.000000
.96	.010663	.005672	.001128	.000035	.000000
1.00	.009174	.004701	.001052	.000046	.000000
1.04	.008065	.004404	.001003	.000046	.000000
1.08	.007048	.003796	.000972	.000040	.000000
1.12	.006118	.003123	.000891	.000040	.000000
1.16	.005295	.002812	.000879	.000039	.000000
1.20	.004483	.002483	.000805	.000039	.000000
1.24	.004033	.002364	.000783	.000040	.000000
1.28	.003728	.002190	.000759	.000043	.000000
1.32	.003298	.002159	.000739	.000044	.000000
1.36	.002857	.002056	.000709	.000045	.000000
1.40	.002718	.002046	.000656	.000046	.000000
1.44	.002478	.001632	.000622	.000050	.000000
1.48	.002081	.001589	.000588	.000048	.000000
1.52	.002148	.001389	.000619	.000041	.000000
1.56	.002069	.001417	.000567	.000037	.000000
1.60	.001814	.001271	.000517	.000043	.000000
1.64	.001763	.001315	.000510	.000035	.000000
1.68	.001593	.001187	.000459	.000035	.000000
1.72	.001377	.000922	.000404	.000042	.000000
1.76	.001253	.000981	.000349	.000040	.000000
1.80	.001232	.000725	.000305	.000040	.000000
1.84	.000855	.000704	.000226	.000040	.000000

DEFLECTION RESPONSE FUNCTIONS
C130 AIRCRAFT-SITE 2

TIME	RESP 0	RESP 1	RESP 2	RESP 3	RESP 4
0.00	.002115	.002658	.000829	.000004	.000000
.04	.002931	.003185	.000978	.000004	.000000
.08	.003922	.004165	.001129	.000010	.000000
.12	.005522	.005624	.001331	.000017	.000001
.16	.008379	.007690	.001609	.000024	.000001
.20	.012903	.010317	.001900	.000032	.000001
.24	.019336	.013530	.002169	.000041	.000001
.28	.025234	.015946	.002415	.000044	.000001
.32	.028180	.017315	.002607	.000044	.000001
.36	.029168	.018223	.002708	.000044	.000001
.40	.030380	.018765	.002761	.000046	.000001
.44	.033319	.019939	.002871	.000048	.000001
.48	.037199	.021372	.002995	.000070	.000001
.52	.041952	.023120	.003116	.000083	.000001
.56	.047268	.024888	.003246	.000079	.000001
.60	.051000	.025778	.003329	.000083	.000001
.64	.050380	.025294	.003307	.000087	.000001
.68	.046558	.023880	.003232	.000094	.000001
.72	.041770	.021884	.003065	.000105	.000001
.76	.037249	.019761	.002864	.000108	.000001
.80	.033524	.018059	.002704	.000109	.000001
.84	.030306	.016477	.002549	.000109	.000001
.88	.028142	.015319	.002390	.000110	.000001
.92	.026767	.014715	.002300	.000108	.000001
.96	.024958	.014218	.002224	.000107	.000001
1.00	.025928	.013997	.002138	.000105	.000001
1.04	.026878	.014237	.002110	.000103	.000001
1.08	.028515	.014660	.002115	.000099	.000001
1.12	.030506	.015034	.002088	.000097	.000001
1.16	.032515	.015547	.002077	.000096	.000001
1.20	.034685	.015854	.002063	.000095	.000001
1.24	.035779	.015921	.002010	.000093	.000001
1.28	.036222	.015869	.001992	.000090	.000001
1.32	.035237	.015328	.001924	.000090	.000001
1.36	.033384	.014415	.001858	.000089	.000001
1.40	.031056	.013330	.001767	.000088	.000001
1.44	.028383	.012074	.001636	.000087	.000001
1.48	.025558	.010565	.001477	.000086	.000001
1.52	.022970	.009147	.001320	.000084	.000001
1.56	.020610	.007764	.001171	.000084	.000001
1.60	.018520	.006553	.001031	.000083	.000001
1.64	.016797	.005267	.000858	.000083	.000001
1.68	.015309	.004205	.000767	.000081	.000000
1.72	.014064	.003540	.000709	.000081	.000000
1.76	.013054	.002818	.000600	.000080	.000000
1.80	.012267	.002518	.000488	.000079	.000000
1.84	.011449	.002096	.000360	.000079	.000000

DEFLECTION RESPONSE FUNCTIONS
C135 AIRCRAFT-SITE 3

TIME	RESP 0	RESP 1	RESP 2	RESP 3	RESP 4
0.00	.000164	.002195	.000677	.000217	.000052
.04	.003392	.004583	.001168	.000279	.000063
.08	.005238	.008671	.002196	.000385	.000075
.12	.008189	.012884	.003536	.000517	.000087
.16	.012830	.019370	.005182	.000724	.000099
.20	.019777	.026787	.007129	.000978	.000112
.24	.030280	.033371	.009263	.001299	.000124
.28	.042851	.036015	.010894	.001589	.000134
.32	.048505	.035209	.011637	.001739	.000139
.36	.044063	.033683	.011692	.001792	.000142
.40	.038199	.030502	.011637	.001841	.000144
.44	.034642	.030546	.011517	.001856	.000145
.48	.034125	.032418	.011540	.001868	.000146
.52	.037696	.035401	.011625	.001895	.000146
.56	.045787	.035994	.011885	.001907	.000144
.60	.052000	.034324	.011965	.001903	.000139
.64	.047899	.029419	.011630	.001854	.000131
.68	.038441	.021910	.010765	.001801	.000122
.72	.029318	.014971	.008831	.001686	.000109
.76	.021388	.009963	.006589	.001525	.000095
.80	.015337	.006363	.004647	.001332	.000082
.84	.010951	.003989	.003062	.001121	.000069
.88	.007993	.002089	.001938	.000908	.000058
.92	.006115	.001543	.001228	.000742	.000049
.96	.004934	.000816	.000775	.000612	.000042
1.00	.004214	.000709	.000489	.000507	.000035
1.04	.003875	.000760	.000413	.000446	.000031
1.08	.003453	.000251	.000295	.000392	.000027
1.12	.003204	.000307	.000221	.000357	.000024
1.16	.003008	.000089	.000166	.000320	.000021
1.20	.001702	.000301	.000147	.000235	.000014
1.24	.001474	.000467	.000147	.000201	.000013
1.28	.001469	.000290	.000147	.000181	.000011
1.32	.001437	.000008	.000102	.000171	.000010
1.36	.001399	.000071	.000139	.000163	.000009
1.40	.001399	.000202	.000132	.000158	.000008
1.44	.001380	.000168	.000125	.000142	.000007
1.48	.001385	.000143	.000055	.000132	.000007
1.52	.001362	.000167	.000009	.000125	.000006
1.56	.001327	.000034	.000009	.000113	.000005
1.60	.001324	.000007	.000009	.000112	.000005
1.64	.001324	.000299	.000055	.000110	.000005
1.68	.001324	.000331	.000009	.000101	.000004
1.72	.001307	.000070	.000009	.000098	.000004
1.76	.001298	.000373	.000009	.000095	.000003
1.80	.001319	.000434	.000009	.000088	.000003
1.84	.001287	.000007	.000009	.000088	.000003

DEFLECTION RESPONSE FUNCTIONS
C131 AIRCRAFT-SITE 3

TIME	RESP 0	RESP 1	RESP 2	RESP 3	RESP 4
0.00	.001195	.001558	.000446	.000162	.000025
.04	.001461	.001550	.000566	.000180	.000028
.08	.001792	.002407	.000725	.000200	.000030
.12	.002238	.003087	.000945	.000233	.000033
.16	.002823	.003942	.001201	.000260	.000036
.20	.003491	.004301	.001459	.000290	.000038
.24	.004309	.005571	.001736	.000324	.000040
.28	.005291	.006185	.002017	.000373	.000042
.32	.006451	.007801	.002305	.000396	.000043
.36	.007829	.009196	.002630	.000443	.000045
.40	.009553	.010373	.002982	.000499	.000046
.44	.011503	.011718	.003325	.000537	.000048
.48	.013670	.012158	.003624	.000581	.000049
.52	.015776	.012467	.003878	.000625	.000050
.56	.017313	.012385	.004048	.000642	.000050
.60	.018000	.012215	.004142	.000660	.000050
.64	.017654	.011883	.004134	.000654	.000050
.68	.016476	.011069	.004087	.000639	.000049
.72	.015069	.010040	.004007	.000637	.000048
.76	.013709	.009384	.003877	.000625	.000047
.80	.012344	.008097	.003679	.000613	.000046
.84	.011069	.007526	.003438	.000613	.000045
.88	.009885	.006574	.003138	.000589	.000043
.92	.008768	.005543	.002830	.000568	.000041
.96	.007727	.004986	.002527	.000540	.000039
1.00	.006809	.004283	.002222	.000514	.000037
1.04	.006014	.003939	.001927	.000479	.000035
1.08	.005285	.003437	.001661	.000455	.000033
1.12	.004664	.003013	.001418	.000429	.000030
1.16	.004149	.002563	.001197	.000395	.000028
1.20	.003694	.002313	.001031	.000363	.000025
1.24	.003326	.002248	.000874	.000334	.000023
1.28	.003103	.002185	.000771	.000317	.000021
1.32	.002856	.001809	.000686	.000297	.000020
1.36	.002663	.001877	.000612	.000271	.000019
1.40	.002558	.001686	.000558	.000269	.000018
1.44	.002440	.001984	.000494	.000246	.000016
1.48	.002337	.001473	.000446	.000232	.000015
1.52	.002253	.001544	.000404	.000220	.000014
1.56	.002158	.001521	.000373	.000204	.000013
1.60	.002074	.001431	.000345	.000190	.000012
1.64	.002039	.001491	.000316	.000172	.000011
1.68	.002001	.001397	.000301	.000170	.000010
1.72	.001954	.001360	.000275	.000153	.000009
1.76	.001905	.001279	.000263	.000144	.000009
1.80	.001914	.001383	.000259	.000149	.000009
1.84	.001879	.001073	.000240	.000133	.000008

DEFLECTION RESPONSE FUNCTIONS
C130 AIRCRAFT-SITE 3

TIME	RESP 0	RESP 1	RESP 2	RESP 3	RESP 4
0.00	.002228	.003533	.000815	.000275	.000049
.04	.002836	.003076	.000972	.000296	.000053
.08	.003548	.005718	.001376	.000336	.000057
.12	.004614	.005735	.001852	.000399	.000062
.16	.005878	.008751	.002389	.000454	.000067
.20	.007304	.010322	.002905	.000511	.000072
.24	.009258	.012749	.003500	.000567	.000077
.28	.011813	.014582	.004292	.000677	.000082
.32	.014704	.017741	.005034	.000785	.000086
.36	.018237	.019583	.005719	.000882	.000091
.40	.022295	.022471	.006508	.001014	.000094
.44	.026881	.024479	.007135	.001111	.000098
.48	.031484	.025993	.007819	.001205	.000101
.52	.035346	.026324	.008258	.001273	.000104
.56	.037938	.027011	.008651	.001348	.000106
.60	.039000	.026126	.008853	.001390	.000108
.64	.038570	.026100	.008974	.001421	.000109
.68	.036819	.024567	.008915	.001430	.000109
.72	.034487	.024153	.008766	.001414	.000109
.76	.032112	.022546	.008649	.001428	.000109
.80	.029962	.023248	.008574	.001422	.000108
.84	.028207	.021018	.008358	.001400	.000108
.88	.026844	.021171	.008222	.001399	.000106
.92	.026115	.020098	.008102	.001401	.000106
.96	.025926	.021402	.007924	.001395	.000104
1.00	.026282	.020089	.007771	.001364	.000102
1.04	.027480	.021715	.007714	.001361	.000100
1.08	.029202	.020858	.007673	.001347	.000098
1.12	.030870	.021358	.007639	.001335	.000096
1.16	.031681	.020317	.007468	.001323	.000093
1.20	.031470	.019285	.007258	.001289	.000090
1.24	.030222	.017145	.006965	.001271	.000088
1.28	.028258	.015557	.006610	.001222	.000084
1.32	.026040	.013821	.006270	.001187	.000081
1.36	.023557	.012865	.005736	.001149	.000077
1.40	.020926	.010308	.005231	.001089	.000073
1.44	.018598	.009020	.004718	.001045	.000069
1.48	.016316	.006737	.004127	.000978	.000065
1.52	.014295	.005755	.003529	.000908	.000060
1.56	.012388	.004153	.002971	.000821	.000056
1.60	.010708	.003911	.002454	.000745	.000052
1.64	.009315	.002072	.001916	.000684	.000049
1.68	.008090	.002313	.001588	.000623	.000045
1.72	.007019	.000878	.001209	.000553	.000042
1.76	.006107	.001376	.000929	.000513	.000039
1.80	.005334	.000529	.000631	.000466	.000036
1.84	.004734	.000437	.000448	.000424	.000033

TDT FUNCTIONS
C135 AIRCRAFT-SITE 1

TIME	FUNC 1	FUNC 2	FUNC 3	FUNC 4
.00	.000000	.002348	.000010	.000000
.04	.101932	.003173	.000011	.000000
.08	.126460	.004057	.000013	.000000
.12	.162192	.004907	.000015	.000000
.16	.227275	.006324	.000016	.000000
.20	.304122	.007877	.000017	.000000
.24	.402837	.009264	.000019	.000000
.28	.506481	.010897	.000019	.000000
.32	.613318	.012445	.000020	.000000
.36	.645742	.013259	.000020	.000000
.40	.504594	.013081	.000019	.000000
.44	.491714	.012357	.000018	.000000
.48	.443401	.011630	.000017	.000000
.52	.463034	.011045	.000015	.000000
.56	.518528	.010616	.000013	.000000
.60	.485399	.009696	.000011	.000000
.64	.339006	.007972	.000009	.000000
.68	.159824	.005617	.000006	.000000
.72	-.011402	.003002	.000003	.000000
.76	-.153995	.000267	.000001	.000000
.80	-.206972	-.002068	-.000001	.000000
.84	-.337872	-.003763	-.000003	-.000000
.88	-.396405	-.005104	-.000004	-.000000
.92	-.418527	-.006024	-.000005	-.000000
.96	-.410740	-.006417	-.000006	-.000000
1.00	-.391693	-.006576	-.000006	-.000000
1.04	-.336395	-.006340	-.000006	-.000000
1.08	-.276573	-.005654	-.000007	-.000000
1.12	-.229256	-.005065	-.000006	-.000000
1.16	-.180225	-.004452	-.000005	-.000000
1.20	-.134951	-.003564	-.000004	-.000000
1.24	-.078527	-.002616	-.000004	-.000000
1.28	-.021219	-.001907	-.000002	-.000000
1.32	.031126	-.000939	-.000001	-.000000
1.36	.083351	.000118	-.000001	-.000000
1.40	.114371	.000713	.000001	-.000000
1.44	.140301	.001298	.000001	.000000
1.48	.147629	.001708	.000002	.000000
1.52	.149450	.002102	.000002	.000000
1.56	.141349	.001942	.000002	.000000
1.60	.123972	.002333	.000002	.000000
1.64	.099501	.001844	.000001	.000000
1.68	.070172	.001454	.000002	.000000
1.72	.046531	.001145	.000001	.000000
1.76	.021628	.000917	-.000000	.000000
1.80	-.009373	.000216	.000000	-.000000
1.84	-.029268	-.000207	-.000001	-.000000

TDT FUNCTIONS
C131 AIRCRAFT-SITE 1

TIME	FUNC 1	FUNC 2	FUNC 3	FUNC 4
1.01	.011698	.004257	0.000000	.000000
1.04	.010513	.004905	0.000000	.000000
1.07	.012147	.005416	0.000000	.000000
1.12	.016102	.005892	0.000000	.000000
1.14	.024081	.006224	.000008	.000000
1.20	.046159	.007098	.000014	.000000
1.24	.087519	.007816	.000012	.000000
1.26	.153254	.008653	.000009	.000000
1.32	.238505	.009809	-.000000	.000000
1.34	.333803	.010499	-.000000	.000000
1.40	.427852	.011457	-.000000	.000000
1.44	.516418	.011726	-.000001	.000000
1.46	.589286	.011901	-.000001	.000000
1.52	.639195	.011965	-.000001	.000000
1.54	.659159	.011471	-.000001	.000000
1.56	.649008	.010406	.000004	.000000
1.60	.621620	.009853	.000009	.000000
1.64	.587400	.008875	-.000003	.000000
1.72	.543529	.007619	-.000004	.000000
1.74	.482562	.006486	.000005	.000000
1.80	.398018	.005603	.000004	.000000
1.84	.289901	.004587	-.000004	.000000
1.86	.165457	.003443	.000008	.000000
1.92	.039767	.002428	.000008	.000000
1.94	-.071733	.001391	-.000003	.000000
1.00	-.165714	.000294	-.000003	.000000
1.04	-.246060	-.000584	-.000003	.000000
1.06	-.313309	-.001201	.000012	.000000
1.12	-.369252	-.001866	.000007	.000000
1.14	-.408798	-.002127	-.000002	.000000
1.20	-.433968	-.002397	-.000002	.000000
1.24	-.439803	-.002439	.000014	.000000
1.26	-.429571	-.002044	.000005	.000000
1.32	-.407000	-.001736	-.000003	.000000
1.34	-.372311	-.001911	-.000003	.000000
1.40	-.324609	-.001585	-.000003	.000000
1.44	-.267174	-.000925	-.000003	.000000
1.46	-.202977	-.000221	-.000003	.000000
1.52	-.134206	.000315	.000017	.000000
1.54	-.062720	.000957	.000001	.000000
1.60	.004964	.001469	-.000003	.000000
1.64	.068879	.001825	-.000003	.000000
1.66	.127336	.002740	-.000003	.000000
1.72	.176789	.003109	.000015	.000000
1.74	.215354	.003297	.000001	.000000
1.80	.243182	.003536	-.000003	.000000
1.84	.262025	.003198	.000021	.000000

TDT FUNCTIONS
1301 AIRCRAFT-SITE 1

TIME	FUNC 1	FUNC 2	FUNC 3	FUNC 4
0.00	.125572	.004541	.000014	.000000
.04	.114530	.005056	.000015	.000000
.08	.118567	.005300	.000016	.000000
.12	.146814	.005372	.000016	.000000
.16	.178370	.006435	.000017	.000000
.20	.222706	.007260	.000018	.000000
.24	.268447	.007897	.000018	.000000
.28	.342216	.008793	.000019	.000000
.32	.383751	.009736	.000019	.000000
.36	.440376	.010597	.000019	.000000
.40	.493338	.010484	.000019	.000000
.44	.561599	.011545	.000018	.000000
.48	.596383	.011475	.000018	.000000
.52	.617431	.012121	.000017	.000000
.56	.603257	.011574	.000016	.000000
.60	.574862	.010903	.000014	.000000
.64	.497403	.010062	.000013	.000000
.68	.394223	.009288	.000011	.000000
.72	.287310	.008508	.000009	.000000
.76	.181011	.007571	.000008	.000000
.80	.076163	.006455	.000007	.000000
.84	-.005918	.005534	.000006	.000000
.88	-.057220	.004570	.000005	.000000
.92	-.103449	.003787	.000004	.000000
.96	-.162275	.002916	.000003	.000000
1.00	-.192273	.002172	.000003	.000000
1.04	-.205527	.001423	.000002	.000000
1.08	-.224237	.000681	.000002	.000000
1.12	-.232725	.000334	.000001	.000000
1.16	-.235738	-.000126	.000000	.000000
1.20	-.253526	-.000577	-.000000	.000000
1.24	-.252428	-.001168	-.000001	.000000
1.28	-.267616	-.001495	-.000001	-.000000
1.32	-.297444	-.002519	-.000001	-.000000
1.36	-.334239	-.002767	-.000002	-.000000
1.40	-.350618	-.003297	-.000002	-.000000
1.44	-.355185	-.003886	-.000002	-.000000
1.48	-.327207	-.004204	-.000003	-.000000
1.52	-.300837	-.004552	-.000003	-.000000
1.56	-.276767	-.004850	-.000003	-.000000
1.60	-.253936	-.005343	-.000003	-.000000
1.64	-.230893	-.005592	-.000003	-.000000
1.68	-.206836	-.005502	-.000003	-.000000
1.72	-.177893	-.005198	-.000003	-.000000
1.76	-.145313	-.005047	-.000002	-.000000
1.80	-.107723	-.004709	-.000002	-.000000
1.84	-.065364	-.004314	-.000001	-.000000

TOT FUNCTIONS
C135 AIRCRAFT-SITE 2

TIME	FUNC 1	FUNC 2	FUNC 3	FUNC 4
0.00	.105370	.036808	.001013	.000019
.04	.133185	.043918	.001340	.000022
.08	.181399	.053357	.001859	.000025
.12	.248802	.064031	.002412	.000028
.16	.352503	.077733	.003005	.000032
.20	.514487	.095359	.003596	.000034
.24	.748338	.114171	.004124	.000037
.28	1.024636	.133632	.004583	.000038
.32	1.206726	.147222	.004833	.000038
.36	1.204223	.146529	.004782	.000037
.40	1.077595	.135344	.004567	.000035
.44	.938273	.122089	.004291	.000032
.48	.854399	.110341	.003981	.000030
.52	.839253	.099298	.003649	.000027
.56	.848752	.089923	.003290	.000024
.60	.767997	.075790	.002887	.000020
.64	.573377	.052412	.002501	.000016
.68	.297813	.024006	.002149	.000012
.72	.035972	-.002166	.001829	.000009
.76	-.189261	-.026286	.001557	.000006
.80	-.369197	-.046932	.001303	.000003
.84	-.516327	-.064227	.001050	.000001
.88	-.622941	-.075612	.000711	-.000002
.92	-.682475	-.081635	.000344	-.000004
.96	-.695831	-.082672	.000040	-.000005
1.00	-.657133	-.078878	-.000250	-.000007
1.04	-.583231	-.071714	-.000435	-.000007
1.08	-.497624	-.062488	-.000565	-.000008
1.12	-.399708	-.052087	-.000624	-.000008
1.16	-.303856	-.040533	-.000663	-.000008
1.20	-.202529	-.029179	-.000598	-.000007
1.24	-.101271	-.017481	-.000491	-.000006
1.28	-.005141	-.006497	-.000355	-.000004
1.32	.094557	.003616	-.000217	-.000003
1.36	.166735	.011881	-.000065	-.000002
1.40	.229653	.018932	.000075	-.000001
1.44	.267963	.024297	.000219	-.000000
1.48	.295408	.027361	.000331	.000000
1.52	.297090	.028177	.000462	.000001
1.56	.281614	.026897	.000550	.000001
1.60	.253336	.023801	.000596	.000001
1.64	.203872	.019282	.000628	.000001
1.68	.153788	.013779	.000635	.000001
1.72	.097461	.007710	.000622	.000001
1.76	.040959	.001476	.000585	.000000
1.80	-.015170	-.004559	.000540	-.000000
1.84	-.063836	-.010072	.000470	-.000001

TDT FUNCTIONS
C134 AIRCRAFT-SITE 2

TIME	FUNC 1	FUNC 2	FUNC 3	FUNC 4
0.00	.469510	.108575	.003264	.000039
.04	.514572	.113856	.004033	.000040
.08	.529570	.112398	.004352	.000040
.12	.591558	.116177	.004230	.000038
.16	.659043	.121376	.003023	.000037
.20	.683867	.117516	.003506	.000037
.24	.782588	.120766	.002650	.000035
.28	.802897	.115559	.002496	.000034
.32	.865913	.117513	.002654	.000032
.36	.903690	.114193	.002162	.000031
.40	.890664	.106706	.002773	.000028
.44	.876625	.099664	.003213	.000026
.48	.894077	.094687	.002251	.000022
.52	.833639	.086427	.002376	.000019
.56	.763037	.074226	.002684	.000018
.60	.674032	.066426	.001106	.000013
.64	.528624	.049279	.001160	.000011
.68	.434085	.036987	.001225	.000009
.72	.274367	.024391	.000926	.000007
.76	.101128	.011828	.000386	.000006
.80	-.028143	.006771	.001009	.000005
.84	-.138347	.000450	.000478	.000003
.88	-.269735	-.011526	.000766	.000003
.92	-.340908	-.018420	.001176	.000004
.96	-.387383	-.015274	-.000026	.000003
1.00	-.484042	-.020244	.001236	.000005
1.04	-.491586	-.020788	.001364	.000006
1.08	-.518817	-.018117	.000788	.000006
1.12	-.538627	-.019791	.000965	.000009
1.16	-.505236	-.012868	.000949	.000009
1.20	-.462206	-.012092	.001104	.000010
1.24	-.386824	-.005152	.001392	.000012
1.28	-.311357	.001557	.001828	.000014
1.32	-.216065	.008575	.002054	.000015
1.36	-.127155	.014280	.002246	.000016
1.40	-.030161	.016896	.002475	.000017
1.44	.018021	.020909	.002910	.000017
1.48	.101124	.024168	.002796	.000017
1.52	.157359	.033539	.002003	.000015
1.56	.227742	.032511	.001537	.000014
1.60	.267284	.030958	.002197	.000014
1.64	.314182	.032972	.001281	.000012
1.68	.328654	.029062	.001188	.000011
1.72	.314970	.024040	.001866	.000011
1.76	.323873	.018143	.001562	.000009
1.80	.285937	.012746	.001475	.000007
1.84	.263898	.003124	.001387	.000006

TDT FUNCTIONS
C130 AIRCRAFT-SITE 2

TIME	FUNC 1	FUNC 2	FUNC 3	FUNC 4
0.00	.131197	.040900	.000187	.000019
.04	.156475	.048017	.000195	.000020
.08	.203638	.055143	.000514	.000023
.12	.273803	.064553	.000856	.000025
.16	.372522	.077414	.001191	.000026
.20	.496840	.090389	.001558	.000027
.24	.646737	.101515	.001975	.000028
.28	.753210	.110728	.002077	.000028
.32	.803862	.116558	.002024	.000027
.36	.827386	.117337	.001985	.000027
.40	.827562	.115047	.001985	.000026
.44	.852771	.114808	.002010	.000026
.48	.883976	.114361	.002982	.000028
.52	.924042	.112914	.003532	.000028
.56	.958862	.110968	.003195	.000026
.60	.944969	.105994	.003215	.000024
.64	.858970	.095490	.003248	.000022
.68	.723282	.082312	.003405	.000021
.72	.555481	.064752	.003718	.000020
.76	.378969	.045757	.003618	.000018
.80	.222696	.029356	.003394	.000016
.84	.075234	.013973	.003138	.000014
.88	-.044476	-.000532	.002947	.000013
.92	-.126661	-.010323	.002627	.000010
.96	-.191576	-.017990	.002346	.000009
1.00	-.230856	-.024698	.002014	.000007
1.04	-.236363	-.027279	.001666	.000005
1.08	-.223165	-.027156	.001273	.000003
1.12	-.203483	-.027694	.000975	.000002
1.16	-.168301	-.026601	.000724	.000000
1.20	-.134953	-.024952	.000547	-.000001
1.24	-.105510	-.024577	.000322	-.000002
1.28	-.075423	-.021964	.000051	-.000003
1.32	-.065051	-.021314	-.000061	-.000004
1.36	-.071253	-.020264	-.000172	-.000004
1.40	-.086657	-.020339	-.000230	-.000005
1.44	-.113285	-.022443	-.000284	-.000005
1.48	-.156589	-.025946	-.000298	-.000006
1.52	-.200034	-.029617	-.000333	-.000006
1.56	-.246300	-.033029	-.000287	-.000007
1.60	-.287817	-.036176	-.000227	-.000007
1.64	-.335619	-.041029	-.000155	-.000007
1.68	-.373257	-.041771	-.000121	-.000007
1.72	-.390379	-.040712	-.000035	-.000006
1.76	-.407322	-.041822	.000037	-.000006
1.80	-.398448	-.042654	.000080	-.000006
1.84	-.388855	-.043719	.000190	-.000006

TDT FUNCTIONS
C135 AIRCRAFT-SITE 3

TIME	FUNC 1	FUNC 2	FUNC 3	FUNC 4
0.00	.106026	.032703	.010495	.002532
.04	.220644	.056214	.013416	.003014
.08	.416254	.105345	.018386	.003568
.12	.615563	.168982	.024544	.004104
.16	.921077	.246380	.034131	.004623
.20	1.265266	.336632	.045737	.005097
.24	1.559334	.433292	.060131	.005511
.28	1.648859	.501743	.072370	.005675
.32	1.554869	.522560	.077216	.005561
.36	1.408451	.504869	.076808	.005331
.40	1.164607	.476384	.075574	.005060
.44	1.061529	.439509	.072003	.004730
.48	1.035923	.405143	.067552	.004360
.52	1.061348	.370943	.063226	.003951
.56	.978078	.344606	.057730	.003427
.60	.798934	.311249	.051508	.002750
.64	.477765	.261086	.043527	.001976
.68	.041675	.188658	.035993	.001217
.72	-.361224	.067540	.025936	.000330
.76	-.667484	-.065466	.014194	-.000497
.80	-.894752	-.180086	.001433	-.001204
.84	-1.034737	-.271256	-.011475	-.001798
.88	-1.105858	-.330487	-.023296	-.002189
.92	-1.056348	-.356649	-.031296	-.002359
.96	-.964062	-.355499	-.035828	-.002334
1.00	-.805693	-.331659	-.037461	-.002206
1.04	-.625011	-.285669	-.035357	-.001918
1.08	-.473515	-.234248	-.031643	-.001554
1.12	-.304512	-.178028	-.026107	-.001176
1.16	-.159616	-.122037	-.020143	-.000761
1.20	-.003092	-.067613	-.016349	-.000551
1.24	.142587	-.016382	-.010351	-.000142
1.28	.260471	.030863	-.004118	.000249
1.32	.355870	.071884	.001988	.000587
1.36	.444015	.111671	.007469	.000878
1.40	.506487	.142240	.012377	.001085
1.44	.528783	.163812	.015903	.001221
1.48	.517889	.171894	.018753	.001288
1.52	.477292	.170059	.020579	.001244
1.56	.402108	.159750	.020832	.001160
1.60	.312138	.140054	.020349	.001026
1.64	.226184	.115233	.018590	.000814
1.68	.124669	.081239	.015557	.000580
1.72	.013338	.047499	.012212	.000338
1.76	-.061044	.014316	.008546	.000082
1.80	-.134085	-.016310	.004649	-.000129
1.84	-.215352	-.042973	.001226	-.000309

TDT FUNCTIONS
C131 AIRCRAFT-SITE 3

TIME	FUNC 1	FUNC 2	FUNC 3	FUNC 4
0.00	.216880	.062023	.022520	.003491
.04	.213904	.078310	.024861	.003809
.08	.331101	.099671	.027422	.004100
.12	.422087	.129089	.031629	.004443
.16	.535797	.163186	.034937	.004799
.20	.578351	.196770	.038595	.005058
.24	.745524	.232171	.042606	.005226
.28	.817773	.267147	.048401	.005335
.32	1.025755	.301800	.050443	.005332
.36	1.197577	.340228	.055572	.005366
.40	1.332550	.380399	.061427	.005359
.44	1.483479	.417103	.064429	.005311
.48	1.499369	.445119	.067754	.005067
.52	1.488029	.463974	.070491	.004836
.56	1.412907	.467954	.069121	.004432
.60	1.316314	.458484	.067375	.003991
.64	1.189179	.432206	.062080	.003434
.68	.987923	.398219	.055347	.002832
.72	.751380	.357674	.050359	.002308
.76	.562961	.308637	.043901	.001746
.80	.284441	.249202	.037530	.001258
.84	.105792	.183583	.032913	.000773
.88	-.123207	.110063	.025226	.000324
.92	-.356459	.036794	.018136	-.000080
.96	-.512436	-.033436	.010449	-.000483
1.00	-.673632	-.100672	.003613	-.000801
1.04	-.765130	-.162069	-.003941	-.001105
1.08	-.855902	-.214088	-.009116	-.001358
1.12	-.911084	-.256627	-.013695	-.001546
1.16	-.943805	-.289005	-.018624	-.001674
1.20	-.923022	-.306380	-.022295	-.001736
1.24	-.852008	-.314865	-.024534	-.001705
1.28	-.758864	-.308338	-.024431	-.001535
1.32	-.690479	-.292388	-.023908	-.001328
1.36	-.545252	-.268360	-.023552	-.001088
1.40	-.425989	-.235829	-.019279	-.000812
1.44	-.232740	-.200228	-.017493	-.000598
1.48	-.151657	-.158963	-.014071	-.000364
1.52	.006905	-.115069	-.010147	-.000132
1.56	.144015	-.068999	-.006616	.000117
1.60	.259411	-.023565	-.002966	.000345
1.64	.379972	.019252	.000061	.000559
1.68	.460549	.060293	.004855	.000764
1.72	.528500	.094961	.007243	.000855
1.76	.568290	.125600	.010139	.000968
1.80	.611541	.150737	.014436	.001049
1.84	.574833	.166791	.015071	.001058

TDT FUNCTIONS
1301 AIRCRAFT-SITE 3

TIME	FUNC 1	FUNC 2	FUNC 3	FUNC 4
0.00	.226576	.052243	.017648	.003150
.04	.195646	.061991	.018826	.003405
.08	.363269	.087354	.021223	.003634
.12	.360690	.116993	.025062	.003876
.16	.549608	.150029	.028268	.004149
.20	.643210	.181216	.031476	.004389
.24	.789190	.216678	.034479	.004599
.28	.893346	.263785	.040776	.004821
.32	1.078420	.306433	.046705	.004969
.36	1.173119	.343867	.051655	.005063
.40	1.328521	.386025	.058547	.005067
.44	1.419298	.415506	.062709	.005032
.48	1.469353	.446029	.066264	.004897
.52	1.433967	.457980	.067687	.004713
.56	1.411776	.463907	.069163	.004435
.60	1.278962	.454567	.068137	.004105
.64	1.192543	.437104	.066017	.003757
.68	1.001230	.405362	.062235	.003336
.72	.875336	.365396	.056589	.002909
.76	.667616	.325487	.052665	.002478
.80	.605314	.286727	.047304	.002074
.84	.353646	.237908	.040804	.001684
.88	.257626	.193915	.035643	.001302
.92	.087755	.151495	.030655	.000965
.96	.078745	.106594	.025316	.000601
1.00	-.087934	.065425	.018569	.000250
1.04	-.052655	.033244	.013902	-.000055
1.08	-.163161	.005417	.008937	-.000322
1.12	-.171169	-.018189	.004585	-.000601
1.16	-.263300	-.046432	.000675	-.000880
1.20	-.340024	-.072823	-.004004	-.001133
1.24	-.474405	-.100120	-.007015	-.001322
1.28	-.561134	-.127140	-.011413	-.001525
1.32	-.647215	-.149139	-.014295	-.001684
1.36	-.674663	-.179862	-.016748	-.001841
1.40	-.798254	-.205366	-.020147	-.001966
1.44	-.834278	-.228251	-.021997	-.002040
1.48	-.928803	-.253293	-.024867	-.002073
1.52	-.934120	-.275995	-.027498	-.002109
1.56	-.972642	-.293385	-.030778	-.002065
1.60	-.915709	-.305316	-.032965	-.001970
1.64	-.951827	-.315688	-.033640	-.001824
1.68	-.842999	-.309251	-.033936	-.001666
1.72	-.830091	-.302829	-.034349	-.001467
1.76	-.680888	-.286540	-.032367	-.001220
1.80	-.607399	-.267914	-.030419	-.000964
1.84	-.476253	-.238721	-.027727	-.000682

APPENDIX II

PREDICTED DEFLECTION RESPONSE FUNCTIONS

The predicted deflection response functions are contained in this Appendix. The functions were calculated by using computer code CONVLE. All nine combinations of aircraft and test sites were employed, and similar results as shown in the typical plots (Figures 47 and 48) were achieved. Computer printouts of the predicted dynamic deflections for four of the nine combinations are provided. These results, labeled cases 1 through 4, are representative of all the combinations. They include:

- Case 1. C131 Aircraft and Site 2 - Standard Predictions provided for C135 and C130 aircraft at both sites 1 and 3.
- Case 2. C135 Aircraft and Site 2 - Standard Predictions provided for C131 and C130 aircraft at both sites 1 and 3.
- Case 3. C130 Aircraft and Site 2 - Standard Predictions provided for C135 and C131 aircraft at both sites 1 and 3.
- Case 4. C131 Aircraft and Site 1 - Standard Predictions provided for C135 and C130 aircraft at both sites 2 and 3.

Case 1

C131 Aircraft and Site 2 - Standard

Predictions for:

C135 Aircraft at Site 1
C130 Aircraft at Site 1
C135 Aircraft at Site 3
C130 Aircraft at Site 3

PREDICTED DEFL. RESPONSE FUNS (BY RATIO MULTIPLICATION)
C135 AIRCRAFT SITE-1

TIME	RESP 0	RESP 1	RESP 2	RESP 3	RESP 4
0.00	.002722	.012436	.000154	.000000	.000000
.04	.004084	.00308	.000184	.000000	.000000
.08	.005336	.00421	.000224	.000000	.000000
.12	.006574	.005804	.000270	.000001	.000000
.16	.013546	.00824	.000330	.000001	.000000
.20	.022699	.012081	.000408	.000001	.000000
.24	.033029	.017645	.000494	.000001	.000000
.28	.065481	.024310	.000583	.000001	.000000
.32	.095708	.028970	.000665	.000001	.000000
.36	.102332	.029527	.000688	.000001	.000000
.40	.086336	.027372	.000663	.000001	.000000
.44	.073621	.02512	.000643	.000001	.000000
.48	.060398	.024445	.000628	.000001	.000000
.52	.074167	.025694	.000622	.000001	.000000
.56	.090539	.027870	.000620	.000001	.000000
.60	.105790	.028193	.000618	.000001	.000000
.64	.096831	.025831	.000563	.000001	.000000
.68	.076640	.021282	.000490	.000001	.000000
.72	.053194	.01666	.000412	.000001	.000000
.76	.040533	.012646	.000336	.000001	.000000
.80	.030005	.009607	.000263	.000001	.000000
.84	.031366	.007317	.000208	.000001	.000000
.88	.026342	.005777	.000166	.000001	.000000
.92	.024137	.004777	.000134	.000001	.000000
.96	.022716	.003975	.000103	.000001	.000000
1.00	.020337	.003492	.000090	.000001	.000000
1.04	.019384	.003177	.000073	.000001	.000000
1.08	.019139	.002815	.000058	.000001	.000000
1.12	.018592	.002653	.000045	.000001	.000000
1.16	.018133	.002435	.000036	.000001	.000000
1.20	.017719	.002317	.000026	.000000	.000000
1.24	.017371	.002170	.000013	.000000	.000000
1.28	.016656	.001962	.000013	.000000	.000000
1.32	.016440	.002044	.000003	.000000	.000000
1.36	.016200	.00183	.000003	.000000	.000000
1.40	.015844	.001812	.000001	.000000	.000000
1.44	.015730	.001669	.000001	.000000	.000000
1.48	.015678	.001724	.000001	.000000	.000000
1.52	.015163	.001632	.000001	.000000	.000000
1.56	.015088	.001570	.000001	.000000	.000000
1.60	.015083	.001594	.000001	.000000	.000000
1.64	.014311	.001420	.000001	.000000	.000000
1.68	.014560	.001440	.000001	.000000	.000000
1.72	.014580	.001423	.000000	.000000	.000000
1.76	.014510	.001404	.000000	.000000	.000000
1.80	.014523	.001337	.000000	.000000	.000000
1.84	.014214	.001320	.000000	.000000	.000000

PREDICTED DEFL. RESPONSE FUNS (BY RATIO MULTIPLICATION)
C130 AIRCRAFT SITE-1

TIME	RESP 0	RESP 1	RESP 2	RESP 3	RESP 4
0.00	.003151	.002741	.000123	.000000	.000000
.04	.004368	.003285	.000145	.000000	.000000
.08	.005344	.004295	.000167	.000000	.000000
.12	.006229	.005801	.000197	.000000	.000000
.16	.012484	.007935	.000238	.000000	.000000
.20	.019225	.010640	.000281	.000000	.000000
.24	.023811	.013952	.000321	.000000	.000000
.28	.037599	.016442	.000357	.000000	.000000
.32	.041988	.017851	.000385	.000000	.000000
.36	.043460	.018785	.000400	.000000	.000000
.40	.045267	.019339	.000408	.000000	.000000
.44	.049645	.020546	.000424	.000000	.000000
.48	.055426	.022018	.000442	.000001	.000000
.52	.062509	.023815	.000460	.000001	.000000
.56	.070429	.025630	.000479	.000001	.000000
.60	.075990	.026540	.000491	.000001	.000000
.64	.075066	.026032	.000488	.000001	.000000
.68	.069372	.024564	.000476	.000001	.000000
.72	.062237	.022495	.000452	.000001	.000000
.76	.055501	.020296	.000422	.000001	.000000
.80	.049951	.018530	.000398	.000001	.000000
.84	.045156	.016888	.000375	.000001	.000000
.88	.041932	.015685	.000351	.000001	.000000
.92	.039884	.015054	.000338	.000001	.000000
.96	.038677	.014536	.000326	.000001	.000000
1.00	.038633	.014303	.000313	.000001	.000000
1.04	.043948	.014547	.000309	.000001	.000000
1.08	.042488	.014984	.000310	.000001	.000000
1.12	.045454	.015367	.000306	.000001	.000000
1.16	.048448	.015900	.000304	.000001	.000000
1.20	.051680	.016220	.000303	.000001	.000000
1.24	.053311	.016293	.000295	.000001	.000000
1.28	.053970	.016243	.000292	.000001	.000000
1.32	.052504	.015631	.000282	.000001	.000000
1.36	.049743	.014755	.000273	.000001	.000000
1.40	.046273	.013641	.000259	.000001	.000000
1.44	.042291	.012351	.000240	.000001	.000000
1.48	.038082	.010799	.000216	.000001	.000000
1.52	.034225	.009341	.000193	.000001	.000000
1.56	.030709	.007917	.000171	.000001	.000000
1.60	.027595	.006671	.000151	.000001	.000000
1.64	.025028	.005346	.000125	.000001	.000000
1.68	.022810	.004254	.000112	.000001	.000000
1.72	.020356	.003570	.000103	.000001	.000000
1.76	.018450	.002822	.000087	.000001	.000000
1.80	.016277	.002522	.000071	.000001	.000000
1.84	.017959	.002091	.000052	.000001	.000000

PREDICTED DEFL. RESPONSE FUNS (BY RATIO MULTIPLICATION)
C135 AIRCRAFT SITE-3

TIME	RESP 0	RESP 1	RESP 2	RESP 3	RESP 4
0.00	.001407	.002863	.003103	.000359	.000056
.04	.002110	.003630	.003715	.000476	.000064
.08	.003017	.004959	.004530	.000662	.000074
.12	.004431	.006822	.005461	.000862	.000084
.16	.007000	.009697	.006669	.001030	.000094
.20	.011730	.014201	.008245	.001302	.000104
.24	.020169	.020741	.009988	.001510	.000113
.28	.033839	.028577	.011395	.001710	.000121
.32	.049460	.034054	.013450	.001855	.000127
.36	.052383	.034709	.013898	.001910	.000131
.40	.044927	.032176	.013510	.001920	.000132
.44	.038046	.029540	.013003	.001919	.000133
.48	.035347	.028735	.012702	.001918	.000134
.52	.033328	.030204	.012568	.001918	.000133
.56	.046789	.032761	.012694	.001920	.000133
.60	.054670	.033141	.012500	.001913	.000131
.64	.050040	.030364	.011484	.001908	.000127
.68	.039606	.025017	.009899	.001902	.000122
.72	.030590	.019593	.008330	.001892	.000119
.76	.024047	.014866	.006784	.001882	.000115
.80	.019640	.011293	.005414	.001862	.000109
.84	.016210	.008602	.004210	.001824	.000103
.88	.013923	.006791	.003351	.001735	.000096
.92	.012473	.005610	.002717	.001613	.000088
.96	.011481	.004673	.002207	.001489	.000080
1.00	.010820	.004105	.001811	.001349	.000071
1.04	.010328	.003735	.001473	.001229	.000063
1.08	.009891	.003309	.001172	.001115	.000056
1.12	.009608	.003118	.000905	.001018	.000049
1.16	.009371	.002863	.000719	.000919	.000043
1.20	.009157	.002723	.000524	.000849	.000039
1.24	.008977	.002551	.000388	.000791	.000034
1.28	.008608	.002307	.000255	.000741	.000031
1.32	.008496	.002403	.000160	.000696	.000027
1.36	.008372	.002151	.000055	.000662	.000024
1.40	.008188	.002130	.000018	.000631	.000022
1.44	.008129	.001961	.000023	.000609	.000020
1.48	.008102	.002027	.000026	.000584	.000018
1.52	.007836	.001918	.000027	.000573	.000017
1.56	.007797	.001846	.000026	.000558	.000015
1.60	.007795	.001873	.000023	.000538	.000014
1.64	.007654	.001680	.000019	.000525	.000013
1.68	.007524	.001703	.000013	.000513	.000012
1.72	.007535	.001673	.000007	.000504	.000011
1.76	.007498	.001651	.000001	.000496	.000010
1.80	.007505	.001572	.000000	.000493	.000010
1.84	.007346	.001561	.000000	.000487	.000010

PREDICTED DEFL. RESPONSE FUNS (BY RATIO MULTIPLICATION)
C130 AIRCRAFT SITE-3

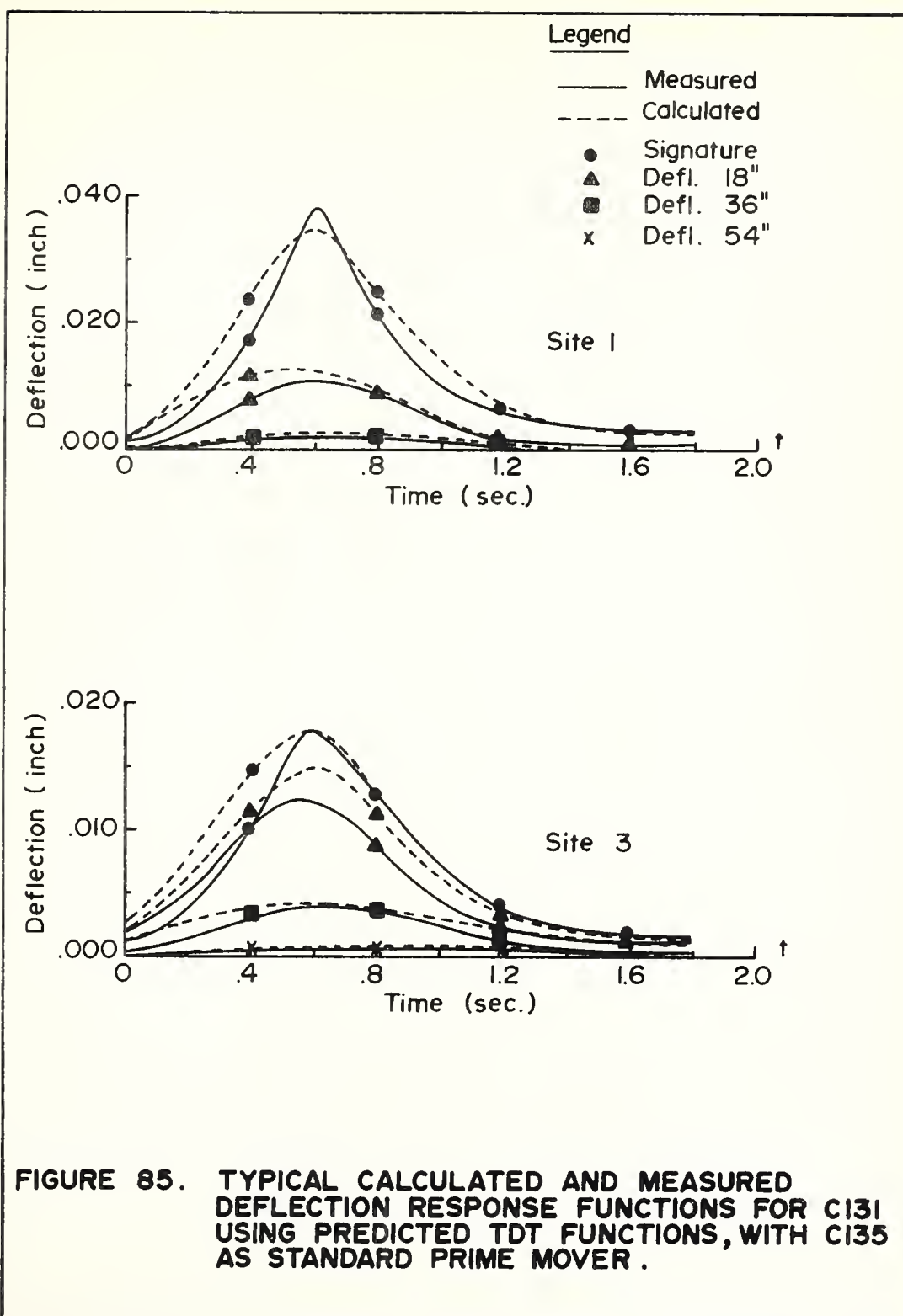
TIME	RESP 0	RESP 1	RESP 2	RESP 3	RESP 4
0.00	.001628	.003223	.002477	.000048	.000039
.04	.002257	.003862	.002922	.000050	.000043
.08	.003020	.005043	.003375	.000131	.000048
.12	.004252	.006811	.003973	.000219	.000053
.16	.006452	.009322	.004803	.000307	.000056
.20	.009335	.012507	.005678	.000403	.000059
.24	.014889	.016406	.006480	.000515	.000063
.28	.019430	.019327	.007215	.000549	.000065
.32	.021699	.020984	.007787	.000547	.000067
.36	.022459	.022082	.008089	.000552	.000069
.40	.023393	.022734	.008244	.000571	.000071
.44	.025656	.024152	.008571	.000601	.000075
.48	.028643	.025882	.008338	.000875	.000081
.52	.032303	.027994	.009298	.001047	.000086
.56	.036396	.030128	.009682	.000937	.000086
.60	.039270	.031193	.009326	.001041	.000088
.64	.038793	.030601	.009357	.001033	.000090
.68	.035850	.028875	.009628	.001132	.000092
.72	.032163	.026443	.009126	.001319	.000094
.76	.028682	.023851	.008520	.001356	.000096
.80	.025914	.021782	.008040	.001364	.000095
.84	.023336	.019852	.007574	.001362	.000094
.88	.021670	.018438	.007096	.001375	.000093
.92	.020611	.017696	.006824	.001353	.000091
.96	.019387	.017086	.006594	.001340	.000090
1.00	.018365	.016813	.006336	.001313	.000088
1.04	.020696	.017102	.006252	.001282	.000085
1.08	.021357	.017614	.006266	.001237	.000082
1.12	.023489	.018067	.006186	.001212	.000080
1.16	.025037	.018691	.006154	.001194	.000079
1.20	.026707	.019067	.006115	.001188	.000077
1.24	.027550	.019152	.005953	.001164	.000075
1.28	.027391	.019094	.005903	.001124	.000073
1.32	.027133	.018445	.005703	.001118	.000071
1.36	.025706	.017344	.005508	.001105	.000070
1.40	.023313	.016035	.005233	.001097	.000069
1.44	.021355	.014519	.004846	.001084	.000067
1.48	.019680	.012694	.004375	.001074	.000065
1.52	.017687	.010980	.003905	.001052	.000061
1.56	.015370	.009307	.003463	.001045	.000058
1.60	.014260	.007841	.003045	.001037	.000056
1.64	.012934	.006285	.002523	.001030	.000053
1.68	.011788	.005000	.002253	.001011	.000050
1.72	.010329	.004196	.002087	.001005	.000048
1.76	.010051	.003325	.001764	.000936	.000046
1.80	.009445	.002965	.001431	.000980	.000043
1.84	.008316	.002458	.001051	.000982	.000039

Case 2

C135 Aircraft and Site 2 - Standard

Predictions for:

C131 Aircraft at Site 1
C130 Aircraft at Site 1
C131 Aircraft at Site 3
C130 Aircraft at Site 3



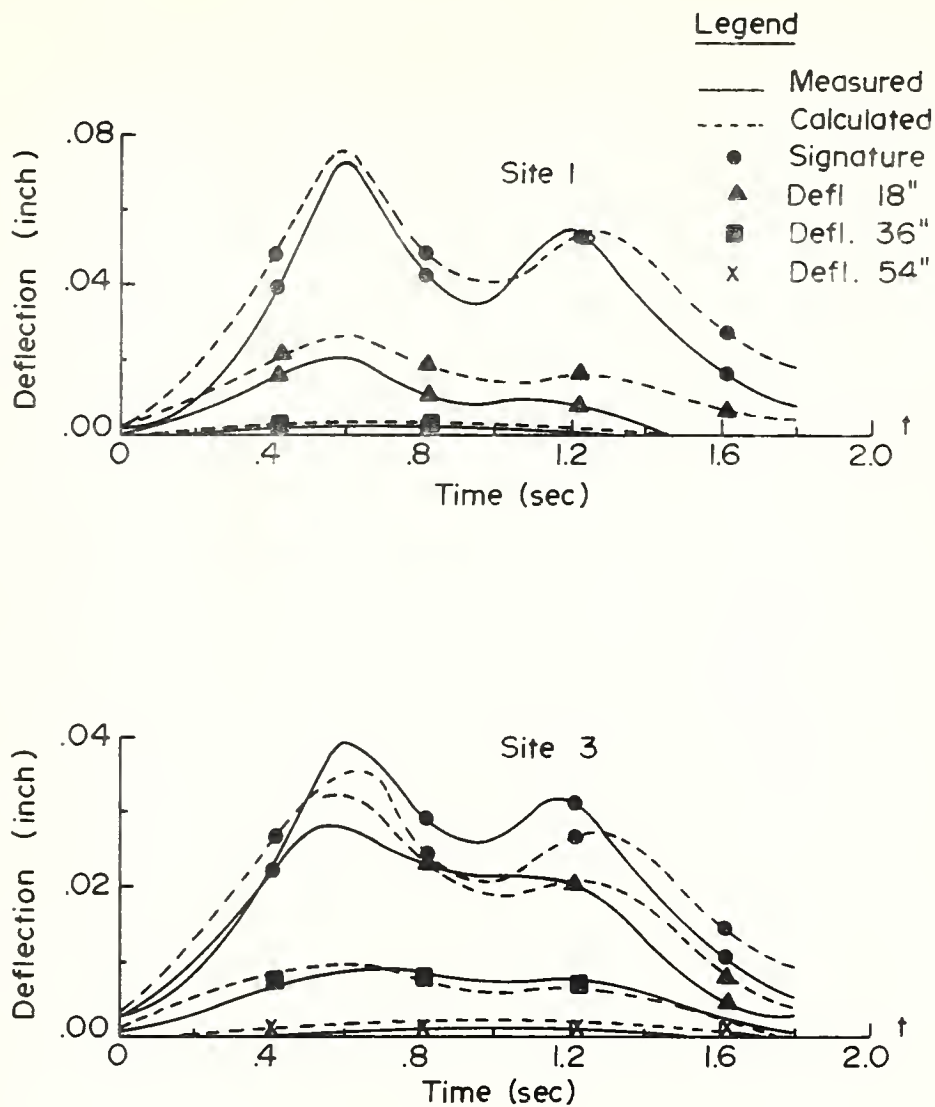


FIGURE 86. TYPICAL CALCULATED AND MEASURED DEFLECTION RESPONSE FUNCTIONS FOR C130 USING PREDICTED TDT FUNCTIONS WITH C135 AS STANDARD PRIME MOVER.

PREDICTED DEFL. RESPONSE FUNCS (BY RATIO MULTIPLICATION)
C131 AIRCRAFT SITE-1

TIME	RESP 0	RESP 1	RESP 2	RESP 3	RESP 4
.00	.004887	.004599	.000134	.000000	.000000
.04	.005944	.005120	.000143	.000000	.000000
.08	.006911	.005367	.000144	.000000	.000000
.12	.008190	.006096	.000152	.000000	.000000
.16	.009837	.006913	.000162	.000000	.000000
.20	.011404	.007349	.000162	.000000	.000000
.24	.013534	.008549	.000172	.000000	.000000
.28	.015736	.009036	.000172	.000000	.000000
.32	.018836	.010000	.000182	.000000	.000000
.36	.021816	.010785	.000187	.000000	.000000
.40	.024748	.011139	.000188	.000000	.000000
.44	.027612	.011544	.000191	.000000	.000000
.48	.030564	.012324	.000197	.000000	.000000
.52	.032652	.012401	.000200	.000000	.000000
.56	.033863	.012417	.000198	.000000	.000000
.60	.034270	.012275	.000202	.000000	.000000
.64	.033412	.011579	.000193	.000000	.000000
.68	.031657	.011351	.000189	.000000	.000000
.72	.030109	.010454	.000183	.000000	.000000
.76	.027425	.009354	.000176	.000000	.000000
.80	.024882	.008598	.000175	.000000	.000000
.84	.022502	.007935	.000171	.000000	.000000
.88	.019910	.006952	.000158	.000000	.000000
.92	.017354	.006425	.000150	.000000	.000000
.96	.015887	.006019	.000151	.000000	.000000
1.00	.013669	.004980	.000141	.000000	.000000
1.04	.012016	.004663	.000134	.000000	.000000
1.08	.010502	.004015	.000130	.000000	.000000
1.12	.009116	.003297	.000119	.000000	.000000
1.16	.007890	.002967	.000118	.000000	.000000
1.20	.006680	.002620	.000108	.000000	.000000
1.24	.006010	.002497	.000105	.000000	.000000
1.28	.005555	.002316	.000102	.000000	.000000
1.32	.004914	.002287	.000099	.000000	.000000
1.36	.004257	.002182	.000095	.000000	.000000
1.40	.004050	.002177	.000088	.000000	.000000
1.44	.003692	.001738	.000084	.000000	.000000
1.48	.003100	.001697	.000079	.000000	.000000
1.52	.003201	.001487	.000083	.000000	.000000
1.56	.003082	.001520	.000076	.000000	.000000
1.60	.002703	.001367	.000070	.000000	.000000
1.64	.002627	.001416	.000069	.000000	.000000
1.68	.002373	.001281	.000062	.000000	.000000
1.72	.002052	.000997	.000054	.000000	.000000
1.76	.001868	.001061	.000047	.000000	.000000
1.80	.001836	.000787	.000041	.000000	.000000
1.84	.001274	.000763	.000030	.000000	.000000

PREDICTED DFEL. RESPONSE FUNS (BY RATIO MULTIPLICATION)
C130 AIRCRAFT SITE-1

TIME	RESP 0	RESP 1	RESP 2	RESP 3	RESP 4
.00	.003151	.002686	.000112	.000000	.000000
.04	.004368	.003218	.000132	.000000	.000000
.08	.005844	.004208	.000153	.000000	.000000
.12	.008229	.005682	.000180	.000000	.000000
.16	.012484	.007769	.000217	.000000	.000000
.20	.019225	.010423	.000257	.000000	.000000
.24	.028811	.013668	.000293	.000000	.000000
.28	.037599	.016107	.000326	.000000	.000000
.32	.041988	.017488	.000352	.000000	.000000
.36	.043460	.018402	.000366	.000000	.000000
.40	.045267	.018946	.000373	.000000	.000000
.44	.049645	.020128	.000387	.000000	.000000
.48	.055426	.021570	.000404	.000000	.000000
.52	.062509	.023330	.000420	.000001	.000000
.56	.070429	.025108	.000438	.000000	.000000
.60	.075990	.026000	.000449	.000001	.000000
.64	.075066	.025503	.000446	.000001	.000000
.68	.069372	.024064	.000435	.000001	.000000
.72	.062237	.022037	.000413	.000001	.000000
.76	.055501	.019883	.000385	.000001	.000000
.80	.049951	.018152	.000363	.000001	.000000
.84	.045156	.016545	.000342	.000001	.000000
.88	.041932	.015366	.000321	.000001	.000000
.92	.039884	.014747	.000308	.000001	.000000
.96	.038677	.014240	.000298	.000001	.000000
1.00	.038633	.014012	.000286	.000001	.000000
1.04	.040048	.014253	.000283	.000001	.000000
1.08	.042488	.014679	.000283	.000001	.000000
1.12	.045454	.015056	.000280	.000001	.000000
1.16	.048448	.015577	.000278	.000001	.000000
1.20	.051680	.015890	.000276	.000001	.000000
1.24	.053311	.015961	.000269	.000001	.000000
1.28	.053970	.015913	.000267	.000001	.000000
1.32	.052504	.015372	.000258	.000001	.000000
1.36	.049743	.014454	.000249	.000001	.000000
1.40	.046273	.013364	.000237	.000001	.000000
1.44	.042291	.012100	.000219	.000001	.000000
1.48	.038082	.010579	.000198	.000001	.000000
1.52	.034225	.009151	.000177	.000001	.000000
1.56	.030709	.007756	.000157	.000001	.000000
1.60	.027595	.006535	.000138	.000001	.000000
1.64	.025028	.005237	.000114	.000001	.000000
1.68	.022810	.004167	.000102	.000001	.000000
1.72	.020956	.003497	.000094	.000000	.000000
1.76	.019450	.002771	.000080	.000000	.000000
1.80	.018277	.002471	.000065	.000000	.000000
1.84	.017059	.002049	.000047	.000000	.000000

PREDICTED DEFL. RESPONSE FUNCS (BY RATIO MULTIPLICATION)
C131 AIRCRAFT SITE-3

TIME	RESP 0	RESP 1	RESP 2	RESP 3	RESP 4
.00	.002525	.006069	.002730	.000369	.000041
.04	.003072	.006756	.002910	.000463	.000043
.08	.003572	.007083	.002931	.000508	.000044
.12	.004233	.008044	.003093	.000505	.000043
.16	.005083	.009122	.003306	.000382	.000043
.20	.005893	.009698	.003307	.000450	.000045
.24	.006994	.011281	.003503	.000369	.000044
.28	.008132	.011924	.003507	.000369	.000045
.32	.009734	.013196	.003715	.000407	.000045
.36	.011274	.014231	.003816	.000376	.000046
.40	.012789	.014698	.003837	.000471	.000046
.44	.014269	.015233	.003890	.000551	.000047
.48	.015795	.016262	.004016	.000476	.000046
.52	.016874	.016364	.004075	.000524	.000046
.56	.017500	.016385	.004040	.000593	.000048
.60	.017710	.016197	.004112	.000449	.000047
.64	.017267	.015280	.003934	.000484	.000047
.68	.016360	.014979	.003851	.000516	.000047
.72	.015560	.013794	.003733	.000503	.000047
.76	.014173	.012343	.003577	.000458	.000048
.80	.012858	.011345	.003569	.000539	.000048
.84	.011628	.010470	.003491	.000487	.000047
.88	.010289	.009173	.003228	.000522	.000047
.92	.008968	.008479	.003046	.000567	.000047
.96	.008210	.007943	.003081	.000428	.000046
1.00	.007064	.006572	.002872	.000562	.000046
1.04	.006210	.006154	.002738	.000567	.000046
1.08	.005427	.005298	.002653	.000490	.000044
1.12	.004711	.004351	.002431	.000495	.000045
1.16	.004077	.003916	.002401	.000478	.000043
1.20	.003452	.003458	.002199	.000478	.000043
1.24	.003106	.003296	.002141	.000494	.000042
1.28	.002871	.003056	.002076	.000528	.000043
1.32	.002539	.003018	.002021	.000540	.000042
1.36	.002200	.002880	.001940	.000550	.000041
1.40	.002093	.002873	.001796	.000568	.000041
1.44	.001908	.002294	.001704	.000611	.000040
1.48	.001602	.002239	.001611	.000595	.000040
1.52	.001654	.001962	.001697	.000506	.000038
1.56	.001593	.002006	.001553	.000453	.000036
1.60	.001397	.001804	.001418	.000531	.000036
1.64	.001358	.001869	.001399	.000433	.000034
1.68	.001226	.001690	.001257	.000428	.000033
1.72	.001060	.001316	.001108	.000512	.000033
1.76	.000965	.001400	.000957	.000487	.000032
1.80	.000949	.001039	.000835	.000487	.000030
1.84	.000658	.001006	.000617	.000487	.000029

PREDICTED DEFL. RESPONSE FUNS (BY RATIO MULTIPLICATION)
C130 AIRCRAFT SITE-3

TIME	RESP 0	RESP 1	RESP 2	RESP 3	RESP 4
0.00	.001628	.003544	.002280	.000047	.000044
.04	.002257	.004247	.002690	.000049	.000048
.08	.003020	.005552	.003107	.000130	.000054
.12	.004252	.007498	.003662	.000216	.000059
.16	.006452	.010251	.004427	.000302	.000063
.20	.009935	.013754	.005227	.000398	.000066
.24	.014889	.018036	.005966	.000508	.000070
.28	.019430	.021254	.006643	.000541	.000073
.32	.021699	.023076	.007169	.000539	.000075
.36	.022459	.024283	.007447	.000544	.000077
.40	.023393	.025000	.007590	.000563	.000080
.44	.025656	.026560	.007891	.000593	.000084
.48	.028643	.028463	.008229	.000863	.000091
.52	.032303	.030785	.008560	.001032	.000096
.56	.036396	.033132	.008913	.000983	.000097
.60	.039270	.034308	.009138	.001027	.000099
.64	.038793	.033652	.009075	.001078	.000101
.68	.035850	.031754	.008864	.001166	.000103
.72	.032163	.029079	.008402	.001301	.000106
.76	.028682	.026237	.007844	.001338	.000107
.80	.025814	.023953	.007402	.001345	.000106
.84	.023336	.021832	.006973	.001344	.000105
.88	.021670	.020276	.006533	.001356	.000105
.92	.020611	.019460	.006283	.001334	.000102
.96	.019987	.018790	.006071	.001322	.000101
1.00	.019965	.018490	.005833	.001295	.000099
1.04	.020696	.018808	.005756	.001264	.000096
1.08	.021957	.019370	.005769	.001220	.000092
1.12	.023489	.019868	.005695	.001195	.000090
1.16	.025037	.020554	.005666	.001177	.000088
1.20	.026707	.020968	.005629	.001172	.000086
1.24	.027550	.021062	.005485	.001148	.000084
1.28	.027891	.020998	.005435	.001109	.000081
1.32	.027133	.020284	.005250	.001102	.000080
1.36	.025706	.019074	.005071	.001089	.000079
1.40	.023913	.017634	.004822	.001082	.000077
1.44	.021855	.015966	.004461	.001069	.000075
1.48	.019680	.013959	.004028	.001059	.000072
1.52	.017687	.012075	.003596	.001037	.000069
1.56	.015870	.010235	.003188	.001030	.000065
1.60	.014260	.008623	.002803	.001023	.000062
1.64	.012934	.006911	.002328	.001016	.000060
1.68	.011788	.005499	.002080	.000997	.000056
1.72	.010829	.004615	.001921	.000991	.000054
1.76	.010051	.003656	.001624	.000982	.000051
1.80	.009445	.003260	.001318	.000967	.000048
1.84	.008816	.002703	.000967	.000968	.000044

Case 3

C130 Aircraft and Site 2 - Standard

Predictions for:

C135 Aircraft at Site 1
C131 Aircraft at Site 1
C135 Aircraft at Site 3
C131 Aircraft at Site 3

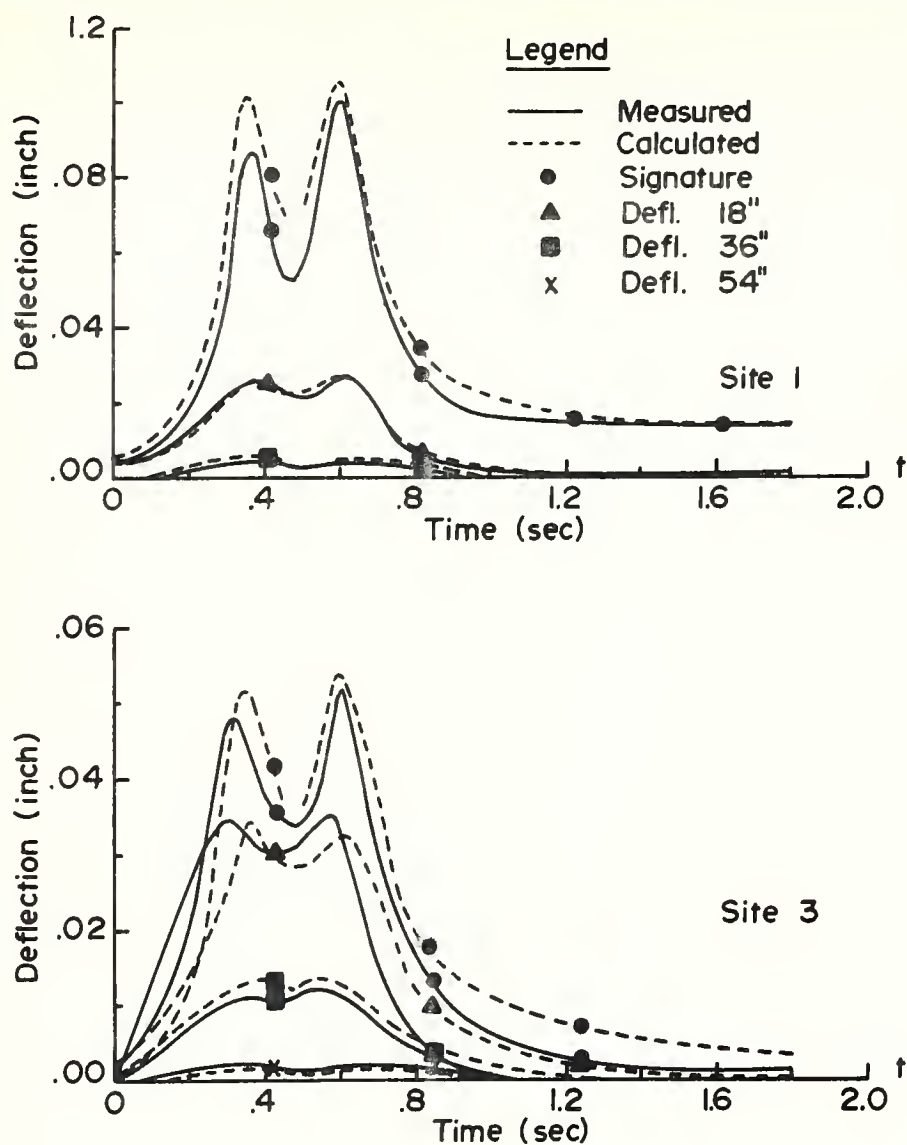


FIGURE 87. TYPICAL CALCULATED AND MEASURED DEFLECTION RESPONSE FUNCTIONS FOR C135 USING PREDICTED TDT FUNCTIONS WITH C130 AS STANDARD PRIME MOVER.

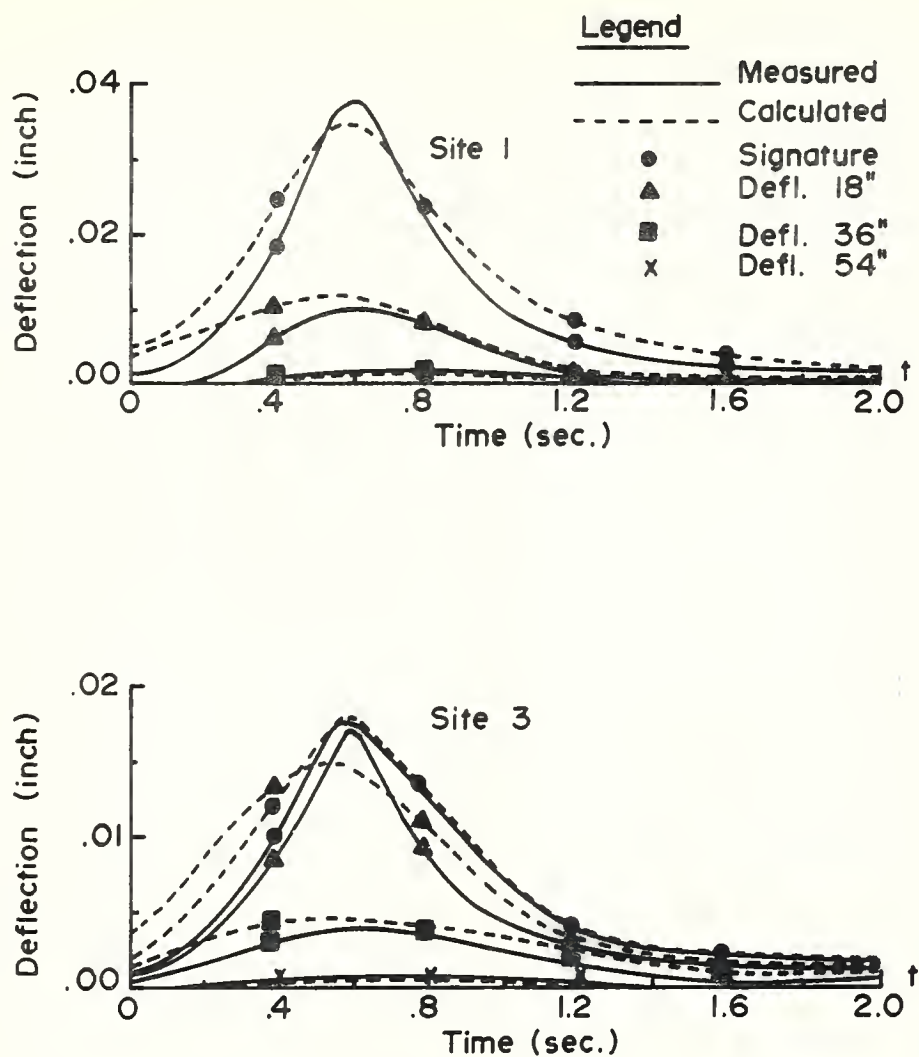


FIGURE 88. TYPICAL CALCULATED AND MEASURED DEFLECTION RESPONSE FUNCTIONS FOR C 131 USING PREDICTED TDT FUNCTIONS WITH C130 AS STANDARD PRIME MOVER.

PREDICTED DEFL. RESPONSE FUNS (BY RATIO MULTIPLICATION)
C135 AI CRAFT SIF-1

TIME	RESP 0	RESP 1	RESP 2	RESP 3	RESP 4
0.00	.002722	.002281	.000161	.000000	.000000
.04	.004084	.002892	.000193	.000000	.000000
.08	.005338	.003951	.000235	.000000	.000000
.12	.006574	.005436	.000283	.000001	.000000
.16	.013546	.017727	.000346	.000001	.000000
.20	.022699	.011316	.000428	.000001	.000000
.24	.039029	.016520	.000518	.000001	.000000
.28	.065481	.022771	.000617	.000001	.000000
.32	.095708	.027136	.000697	.000001	.000000
.36	.102332	.027657	.000721	.000001	.000000
.40	.086936	.02563	.000700	.000001	.000000
.44	.073621	.023539	.000674	.000001	.000000
.48	.068398	.022898	.000653	.000001	.000000
.52	.074167	.024068	.000652	.000001	.000000
.56	.090539	.026106	.000658	.000001	.000000
.60	.105790	.026403	.000648	.000001	.000000
.64	.096831	.024195	.000595	.000001	.000000
.68	.076640	.019935	.000513	.000001	.000000
.72	.059194	.015612	.000432	.000001	.000000
.76	.046533	.011846	.000352	.000001	.000000
.80	.038005	.008999	.000281	.000001	.000000
.84	.031366	.006854	.000218	.000001	.000000
.88	.026942	.005411	.000174	.000001	.000000
.92	.024137	.004471	.000141	.000001	.000000
.96	.022216	.003723	.000114	.000001	.000000
1.00	.020937	.003271	.000094	.000001	.000000
1.04	.019984	.002976	.000076	.000001	.000000
1.08	.019139	.002637	.000061	.000001	.000000
1.12	.018592	.002485	.000047	.000001	.000000
1.16	.018133	.002281	.000037	.000001	.000000
1.20	.017719	.002170	.000027	.000001	.000000
1.24	.017371	.002032	.000020	.000000	.000000
1.28	.016656	.001830	.000013	.000000	.000000
1.32	.016440	.001915	.000008	.000000	.000000
1.36	.016200	.001714	.000003	.000000	.000000
1.40	.015844	.001698	.000001	.000000	.000000
1.44	.015730	.001563	.000001	.000000	.000000
1.48	.015678	.001615	.000001	.000000	.000000
1.52	.015163	.001528	.000001	.000000	.000000
1.56	.015088	.001471	.000001	.000000	.000000
1.60	.015083	.001493	.000001	.000000	.000000
1.64	.014811	.001339	.000001	.000000	.000000
1.68	.014560	.001357	.000001	.000000	.000000
1.72	.014580	.001333	.000000	.000000	.000000
1.76	.014510	.001315	.000000	.000000	.000000
1.80	.014523	.001253	.000000	.000000	.000000
1.84	.014214	.001244	.000000	.000000	.000000

PREDICTED DEFL. RESPONSE FUNS (BY RATIO MULTIPLICATION)
C131 AIRCRAFT SITE-1

TIME	RESP 0	RESP 1	RESP 2	RESP 3	RESP 4
0.00	.004887	.004397	.000154	.000000	.000000
.04	.005944	.004896	.000164	.000000	.000000
.08	.006911	.005132	.000165	.000000	.000000
.12	.008190	.005829	.000174	.000000	.000000
.16	.009837	.006610	.000186	.000000	.000000
.20	.011404	.007027	.000186	.000000	.000000
.24	.013534	.008174	.000197	.000000	.000000
.28	.015736	.008640	.000198	.000000	.000000
.32	.018836	.009562	.000209	.000000	.000000
.36	.021816	.010312	.000215	.000000	.000000
.40	.024748	.010650	.000216	.000000	.000000
.44	.027612	.011038	.000219	.000000	.000000
.48	.030564	.011784	.000226	.000000	.000000
.52	.032652	.011858	.000229	.000000	.000000
.56	.033863	.011872	.000228	.000000	.000000
.60	.034270	.011737	.000232	.000000	.000000
.64	.033412	.011072	.000222	.000000	.000000
.68	.031657	.010853	.000217	.000000	.000000
.72	.030109	.009995	.000210	.000000	.000000
.76	.027425	.008944	.000201	.000000	.000000
.80	.024882	.008221	.000201	.000000	.000000
.84	.022502	.007587	.000197	.000000	.000000
.88	.019910	.006647	.000182	.000000	.000000
.92	.017354	.006144	.000172	.000000	.000000
.96	.015887	.005755	.000173	.000000	.000000
1.00	.013669	.004762	.000162	.000000	.000000
1.04	.012016	.004459	.000154	.000000	.000000
1.08	.010502	.003839	.000149	.000000	.000000
1.12	.009116	.003153	.000137	.000000	.000000
1.16	.007890	.002637	.000135	.000000	.000000
1.20	.006680	.002505	.000124	.000000	.000000
1.24	.006010	.002388	.000121	.000000	.000000
1.28	.005555	.002214	.000117	.000000	.000000
1.32	.004914	.002187	.000114	.000000	.000000
1.36	.004257	.002087	.000109	.000000	.000000
1.40	.004050	.002082	.000101	.000000	.000000
1.44	.003692	.001662	.000096	.000000	.000000
1.48	.003100	.001623	.000091	.000000	.000000
1.52	.003201	.001421	.000096	.000000	.000000
1.56	.003082	.001454	.000087	.000000	.000000
1.60	.002703	.001307	.000080	.000000	.000000
1.64	.002627	.001354	.000079	.000000	.000000
1.68	.002373	.001225	.000071	.000000	.000000
1.72	.002052	.000954	.000062	.000000	.000000
1.76	.001868	.001014	.000054	.000000	.000000
1.80	.001836	.000753	.000047	.000000	.000000
1.84	.001274	.000729	.000035	.000000	.000000

PREDICTED DEFL. RESPONSE FUNS (BY RATIO MULTIPLICATION)
C135 AIRCRAFT SITE-3

TIME	RESP 0	RESP 1	RESP 2	RESP 3	RESP 4
0.00	.001407	.002806	.003152	.000412	.000077
.04	.002110	.003557	.003809	.000547	.000087
.08	.003017	.004859	.004645	.000761	.000101
.12	.004431	.006686	.005601	.000990	.000115
.16	.007000	.009503	.006839	.001240	.000129
.20	.011730	.013917	.008455	.001495	.000143
.24	.020169	.020326	.010243	.001735	.000154
.28	.033839	.026005	.012199	.001963	.000165
.32	.049460	.033372	.013792	.002130	.000174
.36	.052863	.034014	.014252	.002194	.000179
.40	.044927	.031532	.013854	.002205	.000181
.44	.038046	.028948	.013334	.002204	.000183
.48	.035347	.028160	.013026	.002202	.000183
.52	.038328	.029599	.012868	.002203	.000183
.56	.046789	.032105	.013017	.002205	.000182
.60	.054670	.032479	.012819	.002197	.000179
.64	.050040	.029756	.011776	.002191	.000174
.68	.039606	.024516	.010152	.002184	.000168
.72	.030590	.019200	.008542	.002173	.000163
.76	.024047	.014568	.006956	.002161	.000157
.80	.019640	.011067	.005551	.002139	.000150
.84	.016210	.008430	.004318	.002095	.000142
.88	.013923	.006655	.003437	.001993	.000132
.92	.012473	.005498	.002766	.001852	.000121
.96	.011481	.004579	.002264	.001710	.000109
1.00	.010320	.004023	.001857	.001549	.000097
1.04	.010328	.003660	.001510	.001411	.000086
1.08	.009991	.003243	.001201	.001281	.000076
1.12	.009608	.003056	.000929	.001169	.000067
1.16	.009371	.002806	.000738	.001055	.000058
1.20	.009157	.002669	.000539	.000975	.000052
1.24	.008977	.002490	.000398	.000906	.000047
1.28	.008608	.002261	.000262	.000851	.000042
1.32	.008496	.002355	.000164	.000800	.000037
1.36	.008372	.002108	.000057	.000760	.000033
1.40	.008188	.002088	.000019	.000725	.000030
1.44	.0080129	.001922	.000024	.000700	.000027
1.48	.008102	.001986	.000027	.000670	.000024
1.52	.007936	.001880	.000028	.000659	.000023
1.56	.007797	.001809	.000027	.000641	.000021
1.60	.007795	.001836	.000024	.000618	.000019
1.64	.007654	.001647	.000019	.000602	.000018
1.68	.007524	.001669	.000014	.000589	.000016
1.72	.007535	.001639	.000008	.000579	.000015
1.76	.007498	.001618	.000001	.000570	.000014
1.80	.007505	.001541	.000000	.000566	.000014
1.84	.007346	.001530	.000000	.000559	.000013

PREDICTED DEFL. RESPONSE FUNS (BY RATIO MULTIPLICATION)
C131 AIRCRAFT SITE-3

TIME	RESP 0	RESP 1	RESP 2	RESP 3	RESP 4
0.00	.002525	.005408	.003041	.000430	.000050
.04	.003072	.006021	.003242	.000539	.000053
.08	.003572	.006312	.003265	.000591	.000054
.12	.004233	.007168	.003445	.000588	.000053
.16	.005083	.008129	.003683	.000445	.000053
.20	.005893	.008642	.003684	.000523	.000055
.24	.006994	.010052	.003902	.000430	.000054
.28	.008132	.010625	.003907	.000430	.000055
.32	.009734	.011759	.004138	.000474	.000055
.36	.011274	.012682	.004251	.000437	.000056
.40	.012789	.013096	.004274	.000548	.000056
.44	.014269	.013575	.004332	.000642	.000057
.48	.015795	.014432	.004473	.000554	.000056
.52	.016874	.014583	.004539	.000610	.000057
.56	.017500	.014601	.004500	.000691	.000058
.60	.017710	.014434	.004580	.000523	.000057
.64	.017267	.013616	.004382	.000563	.000057
.68	.016360	.013348	.004289	.000601	.000058
.72	.015560	.012293	.004158	.000586	.000053
.76	.014173	.010994	.003984	.000534	.000059
.80	.012858	.010110	.003975	.000628	.000059
.84	.011628	.009331	.003888	.000567	.000057
.88	.010289	.008174	.003556	.000607	.000057
.92	.008968	.007556	.003393	.000660	.000057
.96	.008210	.007078	.003431	.000498	.000056
1.00	.007064	.005856	.003199	.000654	.000057
1.04	.006210	.005484	.003050	.000661	.000056
1.08	.005427	.004721	.002955	.000571	.000054
1.12	.004711	.003877	.002708	.000577	.000055
1.16	.004077	.003489	.002674	.000557	.000053
1.20	.003452	.003081	.002449	.000557	.000052
1.24	.003106	.002937	.002384	.000575	.000052
1.28	.002371	.002723	.002312	.000615	.000052
1.32	.002539	.002690	.002251	.000629	.000051
1.36	.002200	.002566	.002160	.000641	.000050
1.40	.002093	.002560	.002000	.000661	.000050
1.44	.001908	.002044	.001893	.000711	.000049
1.48	.001602	.001996	.001794	.000693	.000049
1.52	.001654	.001748	.001891	.000589	.000046
1.56	.001593	.001788	.001729	.000528	.000044
1.60	.001397	.001607	.001579	.000613	.000044
1.64	.001358	.001665	.001558	.000504	.000042
1.68	.001226	.001506	.001401	.000498	.000041
1.72	.001060	.001173	.001234	.000596	.000041
1.76	.000965	.001248	.001066	.000568	.000039
1.80	.000949	.000926	.000930	.000567	.000037
1.84	.000658	.000897	.000687	.000567	.000036

Case 4

C131 Aircraft and Site 1 - Standard

Predictions for:

C135 Aircraft at Site 2
C130 Aircraft at Site 2
C135 Aircraft at Site 3
C130 Aircraft at Site 3

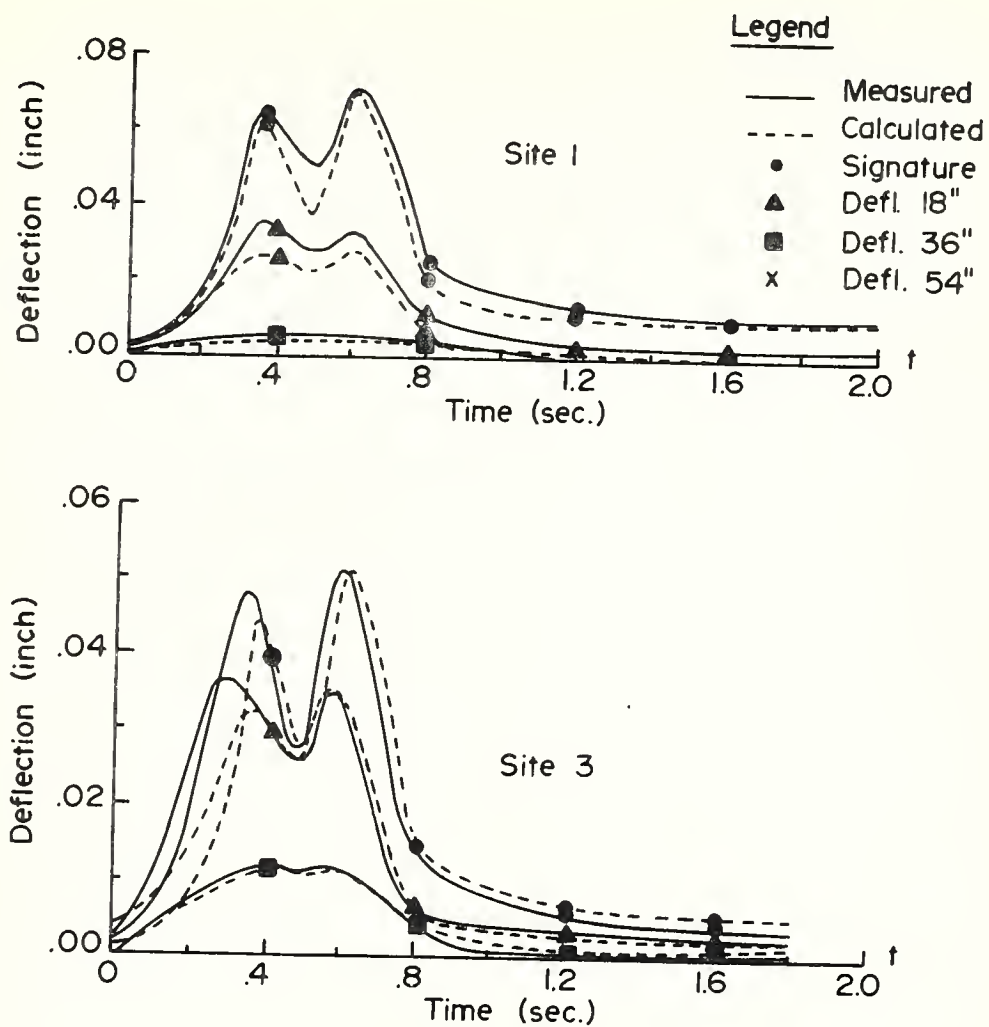


FIGURE 89. TYPICAL CALCULATED AND MEASURED DEFLECTION RESPONSE FUNCTIONS FOR C135 USING PREDICTED TDT FUNCTIONS WITH C131 AS STANDARD PRIME MOVER.

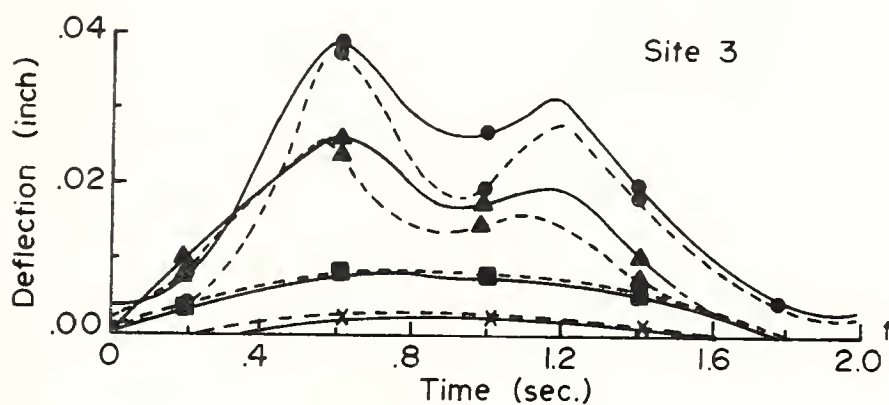
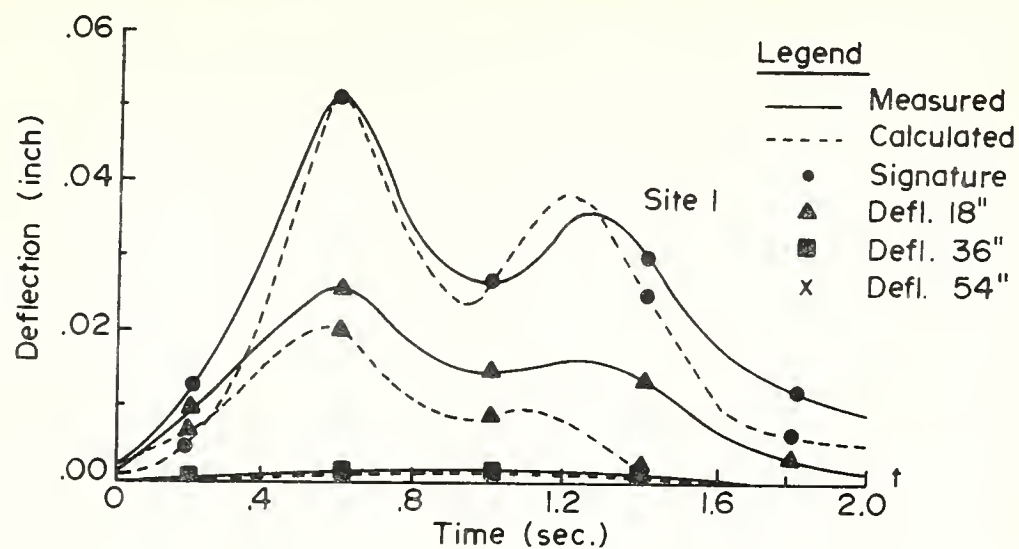


FIGURE 90. TYPICAL CALCULATE AND MEASURED DEFLECTION RESPONSE FUNCTIONS FOR C130 USING PREDICTED TDT FUNCTIONS WITH C131 AS STANDARD PRIME MOVER.

PREDICTED DEFL. RESPONSE FUNS (BY RATIO MULTIPLICATION)
C135 AIRCRAFT SITE-2

TIME	RESP 0	RESP 1	RESP 2	RESP 3	RESP 4
0.00	.001697	.002731	.000673	.000061	.000001
.04	.002255	.004043	.000912	.000067	.000001
.08	.002944	.005029	.001164	.000076	.000001
.12	.004263	.006468	.001419	.000088	.000001
.16	.006380	.009087	.001836	.000097	.000001
.20	.012261	.012407	.002299	.000104	.000001
.24	.021146	.016259	.002728	.000115	.000001
.28	.033874	.020603	.003248	.000121	.000001
.32	.049279	.025211	.003772	.000127	.000001
.36	.060886	.027038	.004117	.000137	.000001
.40	.055969	.025298	.004198	.000140	.000001
.44	.042979	.022422	.004137	.000139	.000001
.48	.037554	.021477	.004094	.000137	.000001
.52	.042083	.023455	.004121	.000137	.000001
.56	.057322	.027125	.004230	.000130	.000001
.60	.070700	.027506	.004231	.000127	.000001
.64	.062311	.023438	.004008	.000124	.000001
.68	.045806	.017879	.003588	.000114	.000001
.72	.033421	.012456	.003067	.000107	.000001
.76	.024882	.007884	.002480	.000098	.000001
.80	.019405	.004602	.001975	.000088	.000001
.84	.016243	.002505	.001626	.000077	.000001
.88	.014236	.001070	.001346	.000070	.000001
.92	.013036	.000700	.001137	.000064	.000001
.96	.012369	.000731	.001004	.000052	.000001
1.00	.011734	.000266	.000849	.000048	.000001
1.04	.011320	.000548	.000726	.000041	.000000
1.08	.011185	.000772	.000674	.000032	.000000
1.12	.010788	.000577	.000562	.000028	.000000
1.16	.010394	.000545	.000442	.000025	.000000
1.20	.010170	.000281	.000391	.000024	.000000
1.24	.010016	.000278	.000348	.000017	.000000
1.28	.009631	.000243	.000233	.000020	.000000
1.32	.009481	.000152	.000200	.000019	.000000
1.36	.009477	.000379	.000217	.000013	.000000
1.40	.009225	.000200	.000143	.000017	.000000
1.44	.009100	.000275	.000118	.000014	.000000
1.48	.009399	.000051	.000097	.000014	.000000
1.52	.008925	.000034	.000125	.000014	.000000
1.56	.008858	.000032	.000050	.000013	.000000
1.60	.009008	.000029	.000179	.000011	.000000
1.64	.008925	.000035	.000098	.000007	.000000
1.68	.008789	.000016	.000077	.000013	.000000
1.72	.009035	.000268	.000101	.000007	.000000
1.76	.009076	.000434	.000153	.000004	.000000
1.80	.008874	.000280	.000085	.000009	.000000
1.84	.008793	.000466	.000088	.000007	.000000

PREDICTED DEFL. RESPONSE FUNS (BY RATIO MULTIPLICATION)
C130 AIRCRAFT SITE-2

TIME	RESP 0	RESP 1	RESP 2	RESP 3	RESP 4
0.00	.001527	.003158	.000942	.000060	.000001
.04	.001856	.003438	.001052	.000063	.000001
.08	.002205	.003576	.001107	.000067	.000001
.12	.002812	.004437	.001252	.000070	.000001
.16	.003732	.005409	.001377	.000073	.000001
.20	.005087	.006777	.001539	.000076	.000001
.24	.006975	.008218	.001687	.000080	.000001
.28	.009702	.010499	.001895	.000083	.000001
.32	.013412	.011868	.002122	.000086	.000001
.36	.018049	.013735	.002345	.000089	.000001
.40	.023858	.015556	.002483	.000091	.000001
.44	.030870	.017913	.002696	.000093	.000001
.48	.038536	.019367	.002862	.000095	.000001
.52	.045155	.020513	.003011	.000097	.000001
.56	.049667	.020712	.003035	.000099	.000001
.60	.051100	.020589	.003047	.000100	.000001
.64	.049669	.019098	.003033	.000101	.000001
.68	.045943	.016932	.003039	.000100	.000001
.72	.041072	.014749	.003045	.000101	.000001
.76	.035908	.012654	.003020	.000101	.000001
.80	.031088	.010674	.002955	.000100	.000001
.84	.027458	.009420	.002928	.000099	.000001
.88	.025059	.009101	.002887	.000098	.000001
.92	.023958	.008896	.002877	.000098	.000001
.96	.024441	.008274	.002839	.000097	.000001
1.00	.026436	.008375	.002816	.000097	.000001
1.04	.029688	.008772	.002780	.000097	.000001
1.08	.033235	.008841	.002772	.000097	.000001
1.12	.036143	.008917	.002747	.000097	.000001
1.16	.037863	.008865	.002721	.000095	.000001
1.20	.038163	.008079	.002677	.000094	.000001
1.24	.037205	.007592	.002606	.000092	.000001
1.28	.035122	.006406	.002530	.000091	.000001
1.32	.032140	.004634	.002417	.000089	.000001
1.36	.028447	.002573	.002243	.000088	.000001
1.40	.024682	.001107	.002100	.000085	.000001
1.44	.021058	.000031	.001934	.000082	.000001
1.48	.017960	0.000000	.001814	.000078	.000001
1.52	.015145	0.000000	.001677	.000075	.000001
1.56	.012773	0.000000	.001540	.000072	.000001
1.60	.010638	0.000000	.001351	.000068	.000001
1.64	.008955	0.000000	.001200	.000065	.000001
1.68	.007687	0.000000	.001104	.000061	.000001
1.72	.006861	0.000000	.001038	.000057	.000001
1.76	.006110	0.000000	.000925	.000054	.000001
1.80	.005444	0.000000	.000835	.000052	.000001
1.84	.004862	0.000000	.000741	.000050	.000001

PREDICTED DEFL. RESPONSE FUNS (BY RATIO MULTIPLICATION)
C135 AIRCRAFT SITE-3

TIME	RESP 0	RESP 1	RESP 2	RESP 3	RESP 4
0.00	.001236	.003301	.001892	.000717	.000053
.04	.001643	.004887	.002563	.000791	.000062
.08	.002145	.006079	.003269	.000899	.000071
.12	.003106	.007819	.003987	.001043	.000080
.16	.005085	.010985	.005156	.001150	.000083
.20	.008933	.014998	.006458	.001228	.000095
.24	.015407	.019654	.007664	.001355	.000102
.28	.024679	.024905	.009124	.001430	.000107
.32	.035903	.030475	.010596	.001502	.000113
.36	.044360	.032684	.011564	.001619	.000119
.40	.040778	.030581	.011792	.001650	.000123
.44	.031313	.027104	.011620	.001641	.000125
.48	.027361	.025962	.011500	.001616	.000126
.52	.030661	.028353	.011576	.001616	.000123
.56	.042127	.032789	.011882	.001534	.000120
.60	.051510	.033250	.011885	.001496	.000113
.64	.045398	.028333	.011257	.001464	.000114
.68	.033373	.021612	.010079	.001350	.000110
.72	.024349	.015057	.008615	.001263	.000105
.76	.018128	.009530	.006965	.001158	.000097
.80	.014138	.005563	.005549	.001039	.000089
.84	.011934	.003028	.004568	.000906	.000080
.88	.010372	.001293	.003780	.000830	.000071
.92	.009498	.000846	.003192	.000757	.000063
.96	.009012	.000884	.002820	.000613	.000056
1.00	.008549	.000322	.002386	.000562	.000049
1.04	.008248	.000662	.002039	.000488	.000043
1.08	.008149	.000933	.001893	.000375	.000036
1.12	.007860	.000698	.001578	.000336	.000032
1.16	.007573	.000658	.001241	.000298	.000027
1.20	.007410	.000340	.001098	.000278	.000023
1.24	.007297	.000337	.000978	.000205	.000021
1.28	.007017	.000293	.000654	.000235	.000019
1.32	.006908	.000184	.000562	.000225	.000016
1.36	.006905	.000458	.000611	.000149	.000015
1.40	.006721	.000242	.000401	.000197	.000014
1.44	.006630	.000332	.000331	.000161	.000013
1.48	.006848	.000061	.000273	.000166	.000012
1.52	.006502	.000042	.000355	.000164	.000011
1.56	.006454	.000039	.000139	.000151	.000010
1.60	.006563	.000034	.000503	.000129	.000009
1.64	.006503	.000042	.000274	.000083	.000008
1.68	.006403	.000020	.000217	.000152	.000008
1.72	.006583	.000324	.000284	.000087	.000007
1.76	.006613	.000524	.000446	.000043	.000006
1.80	.006466	.000338	.000238	.000106	.000006
1.84	.006407	.000563	.000247	.000084	.000006

PREDICTED DEFL. RESPONSE FUNS (BY RATIO MULTIPLICATION)
C130 AIRCRAFT SITE-3

TIME	RESP 0	RESP 1	RESP 2	RESP 3	RESP 4
0.00	.001113	.003818	.002645	.000703	.000054
.04	.001353	.004156	.002954	.000741	.000057
.08	.001606	.004323	.003109	.000786	.000060
.12	.002049	.005364	.003517	.000821	.000063
.16	.002719	.006539	.003868	.000859	.000065
.20	.003706	.008192	.004322	.000901	.000068
.24	.005082	.009934	.004739	.000940	.000070
.28	.007068	.012692	.005324	.000978	.000072
.32	.009771	.014346	.005962	.001011	.000074
.36	.013150	.016604	.006586	.001046	.000076
.40	.017382	.018804	.006975	.001075	.000078
.44	.022491	.021654	.007574	.001097	.000079
.48	.028076	.023411	.008041	.001125	.000080
.52	.032899	.024797	.008459	.001141	.000081
.56	.036186	.025037	.008525	.001168	.000083
.60	.037230	.024888	.008559	.001182	.000085
.64	.036187	.023086	.008520	.001187	.000086
.68	.033473	.020467	.008536	.001182	.000087
.72	.029924	.017828	.008554	.001187	.000089
.76	.026162	.015296	.008483	.001186	.000090
.80	.022650	.012903	.008302	.001175	.000090
.84	.020005	.011387	.008226	.001170	.000091
.88	.018257	.011002	.008110	.001162	.000091
.92	.017455	.010754	.008080	.001154	.000091
.96	.017307	.010001	.007974	.001148	.000090
1.00	.019261	.010124	.007910	.001150	.000090
1.04	.021630	.010604	.007809	.001141	.000089
1.08	.024214	.010688	.007787	.001142	.000088
1.12	.026333	.010779	.007715	.001139	.000087
1.16	.027586	.010716	.007642	.001124	.000086
1.20	.027804	.009766	.007520	.001108	.000085
1.24	.027106	.009178	.007320	.001090	.000083
1.28	.025589	.007744	.007106	.001069	.000082
1.32	.023416	.005602	.006790	.001048	.000081
1.36	.020725	.003111	.006300	.001034	.000080
1.40	.017983	.001338	.005900	.001002	.000078
1.44	.015342	.000037	.005433	.000971	.000076
1.48	.013085	0.000000	.005094	.000922	.000073
1.52	.011034	0.000000	.004710	.000886	.000071
1.56	.009306	0.000000	.004326	.000848	.000068
1.60	.007750	0.000000	.003795	.000808	.000066
1.64	.006524	0.000000	.003369	.000764	.000063
1.68	.005600	0.000000	.003101	.000718	.000059
1.72	.004998	0.000000	.002916	.000678	.000056
1.76	.004452	0.000000	.002598	.000642	.000054
1.80	.003966	0.000000	.002344	.000619	.000051
1.84	.003542	0.000000	.002081	.000589	.000049

